THE EFFECT OF SUPERPLASTICISING ADMIXTURES ON THE PERFORMANCE OF CIMENT FONDU

Thesis submitted in accordance with the requirements
of the University of Liverpool for the degree of
Doctor in Philosophy by Susan Margaret Gill

August 1987

CONTENTS

LIST OF TABLES

LIST OF FIGURES

THE EFFECT OF SUPERPLASTICISING ADMIXTURES ON THE PERFORMANCE OF CIMENT FONDU

S. M. GILL

ABSTRACT

The main objective of the project was to find a superplasticising admixture for Ciment Fondu which is effective at 6-8°C and which does not cause set retardation. An additional objective was to gain understanding of the interaction between superplasticiser and Ciment Fondu to enable improvements in formulation to be investigated.

The influence of three superplasticisers and one accelerator on Ciment Fondu pastes and mortars at test temperatures ranging from 5-45°C was studied using several techniques. The superplasticisers tested were :

S1 sulphonated naphthalene formaldehyde condensate
S2 sulphonated phenol formaldehyde condensate
S3 sulphonated melamine formaldehyde condensate
whilst the accelerator was lithium citrate.

The properties investigated were

(i) rheology; using coaxial cylinders viscometry and "industrial" workability tests,
(ii) hydration kinetics; using isothermal conduction calorimetry,
(iii) setting time; using the Vicat penetration test,
(iv) strength development; using ultrasonic pulse velocity (upv) measurements correlated with compressive strength ,
(v) hydration products; using derivative thermogravimetric analysis (DTG) and X-ray analysis (XRD),
(vi) calcium concentration in solution; by titration with the disodium salt of ethylenediaminetetra-acetic acid (EDTA) and by use of an ion selective electrode and
(vii) aluminium concentration in solution; using atomic absorption flame spectrophotometry.

None of the three superplasticisers improved the workability of Ciment Fondu mixes to the same extent as that normally observed when superplasticisers are used with Portland cements.

The most effective of the three superplasticisers was S2 followed by S1 and then S3. The use of 0.3% S2 with 0.025% accelerator gives improved workability compared to the control mix for up to 25 minutes after mixing at 5°C and up to 10 minutes at 20°C. This combination of admixtures does not cause set retardation. The very poor performance of S3 in the rheological testing led to its exclusion from the other experiments.

The use of either S1 or S2 alone causes set retardation at 20°C or below but accelerates setting at 30°C or above.

At early ages the use of superplasticisers generally causes a reduction in strength compared to control samples at the same temperature. After 18 months there is however little difference between control mixes and those containing admixtures.

ACKNOWLEDGEMENTS

The production of this thesis was made possible by the assistance of many people including my family and friends who provided much tea and a sympathetic hearing during difficult moments.

In particular I would like to thank:

Dr. P.F.G. Banfill for his efficient supervision and invaluable guidance.

The Science and Engineering Research Council for financial support.

FEB (Great Britain) Ltd for financial support and supply of materials.

Lafarge Aluminous Cement Company Ltd for supply of cement.

Dr. B. El-Jazairi (FEB) for his interest and advice.

Les Smith for his technical assistance and unfailing cheerfulness; also Pam Hooper, Mike Reid, Gary Seiffert, Syd Robinson and Bill Baker for their assistance.

Julie Sharman for assistance with X-ray testing.

Alan Thomas for assistance with atomic absorption testing.

Irene Green for typing the thesis.

CHAPTER 1. INTRODUCTION AND LITERATURE REVIEW

INTRODUCTION

High alumina cement was originally developed in response to the severe attack suffered by Portland cements in groundwater containing a high concentration of sulphates. It was soon found that in addition to giving extremely good chemical resistance high alumina cement produced concrete with very high early strength. The rapid rate of strength gain is found to occur even at low temperature thus high alumina cements have been successfully used for construction at temperatures near freezing when the extended setting time of Portland cements would be unacceptable.

The manufacture of high alumina cement will not be described in detail in this thesis for brevity. The raw materials used are generally limestone and bauxite which are combined in a kiln in which fusion takes place producing a clinker which is subsequently ground to the required fineness.

The use of superplasticisers with Portland cement has become increasingly common in recent decades and has extended the range of applications of grouts, mortars and concretes. The use of superplasticising admixtures to improve the workability of high alumina cement mixes is an attractive proposition although the research carried out to date has shown that conventional superplasticisers, used with Portland cements, cause unnacceptable set retardation.

The main objective of the research described in this thesis is the development of a superplasticising admixture for high alumina cement which is effective at the low temperature of 6-8°C commonly encountered in the marine environment and which does not cause excessive set retardation.

Note on Cement Terminology

The term "aluminous cement" is commonly used to describe cement in which the predominant constituent is alumina.

High alumina cement is the name normally given to cement containing approximately 40% alumina although confusion may arise due to the existence of aluminous cements used for refractory purposes containing 50-80% alumina.

The trade name "Ciment Fondu" is used for an aluminous cement with about 40% alumina produced in the UK and Europe by Lafarge Ltd and will be used throughout the thesis rather than high alumina cement.

In the review of literature the terminology used by individual authors is retained to avoid possible errors in the description of experimental work.

1.1 CHEMICAL AND MINERALOGICAL COMPOSITION

1.1.1 Introduction

The conventional abbreviations for the various oxide components of cement are listed below and will be used throughout the thesis.

CaO	=	C	TiO_2	=	T
Al_2O_3	=	A	MgO	=	M
SiO_2	=	S	H_2O	=	H
Fe_2O_3	=	F	SO_3	=	$\bar{S}$
FeO	=	f	CO_2	=	$\bar{C}$

Ciment Fondu is composed mainly of alumina and lime. The aluminate composition is such that the lime/alumina ratio lies between 1 - 1.67. This may be contrasted with a lime/alumina ratio of 3 for the aluminate phase found in Portland cement which leads to increased alkalinity.

A typical oxide composition for Ciment Fondu manufactured in England is given below. (1)

S	4 - 5 %	f	5 - 7 %
A	38 - 40 %	T	< 2 %
C	36 - 39 %	M	1 %
F	8 - 10 %	$\bar{S}$	0.1 %

Until the early 1970's workers in aluminous cement chemistry had concentrated on the lime-alumina-silica system. Much useful information was obtained but the analysis suffered from the major drawback that it ignored the role played by the iron oxides.

In a study of the C-A-F-S phase diagrams Sorrentino and Glasser (2) showed that the introduction of either iron oxide or silica has a large effect on C-A equilibria. Calleja (3) commented that consideration of this system is a reasonable approach since it typically includes approximately 94% of Ciment Fondu. He notes however that in calculations of theoretically possible compositions of high alumina cements the same chemical composition can give rise to the formation of cements with quite different mineralogy which may exhibit markedly different behaviour. No studies have yet been able to take full account of the influence of the ferrous, titanium and magnesium oxides.

George (4) has suggested that full equilibrium may not be reached during crystallisation of Ciment Fondu thus increasing the difficulties encountered in interpretation of phase diagrams. In view of these problems it seems that phase equilibria studies are of limited value in gaining full understanding of Ciment Fondu composition. In addition the practical value of such studies depends on detailed knowledge of the relationship between mineralogy and cement behaviour. This aspect is reviewed in section 1.6.5.

1.1.2 Aluminates

The major constituent of Ciment Fondu is CA (monocalcium aluminate); other aluminates normally present are $C_{12}A_7$ and CA_2. CA normally accounts for up to 50% of Ciment Fondu whilst the amount of $C_{12}A_7$ increases with increasing C/A ratio (1) with up to 15% being present (5). Brisi et al (6) maintain that a stable form of C_5A_3 can exist in the C-A system although its occurrence in Ciment Fondu is not confirmed.

All calcium aluminates can take Fe^{3+} ions into their crystal structure and so are rarely found in pure form in Ciment Fondu. Robson noted that the effect of such "alien" ions in the crystal lattices on the hydration rate and strength development of aluminous cement mixes requires much more investigation (7).

1.1.3 Silicates

Less than 5% of beta C_2S is normally present; other silicates exist as melilite, also found in blastfurnace slags, which is a solid solution whose end members are gehlenite (C_2AS) and akermanite (C_2MS_2) (8). The quanitity of C_2AS increases rapidly if the silica content exceeds 4-5%.

1.1.4 Ferrites

The relative proportions of ferric/ferrous oxides is dependent on the extent to which an oxidising atmosphere is present in the furnace during cement manufacture (7,9).

Ferric oxide can be taken up by $C_{12}A_7$, CA and CA_2 in solid solution. The composition of ferrites in aluminous cements is variable and may lie between C_2F and C_2A thus C_4AF is often used as a general formula. According to Robson (7) however ferrites in Ciment Fondu tend to be iron rich and the formula $C_{10}A_4F$ may be more accurate. The presence of an additional ferrite phase, CF, was reported in 1984 by Harchand et al (10). It should be noted that this work was carried out on an Indian HAC with a low ratio of C/A (0.63) and low ferric oxide content of 5% which may lead to differences in phase composition.

Ferrous oxide can exist freely as wustite or as a glassy phase.

1.1.5 Remaining Constituents

Pleochroite, thought formerly to be unstable C_5A_3 is now considered to be a quaternary compound of variable composition. Midgley (11) proposes a general formula of $(CaNaKFe'')_A \cdot (Fe'''Al)_B \cdot (Al_2O_7)_8 \cdot (AlO_4)_{6-x} \cdot (SiTiO_4)_x$ with typical values of A and B being 28 and 13 respectively.

Titania may be present as perovskite or in solid solution in the ferrite. A small amount of titania is always found since it is present in the bauxite used to manufacture Ciment Fondu (9).

Magnesia is always present, sometimes replacing ferrous oxide in pleochroite, although the proportion does not normally exceed 1%.

Both sodium and potassium oxides are present, the total not usually more than 0.3%. It is possible that most of the sodium oxide is combined in aluminate phases, this suggestion being borne out by the observation that not all the alkalis go into solution when water is added to cement (1).

The amount of sulphur present is usually very low, the amount being affected by the method of manufacture. Traces of compounds of manganese and phosphorus may be found which result from impurities in raw materials, additives and fuel.

It is thus evident that commercially available Ciment Fondu is a combination not only of aluminates, silicates and ferrites but also of numerous impurities in amounts which are likely to vary with changes in raw materials and in production conditions.

1.2. EXPERIMENTAL METHODS

1.2.1 Identification of Hydration Products

1.2.1.1 Thermal Methods

Several thermoanalytical methods which have been used in studies of aluminous cements are briefly described below;

DTA The difference in temperature between the sample and inert reference is recorded as a function of either time or temperature as specimens are subjected to identical temperature regimes in an environment heated at a controlled rate. The area under a peak is related to the energy of the reaction producing it.

DSC The energy required to establish zero temperature difference between sample and reference is plotted against either time or temperature.

DTG The rate of weight change of sample is recorded as a function of time or, more commonly, temperature when the sample is heated at a controlled rate. The area under the DTG curve is directly proportional to the $\overset{\text{weight}}{\wedge}$ change whilst the height of the DTG peak at any temperature gives the rate of $\overset{\text{weight}}{\wedge}$ change at that temperature.

TG The weight change of a material is monitored as a function of time or temperature.

Thermal methods have the advantage that they can detect the presence of non-crystalline hydration products. Baseline drift for both DTA and DSC can cause problems in accurate measurement of peak heights due to the changing heat capacity of the sample as it undergoes chemical and/or physical changes. DTG does not suffer from the same drawback since it depends only on the rate of change of weight.

1.2.1.2 X-ray Diffraction (XRD)

XRD of finely ground samples of either anhydrous or hydrated cement is frequently used to determine the nature and sometimes also amounts of the phases present. XRD is also used to investigate changes in the crystalline structure of compounds resulting from hydration at different temperatures or from the presence of admixtures. Difficulties are encountered in the positive identification of phases present due to the overlapping of lines from the large number of different phases normally present in hydrated cement. XRD is of limited value during early hydration of Ciment Fondu due to the amorphous or very poorly crystalline nature of some of the hydrated phases.

1.2.1.3 Other Methods

Electron microscopy is often used as part of a study on the effect of variables such as hydration temperature or w/c ratio on the shape and size of hydration products.

Infra-red spectroscopy (IRS) and to a lesser extent nuclear magnetic resonance (NMR) are also used and have an advantage over XRD testing in that the position of hydrogen atoms, important to the study of hydrates, may be revealed.

1.2.1.4 Sample Preparation

Investigations of the reaction products formed in the early stages of hydration require water to be removed from the sample in order to prevent further hydration; this process is known as quenching. Organic solvents are normally used which may cause partial dehydration of hydration products (12, 13). Costa et al (13) studied the effects of quenching using ethyl alcohol, isopropyl alcohol and acetone. XRD showed no great differences in relative peak heights but the height of the peaks decreased by approximately 40% for ethyl alcohol and 25-30% for the other 2 solvents.

1.2.2 Method Used to Monitor Hydration and Setting

1.2.2.1 Calorimetry

Several different calorimetric methods, either adiabatic or isothermal, have been used in an attempt to gain insight into hydration. Rodger & Double used a simple adiabatic method in which paste samples in pyrex tubes were surrounded by a thermally insulated container and a thermocouple was used to monitor paste temperature (14). Treffner & Williams used a semi-adiabatic method for studying calcium aluminates binders and castables (15).

It is relevant to note here the frequent use of thermocouples to monitor the setting process. The use of thermocouples is possible because of the spontaneous nature of the exothermic reaction occuring when bulk precipitation of hydrates begins from the solution phase in contact with cement.

1.2.2.2 Ultrasonic Pulse Velocity (Upv)

A small number of workers have used ultrasonic techniques to monitor the build up of paste structure during early hydration, setting and hardening. The velocity of the transmitted wave depends on the structure and density of the transmitting medium and it is not surprising that marked changes in waveform and wave velocity accompany the transition from fresh to hardened paste. The successful interpretation of these changes in terms of physical or chemical alterations to paste structure is extremely difficult.

1.2.2.3 Solution Analysis

The 2 methods of solution analysis described below have been used to monitor the hydration of aluminous cements.

(i) WELLS CURVES (W) Cement and water at high w/c ratio are agitated continuously. Samples of the suspension are taken regularly, filtered and then tested for lime [C] and alumina [A] concentrations by titration and by atomic flame absorption spectrophotometry. The graphs of variation in [C] and [A] with respect to time are known as Wells curves, after their originator.

(ii) FILTRATE DEVELOPMENT CURVES (F) The same process is followed as for W curves but the whole mixture is filtered at one particular time and the liquid obtained is monitored over time for [C] and [A] as above. The difference is thus that there is no original solid phase in contact with the solution.

1.2.2.4 Electrical Conductivity

The electrical conductivity of a paste solution can be continuously monitored although a high water content is usually required.

1.2.2.5 Other Techniques

McCarter & Afshar (16, 17) observed changes in electrical resistivity and dielectric constant during cement hydration.

Rettel et al (18) used NMR to monitor the hydration of CA over a range of temperatures by studying the change in coordination state of aluminium atoms from tetrahedral in anhydrous CA to octahedral in the hydration products.

1.3. HYDRATION

1.3.1 Introduction

A considerable amount of work has been carried out on the hydration of individual phases particularly the major constituent CA, much less on the hydration of commercially available aluminous cements such as Ciment Fondu. Undoubtedly the main reason for this is the great complexity of the reactions, even of one phase, which lead to the formation of differing products under different hydration conditions. The interactions between phase components and the effects of small amounts of impurities in commercial cements are poorly understood.

Any study of calcium aluminates is complicated by the vulnerability of the hydrates to attack by atmospheric carbon dioxide. A further complication is the occurence of compounds as polymorphs and polytypes and in different hydration states.

1.3.2 Hydration of Individual Phase Components of Ciment Fondu

1.3.2.1 CA

A detailed study of the hydration of CA and Ciment Fondu has been undertaken by Barret et al (19) using the 2 methods of solution analysis described in section 1.2.2.3 with w/c 10 to observe the variation in lime and alumina concentrations with time.

When pure CA and water are mixed together at 21°C a metastable solution remains for about 10-30 hours during an induction period of hydrate nucleation (19, 20). During this induction period the values of [C] and [A] remain sensibly constant until a marked drop at a time corresponding to the bulk precipitation of hydrates. The remaining solution has a considerably higher [C/A] ratio and slowly increasing pH. Barret et al (19) found that the maximum values of [C] and [A] were 1.11 g/L and 1.90 g/L respectively with the maximum [C] reached after 2.5 hours; the time to maximum [A] was not reported.

Fujii, Kondo and Ueno (21) have recently monitored the variation of [C] and [A] with time for pure CA at 5, 10, 20 and 30°C at w/c 0.50 and their findings are shown on Figure 1.1. As the hydration temperature increases the levels of both [C] and [A] in solution increase as does the time for which these levels remain unchanged. At 20°C the maximum values of [C] and [A] are 1.34 and 2.14 g/L respectively which are close to the results obtained by Barret et al at 21°C for CA at the considerably higher w/c ratio of 10.

Lea does not distinguish between the behaviour of CA, $C_{12}A_7$ and alkali-free high alumina cement when mixed with water. He reported the variation of [C] and [A] with time, reproduced as Figure 1.2, obtained by shaking 50g of CA with 1 litre of water which show no induction period (9).

Figure 1.1 Effect of Temperature on Concentration of CaO and Al_2O_3 in Solution for CA Paste at w/c 0·5 (21)

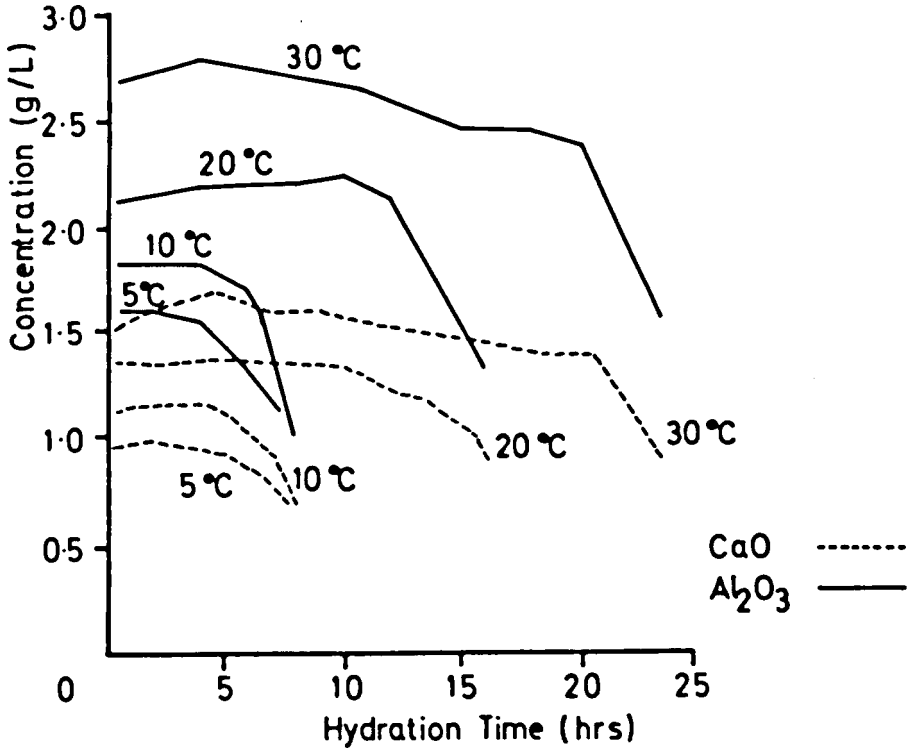

Figure 1.2 Concentration of CaO and Al_2O_3 in Solution for CA Paste at w/c 20 (9)

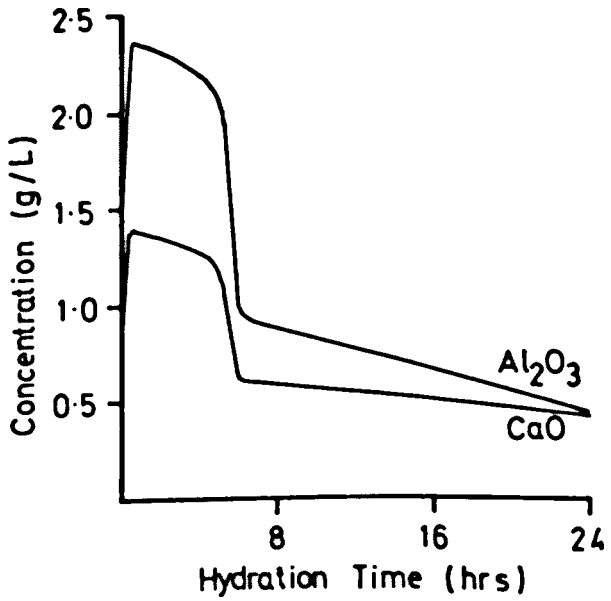

It is not easy to reconcile this major difference although the production of pure CA is known to be very difficult and traces of other aluminates may be present which can alter the hydration characteristics.

The similarity of the W and F curves obtained by Barret et al showed that it is not the presence of anhydrous CA which induces nucleation and precipitation of either calcium aluminate hydrates or aluminium hydroxide although the solution is metastable with respect to these solid phases.

Galtier (12) states that hydration products exist from the first instant of hydration. This early precipitation does not preclude the subsequent gaining of a saturation level which can then be maintained for several hours. The saturation level results from competition between precipitation of hydration products and dissolution of CA. As hydrates nucleate and grow, more anhydrous material can dissolve into solution thus hydration can be seen as a through solution mechanism (22).

This aspect is considered by Barret and Bertrandie (20, 23) who undertook a detailed study of solubility curves for calcium aluminates and propose a minimum instability curve for the formation of C_2AH_8 and alumina gel as shown in Figure 1.3.

For a solution represented by a point to the right of curve I immediate precipitation of C_2AH_8 would occur. To the left of curve II, immediate precipitation of alumina gel would occur. Addition of saturated lime solution causes immediate precipitation of C_2AH_8, otherwise the first hydrate formed is CAH_{10}.

In later work Barret et al extended their study of solubility diagrams to include carboaluminates, carbonates, atmospheric CO_2 and sodium ions in solution (24). The equilibrium diagram obtained thus offers a more realistic description of hydration than one based only on C-A-H since the influence of carbonation and alkali ions is no longer ignored. The situation is modelled by considering i) electrical neutrality of the solution, ii) constant ionic

Figure 1.3. Minimum Instability Curve, m, for Hydration of CA (20)

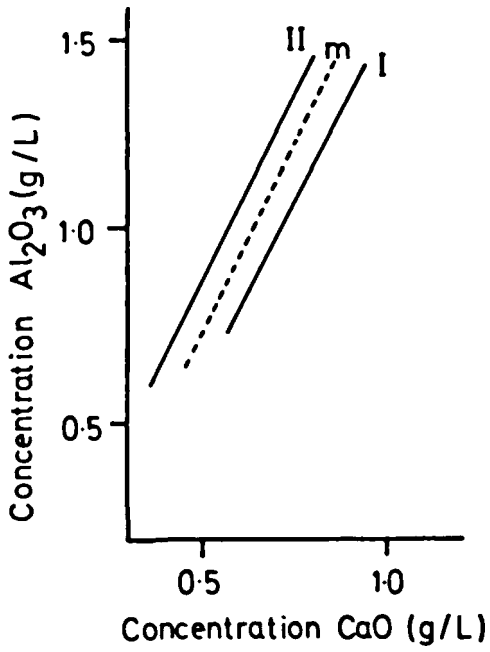

Figure 1.4. Concentrations of CaO and Al_2O_3 in Solution for $C_{12}A_7$ Paste at w/c 1·5 (13)

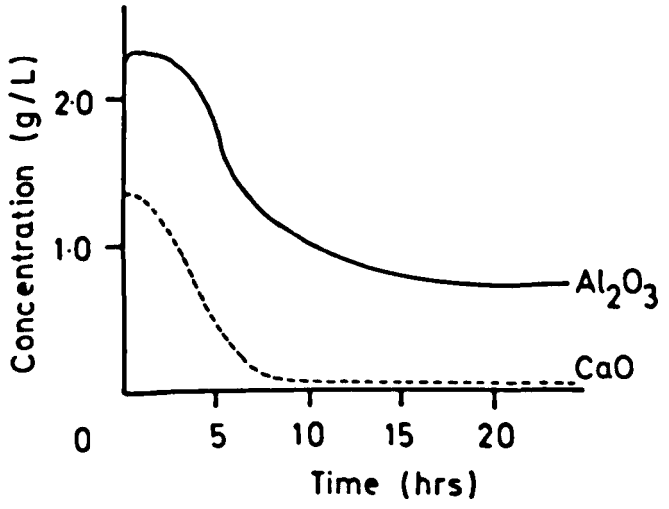

product of water, iii) equilibrium between CO_2 in solution and in the atmosphere and iv) equilibrium between solid phases and solution. The Debye & Huckel equation for activity coefficient γ is used as given below which is valid for dilute solutions.

$$\log_{10}\gamma = A.Z_i^2\sqrt{I}$$

where A = constant (0.509 for water at 25°C)

Z_i = ionic charge

I = ionic strength $(I = 0.5\sum(C_i.Z_i^2))$

C_i = concentration

This work shows the position of hydrate stability curves to be influenced by solution pH, and the concentrations of carbonate and alkali ions in solution.

Soustelle et al (25, 26) have also worked on the C-A-H system for hydrating CA in the presence of atmospheric CO_2 and carbonates in solution. They allow for the experimentally confirmed presence of C_2AH_8 and hydrated carboaluminate in addition to CAH_{10} by supposing that the solution is supersaturated with respect to CAH_{10} and assigning an artificially high solubility product to CAH_{10} for their analysis. Without this amendment they predicted that the only stable hydrate at 21°C should be CAH_{10}.

Barret et al criticised the approach of Soustelle et al and argued that they should have included C_3AH_6 and C_4AH_{13} as allowable stable phases in their analysis (27).

The complication caused by the presence of carbonates was further illustrated by Bachiorrini et al (28) who showed that, if the rate of

dissolution of CA is slow, CAH_{10} crystals originally precipitated near calcite particles may dissolve to allow for the crystallization of carboaluminate hydrate.

Fujii, Kondo and Ueno (21) have recently put forward an alternative to the through solution mechanism for the hydration of CA. They propose that during the induction period the surface of CA particles is superficially hydrated by intrusion although they were not able to confirm this by electron microscopy. The thickness of this layer increases until the build up of stress results in its destruction after which nuclei are generated and the hydration proceeds through a dissolution-crystallisation mechanism.

Investigations using X-ray analysis, electron microscopy and thermoanalytical techniques indicate that the hydration products of CA are as follows:

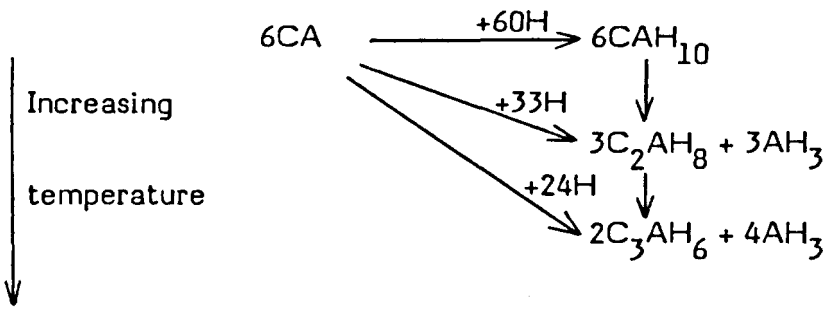

Whilst it is agreed that the hydration products formed are dependent on temperature as indicated above there is considerable disagreement over the transition temperatures. The situation is summarised in Table 1.1.

Table 1.1 Temperatures for formation of hydration products of CA (°C)

Reference	CAH_{10}	C_2AH_8	$CAH_{10} + C_2AH_8$	C_3AH_6
Mishima (29)			<30	>30
Tseung & Carruthers (30)	<21	21-35		>35
Cottin (31)	<20			>60
Murat et al (32)	<15		15-27	>27
Nikushchenko et al (33)	<22			
Schwiete et al (34)		>23		
Wells & Carlson (35)		>20		
Galtier (12)			17-27	
Halsey & Pratt (36)	<23	23-25		

There is also disagreement over the production of alumina gel at low temperatures although most of the literature indicates that it is not formed unless C_2AH_8 is also produced.

The initial presence of a small amount of CAH_{10} at 40°C has been shown by Halsey & Pratt (36).

Some researchers report that even at high temperature the formation of C_3AH_6 is always preceeded by formation of C_2AH_8 while others propose that hydration may lead to the direct formation of C_3AH_6. Mishima (37) found that the initial hydrate formed at 50°C was C_2AH_8 which converted almost immediately to C_3AH_6. Recent work by Gessner (18) and independently by Bushnell-Watson and Sharp (161) has indicated that there is a transition temperature of 55°C above which the direct formation of C_3AH_6 is possible.

Apart from the important effect of temperature, several workers have commented that formation of C_2AH_8 is also favoured by use of high w/c ratios (9, 35).

CAH_{10} is described as a mesh of fine needles composed of hexagonal crystals (38, 39, 40), pseudo-hexagonal (12) or as having rosette-shaped leaves (41) whilst according to others (4, 9, 42) the crystal form is ill defined though having the basis of a hexagonal cell (4, 9). Mehta and Lesnikoff (43) describe CAH_{10} crystals as being well bound agglomerates of hexagonal morphology with average size about 0.5μm.

These differences in observed structure are due possibly to differences in w/c. At low w/c for Portland cement a fine granular mass is formed whilst for high w/c ratios the crystal structure is more distinct. This may apply to aluminous cements (31, 40). The specific gravity of CAH_{10} is reported to be 1.74 (44) or 1.72 (9).

C_2AH_8 has a hexagonal plate-like structure (9, 12) and a specific gravity of 1.95 (9, 44).

C_3AH_6 is a cubic compound (9, 12, 43) with crystal size about 5 μm (43) and specific gravity 2.52 (9, 44).

Both the hydrates CAH_{10} and C_2AH_8 are metastable at ordinary temperatures and tend to convert to the cubic C_3AH_6. This conversion reaction is of great importance since converted pastes usually show a marked reduction in strength. The rate of reaction is dependent on many factors and the exact reasons for the loss of strength are not fully understood. Conversion of Ciment Fondu pastes will be discussed in detail in section 1.6 of this chapter.

Other hydrates which have been reported are C_4AH_{13} (12, 45) and C_4AH_{19} (45).

The alumina gel formed early in the hydration reaction tends to age slowly to crystalline AH_3 known as gibbsite (specific gravity 2.4 (46)). This reaction can take from a couple of months to 2 years (8, 9). Other forms of crystalline AH_3 are norstrandite and bayerite (8). It is suggested by Young (47) that the AH_3 formed by conversion of CAH_{10} differs in crystalline structure from that formed on conversion of C_2AH_8.

Costa, Massazza and Testolin (13) monitored the changes in structure from gel to crystalline by measuring the changes in refractive index. They found that the process was accelerated by contact with lime solutions.

Galtier (12) studied the effect of the fineness of pure CA. At higher temperatures, when C_2AH_8 is formed, increased fineness leads to an increased rate of reaction. At low temperature it was found that finer particles reacted more slowly. For a mixture of fine and coarse particles calorimetric studies showed that a unique peak is formed rather than each size forming its own individual peak. Since the retarding action of finer particles only occured below 27°C, it was concluded that the phenomenon relates in some way to the formation of CAH_{10}.

1.3.2.2 Other Aluminates

Generally aluminates with higher lime content exhibit greater reactivity with water, $C_{12}A_7$ being the most reactive (4, 12, 22, 48, 160) and CA_2 the least reactive (12, 49). In tests on calcium aluminate cements containing varying proportions of $C_{12}A_7$ and C_3A Menetrier-Sorrentino et al (50) obtained values of setting time as given below (test temperature unspecified) which support the above statement. They found that cements containing a higher ratio of C/A tended to form hydrates also with higher C/A.

C/A	Setting Time (mins)
1.18	1
0.91	90

Fournier however found that the C/A ratio of pure pastes did not have a great effect on reactivity as determined by calorimetry (51).

Costa et al (13) and Abdel Razig et al (5) reviewed work on hydration of $C_{12}A_7$. In their own calorimetric studies on pastes at 20°C with w/c 1.5 Costa et al found 2 peaks in heat evolution. Solution analysis was carried out and Figure 1.4 shows that there is no induction period for solutions of $C_{12}A_7$ with saturation levels for [C] and [A] reached very quickly. After about only 1 hour these concentrations begin to decrease and the ratio [C/A] diminishes rapidly. The maximum concentrations reached are close to those for CA given by Lea and Barret et al.

Barret and Bertrandie (20) agree that there is no induction period for solutions of $C_{12}A_7$.

Crystalline hydrates were identified by Costa et al using X-ray diffraction 1.5 hours after the contact of solid $C_{12}A_7$ with water; the first to appear was C_2AH_8 followed by CAH_{10} at 7 hours and C_3AH_6 at 3 days. The amount of C_2AH_8 was seen to diminish after about 3 days, this was interpreted as being due to conversion. XRD testing cannot show the very early gel-like reaction products though their presence was confirmed by optical microscopy. It is suggested that the dissolution of aluminates slows rapidly as i) the solution becomes supersaturated with respect to lime and alumina and ii) gel forms around the anhydrous particles. It was noted that formation of C_3AH_6 was favoured if the solution was rich in lime.

The order of appearance of hydration products is confirmed by Abdel Razig et al (5). They propose that CAH_{10} is not produced from $C_{12}A_7$ at 20°C until the reactions {1} and {2} below have liberated alumina and water thus permitting the formation of CAH_{10} according to equation {3}

$$C_{12}A_7 + 51H \longrightarrow 6C_2AH_8 + AH_3 \ldots\ldots\ldots \{1\}$$

$$3C_2AH_8 \longrightarrow 2C_3AH_6 + AH_3 + 9H \ldots\ldots\ldots\ldots\ldots \{2\}$$

$$C_{12}A_7 + 5AH_3 + 105H \longrightarrow 12CAH_{10} \ldots\ldots\ldots\ldots\ldots \{3\}$$

Bensted, who states that $C_{12}A_7$ typically comprises 2-20% of high alumina cement, confirmed that the main hydration products are C_2AH_8 and alumina gel which subsequently ages to crystalline gibbsite (8).

CA_2 hydrates to form the same products as CA though much more alumina gel, and later gibbsite, is formed due to the different stoichiometry (22).

1.3.2.3 Ferrites

The hydration of the iron phases has not received much attention. Tetracalcium aluminoferrite hydrate, $C_4(AF)H_x$ is formed by the hydration of ferrites with an A/F molecular ratio less than 1. Also formed is an amorphous form of Fe_2O_3 or its hydrate (52). Since ferrites in Ciment Fondu normally have an A/F ratio less than 1, the product $C_4(AF)H_x$ would be expected rather than $C_2(AF)H_x$ formed from ferrites with higher A/F ratios. In fact $C_4(AF)H_x$ has been detected in cement suspensions at w/c 10 but not in cement paste.

It is thought that Fe_2O_3 can replace Al_2O_3 in the compound C_3AH_6 to form a series of solid solutions, with the presence of silica or aluminium necessary for stability.

1.3.2.4 Remaining Phases

Both pleochroite and beta C_2S (a constituent of ordinary Portland cement) are reactive and produce strength. At ordinary temperatures pure gehlenite is unreactive but the slightly impure form thought to exist in Ciment Fondu is known to be reactive (9).

1.3.3 Hydration of Ciment Fondu

Observations of the hydration process show that gelatinous products begin to form around the cement grains after 1 or 2 hours. The amount of gel increases rapidly and crystals soon begin to form (9).

Figure 1.5 shows the hydrates formed at both low and high temperature from Ciment Fondu according to Cottin (38).

Bertrandie and Barret et al (19, 23) found that the W curve for Ciment Fondu showed no latent period. This is in agreement with the results obtained by Lea (9) on shaking 50g of HAC with 1 litre of water.

The F curve obtained by Bertrandie did not show a true latent period but a slow, regular decrease in concentration for about 10 hours prior to bulk precipitation. The possibility was thus that the presence of solid Ciment Fondu particles did induce nucleation and precipitation of hydration products. This was however disproved when addition of cement to a saturated solution of filtrate obtained by prior hydration of cement was found to exhibit a latent period.

An additional series of experiments was carried out in which cement was prehydrated with either water or a non-saturated filtrate before addition to saturated filtrate. Even at very short prehydration times, the time to bulk precipitation of hydrates was considerably reduced due perhaps to the prior formation of nuclei of hydrated phases.

Figure1.5. Hydration Products of Ciment Fondu (38)

a) 12 °C

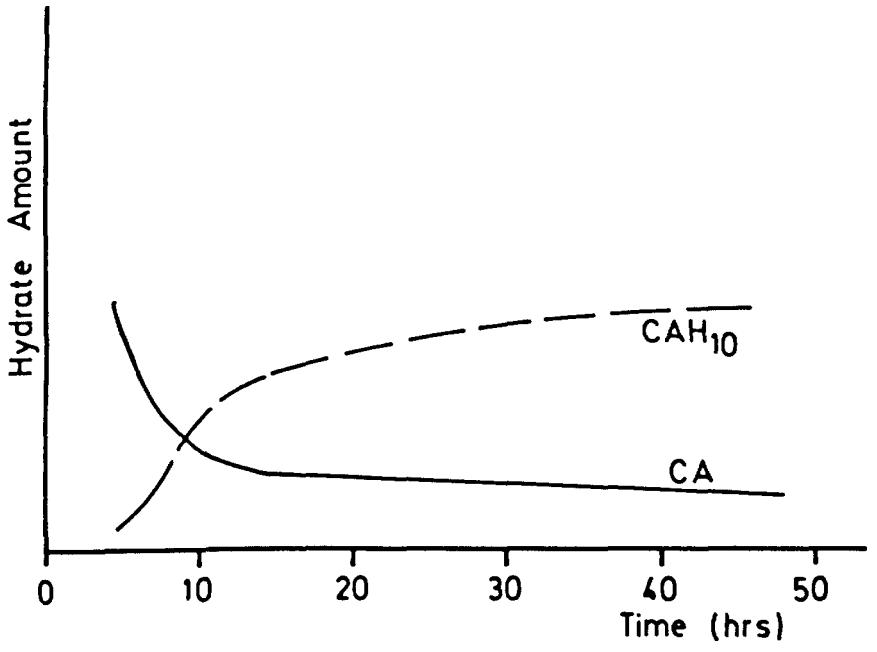

b) 50 C

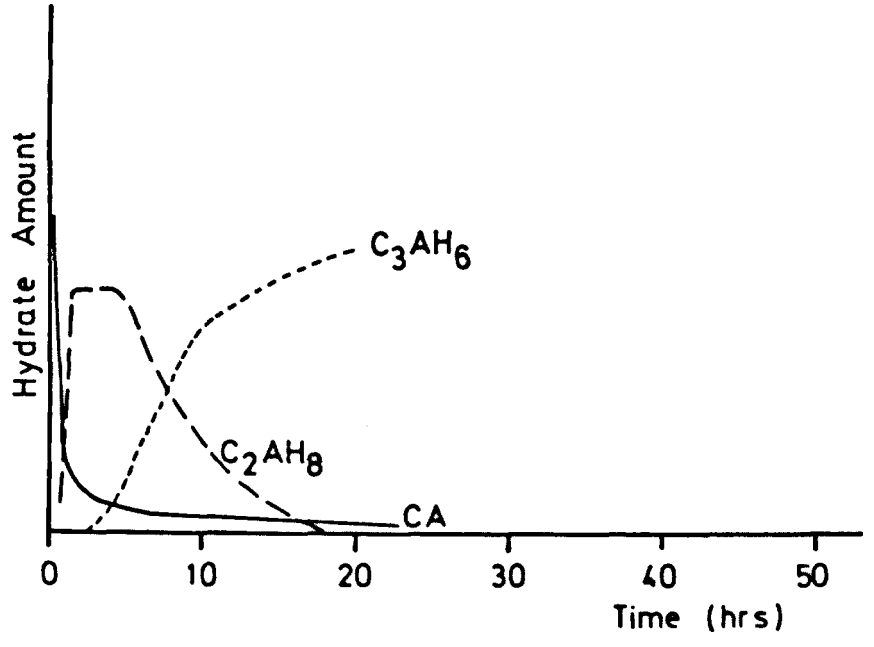

It was concluded that the length of any latent period is closely linked with the ionic concentration of the solution into which the cement is introduced. This concentration determines the amounts of lime and alumina that the cement should supply for it to become saturated. The more supplied, the more rapid was the final precipitation.

Although this work provides additional observations on the hydration of Ciment Fondu, no explanation has been put forward which can take these fully into account. It is likely that the presence of $C_{12}A_7$ and C_2S has an accelerating effect on the predominant constituent CA, the effect of $C_{12}A_7$ being the most marked, thus the hydration of Ciment Fondu shows a very much shorter induction period than for CA (19, 20, 53).

In tests on HAC mortars Van Aardt and Visser noted the presence of C_4A-hydrates and C_2ASH_8 at 5°C (54). The presence of the latter hydrate after prolonged hydration is also reported by Midgley and Bhaskara Rao, the mode of formation being unclear (55).

1.3.4 Hydration Kinetics

In a series of papers on crystal growth Avrami (56) proposes mechanisms for nucleation and crystallisation which have been applied to the hydration of cements. According to Le Sueur & Double (57) the "Avrami equation" is usually given as

$$X = 1 - e^{(-K.t^n)}$$

where X = fraction transformed

K = rate parameter

t = time

n = power exponent

The authors describe the application of the Avrami equation to phase transformations and use it to describe the early stages of hydration of C_3S as measured using a calox calorimeter. This subject will be described in more detail in section 1.5.2.1. Urzhenko and Usherov-Marshak (58) also used a form of the Avrami equation in studies of C_3S hydration and noted that while n was insensitive to temperature, K varied with both temperature and with the presence of admixtures.

Sakovitch (59) indicates that K can be related to the chemical rate constant k by

$$K = \left(\frac{k}{n}\right)^n$$

Where temperature variation of k follows the classical Arrhenius relationship

$$k = A.e^{(-E_a/R.T)}$$

and E_a = activation energy

R = gas constant

T = temp (K)

A = constant

This implies that a value of apparent activation energy can be obtained from a plot of ln(K) vs (1/T) which should give a straight line of slope $(n.E_a/R)$.

1.4 RHEOLOGY

1.4.1 Introduction

A considerable amount of research has been carried out on the rheology of cement pastes although very little information is available on aluminous cement pastes (60). It is reasonable to suppose that there are similarities between the rheology of aluminous and Portland cement pastes. The salient features of the latter are now described.

In a comprehensive study of the rheology of cement pastes Tattersall & Banfill (61) present the generally accepted view that the behaviour of cement pastes at low shear rates or when structural breakdown is complete is represented by the Bingham model whose equation is given below.

$$\tau = \tau_0 + \mu \dot{\gamma}$$

The relationship between shear stress τ and shear rate $\dot{\gamma}$ is thus a straight line that has an intercept on the stress axis τ_0, the yield stress and a slope of $1/\mu$ where μ is the plastic viscosity.

Fresh cement pastes undergo structural breakdown when subjected to shear which is seen as a reduction in the torque on a rotating impeller according to an exponential relationship :

$$T - Te = k.e^{(-Bt)}$$

where Te is the equilibrium value of torque reached when paste is fully dispersed or when rates of build up and reforming are equal, T is the torque at time t and B,K are constants. Subsequently the paste apparent viscosity increases as setting starts and structure builds up resulting in increasing torque (62, 63).

1.4.2 Measurement of Rheological Parameters

Studies of cement paste rheology at early ages are made either by determining flow curves at changing shear rates or by studying the time dependent behaviour at a constant shear rate (64).

Most workers use a coaxial cylinders viscometer to obtain a graph of torque against speed of rotation from which yield stress (τ_o) and plastic viscosity (μ) may be calculated according to the equations given below.

$$\tau_o = \frac{T[(1/R_b^2) - (1/R_c^2)]}{4\pi h.\ln(R_b/R_c)} \qquad \mu = \frac{1}{4\pi h}\left(\frac{1}{R_b^2} - \frac{1}{R_c^2}\right)\frac{1}{S}$$

T,S are the intercept and slope respectively as shown on Figure 1.6.

R_b is the radius of the inner cylinder.

R_c is the radius of the outer cylinder.

h is the height of the inner cylinder.

The results obtained by different workers vary considerably both qualitatively and quantitatively. This is thought to be due largely to differences in experimental technique. Several potential sources of error have been identified which will now be discussed.

FLOW CURVES. The changes in shear stress are monitored as the speed of rotation increases progressively to an arbitrary maximum followed by a decrease to zero. Banfill & Saunders found that the resulting hysteresis loop can take one of 3 forms as shown in Figure 1.7 (65).

Types 1 and 3 are obtained for short and long cycle times respectively whilst type 2 is obtained for intermediate cycle times. The chemical composition of the cement tested was found to alter the time dependence.

MIXING. The use of mixing procedures ranging from gentle hand mixing to use of a colloid mill causes considerable differences in measured values of yield stress and plastic viscosity (66-69).

Figure1.6. Definition of Intercept and Slope used to Calculate Yield Value and Plastic Viscosity

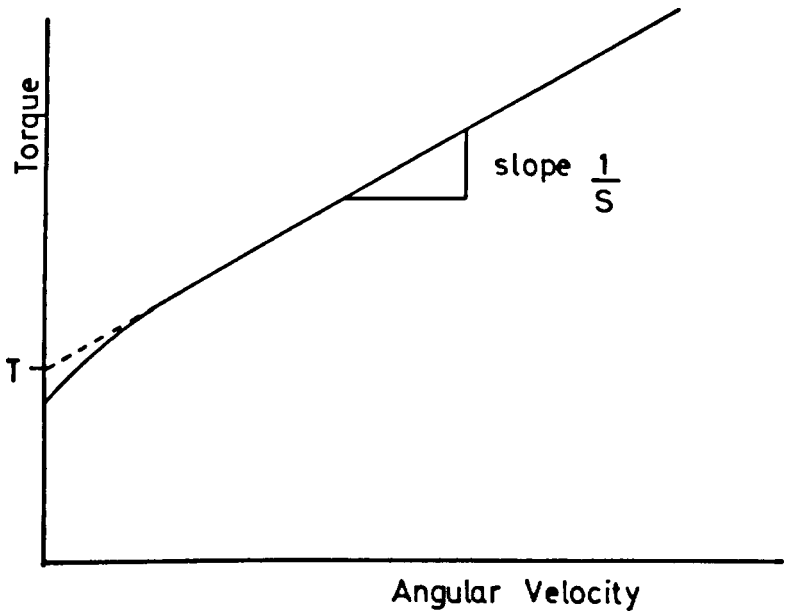

Figure1.7. Effect of Cycle Time on Flow Curve Type (65)

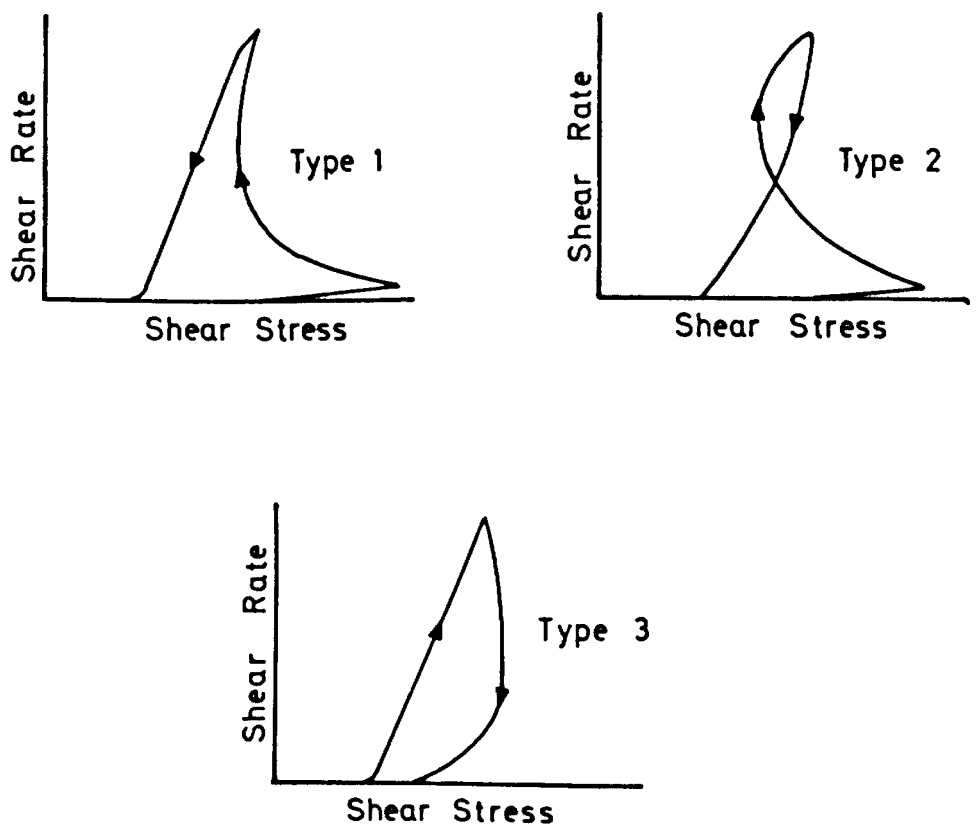

Tattersall and Banfill suggest that a standard test procedure should be adopted so that results obtained by different workers can be compared. To completely characterise a paste, hand mixing at as low a shear rate as possible should be used whilst ensuring that a homogeneous paste is achieved. Measurement of structural breakdown should be carried out at some chosen speed and the down curve from that speed should be obtained. If information only on the broken down paste is required then complete breakdown should be ensured by use of a high shear rate during mixing which is not subsequently exceeded in the test (61).

Orban, Parcevaux and Guilhot (70) have introduced the concept of specific mixing energy which may be used to reconcile differences in laboratory mixing techniques and to match laboratory and field procedures.

They obtain an expression for work done by a mixer (E) as follows:

$$E = k.\ w^2.t.\rho$$

where k = constant

ρ = density of paste or mortar

w = angular velocity of mixer

t = time of mixing

The amount of mechanical work done on a mass M of paste with volume V during mixing is then defined as follows and may be estimated for any type of mixer.

$$E/M = \frac{k\rho w^2 t}{V}$$

A specific mixing energy (SME) of 1.0 is defined as being equivalent to a work input of 5.5 kJ/kg which is the input by the standard API procedure.

It is shown that as the SME increases from 0 to 1 both yield value and plastic viscosity for Portland cement pastes decrease considerably. An SME of 1.0 corresponds to several minutes mixing under a high rate of shear.

CEMENT FINENESS Vom Berg (71) found that yield value and plastic viscosity were both power law functions of specific surface, S_v and quotes relationships of the form

$$\tau_o = k_1 S_v^{3.83} \qquad \mu = k_2 S_v^{2.47}$$

where k_1 and k_2 depend on w/c. The higher power dependence of the yield value indicates that it depends more strongly on attractive forces between surfaces than does the plastic viscosity.

PLUG FLOW. When using a coaxial cylinders viscometer it is possible to have a plug of unsheared material near the wall of the stationary cylinder. Tattersall and Dimond (72, 73) noted that when smooth cylinders were used the solid plug slid round at a velocity less than that of the inner cylinder until it broke up and shearing flow occured across the entire gap. With serrated cylinders, the plug remained stationary and intact until the end of the experiment. These observations could not be explained by normal plug flow theory in terms of the yield value. In a series of tests Banfill (66) showed that the existence of the plug could not be explained by centrifugal separation leading to a more concentrated zone at the outer cylinder wall. When the width of the sheared zone was used as the effective gap width in place of the instrument gap width in calculations of other parameters the data became more rational. This implied that the viscometer behaved as one with an outer cylinder coated in cement paste.

SLIPPAGE. Slippage at the walls of the apparatus due to separation of water is considered likely and many workers have used roughened or profiled cylinders in an effort to overcome this problem (65, 66, 67, 74, 75, 76). With the exception of Tattersall & Dimond's work described above, it has not yet however been convincingly shown either that slippage does occur with smooth cylinders or that it does not occur with roughened cylinders.

Mannheimer (77) has carried out a theoretical study of slippage and concluded that, if slippage occurs during tests using coaxial cylinders, results of yield value and plastic viscosity could be underestimated by a factor of 6. He also showed however that the velocity of the slip layer is negligible at shear rates greater than 50 s^{-1}.

SEDIMENTATION. Sedimentation is a problem which is more apparent for pastes with high water content and can cause considerable errors in rheological measurements. Bhatty and Banfill studied the use of an interrupted helical impeller and concluded that sedimentation was prevented at w/c ratios up to 1.0 for Portland cements (78).

1.4.3 Comparison Between Aluminous and Portland Cements

For a given w/c and cement content Ciment Fondu mixes are more workable than OPC mixes (4,60). As an example, for equivalent flow time through an orifice type workability testing device, HAC paste had a w/c=0.37 whilst a RHPC paste with plasticiser had w/c=0.49 (79). The greater fineness of Portland cement compared to Ciment Fondu is accepted to account for much of this difference.

Tests on cement pastes at 20°C using a coaxial cylinders viscometer gave the results shown in Table 1.2 which also shows the effect of using freshwater and artificial seawater for mixing (60).

The use of seawater in place of freshwater for mixing increases both yield value and plastic viscosity. No explanation is offered for these observations by the authors; it is however possible that the higher ionic strength of seawater hinders deflocculation.

Table 1.2 Comparison between OPC and HAC pastes

	τ_0 (Pa)			μ (Pa.s)		
w/c	OPC (fresh)	HAC (fresh)	HAC (sea)	OPC (fresh)	HAC (fresh)	HAC (sea)
0.30	125.5	26.0	22.8	0.445	0.445	0.593
0.35	73.0	8.0	17.1	0.148	0.163	0.326
0.40	28.5	5.7	9.1	0.089	0.059	0.148
0.45	16.0	3.4	-	0.059	0.037	-

1.5 SETTING

1.5.1 Introduction

It is important to clarify the distinction between setting and hardening. There is a generally held belief that Ciment Fondu is fast setting which is untrue since setting times are often longer than for Portland cements. The misconception is founded on the observation that the time between onset of setting and attainment of final set is extremely short, giving less warning of workability loss.

The rate of heat evolution from hydrating Ciment Fondu is far greater than for Portland cements although the total amount of heat liberated is approximately the same, 100-120 cal/g (1).

The British Standard specification for high alumina cement requires an initial set at 2-6 hours with the final set not more than 2 hours later. The

initial and final setting times are determined by the Vicat method for a fixed w/c of 0.22 at 14-18 °C (80).

1.5.2 Results Obtained from Different Monitoring Methods

1.5.2.1 Calorimetry

A disadvantage of adiabatic as opposed to isothermal calorimetry is that the observed behaviour may be due in part to the temperature increase in the system (12). Most researchers use isothermal methods from which quantitative details of heat evolution rate can be obtained. It is dangerous to make direct comparisons between results obtained from different workers since variations in experimental procedure can affect the findings. This aspect will be considered further at a later stage.

A small initial peak is observed when water first comes into contact with cement. This is followed by a dormant period whose length is determined by temperature, water content and cement composition. After this dormant period the rate of heat evolution increases rapidly until a clearly defined peak is seen. Typically 70-90% of the heat evolved is liberated during the first 24 hours (4). It is generally agreed that the initial peak is due mainly to wetting of solids and chemical dissolution though Magnan (81) states that these factors alone are insufficient to fully account for the peak and that partial hydration is taking place. Menetrier-Sorrentino et al (50) found that the height of this initial peak increased with increasing C/A ratio of aluminous cements, providing further confirmation of the more rapid dissolution of lime into solution.

Figure 1.8 shows the good degree of fit of the Avrami equation to calorimetric data obtained by iterative techniques. The initial peak in heat evolution and the induction period cannot be fitted thus a false origin is established at the end of the induction period as shown (57).

Figure 1.8. Good Degree of Fit of Avrami Equation to Calorimetric Data (57)

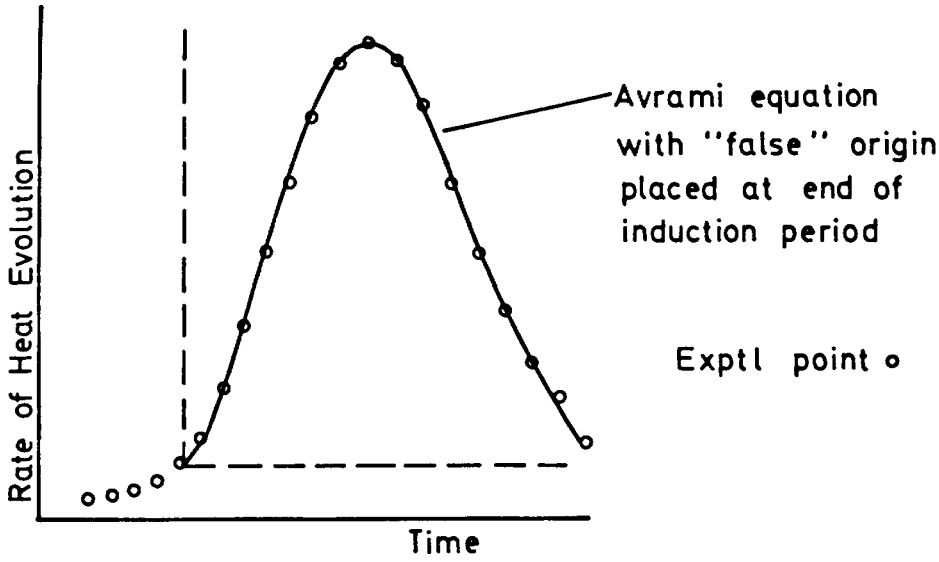

Figure 1.9 Effect of Hydration Temperature on Setting Time

Time after gauging to onset of heat evolution for HAC concrete ——— (1)
– – – (4)
Penetration test results for paste (technique not specified) ------- (4)

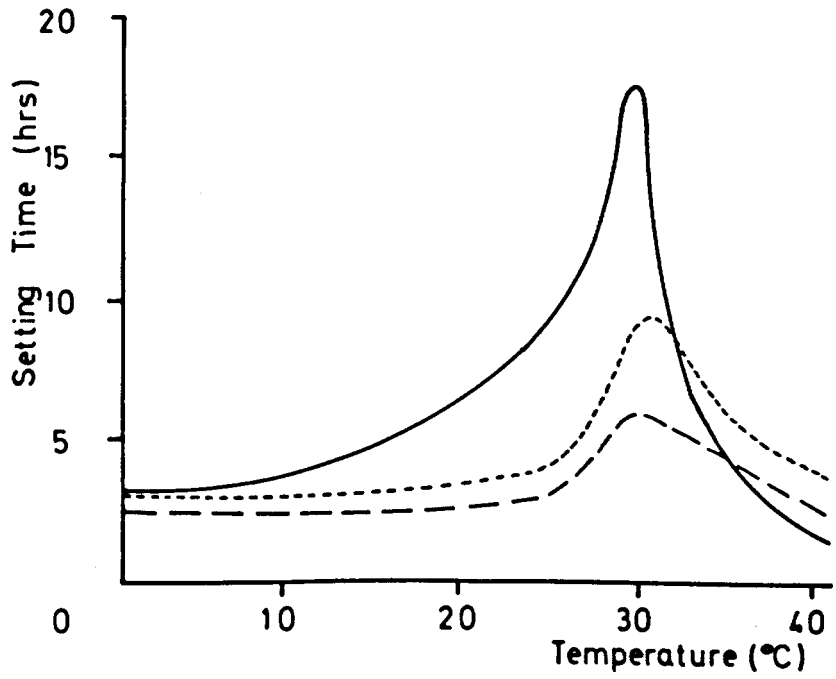

There have been a limited number of reports of multiple peaks in heat evolution. Two distinct peaks for plain HAC pastes were reported, which using DTA testing on samples removed and quenched after the occurrence of each peak, were found to be due to the formation of firstly C-A-H gel and then CAH_{10} (82). Murat, Negro & Bachiorrini showed that some CA pastes modified by the addition of $CaCO_3$ also gave 2 peaks in heat evolution. The first and second peaks being due to the formation of carboaluminate and CA-hydrates respectively (83).

Magnan (81) used microcalorimetry with 0.5g samples of gypsum plaster, Portland cement and aluminous cement. The small sample size implies that the method was isothermal though this was not stated clearly. Empirical expressions were fitted separately to the increasing and decreasing curves forming the main peak. No quantitative information was obtained on heat evolved.

Murat et al also used isothermal calorimetry on pure CA with a sample size of 0.5g and studied the effect of temperature on the length of dormant period and on the time at which the main peak occurred. Their results will be discussed in section 1.5.3 (32).

Galtier & Guilhot (48) comment that the particle size distribution of HAC affects the results obtained although in their work with Murat, grading of pure CA appeared to cause little variation (32). They also note the importance of accurately maintaining the test temperature since a change of only 0.5°C can alter the time to main peak by up to 2 hours. Other workers reported that use of a higher w/c shifted the main peak in heat evolution to an earlier time (82).

Fournier et al used isothermal calorimetry on pure CA pastes at 25°C with w/s 1.0 but did not attempt to fit curves or quantitatively analyse the results obtained (51).

Wilding et al successfully used the Calox isothermal method developed at Oxford University to study the effect of accelerating and retarding admixtures on HAC (84). Treffner & Williams agree that heat evolution is a very sensitive means to check the retarding action of admixtures on aluminous cements (15).

The use of thermocouples to monitor setting is said by George to be successful since bulk precipitation of hydrates corresponds well with the time at which measurable mechanical resistance begins to develop in the paste (4). According to other researchers setting time relates to the maximum rate of formation of C-A-H gel (82). The thermocouple method has the advantage over the Vicat technique that it can be used for mortar or concrete and George further states that it can distinguish between true setting and false setting caused by early stiffening. Robson agrees that the time interval between gauging HAC and the onset of heat evolution has given reasonable agreement with the Vicat initial set (1).

1.5.2.2 Ultrasonic Pulse Velocity

The ultrasonic pulse velocity (upv) for air at 20°C is 0.33 km/s whilst for water it is 1.50 km/s. Very early measurements of upv of cement paste are hampered by the problem of attenuation. Solids and water in the paste move with varying acceleration due to their different densities. The relative motion caused in this way absorbs energy and attenuates the transmitted waves. As the paste structure builds up, drag on individual solid particles is increased so reducing relative motion and attenuation. Sensible values of upv cannot therefore be obtained until sufficient structure has formed, dependent on temperature, paste composition and sample thickness. In tests on calcium aluminates Munir & Taylor found that the first reading could be obtained at 3-5 hours for paste samples 51mm in thickness (85).

Domone & Casson obtained readings after only 15 minutes with 30mm thick samples (86). The presence of air in the paste is known to have a dramatic effect on upv thus good compaction and/or evacuation of samples is important (87, 88).

Casson et al used the technique on OPC cement samples of about 30mm width cast in pastic bags. They showed that the maximum rate of change of upv occurs before setting and development of mechanical properties. This maximum is also before the maximum rate of heat evolution as determined by a Cement and Concrete Association calorimeter. They suggested that the maximum rate of change of upv occurs at the end of an induction period when bridges form between cement grains and the onset of penetration resistance occurs (87).

Munir & Taylor used a thermocouple to monitor paste temperature during upv testing (89). They found that if the transducers were kept on continuously heat was produced which affected the hydration reactions. In a separate programme of testing on calcium aluminates they found good correlation between upv and sample strength. The peak in paste temperature preceded the peak in wave amplitude by about 1 hour. Observations of changes in amplitude and velocity of the ultrasonic waves were found not to correspond with changes in XRD phase analysis. This may be explained by the fact that the initial hydration products are amorphous and thus are not detected by XRD.

Wilding & Double (88) have recently fitted a Calox calorimeter with ultrasonic transducers to allow simultaneous monitoring of upv and heat evolution. The apparatus was successfully used to study the effect of accelerators and retarders on Portland Cement and on Secar 71, an aluminous cement containing about 70% alumina. Testing was carried out at 27°C. The onset of heat evolution according to the calorimeter corresponded to the start of a very sharp increase in upv and was taken to

indicate the onset of setting. Two mixing procedures were tested :

i) By suction under vacuum

ii) By hand

The section method was shown to be more effective with a higher upv obtained until 200 minutes after the start of testing.

1.5.2.3 Other Methods

McCarter & Afshar (16, 17) monitored the setting of Ciment Fondu pastes at 20°C with w/c 0.27 by recording electrical resistivity, dielectric constant and paste internal temperature. They noted a dormant period until 200 minutes followed by a sudden rise in dielectric constant which they attributed to a rupturing of a weak coating around cement particles. This rupturing allowed further hydration and a release of charges which was said to originate from the grain surfaces rather than the bulk aqueous phase since there was no accompanying drop in resistivity. A peak in dielectric constant at 260 minutes coincided with a rise in resistance and in paste temperature, indicative of hydrate formation from solution.

1.5.3 Effect of Temperature

The effect of temperature on hydrate formation has already been described in section 1.3. In most chemical reactions the effect of an increase in temperature is to increase the rate of reaction, with a 10°C rise commonly doubling reaction rate. For Ciment Fondu many workers have reported the rate of hydration slowing considerably above approximately 20°C until 30°C when the rate accelerates. The phenomenon was first described by Periani in 1925 who found that the setting time of HAC increased from 170 minutes at 20°C to 300 minutes at 30°C (90).

Many researchers have since confirmed that the maximum delay in setting of HAC occurs at approximately 30°C (1, 4, 53, 91, 92). George (4) reported setting times for Ciment Fondu pastes and concretes over the range 0-40°C as shown in Figure 1.9 together with Robson's data for HAC paste over the same temperature range (1). Robson noted that the total amount of heat evolved during hydration remained sensibly constant over the temperature range 15. 5-37°C.

Murat et al (32) used conduction calorimetry on pastes of pure CA and observed very similar behaviour as shown in Figure 1.10.

Bushnell-Watson & Sharp (93) undertook a programme of testing to study the effect of hydration temperature on the commercially available refractory aluminous cements listed below and observed a maximum in setting time at 26-30°C for all except Secar 80 :

Cement	% alumina
Secar 51	50
Secar 71	71
Alcoa CA-14	72
Alcoa CA-25	79
Secar 80	81

Several hypotheses have been proposed to provide a satisfactory explanation of this behaviour.

i) the difference in rate of precipitation of CAH_{10} and C_2AH_8 at different temperatures

ii) a reduction in the accelerating tendency of $C_{12}A_7$ near 30°C

iii) the "poisoning" of the surface of CA grains by C_2S due to the low solubility of SiO_2 compared to CaO at higher temperatures (53).

Figure 1.10. Effect of Hydration Temperature on Time to Main Peak in Heat Evolution (T_{peak}) and Time to Onset of Heat Evolution (T_{off}) for CA (32)

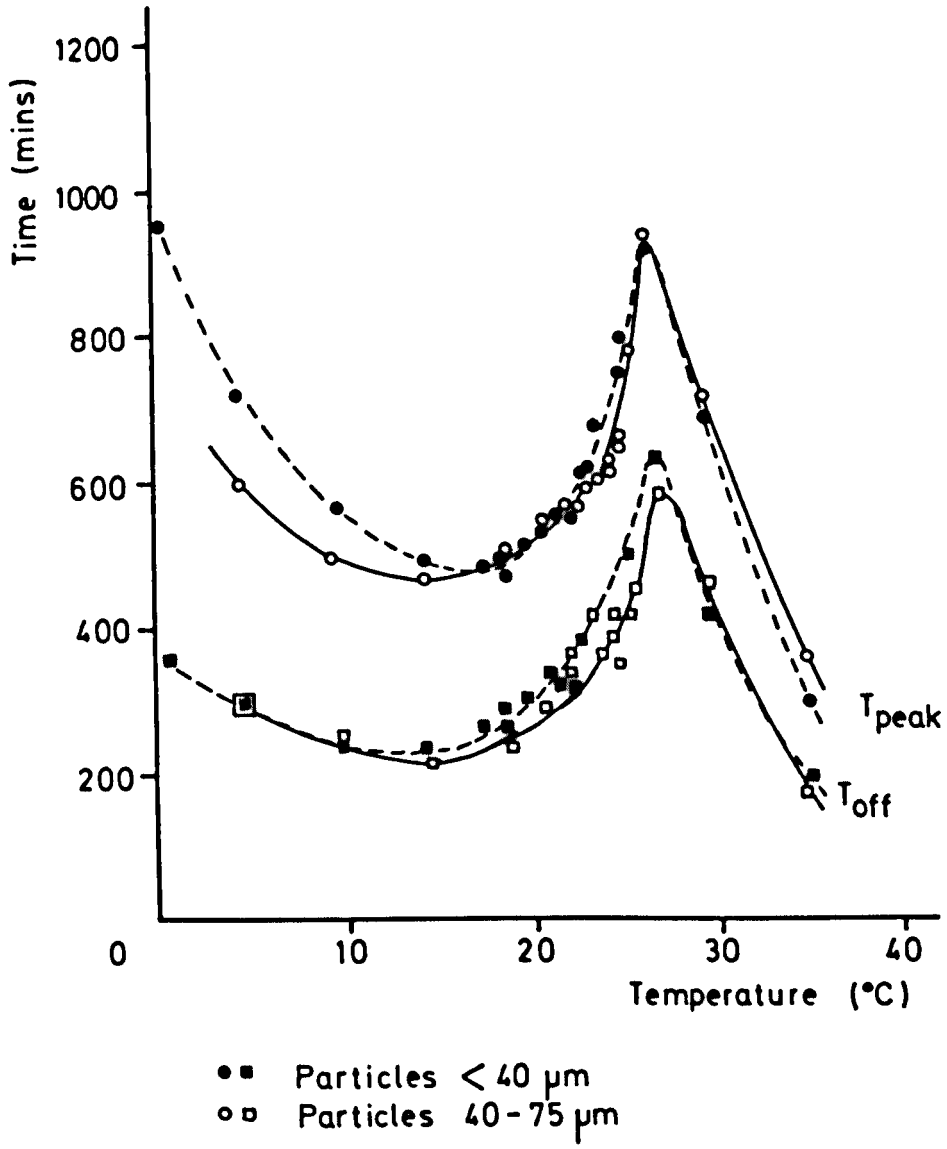

George and Cottin (92) carried out a series of experiments on both Ciment Fondu and on specially prepared aluminates to test various theories. Their findings were inconclusive and indeed they noted that "These test results increased our perplexity".

Bushnell-Watson & Sharp (93) confirmed that C_2S is not responsible since Secar 71 contains only a very small amount of this phase yet still shows a maximum in setting time at 26-30°C.

They propose that the retardation is due to the increasing difficulty in nucleation of C_2AH_8 at temperatures approaching 30°C. Evidence for this proposal is :

i) that increasing the temperature from 20-30°C delays setting but increases both the rate of consumption of CA and the rate of heat evolution when setting commences.

ii) the setting delay is only an initial effect, after 16 hours the rate of hydration increases with increasing temperature as expected.

iii) other authors have proposed similar theories.

The anomalous behaviour of Secar 80 may be due to the presence of a greater amount of alumina (as indicated by XRD) which in some way encourages formation of C_2AH_8 or to the presence of an admixture in the cement. There is no published information giving details of such admixtures but their use is inferred from discussions with personnel from cement manufacturing companies.

Ramachandran & Feldman (94), in a study of pure CA, found that hydration at 80°C gave much higher strengths than at 20°C on the basis of microhardness testing. Kula et al (95) also found that Ciment Fondu paste at w/c 0.30 gave higher flexural strength at 60°C with C_3AH_6 and AH_3 as

the hydration products than at 21°C when CAH_{10} was formed. In contrast French et al (91) found that the strength of HAC concrete cured at 20°C was greater than that cured at 80°C and Mishima (29) reported that mortar cured below 30°C had higher strength than that cured above 30°C. He suggests that mortar containing CAH_{10} is stronger than that containing C_2AH_8 which is in turn stronger than that with C_3AH_6. George (96) reports tests on HAC concrete prisms stored for up to 10 years which show that the strength of mixes cured at high temperature (> 50°C) is consistently lower than those stored at room temperature.

Beaudoin showed that pastes containing both hexagonal and cubic phases had greater fracture toughness than those containing only hexagonal phases. It was suggested that the denser C_3AH_6 crystals act as crack arresters (97).

Cottin & Reif (98) found that for pastes at the same w/c, those containing CAH_{10} have lower penetration resistance (using microhardness measurements) than those containing C_3AH_6/gibbsite. Since the w/c required for complete hydration of CA to C_3AH_6/gibbsite is only 0.455 compared with 1.140 for hydration to CAH_{10} (according to the equations given below) this may provide an explanation for the observation on penetration resistance.

At high temperature $\quad 3CA + 12H \longrightarrow C_3AH_6 + 2AH_3$

At low temperature $\quad CA + 10H \longrightarrow CAH_{10}$

Lea comments that in cements containing pleochroite the CA content is reduced and thus strength is reduced (9). Midgley agrees that it is the production of calcium aluminate hydrates which leads to the rapid strength gain of Ciment Fondu (99).

1.6 STRENGTH DEVELOPMENT AND CONVERSION

1.6.1 Introduction

Since the conversion of aluminous cements has such a profound impact on strength development it was considered inappropriate to discuss the strength characteristics before describing the reaction in some detail. Possible explanations for the strength loss are reviewed in section 1.6.5.

The equations governing the conversion reactions are given below :

$$3CAH_{10} \longrightarrow C_3AH_6 + 2AH_3 + 18H \qquad \text{(i)}$$

$$3C_2AH_8 \longrightarrow 2C_3AH_6 + AH_3 + 9H \qquad \text{(ii)}$$

Although water is a product of the conversion reactions, conversion can only take place in the presence of water since dissolving and precipitation are involved. According to Neville (100) the relative humidity of the interior of solid cement paste of thickness greater than 25mm is 100% regardless of external environment thus conversion can occur in apparently dry concrete.

Since C_3AH_6 and gibbsite are formed following high temperature hydration, their presence in hardened paste is not necessarily indicative of conversion (101).

Neville (102) describes in great detail a number of failures of HAC structures in Europe and elsewhere. In the U.K. the major failures occurred in 1973 at

i) Camden School for Girls (roof of assembly hall)

ii) University of Leicester (roof of Bennet Building)

and in 1974 at Sir John Cass's Foundation and Red Coat Church of England School in Stepney (roof of swimming pool hall).

Investigations of these and other incidents showed that while conversion was not the only cause of failure, it was an important contributor (103, 104). As a result in 1975 HAC was deemed not to satisfy the U.K. Building Regulations, bringing this country into line with most others worldwide.

1.6.2 Determination of Degree of Conversion

Since it is agreed that the strength of HAC concrete is adversely affected by the conversion reaction, it seems reasonable to suggest that if the degree of conversion is accurately determined then an estimate may be made of the loss in strength of a concrete member.

The degree of conversion D_c can be estimated from the percentage of C_3AH_6 present as a proportion of the sum of C_3AH_6 and CAH_{10}.

$$D_c \ (\%) = \frac{\text{Weight of } C_3AH_6 \times 100}{(\text{Weight of } C_3AH_6 + CAH_{10})}$$

The relative weights of the phases present can be determined by thermal techniques as described in section 1.3.1. There are however several potential problems which should be highlighted.

Although it is the areas under peaks which relate to mass/energy changes difficulties in measurement have lead to the use of peak heights as a relative measure of the amounts of various phases present (105). El-Jazairi found that the shape and area under the DTG curve for the CAH_{10} peak is dependent on the humidity of the storage conditions for the sample. A larger peak resulted from more humid conditions (106).

Whilst the position of DTA and DTG peaks is similar and the same order of peaks is followed, they do not occur at exactly the same temperature. The DTA peak position does not correspond to a specific stage in the reaction but occurs when the heat supplied is equal to the heat absorbed by the specimen. The maximum rate of reaction is reached before the peak whereas for DTG testing the peak corresponds to the maximum rate of reaction. Results from DTA testing by Bensted (7) and by the Building Research Establishment (BRE) (107) are given below.

Phase	Peak Temperature (°C)	
	Bensted	BRE
CAH_{10}	115	110-120
C_2AH_8	150	140-190
C_2ASH_8	230 (shoulder)	250
AH_3	285	270-290
C_3AH_6	320	300-310

Complications arise in the detection of aluminium hydroxide, present in crystalline or gel form, since Frenkel et al (108) report that the dehydration of most types of aluminium hydroxide is a 2 step mechanism with dehydration temperatures as shown below.

	Dehydration Temperature (°C)	
	I	II
Pseudoboehmite	140	460
	180	435
Boehmite	-	360
Bayerite	130	300

A further problem reported by Halsey & Pratt (36) is that the alumina gel formed at 40°C has a lower dehydration temperature (90°C) than the alumina gel formed at 8 or 23°C (130°C).

Oger suggested that differences for peak temperatures allotted to a given phase in separate tests can be $\pm$ 15°C (109).

Differences in experimental technique can lead to discrepancies between reported work. An increase in heating rate results in an increase in DTG peak temperature as reported by Barnes and Baxter (110) and Oger (109).

Heating rate (°C/min)	Peak temperature (°C) CAH_{10}	AH_3	
20	95	266	Barnes and Baxter
50	116	302	Barnes and Baxter
100	163	308	Barnes and Baxter
10	95		Oger
40	123		Oger

Wilburn et al recommend a heating rate of 10-30 °C/min (105).

Bushnell-Watson and Sharp highlighted the problem caused by the presence of the carboaluminate phase which can give a DTA peak in the same region as C_2AH_8 (given as 180-200°C). To avoid errors in interpretation they recommend the use of supplementary XRD testing (111).

Unless testing is carried out in a CO_2-free atmosphere the carbonation of C_3AH_6 can cause an apparent reduction in measured D_c. The alternative formula given below is often used since, fortunately, the quantities of C_3AH_6 and AH_3 produced during conversion are similar; 1.0g of CAH_{10} tranforming to 1.12g C_3AH_6 and 0.92g AH_3 (4).

$$D_c\ (\%) = \frac{\text{Weight of } AH_3 \times 100}{(\text{Weight of } AH_3 + CAH_{10})}$$

Errors can occur when using this equation since AH_3 is formed during the production of C_2AH_8 from CA as well as during conversion (4, 8). George suggests that AH_3 is also formed from the hydration reaction of ferrites thus test results may suggest the onset of conversion without any decomposition of either CAH_{10} or C_2AH_8 (4).

Further difficulty may arise in accurate determination of degree of conversion if the HAC has been subject to sulphate attack since the ettringite formed produces a peak during DTA/DTG testing near to that of CAH_{10} (8). There have been suggestions that heat generated during the removal of a sample by rotary drilling may cause conversion (8). Neville reports tests carried out by the BRE, Local Authorities & Test Houses which showed that provided the drill was sharp and good practice employed there was a negligible increase in measured D_c (102).

In an information paper published in 1981 the BRE drew attention to the possibility that AH_3 may even be produced when heating CAH_{10} during thermal analysis (107). Ruiz de Gauna et al agreed but state that this is likely to occur only if the samples are not sufficiently dry (112). Barnes & Baxter (110) make the point that heating rate and sample size can affect D_c determined in thermal analysis.

Midgley (46) investigated the accuracy of various thermoanalytical techniques by the repeated determination of D_c, the analyses being carried out by different analysts. The estimated standard deviation of mean D_c due to the instrument was 0.5% and that due to sampling differences on apparently homogeneous concrete was 5%. Inter-laboratory comparison

gave a standard deviation of 7.7% suggesting that results obtained by analysts are meaningful at 95% confidence limits of $\pm$ 15.4%.

El-Jazairi (106) proposes a semi-isothermal thermogravimetric approach for which determination of D_c is based on the weight losses due to the dehydration of CAH_{10} and of AH_3. When the DTG trace reaches a peak maximum, heating is switched to isothermal mode and the temperature held constant for 30 minutes to allow that reaction to proceed to completion before returning to dynamic heating until the next peak is reached. This method has the advantage of separating peaks which occur close together although there is always the possibility of 2 phases having identical decomposition temperatures. A disadvantage of this technique is the considerably lengthened test time for each sample.

Some sources quote suggested tolerances of $\pm$ 5% for D_c (105, 110) though this is now considered to be rather optimistic and Midgley suggests that the results of tests should be reported as 0, .25, .50, .75 or fully converted (113).

Thus it can be seen that the determination of degree of conversion is not a straightforward matter and since strength cannot be readily related to D_c other techniques are used to assess the strength of existing concrete structures. Core testing provides a direct measurement of compressive strength although interpretation of results is complicated by many factors such as curing history, presence of reinforcing steel, aggregate, core height/diameter ratio, direction of drilling and voidage. This is discussed in detail in a Concrete Society Technical Report (114).

Upv is a non-destructive testing technique which has been used by several researchers and is recommended as a good method for monitoring long term changes in concrete due to conversion (115). Bungey (116)

suggests that a upv greater than 4.4km/s indicated good concrete, 4.0-4.4km/s doubtful and less than 4.0km/s poor. He found however that although "naturally occurring" conversion causes a marked reduction in upv accelerated conversion does not necessarily lead to a decrease in upv even though strength decreased (117). Mayfield & Bettison agree that rapid laboratory conversion does not mirror reality (118). An article by Reynolds indicates that combining density measurements with upv gives a better indication of strength (119). The main difficulty is that a very small change in upv corresponds to a considerable change in strength (102, 117).

Neville notes generally poor correlation between upv and strength with problems caused by aggregates, reinforcing steel and variable moisture content (102).

A further difficulty encountered when determining degree of conversion for an existing structure is that inevitable differences in w/c cause an uneven pattern of conversion (120).

A colour change from grey to brown is often noted on conversion, due to the oxidation of ferrous to ferric oxide (121 cited by Neville in 122). Although this oxidation is facilitated by the higher porosity of converted concrete it may occur for "naturally" porous concrete which is unconverted.

1.6.3 Factors Affecting Conversion

The rate of reaction depends on temperature, w/c ratio, stress and the presence of releasable alkalis (123).

In 1958 Neville investigated the effect of storing HAC concrete at 25-40°C for extended periods. He found that a loss in strength occurred in all cases with the greatest losses for weaker mixes and at higher temperature and humidity (124). Intermittent storage at higher temperature gave a lower rate of strength loss. Other work has confirmed that the minimum strength occurs earlier at higher temperatures (7, 91, 122, 125).

Bradbury et al reported that for Secar pastes with w/c ratios 0.20, 0.60 at 18, 40°C conversion was less at lower w/c ratio (120). This finding is confirmed by Midgley and Midgley: the greater the original w/c ratio, the faster the rate of conversion (123). Midgley and Pettifer demonstrated that the higher the w/c ratio of HAC pastes the larger the crystal size of the hydration products (40). Crystal size has a considerable effect on strength; the smaller the crystal the greater the strength. This is said to be due to improved packing of the small crystallites, reduced average pore size and the greater difficulty of crack propagation.

According to Midgley (123) stress should favour conversion since the products of conversion have a higher density and thus occupy a smaller volume. There is however little experimental work to confirm this theory.

Several workers have reported the influence of alkali solutions on the rate of conversion : solutions of sodium or potassium hydroxide of increasing concentration have a progressively accelerating effect (1, 107, 123, 126). The explanation of this behaviour is unknown.

1.6.4 Influence of Conversion on Strength

There is no simple relationship between the degree of conversion and strength, the degree of conversion at the minimum strength being variable. A further complication is that the time to reach the minimum is not directly related to the rate at which conversion takes place.

Midgley & Midgley (123) propose a relationship between strength as a percentage of one day strength, w/c ratio and rate of conversion as follows:

$$S = (k.\ln R + p) + q(w-m)$$

where S = strength as a percentage of one day strength, known as the normalized strength

R = rate of conversion $= \frac{\log D_c\ (\%)}{\log \text{age (years} \times 10^6)}$

w = w/c ratio

k, p, q, m are constants

For laboratory prepared specimens good correlation was obtained between calculated and measured strengths using

$$S = (-37.8\ \ln R + 39.5) - 100\ (w-0.4)$$

Bensted confirms that it is the rate, not degree of conversion that is of prime importance. Since the rate of conversion cannot be accurately determined for a concrete structure later on in its lifetime, he suggests that thermal analysis techniques should be used to describe concrete as little, moderately or highly converted. A high strength member, even if highly converted, is probably safe (8).

In a long term programme of research into the characteristics of HAC concrete Teychenne has produced a considerable amount of relevant data (127). He studied strength development in water at 18, 38°C for a range of w/c ratios and looked at the effect of initial curing conditions on later behaviour. At 38°C conversion was rapid, 80% at 3 months, with mix proportions having little effect. At 18°C conversion was much slower, 25% at 1 year, with mix proportions unimportant at early ages. After 5 years however leaner mixes, having higher w/c ratios, converted more rapidly. The reduction in strength due to conversion was not as serious for concrete with w/c less than 0.40. The effect of free w/c and water storage temperature on HAC concrete strength is shown in Figure 1.11. Figure 1.12

Figure 1.11. Effect of Free w/c and Storage Temperature on Strength of HAC Concrete (127)

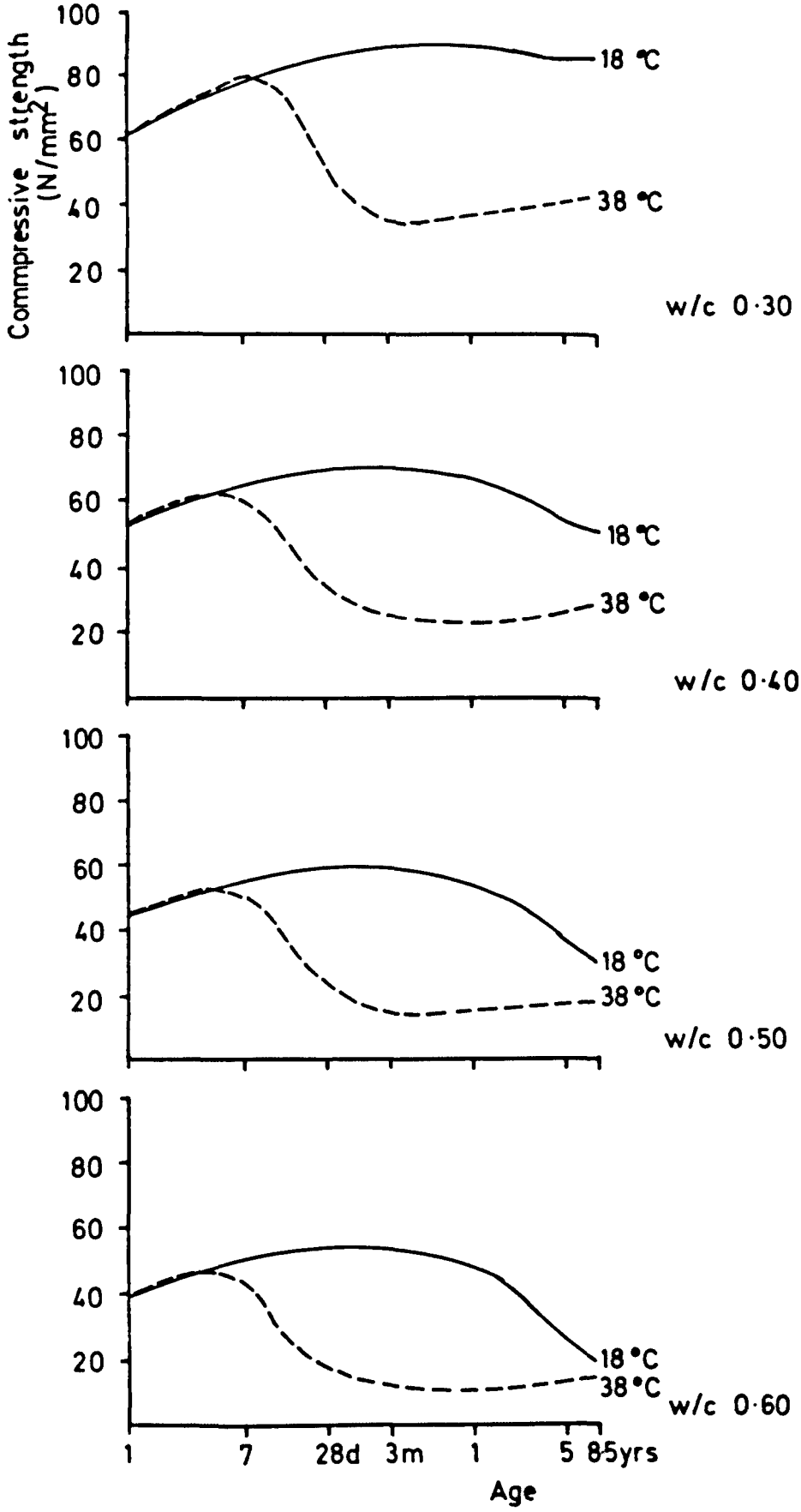

Figure 1.12. Effect of Curing Temperature on Strength of HAC Concrete with w/c 0·38 (91)

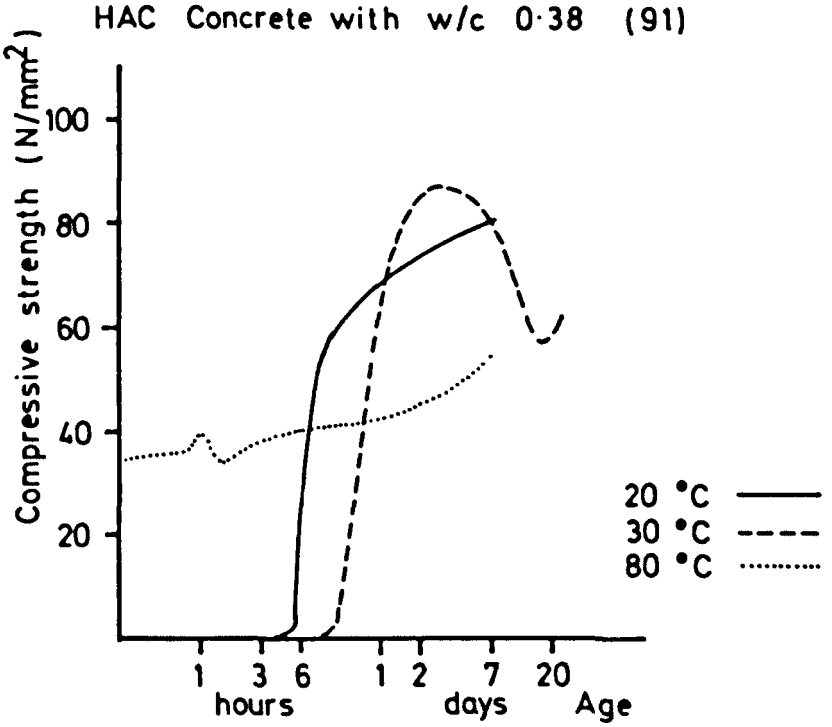

Figure 1.13. Effect of w/c and Porosity on Strength of Aluminous Cement Pastes (98)

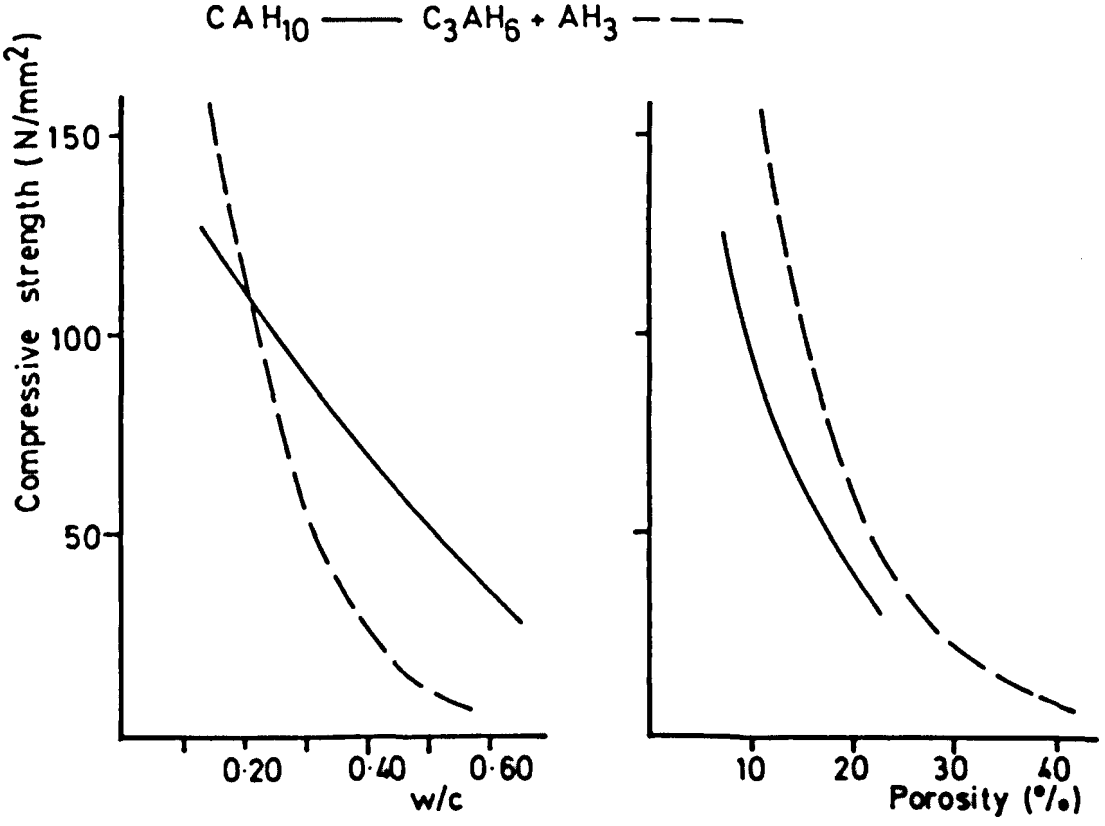

shows the results obtained by French et al on HAC concrete cured continuously at 20, 30 and 80°C (91).

Teychenne (127) and George (53) showed that the initial curing temperature is extremely important. Teychenne found that concrete cured at 35°C or above immediately after placing had lower strength at early age than if high temperature curing was delayed for 3-6 hours.

Quon & Malhotra (115) carried out a series of tests on HAC concrete cast at 21°C and subsequently stored in water or dry heat at 25, 35 or 50°C. Up to 1 year, D_c increased with age for specimens at 25, 35°C and was independent of w/c, in agreement with Teychenne's results. At 50°C the change in strength was dependent on w/c : at low w/c (0.31) there is insignificant early strength drop in spite of high D_c whereas at high w/c (>0.37) there is considerable strength loss.

It has been shown that there is usually a slow increase in the strength of HAC concrete at low w/c ratio after reaching the minimum (91). This may be due to the reaction of anhydrous cement with free water produced during conversion or of C_2S with water and alumina to form Stratlingite, C_2ASH_8 (55, 120). In a separate paper Midgley discusses the possible reasons for some non-UK HAC concrete not showing any strength recovery even after 21 years. After comparing HAC from several sources he concludes that strength recovery can be correlated with the presence of the hydratable silica bearing minerals pleochroite and beta C_2S. It is not however related to total silica content since at higher silica contents, more of the less reactive gehlenite is formed at the expense of C_2S (128).

1.6.5 Explanations for Strength Loss

Several theories have been suggested as explanations for the strength loss occurring on conversion and are described in detail by Midgley (125).

These are summarized as follow:

(i) Mechanical breaking of cementitious bond by the chemical reaction $CAH_{10} \longrightarrow C_3AH_6 + AH_3$

(ii) The binding strength of C_3AH_6 is less than that of CAH_{10}

(iii) Dehydration and ageing of the alumina gel

(iv) Increased porosity

Wells & Carlson (35) believe that alumina gel acts as a glue and propose that strength loss is due to crystallization of this gel to gibbsite. This theory was disproved by Chatterji & Majumdar (129) who showed that pure CA pastes could harden to CAH_{10} without the presence of gel. More recently Chatterji & Jeffery (39) suggested that CAH_{10} crystals are stronger than C_3AH_6 since they contain fewer dislocations while Mehta & Lesnikoff (43) and Lehman and Leers (130) propose that the higher surface area of the CAH_{10} needles gives them higher strength. Mehta & Lesnikoff also suggest that the smoother surface of the cubic crystals may lead to poor interparticle adhesion. These proposals are in contrast to that of Cottin & Reif (98) described later which suggests that the intrinsic strength of C_3AH_6 is greater than that of CAH_{10}.

The most likely explanation for the loss in strength is generally held to be the increase in porosity (98, 101, 102, 123). Cottin & Reif show the relationship for strength vs w/c and strength vs porosity for different hydrates, reproduced here as Figure 1.13. It can be seen that at equal w/c the porosity of C_3AH_6/gibbsite paste is greater than that of CAH_{10}. This is reasonable when considering the higher water content required for complete hydration of CAH_{10}. Mercury porosimetry tests were used to show that there are also differences in pore size distribution (98).

The volume changes accompanying conversion can be calculated from the equations (i) and (ii) given in section 1.6.1. In the formation of C_3AH_6 from CAH_{10} there is a solid volume decrease of approximately 50%, from C_2AH_8 the decrease is approximately 65%. According to George (131) the porosity of fully converted aluminous cement concrete is not greater than that of Portland cement concrete at the same w/c ratio but this is not in agreement with data given by Robson (1) which clearly shows a higher porosity for fully converted HAC concrete. In practice the porosity of HAC concrete does not increase by the amount expected since water produced by the conversion reaction can react with anhydrous cement remaining in the mix. Midgley & Midgley report that in tests on specimens with w/c greater than 0.27, greater porosity results from faster conversion (123).

George discusses the relationship between strength, porosity and the hydrates present. He considers a cement containing 50% CA, 30% C_4AF and 20% inert material and calculates volume changes and water requirement for complete hydration (critical w/c ratio). At low temperature, say 10°C, CA hydrates to form CAH_{10} with a resulting decrease in volume of 15.7% and a critical w/c of 1.14. It is assumed that iron in the ferrite phase plays a minor role thus C_4AF is said to form only C_3AH_6 and AH_3. The decrease in volume for this reaction is 15.5% and the critical w/c is 0.421. At high temperature, say 50°C, CA also hydrates to C_3AH_6 and AH_3 with a larger decrease in volume of 25.3% and a critical w/c of 0.456, the reaction of C_4AF is unchanged. He concludes that at low temperature the required w/c ratio is 0.70 for this particular cement but at high temperature it is only 0.35.

Cottin & Reif (98) studied pastes over a wide range of water contents and by measuring porosity found the critical w/c for full hydration of Ciment Fondu to C_3AH_6/gibbsite to be 0.332. The curing regime used to

obtain these hydrates was 7 days at 70°C.

In the same paper, Cottin & Reif report the following relationship, common to the behaviour of many materials, between porosity and compressive strength :

$$\text{compressive strength} = k_1 . e^{(-k_2 \cdot \text{porosity})}$$

where k_1, k_2 are constants

The constants k_1 and k_2 have different values depending on the hydrates present and hence on hydration temperature. The constants for high temperature hydration are approximately 2.5 times greater than for low temperature. This suggests that the intrinsic strength of the high temperature hydrates (C_3AH_6,AH_3) is greater than for CAH_{10}.

Midgley (132) used QXRD on neat Ciment Fondu pastes and concretes of w/c ratio 0.25-0.61 cured at 18-60°C to predict compressive strength after determination of hydrate quantities using k values to predict compressive strength assuming that a cube contained only 1 hydrate. The relationship between mineral content and strength was assumed to be linear. The strength of a cube containing a known combination of hydrates could then be calculated by adding the contribution from each hydrate. The strength combination of C_3AH_6 was found to decrease with increasing temperature and w/c ratio. This was shown to be due to the increasing average crystal size of the hydrate. The overall correlation coefficient for measured and calculated strengths was better than 0.9. Midgley & Pettifer suggest that the larger crystal size of hydrates at high w/c leads to poorer packing and hence increased porosity (40).

Confirmation of the porosity theory comes from results of tests carried out at the Building Research Establishment which found that an increase in porosity corresponded with an increase in measured degree of conversion (133). Neville also cites measurements showing an increase in porosity on conversion (102).

1.6.6 Prevention of Strength Loss

Some research has been carried out in an attempt to find a means of preventing the loss in strength due to conversion. Perez et al (134, 135) suggest curing HAC above 30°C to ensure immediate formation of C_3AH_6 thus preventing conversion. Using HAC mortar at w/c 0.42 they used XRD testing to show that at 40°C C_3AH_6 was formed directly with no CAH_{10} evident. It is interesting to note the apparent disagreement over the effect of high temperature curing since Figure 1.12 giving the results of French et al (91) for HAC at various curing temperatures clearly shows a drop in strength for curing above 20°C. Conversion is the only realistic explanation for such behaviour yet, if C_3AH_6 is formed directly, no conversion is possible. A possible explanation is that as curing temperature increases to 30°C the amount of CAH_{10} formed does decrease to zero but C_2AH_8 is still formed until considerably higher temperature. It is the conversion of the latter hydrate which may account for the observed strength loss.

Perez et al also suggest deliberate carbonation by addition of 20% $CaCO_3$ to the anhydrous HAC since this was found to improve both flexural and compressive strength. Later work by both Fentiman (136) and Trivino (137) has provided further information on this subject.

Fentiman used a blend of 30% $CaCO_3$ filler with 70% Ciment Fondu and followed reactions by XRD. At 20°C this carboaluminous cement hydrated mainly to CAH_{10}. At higher temperature the formation of C_3AH_6 is supressed by formation of the carboaluminate hydrate, $C_4A\bar{C}H_{11}$. This

indicates that carboaluminous cements could be of use only at high temperature by supressing initial formation of C_2AH_8 although even then there is a possibility of decomposition (with increasing time/temperature) of the carboaluminate hydrate to C_3AH_6, $C\bar{C}$ and water.

Trivino used both carboaluminous cement, containing 20% $CaCO_3$, and thermal treatment in an atmosphere of CO_2. He showed increases in compressive strength using either treatment at up to 14 days compared to control and attributed this to the formation of carboaluminate hydrate rather than C_3AH_6.

Tests by Mehta on an aluminous cement containing 5% calcium sulphoaluminate, $4CaO.3Al_2O_3.SO_3$, showed a much lower loss of strength on hot curing compared to the control mixes. XRD testing showed that the conversion of CAH_{10} to C_3AH_6 was apparently prevented by the sulphoaluminate. The early hydration rate was unaffected (138). These findings are not however substantiated by Ueda & Kondo in a discussion to Mehta's paper. Differences in cement composition and uncertainties in experimental details lead to difficulties in comparing results.

In studies of the hydration of CA with additions of organic compounds, Young showed that the conversion reaction from C_2AH_8 to C_3AH_6 is inhibited due to the organic compounds sorbing into the structure of the hydrate (47).

Another suggestion is to encourage the formation of Stratlingite rather than C_3AH_6 from CAH_{10} by reacting CAH_{10} with C-S-H gel added to an HAC mix (55, 139). Some C-S-H gel may be formed by the hydration reaction of beta C_2S. Whilst the presence of C_2ASH_8 is confirmed by XRD and DTA, there is no evidence of higher strengths.

1.7 CHEMICAL RESISTANCE

1.7.1 Introduction

One of the major causes of the vulnerability of Portland cements to chemical attack is the presence of free lime which is not liberated during the hydration of aluminous cements. Aluminous cement is however vulnerable in alkaline conditions since AH_3 becomes soluble (4). It is suggested that the good resistance of HAC to dilute mineral acids such as sulphuric may be due to the enveloping of more susceptible lime compounds by alumina gel (140).

HAC concrete does however suffer severe attack by :

strong hydrochloric, hydrofluoric, nitric, sulphuric acids;
caustic soda or potash; highly alkaline salts

and moderate attack by :

aluminium chloride, sodium carbonate; castor, linseed or rapeseed oil; some industrial liquors and detergents (if containing alkali hydroxides) (141)

It should be noted that the presence of free water is required before any form of chemical attack can proceed (107).

Porosity, pore size distribution and permeability are important factors in the chemical resistance of concrete. Since porosity is known to increase on conversion it is reasonable to suppose that converted HAC would be more susceptible to chemical attack.

1.7.2 Sulphates

Although the absence of free lime gives HAC much improved sulphate

resistance the cubic hydrate C_3AH_6 is vulnerable and attack can lead to the formation of calcium sulphoaluminate hydrate known as ettringite (4, 8, 107, 142). Lafuma (143) proposed that the disruptive influence of ettringite in aluminous cement is reduced since the absence of free lime increases its solubility. It is suggested by Lea however that the primary cause is the formation of protective surface films (9). In accelerated tests George (4) found that the aggressivity of sulphate salts to aluminous cements increases in the order

$$Ca < Mg < Na$$

which is a reversal of the findings of tests on Portland cement.

HAC concrete is much more vulnerable to sulphate attack after conversion especially if this occurred at a high rate leading to considerably increased porosity (107).

In tests on mortars and concrete containing aluminous cements at up to 7 years, Bachiorrini & Cussino found that the use of calcareous rather than silicious aggregates led to improved resistance to sulphate attack in addition to higher strength and reduced porosity. These changes can be attributed to the formation of carboaluminous hydrate in preference to C_3AH_6 (144).

Concrete cubes with w/c 0.38 cured for 4 hours at 18°C, then 1 hour at 100°C, then immersed in $MgSO_4$ (3.5% SO_3) at 18°C showed a 10% drop in compressive strength after 2 years (91). Other tests on mortar samples stored in 5% sodium sulphate solution showed no conclusive signs of sulphate attack after 1 year (54).

1.7.3 Chlorides

Very little work has been carried out on this subject. The formation of

chloroaluminate $C_3A.CaCl_2.12H_2O$ has been noted in a failed prestressed beam though it is unclear if this contributed to the failure (142).

1.7.4 Sea Water

The conversion of HAC concrete in sea water is very slow, presumably a result of the normally low temperature, and Midgley reports values of 0-15% after 34 years (142). Long term (20 year) tests on concrete specimens show that the only mixes attacked were those at high (> 0.60) w/c which were hot cured and thus rapidly converted (145).

1.7.5 Carbonation

The tendency for atmospheric carbon dioxide to react with calcium aluminate hydrates to form the carboaluminate $C_3A.CaCO_3.11H_2O$ has already been mentioned and can cause problems in studies of aluminous cements (111). Raask notes that rapid carbonation can take place only in the presence of liquid water held in small capillaries and that the reaction stops when water has evaporated from pores greater than about 50 Angstroms in diameter (146).

A potentially severe problem occurs for HAC concrete when CO_2 and alkali hydroxides are available in moist concrete. The reaction, known sometimes as alkaline hydrolysis, is worse for porous concrete and can reduce the cementitious part of a mix to powder (142). The source of alkali hydroxides is usually external (for example, water leaching from OPC concrete) or solutions produced by the release of sodium or potassium from certain aggregates such as mica. Such solutions are harmful in 2 ways; not only is the rate of conversion increased, but the hydration products are decomposed to give alkali aluminate and calcium hydroxide. In the absence of CO_2 the reaction stops here but if CO_2 and water are available then the

alkali aluminate and calcium hydroxide are transformed to calcium carbonate and hydrated alumina thus allowing the alkali hydroxide (or carbonate) to be regenerated and so react again with hydrated cement compounds (107).

As part of a detailed study of carbonation, Blenkinsop et al (147) studied the carbonation of both synthetically prepared C_3AH_6 and highly converted HAC concrete by sodium, potassium and lithium carbonate solutions. The equations governing the reactions are given below:

$$3CaO.Al_2O_3.6H_2O + 3M_2CO_3 \rightarrow 3CaCO_3 + M_2O.Al_2O_3.2H_2O + 4H_2O$$

$$(z - 2)H_2O + M_2O.Al_2O_3.2H_2O + CO_2 \rightarrow M_2CO_3 + Al_2O_3.zH_2O$$

Formation of $CaCO_3$ is rapid whereas formation of the alumina hydrates is slower. Initially the rate of reaction is similar for sodium, potassium or lithium ions but at later ages it is greatest for sodium then potassium then lithium. Indeed the reaction for lithium carbonate does not always proceed to completion, this behaviour being attributed to the comparatively large solvated ionic radius and hence reduced mobility of the lithium ion.

It was found that the rate of carbonation was greater for synthetic C_3AH_6 than for highly converted HAC. This was explained by the formation of gels containing iron hydrates in HAC concrete which are less permeable than pure alumina gels. The depth of penetration of carbonation was found to be proportional to the concentration of carbonate solution, the time of immersion and to paste porosity.

Brocard immersed prisms of Ciment Fondu paste in solutions of sodium and potassium hydroxide and recorded strength losses of up to 50% (126).

Carbonation in the absence of water-soluble alkalis is not necessarily detrimental to HAC concrete and can lead to increased strength as discussed in section 1.6.6. Cussino & Negro also confirmed this and proposed that the lamellar nature of the carboaluminate gives a less porous structure (148).

Soukatchoff compared the durability of 1:2 cement : sand mortars at w/c 0.45 stored in mountain water at 0-10°C with a free CO_2 content of 13-15 mg/L for 15 years. Mortars made from aluminous cement (40% alumina) suffered almost no attack whereas both Portland and Portland slag cement mortars were severely attacked (149).

1.8 USE OF ADMIXTURES WITH CIMENT FONDU

1.8.1 Introduction

In view of the objectives of this project, discussion on the use of admixtures will be limited to superplasticisers, accelerators and retarders.

Admixtures are used to a far lesser extent with Ciment Fondu than with Portland cement and this is reflected in the small amount of research carried out. It appears that considerably more effort has been aimed at understanding acceleration and retardation compared to plasticisation.

Bearing in mind the very different hydration chemistry of Ciment Fondu compared to Portland cement it is reasonable to suppose that :

(i) admixtures do not have the same effect on both types of cement and therefore

(ii) admixtures ineffective for Portland cements may be the most suitable for Ciment Fondu and vice versa.

1.8.2 Superplasticisers

Chemicals used as superplasticisers include lignosulphonates, sulphonated naphthalene or melamine formaldehyde condensates (SNFC, SMFC), hydroxylated carboxylic acids and phenol formaldehyde condensation products. With the exception of the latter product, all these chemicals are commonly used for Portland cements.

The nature of the polymerisation process used during the production of superplasticisers leads inevitably to the presence of molecules with varying chain length and for a given chain length there are many possible molecular configurations. Research carried out using Portland cement showed that an increased monomer content is detrimental to plasticisation and that the higher polymerised fraction is more effective (162).

Other research with Portland cements has indicated that the plasticising action is due to adsorption of superplasticiser molecules onto the surface of cement particles. This adsorption occurs as sulphonate groups are attracted to positively charged sites resulting from imperfections in the crystal structure near the surface. It is thought that adsorption can also occur onto hydrates although their extremely high surface area, at least 100 times greater than anhydrous cement, would result in far poorer plasticisation. The adsorption of superplasticiser molecules has 3 main effects:

i) particle surface charge is altered

ii) steric repulsion occurs between cement particles

iii) the adsorbed layer forms a barrier to effective water penetration thus hydration may be retarded (163).

Very little research has been carried out on the use of

superplasticising admixtures with aluminous cements.

Massazza et al (150) studied the effect of sugar free sodium lignosulphonate, SNFC and SMFC on pure C_4AH_{13} and C_3AH_6 at 20°C. Properties investigated were surface adsorption, zeta potential and rheology. A coaxial cylinders viscometer was used to find the apparent viscosity at a shear rate of 40 s^{-1}. For the same apparent viscosity it was found that a w/s ratio of 1.6 was required for C_4AH_{13} but only 0.4 for C_3AH_6. This was attributed to the difference in specific surface of the two compounds. Both SNFC and SMFC had little effect on the viscosity of C_3AH_6 paste but caused an increase for C_4AH_{13} pastes up to a dosage of 5% before a sharp decrease. The existence of a maximum paste viscosity is explained by a bridging effect. This is caused by the reduction in electrical repulsive forces between particles as plasticiser molecules adsorb on to the particle surfaces. This causes increasing particle agglomeration as the dosage is increased until at a certain, saturation dosage each particle is fully coated with plasticiser molecules and viscosity reduces sharply as deflocculation occurs. The adsorption of the 2 polycondensate molecules was found to be different to that of the lignosulphonate. This was attributed to the difference in the location of the active SO_3^{2-} groups within the molecules.

There is disagreement over the wavelength used in UV spectrophotometry to monitor changes in concentration of SNFC with Massazza et al (150) using 330 nm and Michaux and Defosse (151) using 280-300 nm.

Sakai et al (152) report work which shows that calcium aluminates react with organic compounds to form complexes hence decreasing their water-reducing capability.

Quon & Malhotra (153) used a modified lignosulphonate, SNFC and

SMFC in concrete containing commercial HAC. The concrete contained 25mm limestone with an unspecified sand and had an aggregate/cement ratio of 4.3, testing was carried out at approximately 20°C. The modified lignosulphonate gave a considerably retarded setting time and all admixtures caused rapid slump loss, even at very high dosages. Early age strength (up to 7 days) was found to be much lower for mixes containing admixture though the difference decreased with age until at 180 days, strengths were generally similar. The exception to this was concrete containing a very high dosage of admixture which continued to have reduced strength. Malhotra found that the degree of conversion was not affected by the presence of admixtures. He attributed the poor performance of the superplasticisers to the high heat of hydration of HAC. This explanation does not appear to make sense since the main peak in heat of hydration for HAC at ambient temperature does not occur for several hours after mixing and so cannot account for the rapid workability loss at very early age.

Lankard & Hackman (154) studied high and low purity castables (mixes normally used for refractory purposes). The low purity castable cement contained about 45% alumina and so is comparable to Ciment Fondu. All work was carried out at room temperature, presumably 20°C. The influence of sodium lignosulphonate, hydroxylated carboxylic acid, SNFC, SMFC and sodium citrate on workability, setting time, strength, porosity and thermal properties was investigated.

Sodium lignosulphonate was found to cause a large set retardation and strength loss, in agreement with Malhotra. SNFC and SMFC were said to improve flow without set retardation or strength loss whilst hydroxylated carboxylic acid had little effect. The behaviour of paste containing sodium citrate was found to be complex. In isolation it retarded considerably at dosages above 0.1% and at 0.3% had a fluidizing effect. When 1.0% sodium citrate was used in combination with SNFC or SMFC, a very large water

reduction of 33% was possible to give equivalent workability; set was accelerated and strengths improved. Dragoman (155) used SNFC and SMFC in HAC refractory concretes and found that compressive and flexural strengths at temperatures below 1000°C improved with dosages up to 1.5% although the optimum dosage was 1.0%.

Perez et al (135) studied the effect of a naphthalenic resin superplasticiser on the hydration of HAC mortar at 80°C. Workability was improved even when reducing w/c from 0.42 to 0.38. At the highest dosage used, 1.0%, strength was reduced by approximately 20%.

1.8.3 Accelerators and Retarders

Generally alkalis and alkaline compounds accelerate the set of aluminous cements while acids and acidic compounds retard. Some compounds may however either retard or accelerate depending on concentration.

There is confusion over the mechanism of acceleration and retardation, the theory of pH being disproved since both hydroxide solutions and dilute sulphuric acid are accelerators (82).

Substances normally acting as accelerators are sodium, potassium or calcium hydroxide, sodium or potassium carbonate or silicate, triethanolamine (an organic base) and many lithium salts. According to Lankard & Hackman (154) however triethanolamine is a retarder for calcium aluminate cement.

Many organic compounds such as glycol, glycerine, casein, starch and also citric, tartaric or gluconic acids have a retarding action. According to Young (47) the hydration products remain unchanged. Inorganic retarders include borax, lead salts, phosphates, sulphates and nitrates.

Banfill studied the effect of sulphates on the hydration of Ciment Fondu from the same batch as that used for the work described in this thesis. He found that sulphate retarded only at dosages exceeding 0.5% by weight of cement. These results indicate that no retardation should be expected if seawater is used for mixing since the amount of sulphate normally found in seawater would be effectively less than 0.1% by weight of cement (156). Halsey & Pratt however reported retardation at 8°C caused by the use of seawater with high alumina cement. This may have been caused by an unusually high sulphate content or by the presence of other compounds (36).

Rodger & Double (14) studied the effect of various lithium salts and other chlorides as accelerators and citric acid as a retarder for Ciment Fondu. Testing carried out at 22 ± 2°C included a simple adiabatic form of calorimetry, solution analysis and XRD. All the lithium salts tested, including lithium citrate, were found to be very effective accelerators with only slight variations in final setting time for the same dosage. A range of other chloride salts of uni, di and trivalent cations was also investigated. None of these salts was found to have an accelerating effect comparable to that of lithium compounds. The inclusion of lithium was found to promote the formation of C_2AH_8 at the expense of CAH_{10}. This trend was also noted by Crepaz & Raccanelli who found that the formation of CAH_{10} was increasingly suppressed as the dosage of lithium chloride increased until, at a concentration of N/5 the amounts of CAH_{10}, C_2AH_8 and C_3AH_6 were roughly equal (157). Rodger & Double proposed that the formation of lithium aluminate promotes nucleation of calcium aluminate hydrates thus lithium aluminate acts as a heterogeneous nucleation substrate. This was confirmed when addition of dry, powdered lithium aluminate was seen to caused marked acceleration.

The presence of metal ions affects the form of aluminium hydroxide precipitated. Van Straten et al found that without lithium the order of crystalline phases appearing from a supersaturated aluminate solution was an amorphous phase followed by pseudoboehmite and finally bayerite. With lithium however bayerite precipitated preferentially and rapidly (158). Frenkel et al studied the effect of many ions and found that the tendency for pseudoboehmite to be formed rather than bayerite decreases as cationic radius increases; thus sodium has the largest effect compared with either potassium or caesium. They found that while none of these ions were incorporated into the crystal structure, XRD suggested that lithium ions were intercalated between layers of aluminium in pseudoboehmite (108). This modified phase was found to dehydrate at different temperatures compared to the same phase without lithium, thus providing further evidence for a structural change.

Crepaz & Raccanelli (159), in studies of the C-A-H system, used solution analysis to show that lithium salts accelerated the precipitation of hydrates.

Rodger & Double (14) found that citric acid caused marked retardation. Their explanation, based on solution chemistry, is that citric acid in solution initially promotes precipitation of alumina gel by preferential complexation of calcium and that the citrate is finally precipitated with the calcium aluminate hydrates over several hours. The retardation action is visualised as precipitation of gel coatings around cement particles impeding hydrolysis and inhibiting growth of the normal products of hydration.

In an investigation into accelerators and retarders the effect of cations on the setting of HAC (measured by depth of penetration of a metal

cone into the hardening paste) was found to be as follows, with lithium causing the greatest acceleration and the ammonium ion causing the greatest retardation (82) :

$$Li < Na < none < K,Ca < Mg < Sr < NH_4$$

and the effect of anions as :

$$OH < none < Cl < NO_3 < Br < acetate$$

An interesting feature of the influence of lithium chloride and carbonate is the apparent existence of an optimum dosage after which the accelerating effect decreases.

It is suggested that the mechanism for the cation action is the bringing together of the OH ions bonded to the aluminium hydroxides produced during hydration. Lithium, being the smallest ion and favouring tetrahedral rather than octahedral coordination, should be best. Water is removed during the reaction and oxobridges are formed to precipitate CAH_{10}. The anion effect is said to be caused by replacement of one of the OH ions coordinated to the aluminium which prevents formation of oxobridges, this reaction being known as anion penetration. The order corresponds to the order of stability of the aluminium-anion coordinate bond.

A useful technique for categorising the accelerating or retarding action of admixtures was developed by Wilding et al (84). Plots of maximum rate of heat evolution vs 1/(time to peak) are obtained using conduction calorimetry as shown in Figure 1.14. This is based on the assumption that the hydration mechanism remains unchanged.

Figure 1.14. Illustration of Accelerating / Retarding Action of Admixtures Using Calorimetric Data (84)

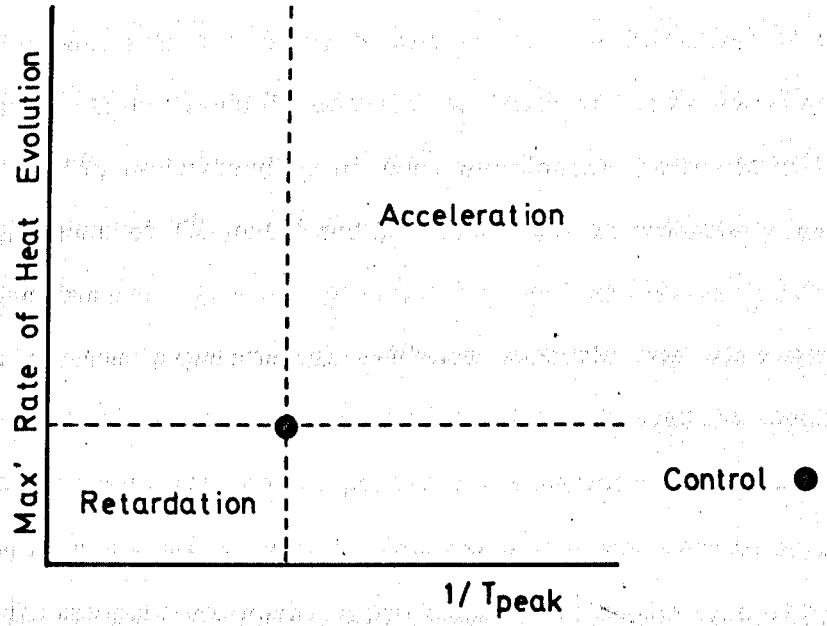

1.9 CONCLUSIONS

The review of literature shows that research carried out on aluminous cements has concentrated on i) hydration, ii) the influence of hydrate composition on strength and iii) conversion. Much of the research has been aimed at gaining understanding of pure aluminates, particularly CA the major constituent of Ciment Fondu, rather than commercially available aluminous cements.

Most of the experimental evidence supports the view that the hydration of aluminous cements occurs as a through solution mechanism. Dissolution of anhydrous cement produces a supersaturated solution from which an amorphous gel is formed. This gel is the precursor to crystalline hydrates with temperature having a profound effect on the type of hydrates produced. The influence of ferrites and silicates on the hydration of aluminous cements is very poorly understood.

Conflicting evidence is available concerning the influence of hydrate composition on strength. It is agreed however that the initial hydration temperature is of great importance in determining later behaviour.

Conversion can cause a major problem in the use of aluminous cements. The mechanism is not completely understood although it is generally accepted that the increased porosity after conversion is largely responsible for the loss in strength.

Very little information has been obtained on either the rheology of aluminous cement pastes or on the influence of superplasticising admixtures. A limited amount of information has been obtained on the chemical resistance of aluminous cements with effort being concentrated on the problem of carbonation.

With this background of existing knowledge the objective of the project described in this thesis was to carry out a systematic study of the effect of superplasticising admixtures on the rheology, hydration, setting and strength development of Ciment Fondu.

CHAPTER 2 INTRODUCTION TO EXPERIMENTAL WORK

2.1 MATERIALS

Cement

Ciment Fondu from one batch produced by the Lafarge Aluminous Cement Company Ltd. Physical characteristics and chemical composition are given in Appendix 1.

Sand

1. Clean silica sand with grading given in Appendix 2.
2. North Nottinghamshire quartzitic sand zone 2/3.

Superplasticisers

S1 Sulphonated naphthalene formaldehyde condensate

S2 Sulphonated phenol formaldehyde condensate

S3 Sulphonated melamine formaldehyde condensate

Accelerator (A)

Lithium citrate

Retarder (R)

Sodium gluconate

Water

De-ionised water for all mixes except the mortars described in Chapter 5 for which tap water was used.

Notes

1. Admixture dosages are given as the percentage by weight of cement.
2. Admixtures were dissolved in the mixing water prior to addition of cement.

2.2 OUTLINE OF EXPERIMENTAL PROGRAMME

The following brief description of the testing sequence is given to assist the reader in understanding the structure of the project.

The overall objective was to find an effective plasticising admixture for Ciment Fondu, thus a rheological study of cement pastes provided the starting point for the work. An initial appraisal of plain Ciment Fondu pastes was made before assessing the effect of the superplasticisers. The rheological investigation is described in Chapter 3.

The influence of admixtures on the setting time of Ciment Fondu is of great importance. An extensive study of hydration kinetics was therefore undertaken using conduction calorimetry at a range of test temperatures. This work is described in Chapter 4 together with additional tests on setting using the Vicat apparatus.

The long term behaviour of Ciment Fondu mortars containing admixtures was investigated for a range of storage temperatures. Strength was monitored indirectly by measuring ultrasonic pulse velocity (upv) up to 18 months and establishing the correlation between upv and strength. The hydrate compositions were investigated by DTG and XRD. The work on long term behaviour and hydrate compositions is described in Chapter 5.

The effect of the admixtures on the concentration of lime and alumina in solution during early hydration was then studied. This work, described in Chapter 6, was to provide information on the admixture mechanisms and to enable improvements in formulation to be investigated.

CHAPTER 3 RHEOLOGY

Key to Symbols Used in Chapter 3

Symbols used only immediately after they have been defined are not included.

D	Impeller diameter
N	Rotational speed of impeller
Np	Power number
R_b	Radius of inner cylinder
R_c	Radius of outer cylinder
Re	Reynolds number
T	Torque
$\dot{\gamma}$	Shear rate
μ	Plastic viscosity
ρ	Density
τ_o	Yield value
Ω	Angular velocity

3.1 INTRODUCTION

The rheological study of aluminous cements is fundamental to the project. The review of published literature showed that very little information is available, thus a detailed study of plain pastes was carried out before moving on to investigate the effect of admixtures.

The testing of cement pastes can be conveniently divided into 2 sections:

i) quantitative determination of yield value and plastic viscosity from flow curves

ii) study of time dependent behaviour under continuous shear

Work carried out in both these areas for plain pastes and for pastes containing admixtures provides the rheological background to the project.

Also included in this chapter is the description of a small test programme to correlate mortar and paste behaviour using "industrial" workability tests on Ciment Fondu mortars.

3.2 EQUIPMENT

3.2.1 Viscometric Equipment

3.2.1.1 Viscometer

All rheological work on cement pastes was carried out using a Haake Rotovisco RV2 viscometer with MK500 torque measuring head and PG142 external speed programmer.

3.2.1.2 Impellers

Helical : 3 interrupted helical ribbon impellers IHA, IHB and IHC of varying size as shown on Figure 3.1

Cylindrical : 3 profiled and 1 smooth cylinder as detailed in Table 3.1.

Figure 3.1 Dimensions of Helical Impellers

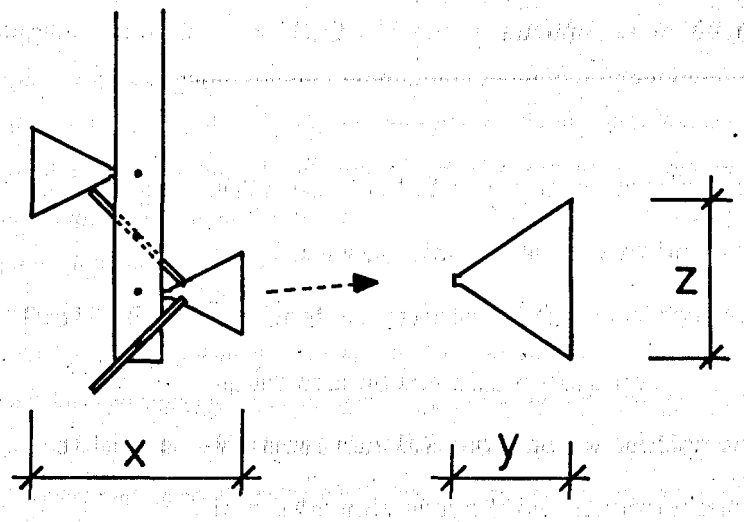

Impeller	Dimensions (mm)		
	x	y	z
IHA	26·0	9·0	12·5
IHB	33·6	12·8	18·6
IHC	37·0	14·5	20·1

Table 3.1 Cylindrical Impeller Details

Reference	External Radius (mm)	Height (mm)	Profile
ICA	10.0	19.6	A
ICB	13.0	50.0	B
ICC	18.4	60.0	C
ICD	20.04	60.0	smooth

Profile A : Vertical ribs 0.2 mm square section spaced at approximately 2 mm intervals around the circumference.

Profile B : Vertical serrations of 0.5 mm square section spaced 0.5 mm apart around the circumference.

Profile C : Vertical ribs 0.2 mm square section spaced at approximately 1 mm intervals around the circumference.

3.2.1.3 Cups

Three profiled and 1 smooth cup were used as detailed in Table 3.2.

Table 3.2 Viscometer Cup Details

Reference	Internal Radius (mm)	Profile
CA	11.55	A
CB	15.0	B
CC	21.0	D
CD	21.0	smooth

Profile D : Vertical ribs 0.2 mm square section spaced at approximately 1.5 mm intervals around the circumference.

The notation IHA/CD thus refers to the smallest helical impeller used with the smooth cup.

3.2.2 Industrial Workability Tests for Mortars

3.2.2.1 West Midlands County Council Flow Trough

Dimensional details of the flow trough are as shown on Figure 3.2.

3.2.2.2 Flow Table

The flow table conformed to BS 4551 : 1980 ((1)).

3.2.2.3 Spread Test

For this test a smooth glass plate approximately 300 mm x 300 mm and a metal cylinder 52 mm high with internal diameter 40 mm are required.

3.3 CALCULATION OF YIELD VALUE AND PLASTIC VISCOSITY

3.3.1 Coaxial Cylinders

The relationship between stress and shear rate for a Bingham material such as cement paste is shown on Figure 3.3. Plastic viscosity (μ) and yield value (τ_o) may be calculated using the Reiner-Rivlin equation in which τ_o is determined from T_2 (see Figure 3.3). The curved portion of the graph is due to the gradual overcoming of plug flow at low stresses until at T_3 all the paste is flowing.

Reiner-Rivlin equation

$$\Omega = \frac{T}{4\pi h_b \mu}\left(\frac{1}{R_b^2} - \frac{1}{R_c^2}\right) - \frac{\tau_o}{\mu} \ln\left(\frac{R_b}{R_c}\right)$$

Figure 3.2. W. Midlands C.C Flow Trough

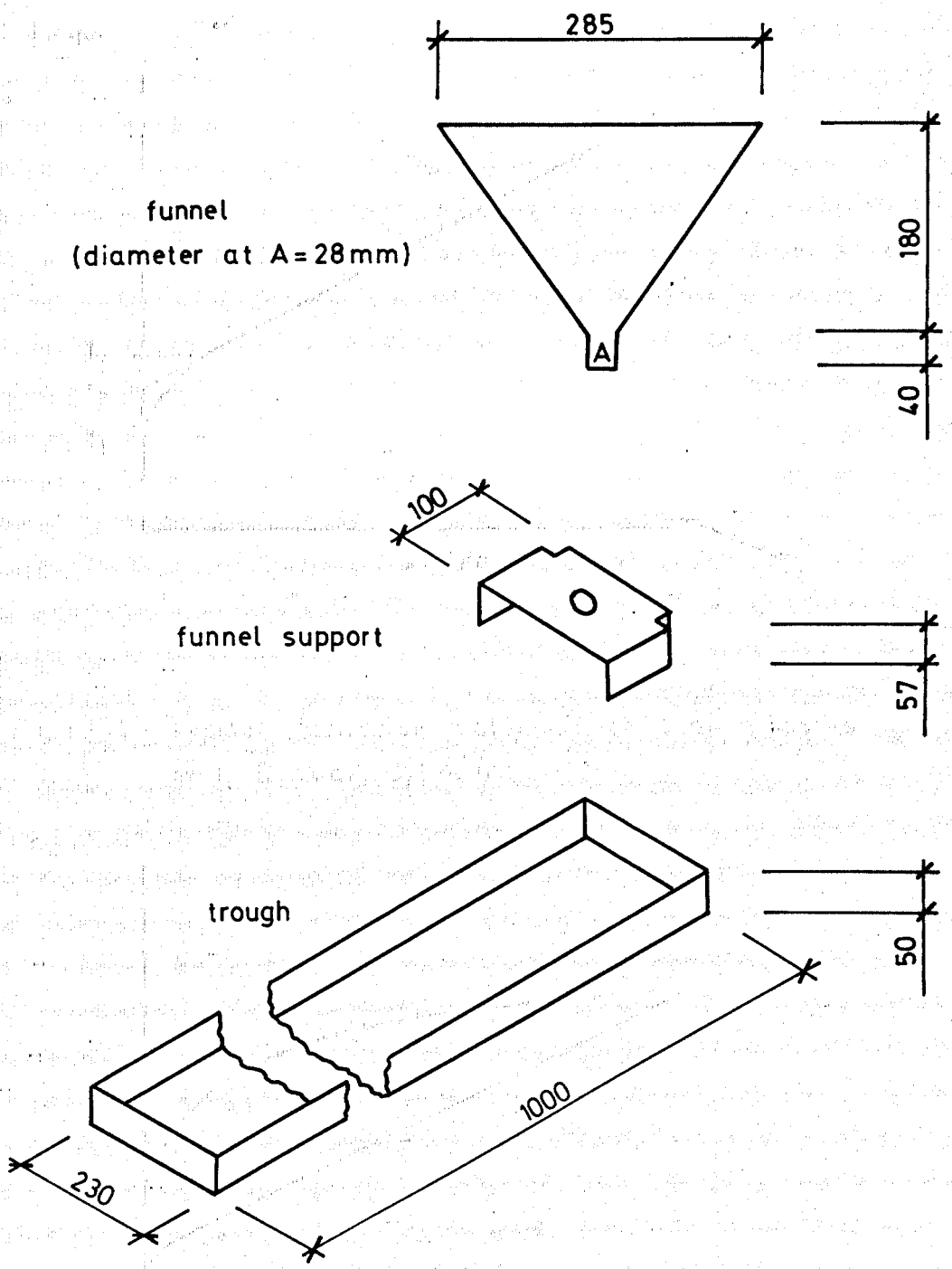

dimensions in mm
not to scale

Figure 3.3 Relationship Between Torque and Angular Velocity for a Bingham Material. (Reiner Rivlin Equation)

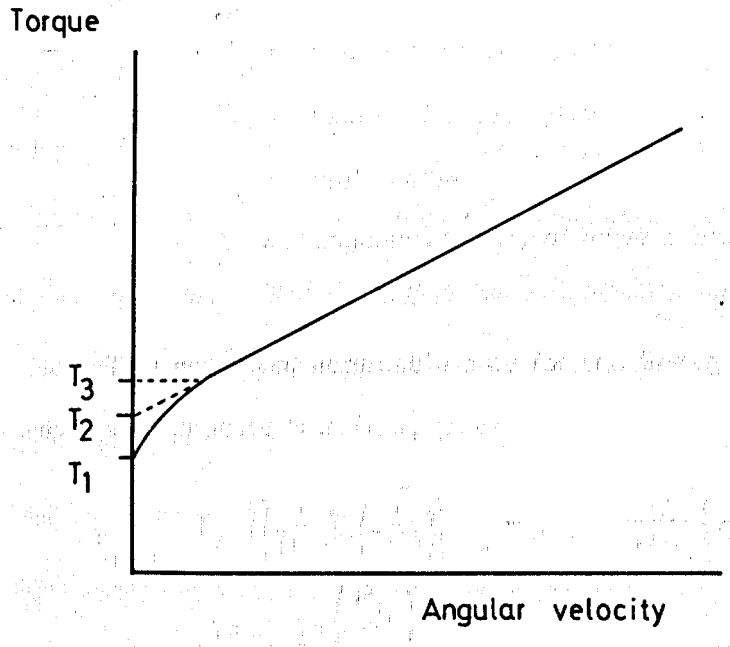

Figure 3.4 Typical Flowcurve Obtained for Plain Pastes with Coaxial Cylinders

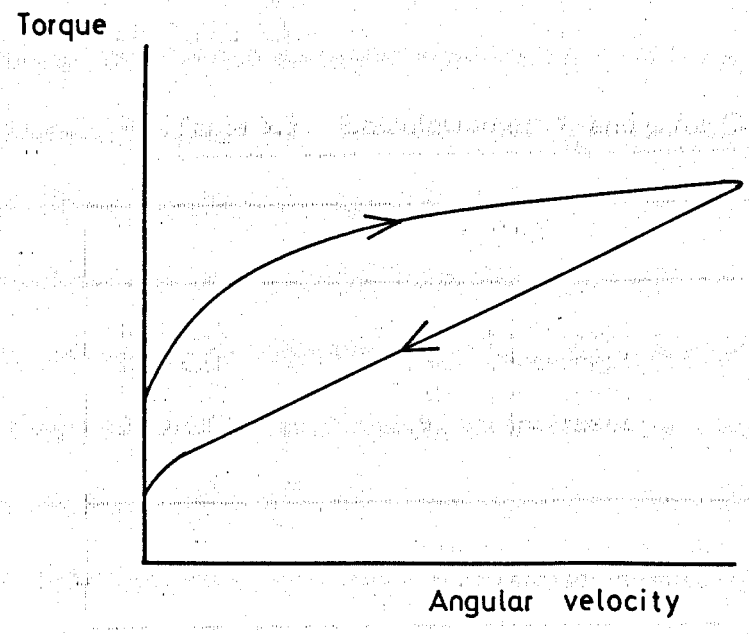

where T = torque on inner cylinder

μ = plastic viscosity

h_b = height of inner cylinder

R_b = radius of inner cylinder

R_c = radius of outer cylinder

τ_o = yield value

Ω = angular velocity of inner cylinder

This equation, applicable only for the linear portion of the flow curve when all the paste is in flow, gives

$$\tau_o = \frac{T_2\left[\left(\frac{1}{R_b^2}\right)-\left(\frac{1}{R_c^2}\right)\right]}{4\pi h_b \ln\left(\frac{R_b}{R_c}\right)} \quad ; \quad \mu = \frac{1}{4\pi h_b}\left(\frac{1}{R_b^2}-\frac{1}{R_c^2}\right)\cdot\frac{1}{S}$$

where S = slope $\left(\frac{\Omega}{T}\right)$ of the linear portion

Thus τ_o and μ can be calculated for impeller/cup combinations as shown in Table 3.3.

Table 3.3 Calculation of τ_o and μ for Coaxial Cylinders

	τ_o (Pa)	μ (Pa.s)
ICA/CA	32.40 x intercept	41.50 x 1/S
ICB/CB	7.66 x intercept	10.50 x 1/S
ICC/CC	3.20 x intercept	4.03 x 1/S
ICD/CD	2.92 x intercept	1.31 x 1/S
intercept as scale units S as rpm/scale units		

The viscometer scale reading indicates the torque on the inner, rotating cylinder and can be converted to fundamental units by multiplying by the calibration factor 0.000464 Nm/scale unit. This calibration factor was obtained by measuring the increase in scale reading as known weights were added to a thread fixed to the viscometer measuring head. The measuring head was placed horizontally so that the weights could be raised by rotating the viscometer spindle at low speed.

3.3.2 Helical Impellers

The geometry of the helical impeller is too complicated to allow for direct calculation of τ_0 and μ. Instead the system is calibrated using fluids whose properties are established by testing with coaxial cylinders. The theory of the helical impeller was developed by Tattersall and Bloomer for the 2 point concrete workability apparatus ((2)). A mean equivalent shear rate in the system is calculated as $\dot{\gamma} = KN$ where N is the impeller speed in rps ((3)). The calibration procedure is described in Appendix 3.

Two constants G and K, obtained from the calibration procedure, are used to calculate τ_0 and μ in fundamental units from the graph of T against N as follows:

τ_0(Pa) = K/G x intercept (intercept in Nm)

μ (Pa.s) = 1/G x 1/slope (slope in rps/Nm)

Values of G and K for different impeller/cup combinations are given in Table 3.4.

Table 3.4 Constants Obtained from Calibration of Helical Impellers

System	K (dimensionless)	G (x 10^{-3} m^3)
IHA/CD	11.2 *	0.345 *
IHA/CB	25.7 *	0.56 *
IHB/CD	8.5	0.787
IHB/CC	8.1	0.710
IHC/CC	9.6	1.301

* personal communication from Dr. P.F.G. Banfill

3.4 EXPERIMENTAL DETAILS

General Comments

i) Mixing Procedures : Cement was always added to the mixing water. For hand mixing a metal spatula was used to stir the paste in a 250 ml glass beaker. For mechanical mixing a laboratory stirrer with propeller shaped impeller was used taking care to keep the rotational speed constant for all mixes.

ii) Sequence of Testing : The order of tests within any experiment, such as the effect of mixing time on yield value, was always randomised.

3.4.1 Plain Pastes

3.4.1.1 Yield Value and Plastic Viscosity

A series of tests was carried out to check the effect of alterations in experimental techniques so that a standard procedure could be adopted for determination of yield value and plastic viscosity. The following variables were studied:

a) mixing regime

b) mixing time

c) paste age at test

d) impeller/cup system and w/c

e) maximum impeller speed and additional shearing of samples between tests

Coaxial cylinders were used for (a) - (d) and helical impellers used for the remaining tests.

Tests were carried out at laboratory temperature, approximately 20 ± 2°C.

The results of these tests are not included for brevity although a copy of the paper on the rheology of aluminous cement pastes by Banfill and Gill is appended to this thesis ((4)). The form of flow curve obtained from all coaxial cylinders tests is shown on Figure 3.4. The downcurves obtained from the IHC helical impeller are shown on Figure 3.5. The reasoning behind the adoption of the standard procedure for determination of yield value and plastic viscosity is given in section 3.5.1.3.

3.4.1.2 Time Dependent Behaviour Under Continuous Shear

For all tests 150 g of cement was added slowly to the appropriate amount of water and mixed by hand for 1 minute before being placed in the viscometer and sheared for up to 45 minutes at a uniform rate. During each test the viscometer scale reading was recording using a Linear 1200 chart recorder.

All tests were carried out at laboratory temperature, approximately 20 ± 2°C.

Figure 3.5. Downcurves Showing Deviation from Bingham Behaviour Obtained with IHC Helical Impeller

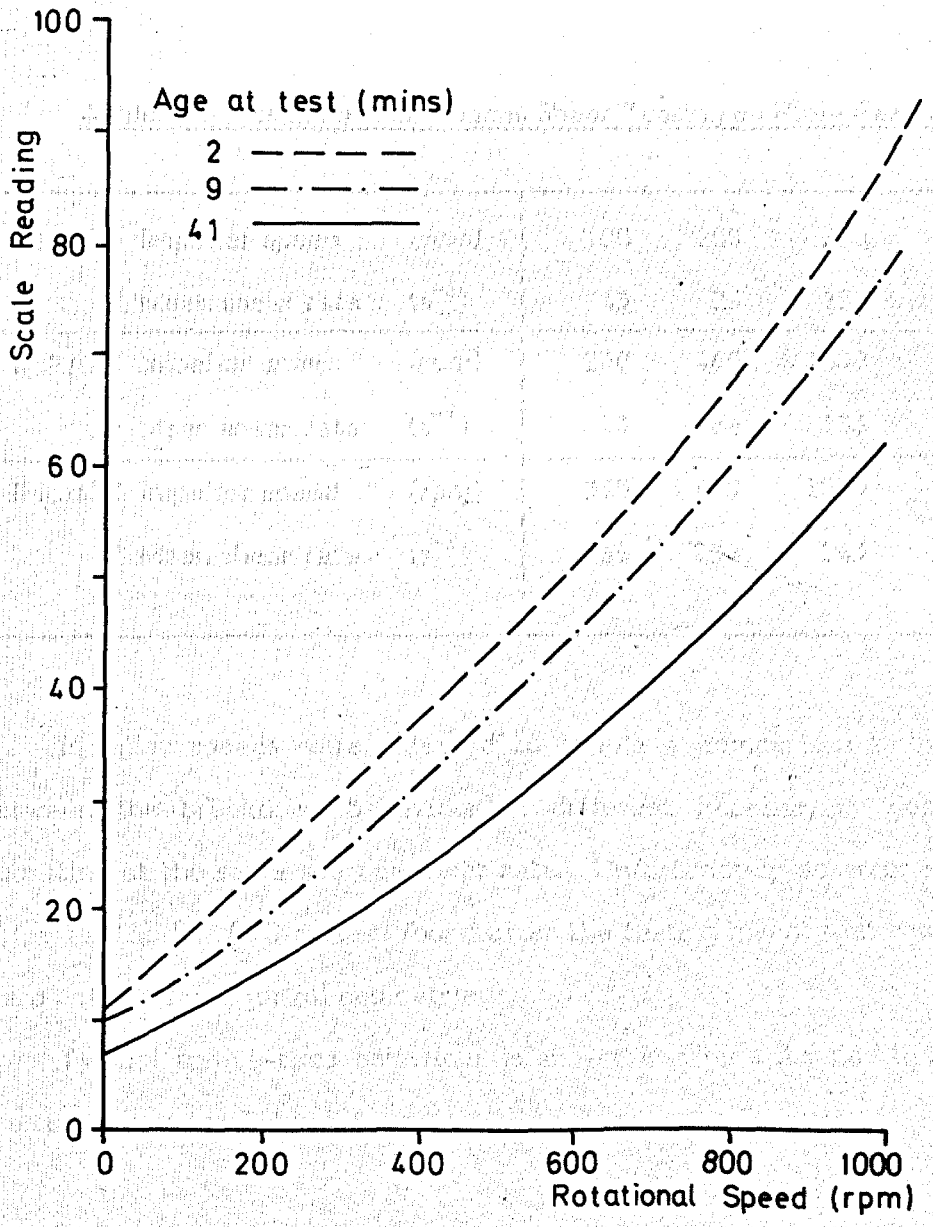

Other experimental details are given in Table 3.5 and apply to tests at both 0.30 and 0.40 w/c. Mean equivalent shear rates are calculated using $\dot{\gamma} = KN$ with K values as given in section 3.3.2. (The K value for IHA/CC was assumed to be the same as for IHA/CD).

Table 3.5 Details of Continuous Shear Testing on Plain Pastes

IHA/CB	Impeller speed	(rpm)	100	200	600	1000
	Mean shear rate	(s^{-1})	43	86	257	427
IHA/CC	Impeller speed	(rpm)	230	460	1000	
	Mean shear rate	(s^{-1})	43	86	186	
IHC/CC	Impeller speed	(rpm)	330	610	1000	
	Mean shear rate	(s^{-1})	69	138	243	

Impeller speeds were selected to enable a comparison to be made between the breakdown behaviour of different impeller/cup geometries operating at the same average shear rate. Unfortunately an error in the K value for the IHC/CC system found after the testing meant that shear rates were not the same for all geometries.

Typical torque-time behaviour is shown on Figure 3.6 and the results are summarised in Table 3.6.

3.4.2 Pastes Containing Admixtures

3.4.2.1 Yield Value and Plastic Viscosity

Initially a helical impeller as used by Bhatty and Banfill (78) was considered to be more suitable than coaxial cylinders since sedimentation in high workability pastes would be prevented. However the tests on plain

Figure 3.6 Typical Torque vs Time for Plain Paste Under Constant Shear (Obtained for all helical systems)

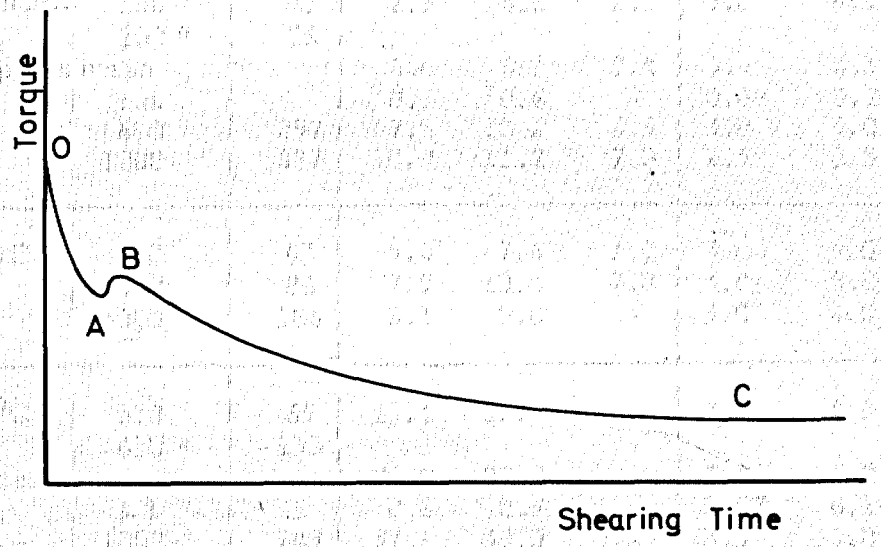

Table 3.6 Behaviour of Plain Pastes Under Continuous Shear
(see Figure 3.6)

w/c 0.30

System	Shearing Speed (rpm)	Mean Equiv' Shear Rate (s^{-1})	Torque (Nm x 10^{-3}) A	B	C	Paste Age (mins) A	B	C	Slope of Semi Log Plot BC
IHA/CB	100	43	2.9	4.6	2.1	3.0	4.5	15.0	2.69
	200 *	86							
6 repeats mean			4.6	6.2	3.4	3.3	4.1	15.0	2.64
	s.d.		0.5	0.6	-	0.08	0.20	-	-
	600	257	7.9	10.2	6.5	3.0	5.0	33.0	5.68
	1000	427	10.7	11.2	7.0	2.5	3.5	20.0	3.15
IHA/CC	230	43	5.4	7.4	3.0	3.0	4.0	20.0	3.85
	460	86	7.9	10.4	7.0	3.0	5.0	38.0	7.44
	1000	186	8.1	9.0	-	3.0	4.0	>45.0	**
IHC/CC	330	69	17.1	22.0	-	3.5	4.5	>35.0	**
	610 *	138							
4 repeats mean			24.9	27.3	-	3.4	4.2	>35.0	**
	s.d.		0.8	0.9	-	0.07	0.20	>35.0	**
	1000	243	37.6	39.0	-	3.5	4.0	>35.0	**

w/c 0.40

IHA/CB	100	43	0.5	1.2	0.8	4.0	6.0	9.0	***
	200	86	0.9	1.6	1.2	3.0	4.5	9.0	***
	600	257	1.9	2.1	1.9	3.0	4.5	unclear	***
	1000	427	unclear		2.4	unclear		15.0	***
IHA/CC	230	43	0.9	1.4	1.1	3.5	5.0	9.0	***
	460	86	1.3	1.7	1.4	3.5	5.0	10.0	***
	1000	186	2.8	3.0	2.8	3.0	4.5	11.0	***
IHC/CC	330	69	2.6	3.3	2.7	4.0	5.5	12.0	***
	610	138	4.7	5.3	4.6	4.0	5.0	20.0	***
	1000	243	8.2	8.6	7.7	4.0	4.5	25.0	***

Note : * Repeats to show variation of initial minima and small peak. For IHA/CB only 1 run gave information up to 30 minutes so only 1 result at point C.

** Equilibrium not reached therefore not possible to calculate slope.

*** Difference BC too small to allow accurate calculation of slope.

s.d. Standard deviation

pastes of high workability highlighted the problem of turbulence caused by helical impellers which leads to errors in the determination of rheological parameters. This problem is discussed in detail in section 3.5.1.2.

Simple sedimentation tests were carried out on plain paste and pastes containing 0.1% superplasticiser which showed that at w/c < 0.4 the amount of segregation before 10 minutes was negligible. It was thus considered acceptable to use coaxial cylinders.

The following standard procedure was adopted after considering the results from plain pastes; the reasons are explained in section 3.5.1.3.

Weight of cement : 150 g

Maximum impeller speed : 1000 rpm for w/c 0.40
400 rpm for w/c 0.30

Impeller/cup : ICC/CC

Mixing : 1 minute hand followed by 4 minutes mechanical

Paste age at test : 6 minutes, unless stated otherwise

Temperature : 20 $\pm$ 2°C

Superplasticised Pastes

Superplasticers : S1, S2, S3

Dosages : 0.01, 0.05, 0.10, 0.50, 1.0, 2.0 % at 6 minutes
0.10, 0.50, 1.0 % at 15, 30 and 45 minutes

Paste w/c : 0.30, 0.40

The effect of superplasticiser dosage on the results at 6 minutes is shown on Figure 3.7.

Figure 3.7a Effect of Superplasticiser Dosage on Yield Value at 6 Minutes

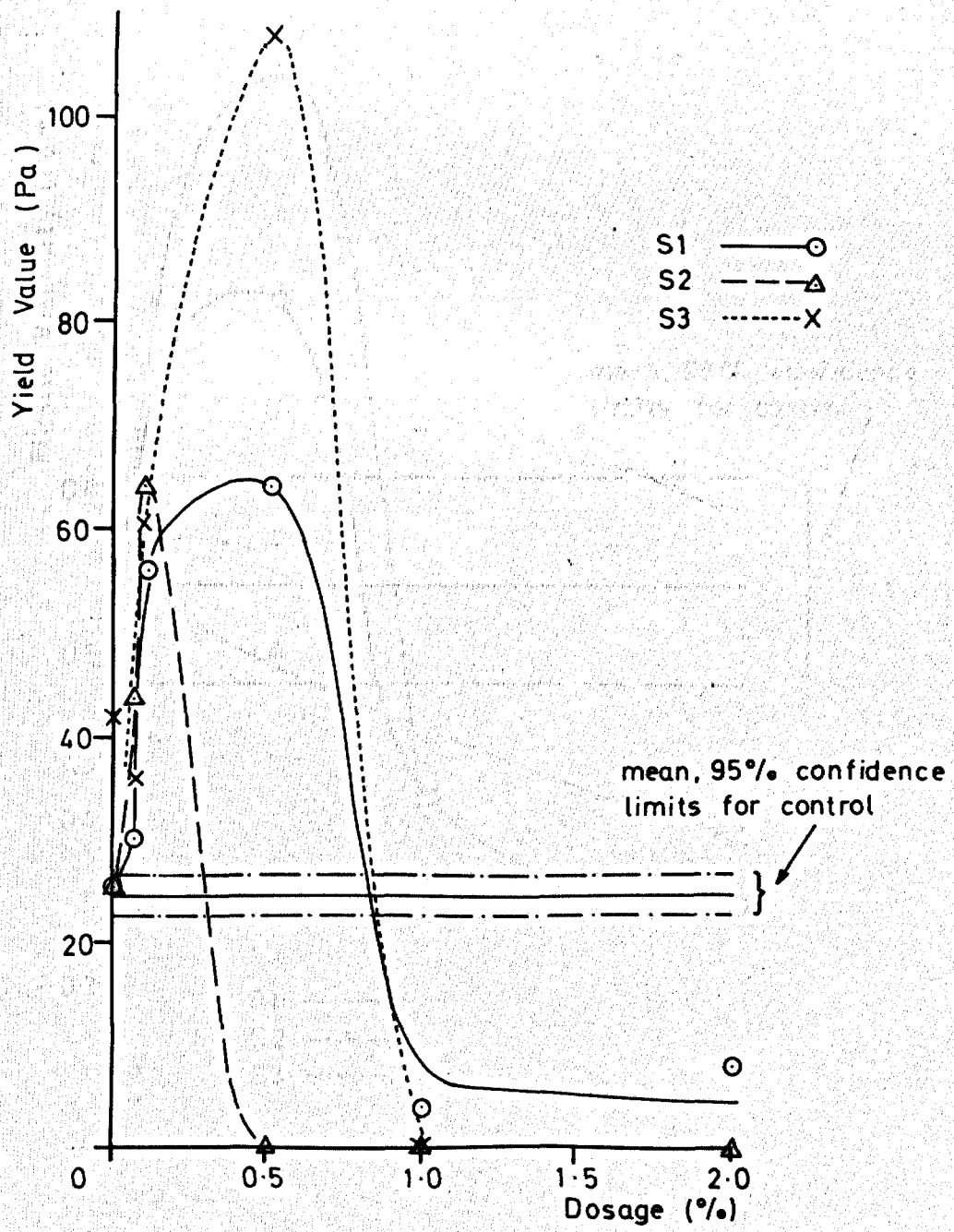

Figure 3.7b Effect of Superplasticiser Dosage on Plastic Viscosity at 6 Minutes

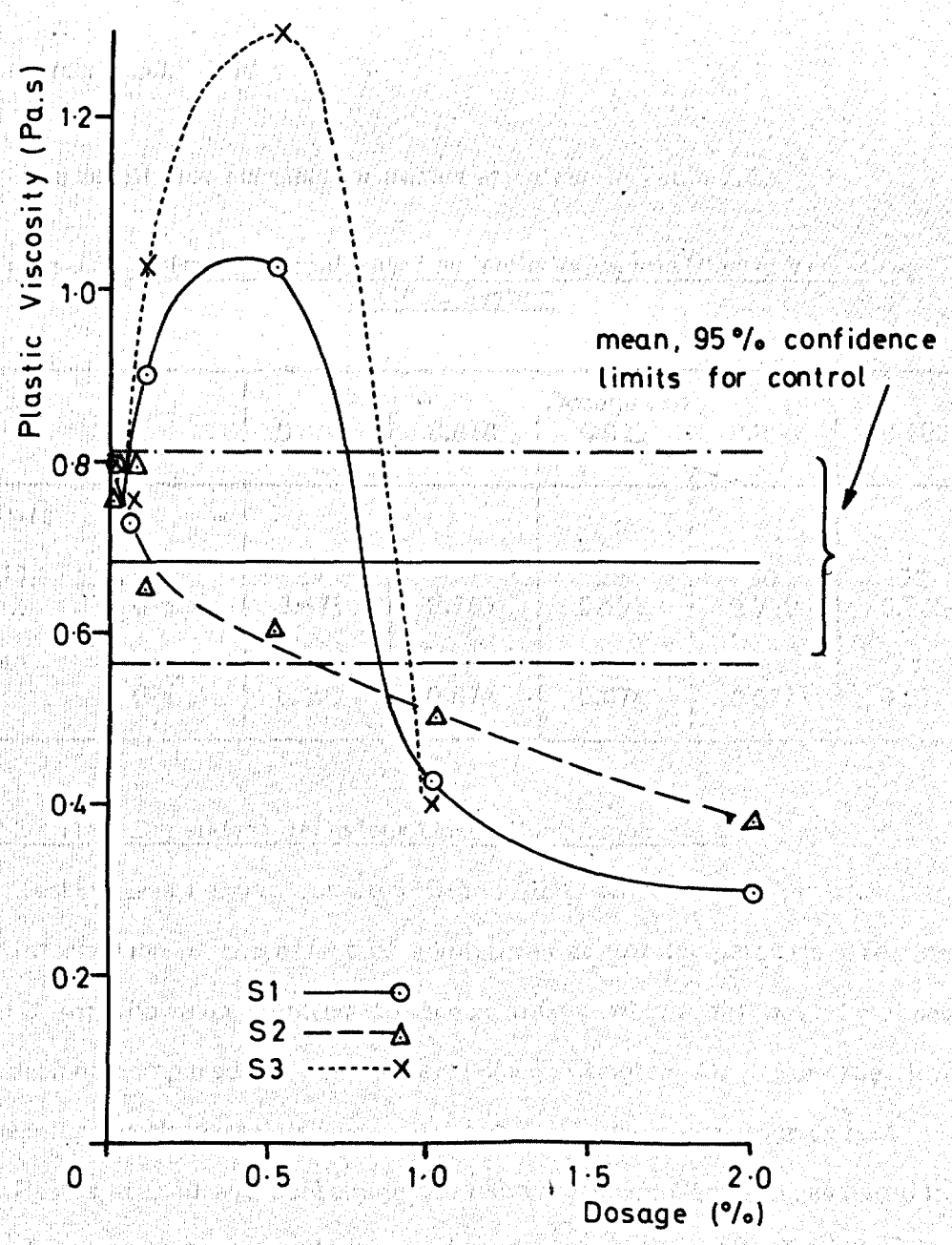

All results for superplasticised pastes are presented in Table 3.7 together with the mean results for plain pastes from 15 tests at w/c 0.30 and 9 tests at w/c 0.40.

Accelerated Pastes

Accelerator dosage : 0.01, 0.025, 0.05, 0.10%

Paste w/c : 0.30, 0.40

The results for accelerator pastes are given in Table 3.8.

Table 3.8 Effect of Accelerator on Yield Value and Plastic Viscosity, ICC/CC System

		Dosage (%) 0	0.010	0.025	0.050	0.100
w/c						
0.30	τ_0 (Pa)	29	70	28	60	32
	μ (Pa.s)	0.671	0.985	0.558	0.720	0.560
0.40	τ_0 (Pa)	9	19	10	8	7
	μ (Pa.s)	0.097	0.074	0.076	0.071	0.072

3.4.2.2 Time Dependent Behaviour Under Continuous Shear

Testing was carried out at 5°C and 20°C since it was important to have information on the effect of admixtures at low temperature. Testing at 5°C was however limited to those mixes which did not show set retardation compared to the control (see Chapter 4). For the low temperature work materials were stored at 2-3°C overnight prior to test.

Pastes at 0.40 w/c containing the combinations of admixtures listed in Table 3.9 were tested using the procedure described in section 3.4.1.2. The IHC/CC system was used in the knowledge that turbulence was likely to occur. It will be shown later in section 3.5.1.3 that this did not affect the form of the flow curves. The use of the helical impeller was justified by the need to prevent sedimentation during the tests.

Table 3.7 Effect of Superplasticisers on Yield Value and Plastic Viscosity

w/c 0.30

Paste Age at Test (mins)	Dosage %	Yield Value (Pa) S1	S2	S3	Plastic Viscosity (Pa.s) S1	S2	S3
6	0	15 results mean		24.4	mean		0.684
		s.d.		4.1	s.d.		0.062
6	0.01	25.6	25.6	41.6	0.806	0.762	0.797
6	0.05	31.0	43.5	35.2	0.717	0.790	0.759
6	0.10	56.0	63.4	60.8	0.907	0.639	1.034
6	0.50	64.0	0	107.2	1.024	0.611	1.290
6	1.00	4.8	0	0	0.422	0.512	0.403
15	0.10	54.4	61.8	52.8	0.994	0.706	0.954
15	0.50	72.0	11.5	*	1.209	0.660	*
15	1.00	16.6	0	*	0.730	0.578	*
30	0.10	43.2	49.6	43.2	0.911	0.717	1.269
30	0.50	63.0	21.1	*	0.932	0.689	*
30	1.00	45.8	17.6	*	0.802	0.766	*
45	0.10	48.0	67.2	59.8	1.008	0.833	1.366
45	0.50	73.6	26.2	*	1.397	0.705	*
45	1.00	112.0	28.2	*	1.128	0.825	*

w/c 0.40

6	0	9 results mean		4.1	mean		0.116
		s.d.		1.0	s.d		0.009
6	0.01	5.8	1.6	10.2	0.098	0.123	0.107
6	0.05	6.4	6.4	8.0	0.124	0.108	0.109
6	0.10	7.4	18.2	10.6	0.126	0.093	0.118
6	0.50	6.7	0.6	18.6	0.105	0.079	0.102
6	1.00	17.6	0	16.0	0.093	**	0.101
15	0.10	6.1	11.2	9.6	0.130	0.102	0.115
15	0.50	11.2	2.6	21.4	0.102	0.084	0.122
15	1.00	18.6	4.2	37.8	0.118	0.098	0.133
30	0.10	7.0	9.6	5.8	0.126	0.105	0.146
30	0.50	19.2	4.5	25.6	0.102	0.115	0.136
30	1.00	12.8	7.0	19.2	0.150	0.134	0.224
45	0.10	5.8	6.7	6.4	0.125	0.107	0.143
45	0.50	16.0	4.8	24.0	0.115	0.117	0.104
45	1.00	6.4	16.0	17.6	0.145	0.140	0.214

Note: * Paste too stiff to test
** No result obtainable due to change in shape of downcurve
s.d. Standard deviation

Table 3.9 Details of Continuous Shear Testing of Pastes Containing Admixtures

Mix	Impeller Speed (rpm)	Superplasticiser Dosage (%) S1	S2	Accelerator Dosage (%)	Temperature (°C)
1	250	0	0	0	5, 20
2	500	0	0	0	20
3	500	0	0	0.01	20
4	250	0	0	0.025	5, 20
5	500	0	0	0.05	20
6	500	0	0	0.10	20
7	250	0.3	0	0	5, 20
8	250	0.3	0	0.025	5, 20
9	250	1.0	0	0	20
10	250	1.0	0	0.025	5, 20
11	250	0	0.3	0	20
12	250	0	0.3	0.025	5, 20
13	250	0	1.0	0	20
14	250	0	1.0	0.025	20

The results are presented as follows

Figure 3.8 Mixes 1, 4, 7, 8, 10, 12 (5°C)

Figure 3.9 Mixes 1, 4, 7, 8, 9, 10 (20°C, S1)

Figure 3.10 Mixes 1, 4, 11, 12, 13, 14 (20°C, S2)

Figure 3.11 Mixes 1, 4, 8, 12 (5, 20°C comparison)

Figure 3.12 Mixes 2, 3, 5, 6 (20°C, Accelerator)

All runs were duplicated with the exception of mixes 2, 3, 5 and 6.

3.4.3 Mortar Testing

3.4.3.1 Industrial Workability Test Methods

The investigation of "industrial" workability tests described in this section was carried out at the laboratory of Feb Ltd, Manchester.

All mixes were 1:1.5 cement:sand (sand 1) at w/c 0.40 and contained admixtures as follows :

Figure 3.8 Torque vs Time, 5 °C

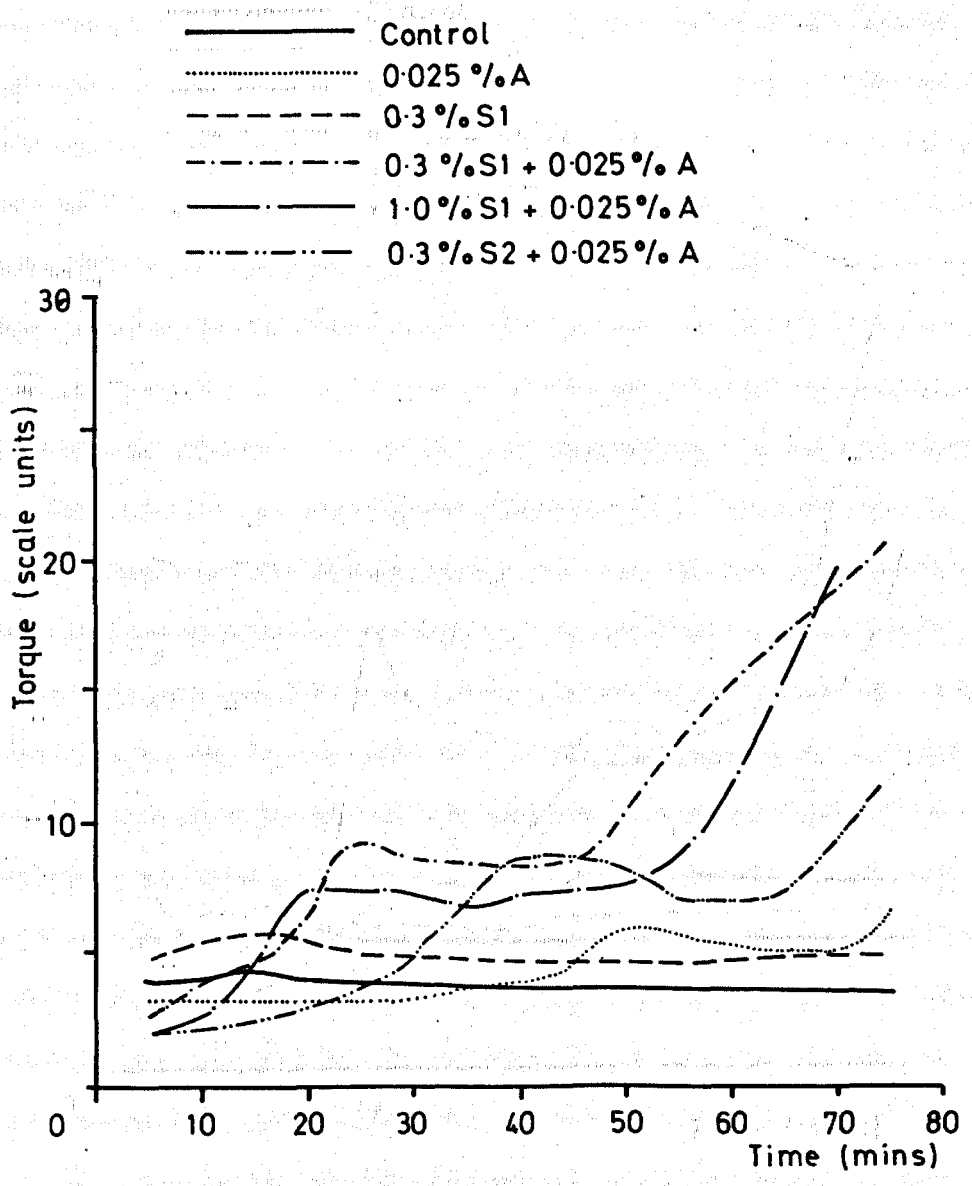

Figure 3.9 Torque vs Time, 20 °C, S1, 0·40 w/c

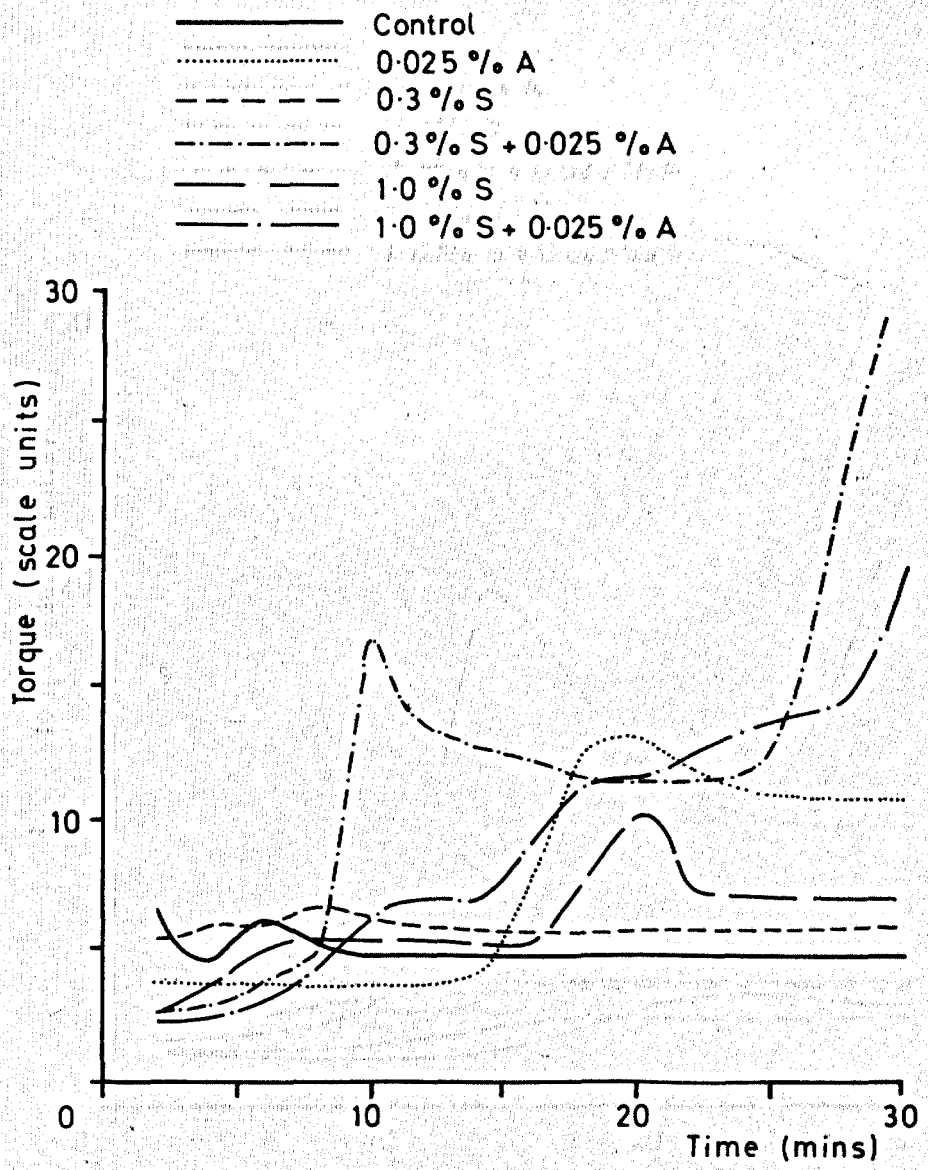

Figure 3.10 Torque vs Time, 20 °C, S2 0·40 w/c

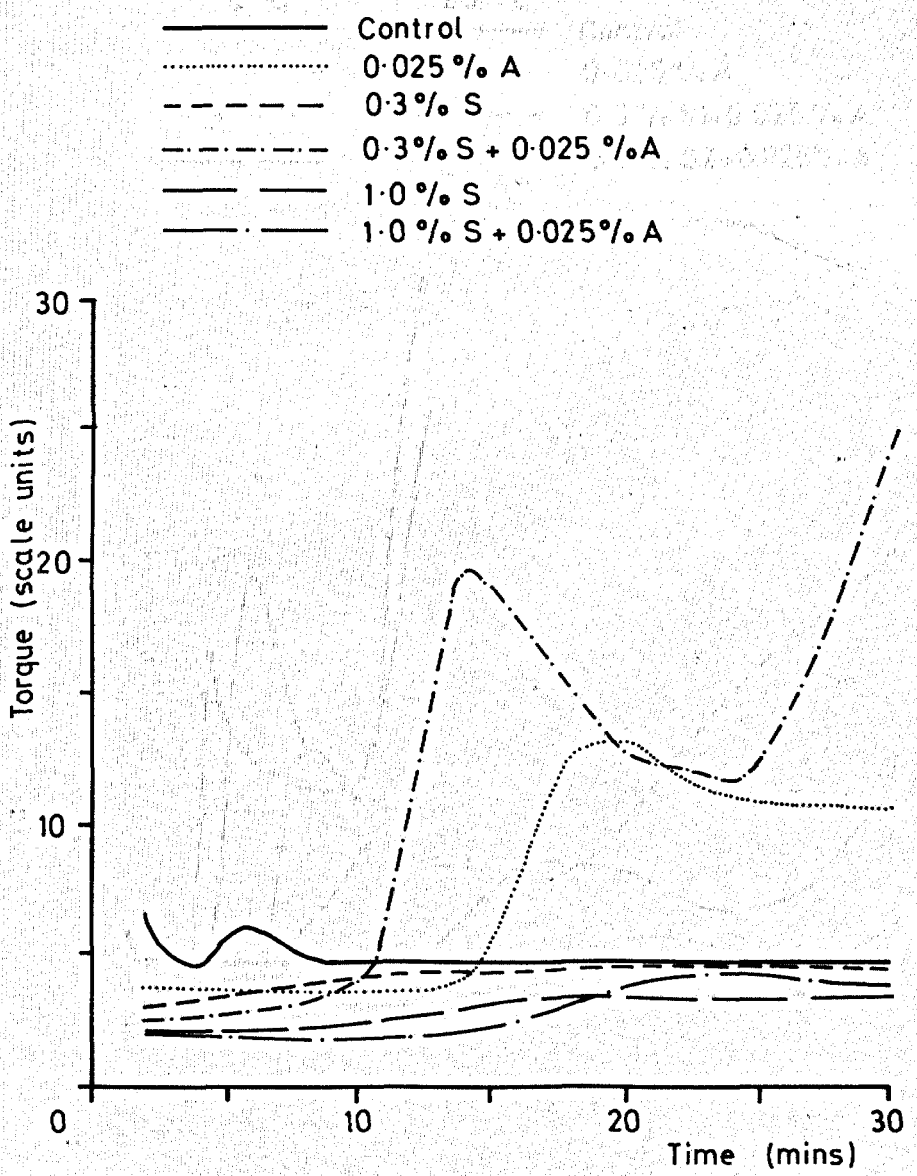

Figure 3.11 Torque vs Time : Comparison of Behaviour at 5, 20 °C

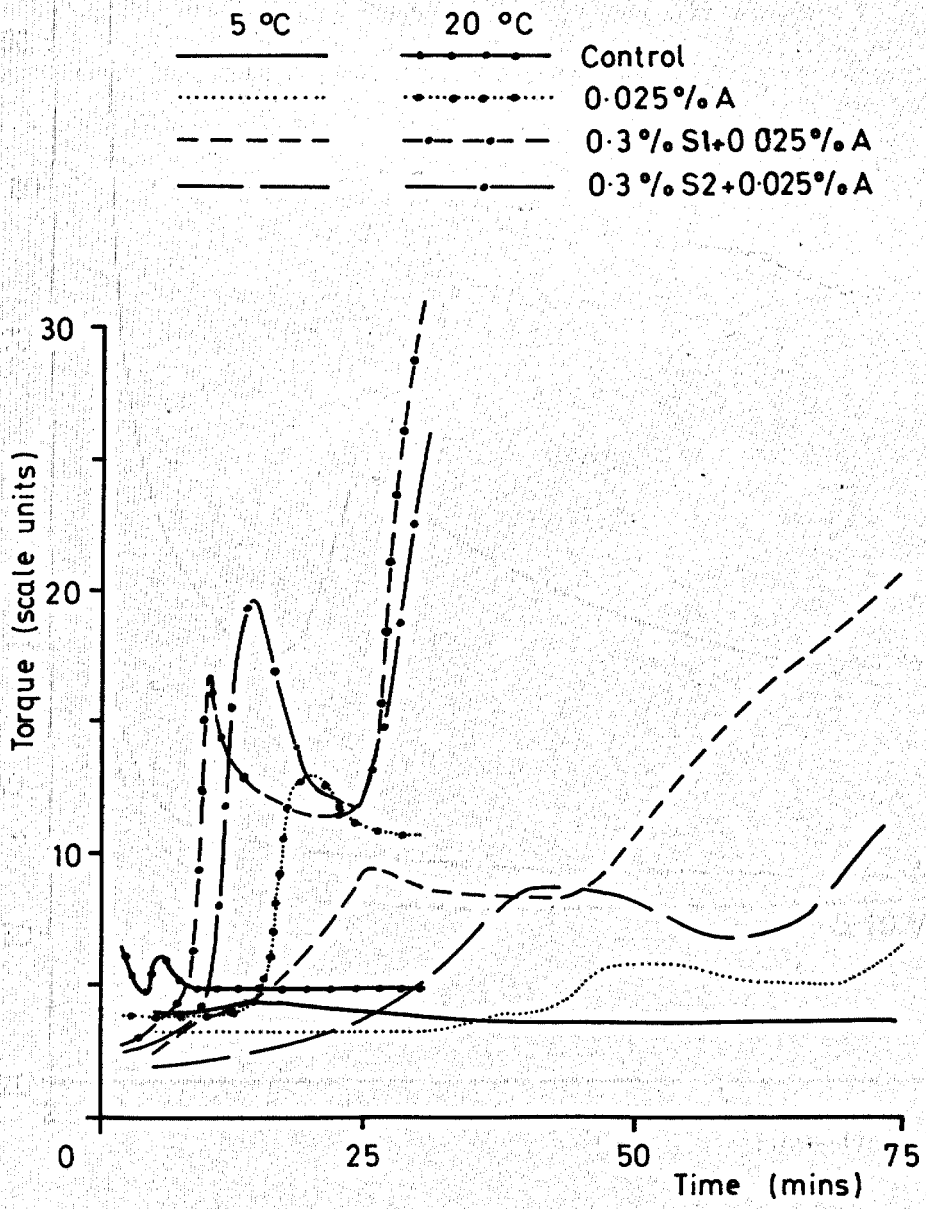

Figure 3.12 Effect of Accelerator Dosage on Early Age Torque vs Time Relationship, 20 °C

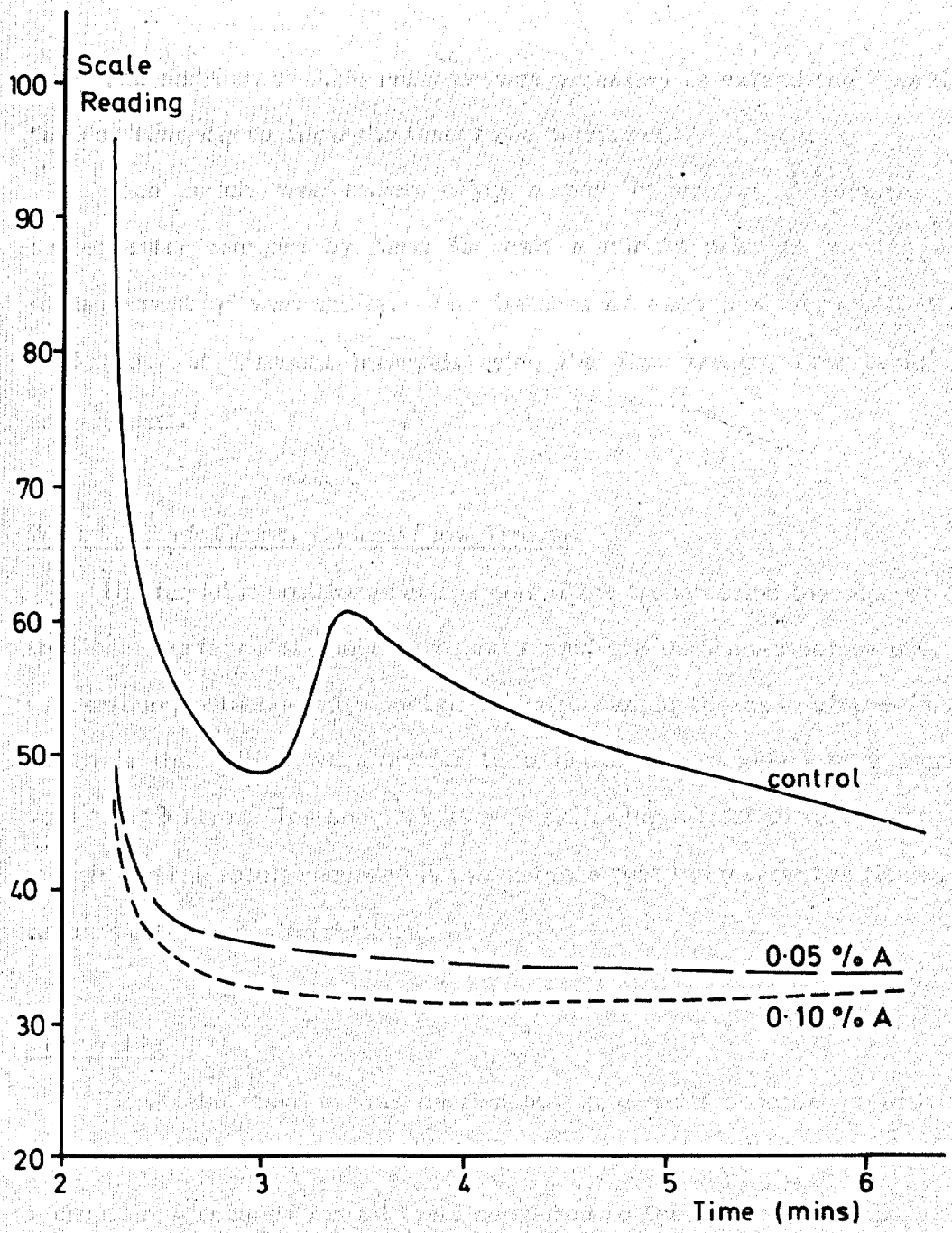

1. Control
2. 0.3% S2
3. 0.3% S2 + 0.025% A + 0.1% retarder
4. 0.6% S2
5. 0.6% S2 + 0.025% A + 0.1% retarder

The addition of 0.1% retarder was necessary to extend the "working" time sufficiently to allow the tests to be carried out.

Each batch was mixed using a pan mixer for 3 minutes and subsequently remixed by hand for half a minute prior to making each measurement of workability. Two batches of each mix were tested for workability at frequent intervals using the flow trough, flow table and spread tests.

West Midlands County Council Flow Trough

The funnel is positioned at one end of the trough using the support and the inner surfaces of the trough and funnel are dampened before use. A rubber bung attached to a metal rod is placed in the base of the funnel which is then filled with mortar to a depth corresponding to a mortar volume of 3 litres. The bung is withdrawn allowing mortar to flow along the trough and the result recorded is the distance that the mortar has flowed 30 seconds after removing the bung.

Flow Table

Flow table testing was carried out in general accordance with BS 4551:1980 ((1)). The highly fluid nature of the mortars led to the use of only 5 drops in 5 seconds for all tests compared to the normal 25 drops in 15 seconds.

The diameter of the mortar sample after spreading is calculated as the mean of 4 diameters at equal intervals and the result reported as

$$\% \text{ flow} = \frac{\text{sample diameter after flow}}{\text{sample diameter before flow}} \times 100$$

Spread Test

Sufficient mortar is poured in to fill the metal cylinder which is placed on the horizontal, dry glass plate. The cylinder is then lifted vertically allowing the mortar to spread freely over the plate. The final diameter of the sample is recorded as the mean of 4 diameters at equal intervals.

Figures 3.13, 3.14 and 3.15 show the effect of admixtures on the loss of workability with time using flow table, flow trough and spread tests respectively.

The correlation between results from different tests is shown on Figures 3.16 and 3.17.

3.4.3.2 Subjective Comments on Mortar Workability at 5-40°C

Observations on the workability of mortars used to make cube specimens for the Pundit test programme (see Chapter 5) are recorded in Table 3.10. These mortars were 1:1.5 cement:sand mixes at w/c 0.40 containing sand 2.

3.5 DISCUSSION

3.5.1 Plain Pastes

3.5.1.1 Flow Curves

The flow curves obtained from coaxial cylinders were always of the form shown on Figure 3.4 designated Type I by Banfill and Saunders (65).

Figure 3.13 Flow Table Results

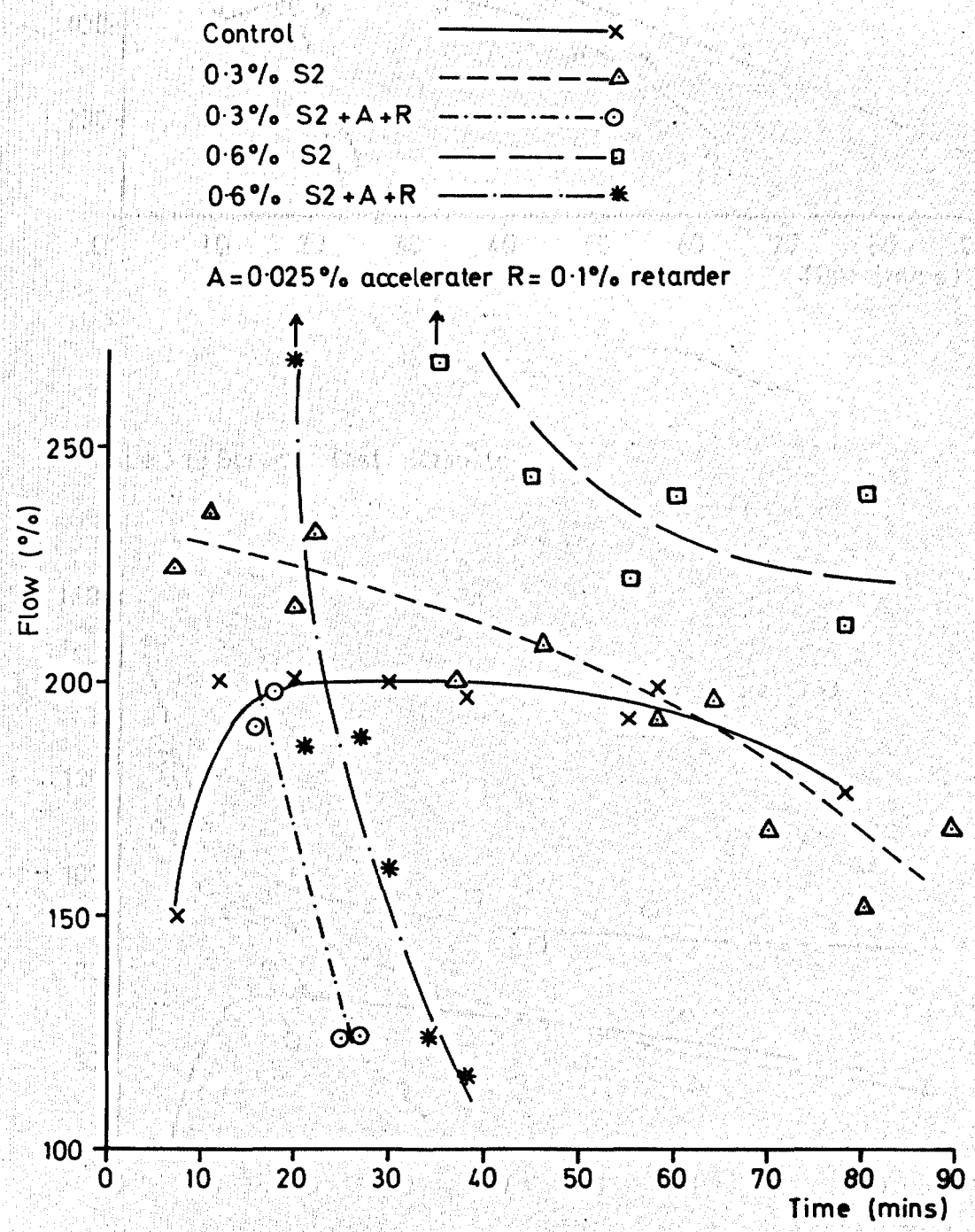

Figure 3.14 Flow Trough Results

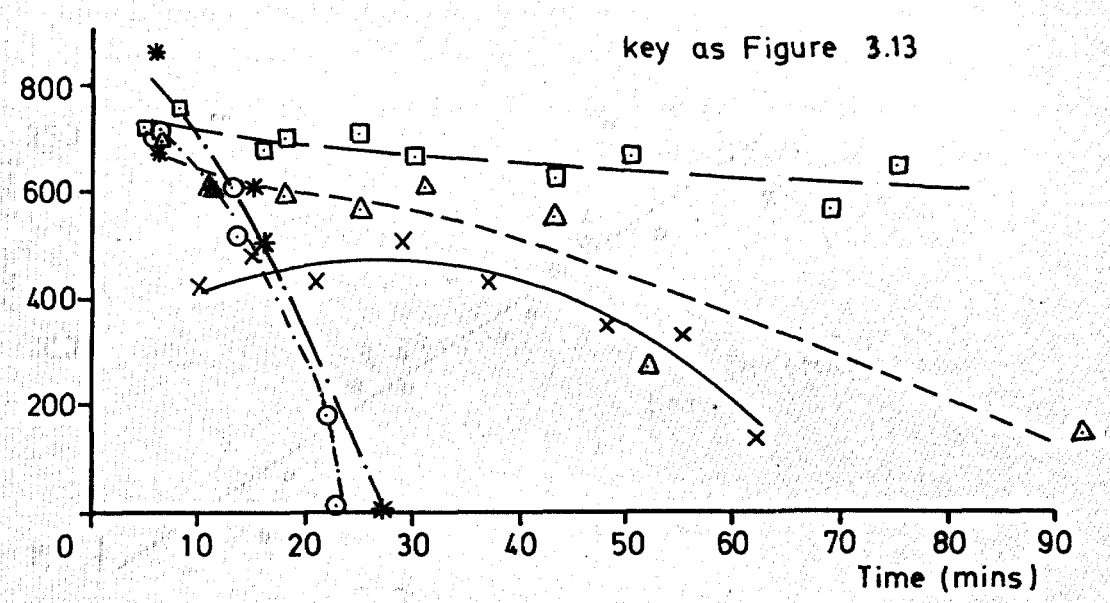

Figure 3.15 Spread Test Results

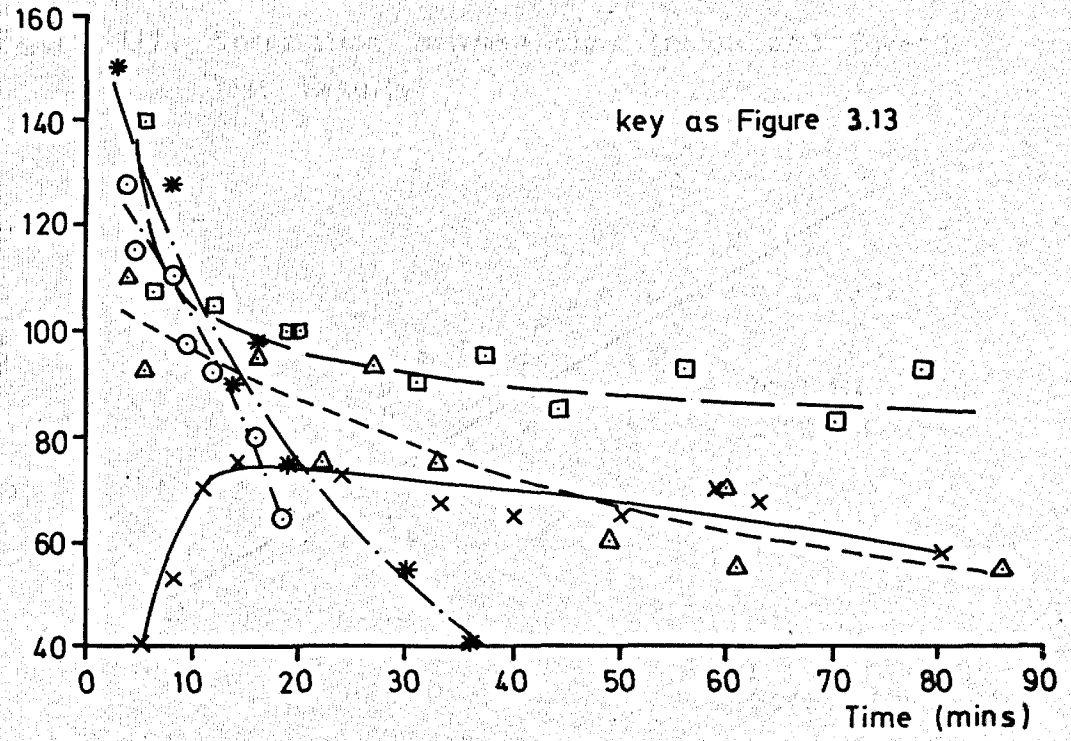

Figure 3.16. Correlation Between Flow Table and Spread Test Results

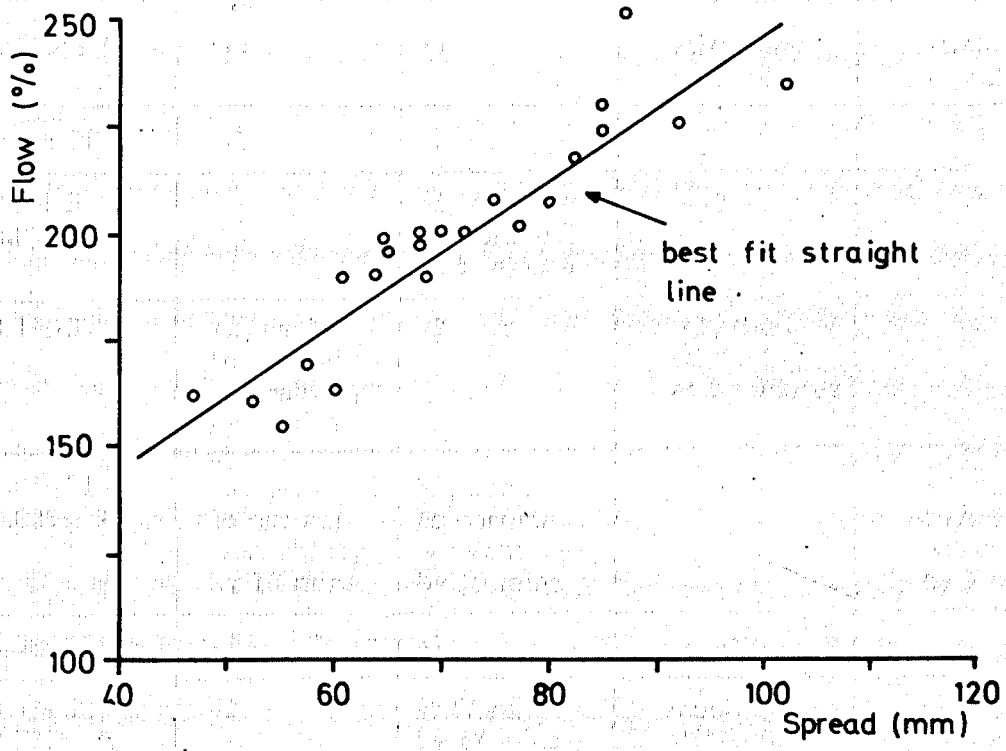

Figure 3.17. Correlation Between Flow Trough and Spread Test Results

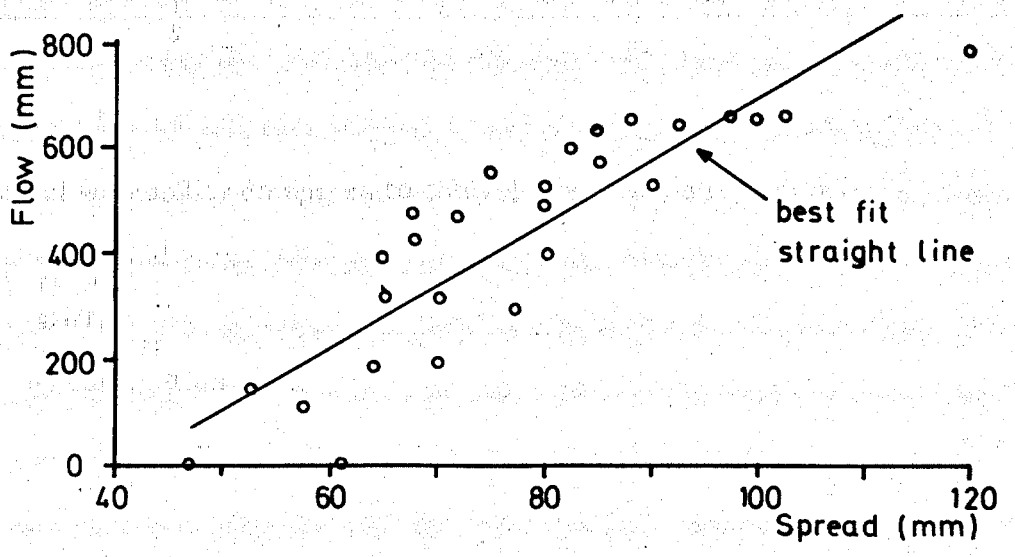

Table 3.10 Subjective Comments on Workability of Mortars Made for Pundit Test Programme

	5°C	20°C	30°C	40°C
0.025% A	+2	+1	stiffening by 8 mins	stiffened rapidly
0.3% S1	-1	-1	-	-1
0.3% S1 + 0.025% A	-	+1, then stiffening at 5 minutes	-2	-2
0.1% S1	+2, back to normal workability by 8 mins	+2	+1, then stiffening at 5 minutes	-
1.0% S1 + 0.025% A	+1, back to normal workability by 10 mins	+1, back to normal workability by 10 mins	-	+2, back to normal workability by 5 mins
0.3% S2	+1	+1	-	-
0.3% S2 + 0.025% A	+2	stiffening by 12 mins	much stiffening at 10 mins	very stiff by 6 mins
1.0% S2	+2	+1	+2	+2
1.0% S2 + 0.025% A	+2	+2	+1, losing workability at 15 mins	+1, losing workability at 8 mins

Key :

Initial workability compared to control mix at same temperature

+2 very fluid
+1 fluid
-1 stiff
-2 very stiff
- no observation

The paste undergoes structural breakdown as the shear rate is increased and the Bingham model is valid for the downcurve.

In contrast the downcurves obtained from the IHC/CC helical system shown on Figure 3.5 tend to curve away from the speed axis which precludes the determination of yield value and plastic viscosity according to the Bingham model. The deviation suggests shear thickening, yet it is shown in section 3.5.1.4 that the paste structure breaks down under shear. The possibility of turbulence in the helical system was considered as an alternative explanation and is discussed in section 3.5.1.2

3.5.1.2 Turbulence

The theoretical background to this discussion is given in Appendix 3.

Earlier work by Tattersall and Bloomer ((2)) showed that turbulence was likely to occur for a helical impeller at a Reynolds number (Re) greater than 10. Thurairatnam and Domone (60) confirmed the occurrence of turbulence for a helical impeller at Re $\approx$ 10 for Newtonian and non-Newtonian fluids although not specifically for cement pastes. If turbulence does occur then resistance to flow is due to inertial as well as viscous forces, hence torque values are higher than expected.

To investigate the possibility of turbulence for the IHC impeller a series of flow curves was obtained for Newtonian fluids of varing viscosity and density such as motor oil and glycerol. To obtain an estimate of Re at the onset of turbulence the speed and corresponding scale reading were noted at the point where deviation from a straight line occurs, shown as point X on Figure 3.18. Re at point X was then calculated using

$$Re = \frac{D^2.N^2.\rho.G}{T}$$

Figure 3.18. Onset of Turbulence for Newtonian and Pseudoplastic Materials

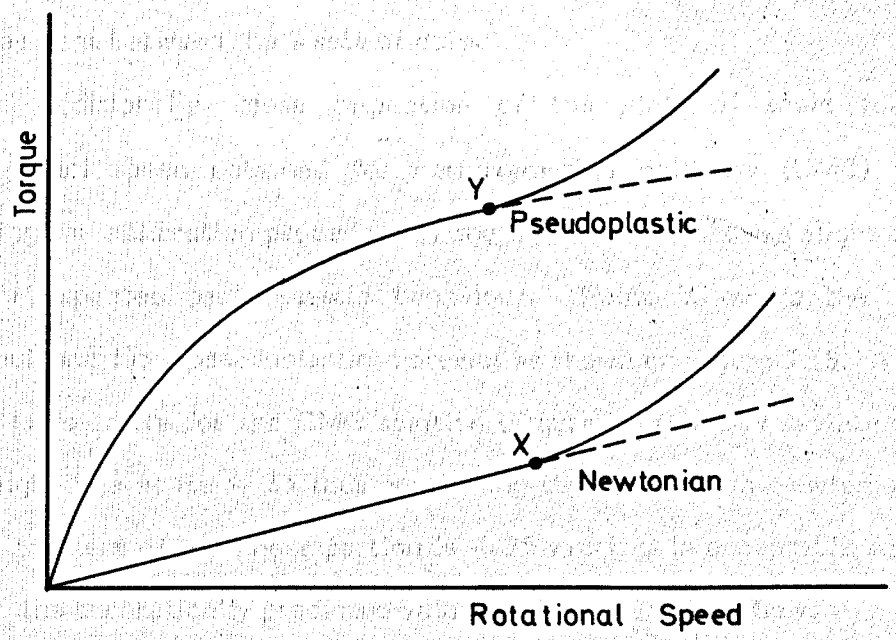

where D = impeller diameter (m)

N = impeller speed at onset of turbulence (rps)

T = torque at onset of turbulence (Nm)

ρ = fluid density (kg/m^3)

G = Calibration constant (m^3)

Re at point X is 13 suggesting that the curvature at higher speeds is indeed due to the onset of turbulence. Considering that this impeller is 1/5 of the size used by Tattersall and Bloomer this may be considered to be good agreement between the 2 sets of data.

Additionally, close inspection of the plots of scale reading vs rotational speed obtained for carboxymethyl cellulose (CMC) solutions during the calibration procedure of the IHC impeller showed slight deviation from expected pseudoplastic behaviour. Point Y marks the onset of turbulence for a pseudoplastic material as shown on Figure 3.18. A graph of ln Np vs ln Re for the CMC solution (Figure 3.19) shows deviation from a straight line at Re $\approx$ 13 thus confirming the result from Newtonian fluids. The gradient of the linear portion is -0.95 which is in acceptable agreement with the theoretically predicted value of -1.0 for laminar flow.

Figure 3.20 shows the likely transition between laminar and turbulent flow for the IHA and IHC impellers with cement paste. This was prepared by assuming the critical Re number to be 13 and paste density 2000 kg/m^3.

Figure 3.21 shows downcurves for Ciment Fondu paste at w/c 0.30 and an ordinary Portland cement paste at w/c 0.35 obtained using the IHC/CC system. Both downcurves clearly deviate from linearity at Re close to 13 thus confirming the occurrence of turbulence for cement pastes.

Whilst it would be possible to obtain yield value and plastic viscosity from the linear portion of the curve for Ciment Fondu at w/c 0.30, it is clear that pastes of higher workability would have flow curves almost

Figure 3.19 ln Np vs ln Re for CMC Solution

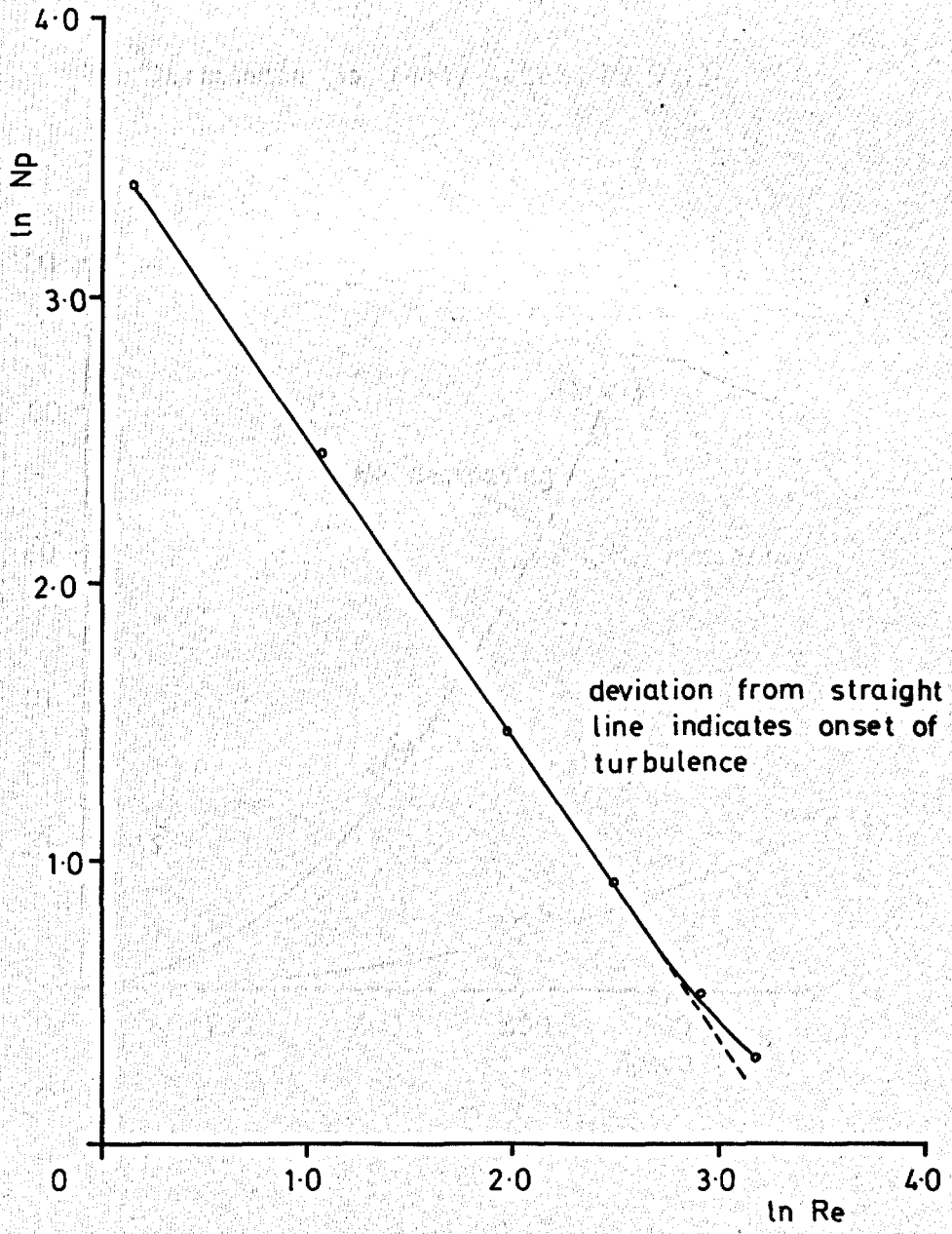

Figure 3.20 Indication of Laminar / Turbulent Regions for Helical Impellers

Turbulence is likely when $Re > 13$

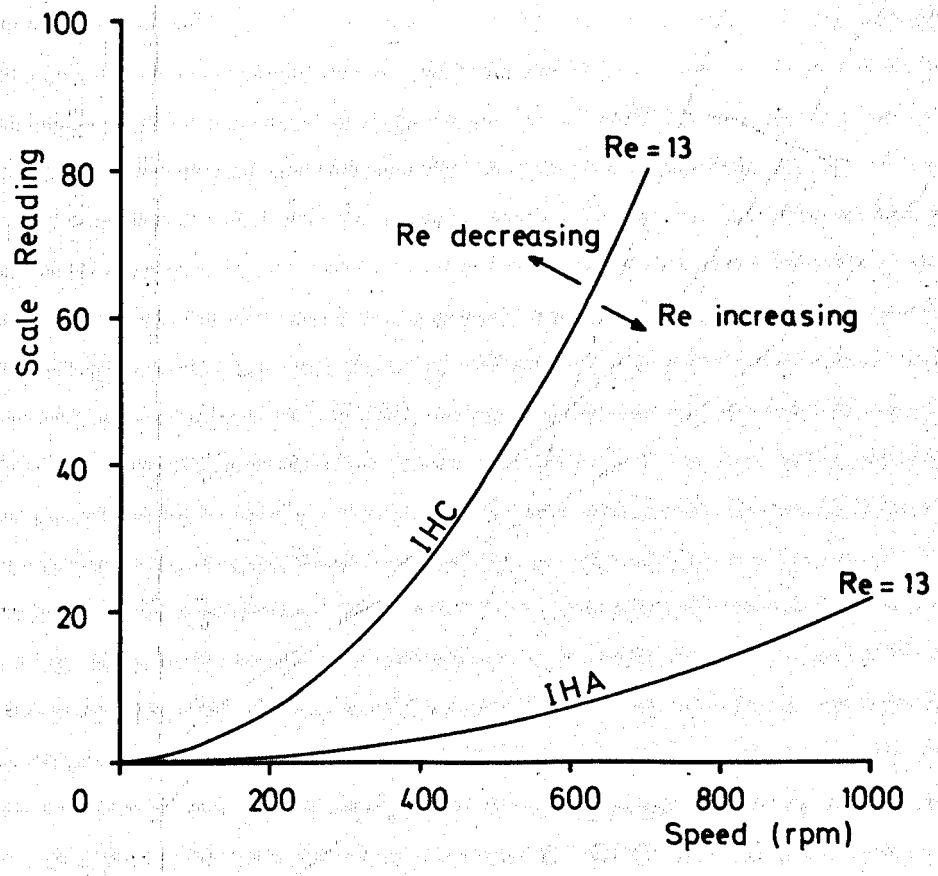

Figure 321 Downcurves Showing Onset of Turbulence ICC/CC System

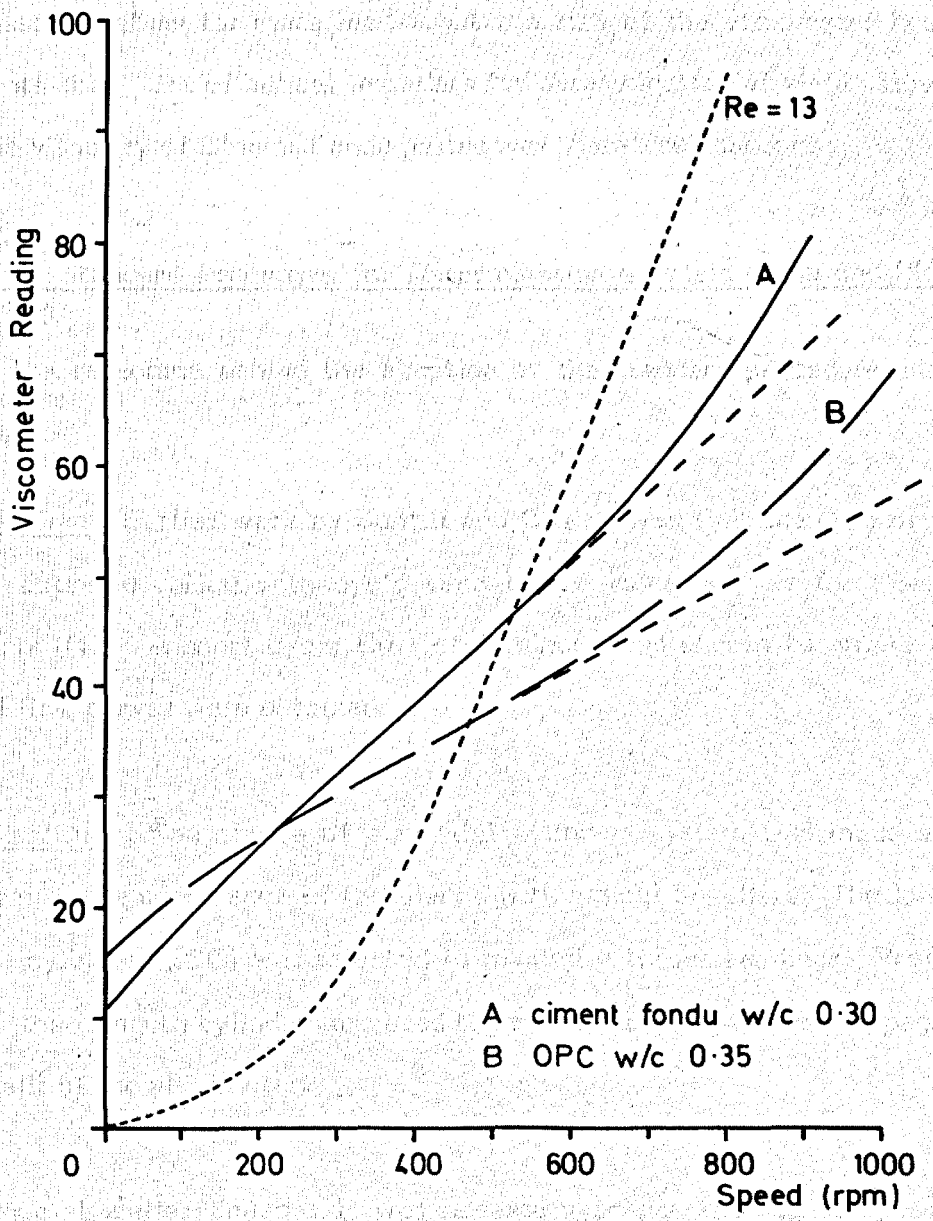

entirely in the turbulent zone. The IHC impeller was thus unsuitable for the study of superplasticised pastes.

A potential solution to the problem is to use the smaller diameter IHA impeller (Re being directly proportional to D) with more blades. The idea was discarded since the maximum number of additional blades was 4 which would result in only a doubling of torque, insufficient for paste of high workability. An alternative option is to increase the depth of immersion in the paste to allow for more blades but the size of the viscometer housing prevents this. Use of helical impellers for determination of yield value and plastic viscosity of Ciment Fondu pastes was therefore abandoned.

3.5.1.3 Standard Procedure for Determination of Yield Value and Plastic Viscosity

The reasoning behind the adoption of the standard procedure was as follows:

Cycle Time : Earlier work by Banfill and Gill showed that the type of flow curve obtained varied with cycle time in the same way as for Portland cements ((4)). A short cycle time of 1 minute was chosen to ensure that type I flow curves were obtained.

Impeller/Cup : The choice of a coaxial cylinders system was made after confirming the occurrence of turbulence with helical impellers. The largest of the cylinders (ICC) was selected to maximise torque readings. Profiled rather than smooth cylinders are used to reduce the likelihood of slippage at the walls of the viscometer.

Maximum Impeller Speed : It was necessary to use the highest possible impeller speed in order to maximise torque readings. This led to the use of 1000 rpm for paste at 0.4 w/c and 400 rpm for 0.30 w/c.

Mixing Regime and Paste Age at Test : It was desirable for pastes to be tested as early as possible in order to study the initial effect of admixtures. This requirement was balanced by the need to ensure that the paste was fully broken down at the time of test. Consideration of the results of time dependent behaviour under shear led to the decision to mix for 5 minutes and begin the test cycle at 6 minutes.

The use of mechanical rather than hand mixing was preferred since it is far more reproducible.

3.5.1.4 Time Dependent Behaviour Under Continuous Shear

The results show that Ciment Fondu pastes undergo structural breakdown under shear in a similar way to Portland cement pastes. However a notable difference is the presence of a double minima in the torque vs time curve. The first minima and subsequent small peak (A and B respectively on Figure 3.6) are always present. Equilibrium was not reached for some pastes, particularly at w/c 0.30 with the IHC/CC system, thus torque continues to decrease after B until the end of the test. The times to A and B appear to be independent of w/c and impeller/cup system. For tests where there is a second minimum in torque (C on Figure 3.6) this value is less than at A for w/c 0.30 but more than at A for w/c 0.40 regardless of impeller/cup system.

These findings are in good qualitative agreement with results for coaxial cylinders reported by Banfill and Gill ((4)).

Further complications are :

i) The observed occurrence of plug flow in the IHA/CC system particularly for paste at w/c 0.30. This is not surprising given that the radius ratio of 1.62 is considerably larger than for either the IHA/CB (1.15) or IHC/CC (1.14) systems.

ii) Almost all of the tests were carried out in turbulent flow. The result for the IHC/CC system at 330 rpm with paste at 0.30 w/c was however in laminar flow. Since the same form of variations in torque was observed for this test it may be said that the form of curve obtained is independent of the flow conditions. This is confirmed by the good agreement between results obtained from coaxial cylinders in laminar flow and the helical systems in turbulent flow as noted above.

The time taken to reach an equilibrium value of torque is greater when using the IHC/CC or IHA/CC systems compared to the ICA/CB system. This is contrary to the expectation that time to equilibrium would be related to shear rate and indicates that the assumption of simple proportionality between $\dot{\gamma}$ and N may not be valid for the helical impeller. It is inevitable that there is a large range in the actual shear rate within the paste under test in the helical system.

The model for the structural breakdown of Portland cement pastes proposed by Tattersall was given in section 1.4.1 of the literature review (62, 63).

According to Tattersall the constant B, obtained as the gradient of a plot of $\ln (T - T_E)$ vs t, may be expressed as

$$B = \frac{2\pi k}{n_o \Psi} . \dot{\gamma} (\dot{\gamma} - \dot{\gamma}_1)$$

where $k, \dot{\gamma}_1$ = constants

n_o = number of structural linkages

Ψ = linkage strength

The occurrence of turbulence for the helical systems leads to errors in torque values and thus numerical analysis of the data presented in this chapter is inappropriate. Values of B obtained for the coaxial cylinders system are given in Table 3 of the report on rheology appended to this thesis. The results show that for the curve OA the value of B is generally higher than for the curve BC indicating a greater number or strength of linkages to be broken after the peak in torque. There are insufficient results to confirm Tattersall's prediction of the dependence of B on $\dot{\gamma}$.

Explanation of Structural Changes

There are 3 possible explanations for the structural changes described above based on (i) chemical, (ii) physical or (iii) a combination of physical and chemical effects.

It is appropriate here to consider the interparticle forces which affect the cement/water system.

The cement particles gain a surface electrical charge due partly to the unequal adsorption of H^+ and OH^- ((5)) and partly to the presence of imperfections in the crystal structure near the surface. This surface charge is compensated by the attraction of ions of opposite sign from solution near the particles and results in the formation of an electrical double layer. Interaction of the electrical double layers as particles approach each other in solution leads to repulsion between the particles. If an electric field is applied to the system a shear plane is formed between the bulk solution and the ions which are strongly attracted to the particle surfaces at an unknown distance from the surface. This potential, which can be measured by electrophoresis, is known as the zeta potential and has been measured by several researchers investigating the effect of admixtures.

Van der Waals interparticle forces arise due to the attraction between atoms which constitute systems of oscillating charges because of the presence of positive nuclei and negative electrons.

The combination of Van der Waals attraction and electrostatic repulsion provides the basis for the classical DLVO theory of colloidal stability developed independently by Deryaguin and Landau ((6)) and Verwey and Overbeek ((7)). The effect of interparticle distance on this combination of forces is shown on Figure 3.22 (61). At low ionic strength the energy barrier to aggregation, which can be overcome only by particles with sufficient kinetic energy, is high and so a stable suspension is formed. As ionic strength increases, the double layer thickness decreases and the energy barrier reduces or disappears altogether resulting in rapid coagulation of the system.

For systems with an extended double layer there can be a secondary minimum in interparticle energy as shown in Figure 3.22. This can occur for coarse suspensions such as cement in water and results in particle flocculation. Flocs are broken down to some extent by shear and may reform when stresses are removed.

It must be noted that the system of hydrating Ciment Fondu is not truly colloidal since many of the particles are too coarse. Forces of attraction and repulsion will still exist as described above but their effect will be less marked.

The following model is proposed as a plausible explanation of the observed behaviour of Ciment Fondu pastes under continuous shear:

The reduction in measured torque is due to deflocculation of groups of cement particles under shearing in accordance with Tattersall's model. At approximately 3 minutes after addition of cement to water changes in solution chemistry cause the sudden precipitation of gel which itself

Figure 3.22 Resultant of Attractive and Repulsive Potential Energy Curves

a) At 3 Electrolyte Concentrations

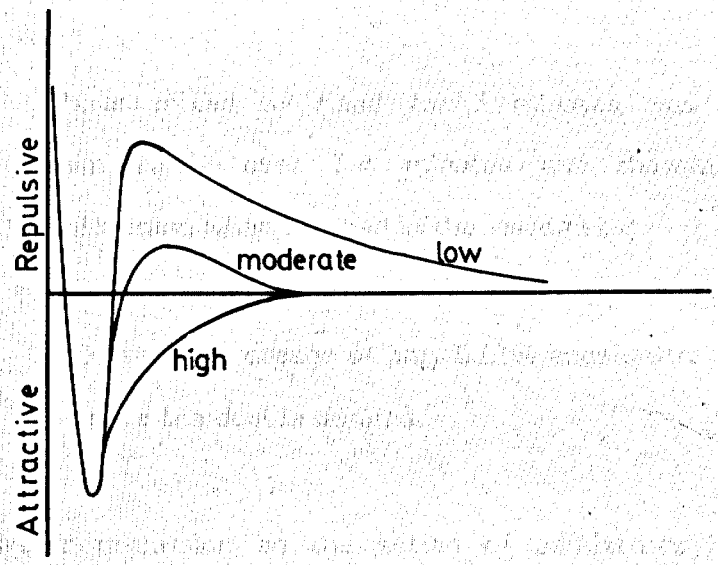

b) Possible Secondary Minimum

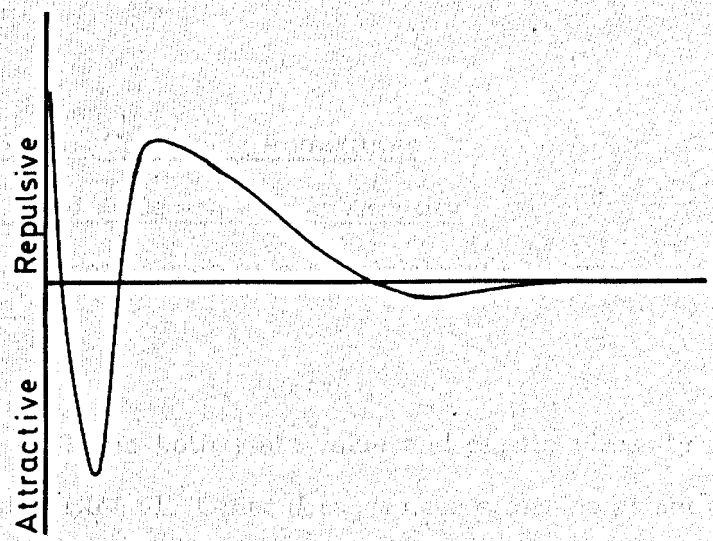

undergoes some breakdown. The difference in behaviour observed for pastes at w/c 0.30 and 0.40 may be explained by differences in the relative contributions of torque from the original cement/water system and newly formed gel as illustrated on Figure 3.23.

The following observations are put forward as evidence in support of this model :

i) Paste mixed by hand for 5 minutes was seen to thicken temporarily over 3-4 minutes and showed no subsequent thickening when sheared in the viscometer.

ii) The double minima are absent when any admixture is included in the paste. A dosage of only 0.01% accelerator was sufficient to remove the double minima.

Further discussion on the action of admixtures is deferred until Chapter 6 when the results of all experimental work will be considered together.

3.5.2 Pastes Containing Admixtures

3.5.2.1 Yield Value and Plastic Viscosity

The effect of each superplasticiser will be considered in turn :

S1

At 0.30 w/c both yield value and plastic viscosity at 6 minutes are improved at 1.0% S1. Other dosages have either no effect or actually cause stiffening compared to the control. In their work on oilwell cements Michaux and Defosse (151) found a similar increase in yield value, although not in plastic viscosity, at a low dosage of a superplasticiser similar to S1. The increase in yield value was attributed to changes in the particle charge

Figure 3.23. Possible Explanation for Double Minimum in Torque vs Time Relationship Observed for Plain Pastes

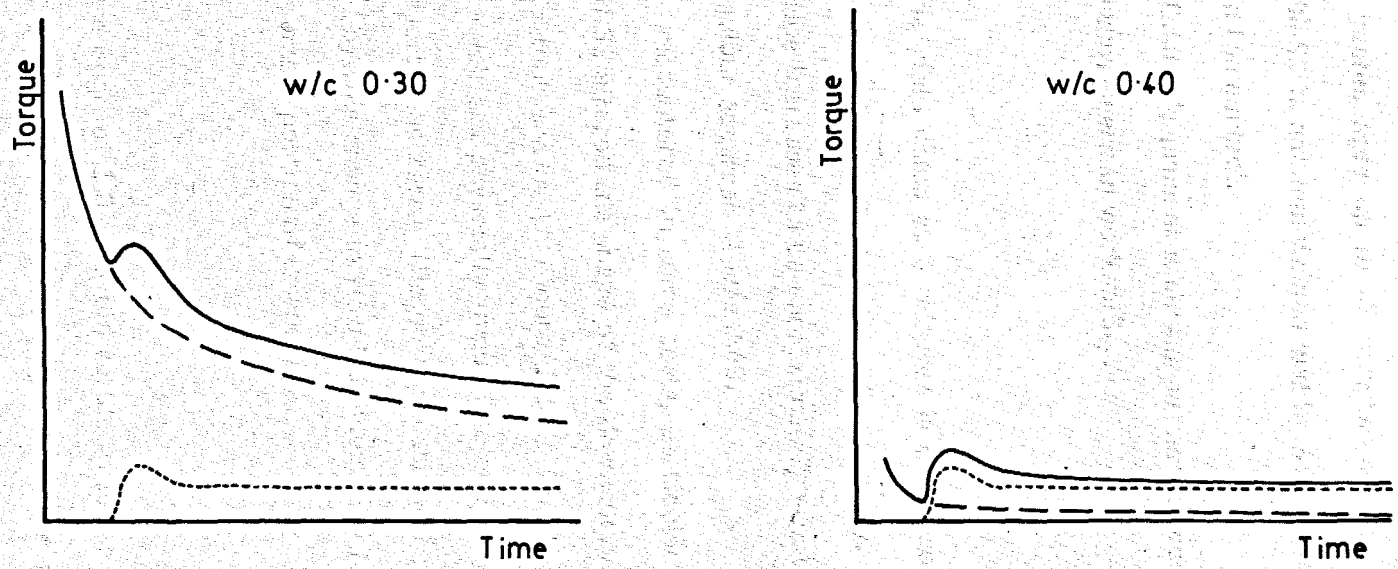

as superplasticiser molecules adsorbed onto the surface.

Very early improvements in workability were noted for 0.01% (up to 25 seconds) and 0.05% (up to 30 seconds) after which marked stiffening occurred. Tests at pastes ages up to 45 minutes showed that the early improvement for 1.0% S1 is not maintained and by 45 minutes the paste is stiffened compared to the control.

The results at 0.40 w/c present a similar pattern of behaviour with no lasting worthwhile improvement in workability.

S2

At w/c 0.30 the yield value at 6 minutes is decreased for 0.5% and 1.0% S2 although there is little effect on plastic viscosity. At later times however the yield value increases to be approximately equal to that for the control. Similar behaviour occurred at w/c 0.40.

Difficulty was encountered in some tests, particularly at 0.40 w/c, since the presence of S2 altered the shape of the downcurve from that of a Bingham material to that shown in Figure 3.24. This led to apparently negative intercepts which are physcially impossible and so yield values for these mixes were reported as zero. The determination of plastic viscosity was also complicated by this change in flow behaviour and for 1.0% S2 at 6 minutes there was no linear portion of downcurve.

S3

At w/c 0.30 a dosage of 1.0% S3 did result in lower yield value and plastic viscosity at 6 minutes. At later ages however rapid stiffening occurred for both the 0.5% and 1.0% mixes to such an extent that some pastes could not be tested in the viscometer.

At w/c 0.40 the behaviour was similar although less pronounced but no improvements in yield value or plastic viscosity were noted.

Figure 3.24. Downcurve Obtained for Some Mixes Containing S2

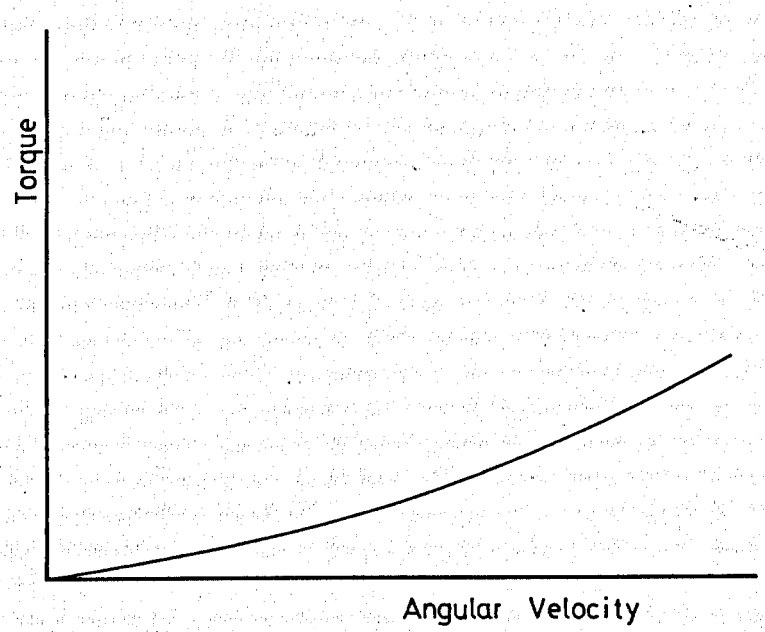

The poor performance of S3 in these tests resulted in its exclusion from other test programmes.

Accelerated Pastes

It was considered necessary to check the plasticising effect of the accelerator after observing that initial workability seemed to be improved.

However the yield value and plastic viscosity of pastes containing up to 0.1% accelerator show no clear trends with increasing accelerator dosage and results at 0.30 w/c are very scattered.

3.5.2.2 Time Dependent Behaviour Under Continuous Shear

The plots of scale reading vs time provide a very useful indication of the time dependent behaviour of pastes containing admixtures. The results for mixes containing either S1 or S2 alone are in good agreement with the results of yield value and plastic viscosity discussed earlier.

An improvement in workability over the control is indicated by a lower scale reading at a given time. Improvements in workability compared to control, according to Figures 3.8 - 3.11 are given in Table 3.11.

Table 3.11 Improvement in Workability due to Superplasticisers

Mix	Improvement in Workability (minutes)	
	5°C	20°C
0.025% A	33	14
0.3% S1	0	0
0.3% S1 + 0.025% A	12	8
1.0% S1	-	7
1.0% S1 + 0.025% A1	14	8
0.3% S2	-	>30
0.3% S2 + 0.025% A	26	10
1.0% S2	-	>30
1.0% S2 + 0.025% A	-	>30

These results confirm the superior performance of S2 compared to S1 at 20°C and at 5°C, although only 1 mix containing S2 was tested at both temperatures. The initial plasticising effect of the accelerator is also shown by these results. Figure 3.12 shows that there is a reduction in initial torque which becomes progressively larger as accelerator dosage increases. This difference becomes less pronounced as time increases until at 6 minutes it no longer exists. Since tests for yield value and plastic viscosity were carried out at 6 minutes it is now clear why no plasticising effect was observed.

The smallest dosage of accelerator was sufficient to cause the absence of the first minimum and subsequent small peak observed for plain paste. This suggests that (i) the accelerator acts as a deflocculating agent and/or (ii) the accelerator causes changes in solution chemistry such that early gel precipitation does not occur.

3.5.3 Mortars

3.5.3.1 Industrial Workability Tests

Before discussing the results in detail it is appropriate to consider (i) the mixing procedure and (ii) the merits of the 3 test methods used.

(i) A pan concrete mixer is generally considered to be unsuitable for fluid mortars. Poor mixing was observed for all batches and additional mixing by hand was required to produce a homogeneous mix. Pan mixers are however in common use on site and so the testing conformed to normal practice.

(ii) The flow table is useful only for mixes of low or medium workability since very fluid mortars flow off the table during the test. In contrast the flow trough is good for very fluid mixes but not for stiffer mixes which do not "flow" at all along the trough. Differences in surface wetness of the trough cause variation in results for the same mix and the test is cumbersome and inconvenient to use. The spread test is by

far the quickest to carry out and gave results over a wide range of workability. Results less than about 60 mm should be considered of doubtful value since mortar of such low workability cannot be poured into the mould.

Figures 3.13, 3.14 and 3.15 show that each test method gave similar patterns of behaviour for the mixes tested.

The workability of the control mix increases up to about 15 minutes before remaining virtually constant until 60 minutes.

Each of the mixes containing admixtures showed improved workability compared to the control mix as shown below:

0.3% S2	60 minutes
0.3% S2 + A + R	15 minutes
0.6% S2	> 80 minutes
0.6% S2 + A + R	20 minutes

Tests on mixes of smaller volume showed that the rate of stiffening increases with increasing mix volume. This is probably due to the greater amount of heat evolved.

There is reasonably good correlation between flow table and spread ($r = 0.91$) and flow trough and spread ($r = 0.88$) according to linear regression analysis. Better correlation is unlikely since each test depends to a different extent on yield value and viscosity which are varied disproportionately by the admixtures.

Mixes containing 0.6% S2 have a beige surface layer which disappears after 5-10 minutes if mixing is continued. This was also noted on earlier testing of pastes containing 1.0% S1 or S2 but was not observed for 0.3%

mixes. The disappearance of the surface colour corresponded closely with a marked drop from very high to high workability for the 0.6% S2 mortar mix.

The possible superplasticiser mechanisms are discussed in Chapter 6.

Tests were carried out on a small number of mixes containing varying proportions of S2 and accelerator with the aim of producing a water reduced mortar with improved workability. This was unsuccessful since it was found that even a 5% reduction in water content led to a very rapid loss of workability.

3.5.3.2 Subjective Comments on Mortar Workability at 5-40°C.

There is very good agreement between the subjective comments for mixes at 5 and 20°C with both the structural breakdown curves for pastes and with the results of workability tests on mortars at 20°C. It is encouraging that laboratory tests on cement pastes provide a good indication of the behaviour of large scale mortar mixes. Batch size was however shown to have an effect on mortar stiffening with larger batches stiffening more rapidly.

3.6 CONCLUSIONS

3.6.1 Plain Pastes

1. The behaviour of Ciment Fondu pastes is broadly similar to that of Portland cement pastes in that structural breakdown occurs under shear and they show Bingham type behaviour.

   The yield value and plastic viscosity of Ciment Fondu pastes are slightly lower than those for Portland cement pastes at the same w/c ratio.

2. Rheological testing of Ciment Fondu pastes should be carried out with strict control of temperature.

3. Results from time dependent behaviour under continuous shear suggest that there is no real increase in paste stiffness up to 40 minutes with slight stiffening occurring after this time.

4. Turbulent flow in cement pastes was shown to occur for the helical impellers operating at Reynolds numbers exceeding approximately 13. This problem makes the helical system unsuitable for determination of yield value and plastic viscosity of high workability Ciment Fondu pastes.

5. In continuous steady shear experiments a double minima occurs in the torque vs time curve. This may be explained by the interaction between paste deflocculation and gel formation.

6. There is good qualitative agreement between results of time dependent behaviour under continuous shear obtained in laminar and turbulent flow. The use of the helical impeller to prevent sedimentation is therefore justified for such experiments although quantitative analysis of the data is not possible.

3.6.2 Pastes Containing Admixtures

1. None of the 3 superplasticisers tested gave the very large improvements in workability normally seen when superplasticisers are used with Portland cement. The effectiveness of the superplasticisers decreases in the order S2 > S1 > S3 with S2 capable of improving workability compared to the control for longer than 30 minutes at both 5 and 20°C.

Pastes containing S3 generally showed stiffening compared to the control and so S3 was not included in the testing described in Chapters 4, 5 and 6.

2. At low dosages all superplasticisers actually caused increases in both yield value and plastic viscosity.

3. The use of S2 at a dosage of > 0.5% alters the form of the flow curve obtained and reduces the yield value at early ages to zero.

4. The presence of any admixture at any of the dosages tested removes the double minima in the torque vs time curves obtained under steady continuous shear.

5. Use of the accelerator alone has an initial plasticising effect which increases with increasing dosage. At 6 minutes there is however no difference compared to the control paste.

6. The continuous steady shear experiments provide a good indication of the time dependent behaviour of mixes containing admixtures. There is good agreement with results of yield value and plastic viscosity determinations at different ages and with large scale tests on Ciment Fondu mortars.

   The results of these tests confirm the superior plasticising effect of S2 compared to S1.

7. Of the 3 "industrial" workability methods investigated the spread test is the most convenient to use and gives reasonably reproducible results provided that the spread value exceeds 60 mm.

REFERENCES

Reference numbers in double brackets refer to references used only in this chapter. Numbers in single brackets refer to references included in the review of literature in Chapter 1.

1. BS 4551: 1980. Methods of Testing Mortars, Screeds and Plasters.
2. TATTERSALL G.H, BLOOMER S.J; Mag of Concr Res. Vol 31, No 109, Dec 1979, pp 202-210.
3. METZNER A.B, OTTO R.E; J. Amer Inst of Chem Engineers, 1957, pp 3-10.
4. BANFILL P.F.G, GILL S.M; 8th Conf on Chem of Cement, Brazil, 1986, Vol. VI, pp 223-227.
5. FURLONG D.N, YATE D.E, HEALY T.W; "Fundamental properties of the oxide/aqueous solution interface" in "Electrodes of Conductive Metallic Oxides", part B, S. TRASSATI ed., Elsevier 1981. Quoted by CHAPPUIS J; 8th Int Conf on Chem of Cem Brazil 1986 Vol VI pp 544-549.
6. DERYAGUIN B.V, LANDAU L; Acta Physiochem. URSS, 14, 1941 p 633. Quoted by TADROS Th F Colloids and surfaces 18 (1986) pp 137-173.
7. VERWEY E.J.W, OVERBEEK J.Th.G; Theory of Stability of Lyophobic Colloids, Elsevier, Amsterdam, 1948. Quoted by TADROS Th F, reference as in ((6)).

CHAPTER 4 HYDRATION KINETICS

4.1 INTRODUCTION

The problem of set retardation caused by the use of superplasticising admixtures with Ciment Fondu has already been identified (153, 154). It was important to quantify such retardation and therefore a comprehensive study of hydration kinetics was undertaken.

Isothermal conduction calorimetry is a very useful technique for studying rates of reaction and most of the work described in this chapter was carried out using this method. The type of calorimeter used was the Oxford Conduction Calorimeter (Calox) developed at Oxford University by Dr. D. Double.

Also described is the use of the Vicat needle penetration test to measure setting times. A thermocouple was embedded in the specimen to enable paste temperature to be monitored during setting.

Initially testing was carried out on plain pastes over a range of temperatures in order to establish a background against which the effect of admixtures could be compared. Subsequently the influence of a large number of admixture combinations was investigated at several test temperatures.

4.2 THEORETICAL BACKGROUND TO CONDUCTION CALORIMETRY

4.2.1 Tian's Analysis ((1))

The Calox calorimeter does not operate under truly isothermal conditions since the monitoring of heat evolution is dependent on the measurement of a small temperature difference between the specimen container and the heat sink, the latter being maintained at constant temperature.

Tian's analysis may be applied provided that this temperature difference is small, in practice less than 1°C.

The calorific power W developed in a calorimeter at any time t is partly lost to the heat sink via the thermoelectric sensors and partly used to raise the temperature of the calorimeter cell and its contents.

The heat exchange from the container to the heat sink is proportional to the temperature difference ΔT across the interface with c_1 (the constant of proportionality) being the heat transfer coefficient. The heat exchange loss w_1 is thus given by

$$w_1 = c_1 . \Delta T$$

The amount of heat w_2 required to raise the temperature of the cell and its contents is given by

$$w_2 = c_2 . \frac{d(\Delta T)}{dt}$$

where c_2 is the heat capacity of the system.

The total calorific power is thus given by:

$$W = w_1 + w_2 = c_1 . \Delta T + c_2 . \frac{d(\Delta T)}{dt}$$

For small temperature differences, the voltage output V from the thermoelectric sensors is proportional to the temperature difference ΔT. The equation may thus be written:

$$W = k_1.V + k_2.\frac{dv}{dt} \qquad \text{(Tian's equation)} \qquad ((1))$$

where k_1 and k_2 are constants

The use of Tian's equation thus enables calculation of the rate of heat evolution provided that the voltage output and rate of change of voltage are known. The cumulative amount of heat produced may be calculated as the area under the graph of the rate of heat evolution against time.

Evaluation of k_1 and k_2

The constants k_1 and k_2 are determined by measuring the voltage response with time when a known electrical resistance embedded in a block of cement is supplied with a known voltage and hence a known rate of heat evolution. The voltage output obtained is of the form shown in Figure 4.1.

Integration of Tian's equation for the period when heat is being produced gives :

$$\ln\left(1 - \frac{V}{V_o}\right) = -\left(\frac{k_1}{k_2}\right).t$$

and during the cooling period gives :

$$\ln\left(\frac{V}{V_o}\right) = -\left(\frac{k_1}{k_2}\right).t$$

In both cases V_o is the steady state output voltage as shown on Figure 4.1 and is given by

$$W = k_1.V_o$$

Figure 4.1. Voltage Output from Calox During Calibration

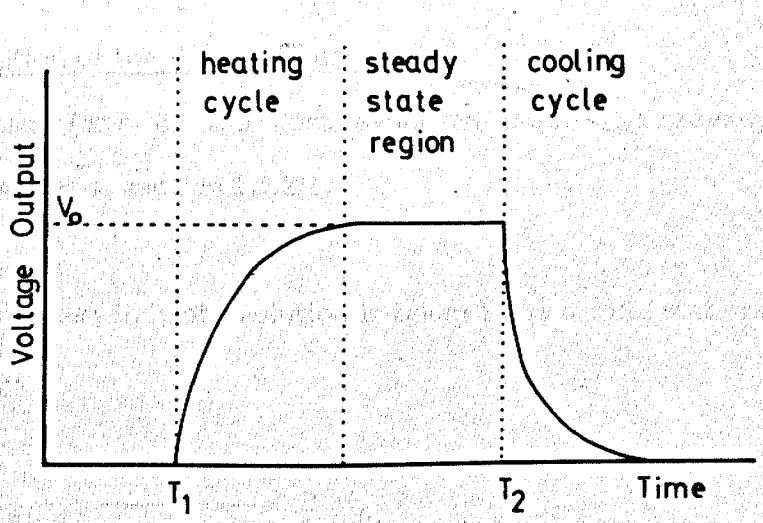

T_1 Time zero for heating cycle
T_2 Time zero for cooling cycle

Where $W = \frac{(\text{voltage applied to resistor})^2}{\text{resistance}}$

and t is the time measured from the start of the cycle. The constant k_1 can thus be found. A graph of $(1 - V/V_o)$ or $\ln (V/V_o)$ vs t should give a straight line of slope $-k_1/k_2$ from which k_2 can be determined.

In practice the occurrence of small heat losses means that the graph is not a perfect straight line, rather a shallow curve. To avoid variation in fitting the best straight line it is prudent to standardise on a certain arbitrary set of times from which to obtain k_2.

4.2.2 Application of the Avrami Equation (56)

The general form of the heat evolution curve has already been described in Chapter 1, section 1.5.2.1.

If the main peak in heat evolution is taken to be a solid state reaction of the type

$$A_{solid} \longrightarrow B_{solid} + \text{heat} \quad \ldots \quad \{1\}$$

the rate of heat evolution at any time can be taken to be proportional to the rate of reaction. The kinetics of many solid state reactions such as growth of nuclei in metals and crystallisation fit the Avrami equation given below:

$$X = 1 - e^{-K.t^n} \quad \ldots \quad \{2\}$$

where X is the fraction transformed at time t and K,n are constants. It has been found that the hydration of pure cement compounds fits the equation

very well (57) while that of real cement deviates somewhat due to the contributions of the different phases at different times to the overall hydration. Nevertheless the Avrami parameters can provide a useful indication of the way in which hydration mechanisms are altered by changes in cement composition or temperature.

It is relevant to comment here on the process of crystal nucleation and on crystal growth which is responsible for the evolution of heat from the hydrating system.

Nucleation of crystals from solution can occur as a homogeneous or heterogeneous process.

Homogeneous nucleation : occurs spontaneously from supersaturated solutions when the degree of supersaturation governs the rate of nucleation.

Heterogeneous nucleation : crystals form due to the presence of foreign, insoluble material which provides sites for nucleation at reduced energy levels. Crystalline hydrates act as further nucleation sites thus "secondary" nucleation will accelerate the production of hydrates.

The inevitable presence of foreign material in commercial Ciment Fondu means that heterogeneous nucleation is the most likely mechanism although the degree of supersaturation still governs the rate of nucleation. As the degree of supersaturation increases the critical size of a nucleus decreases thus more viable crystals will form. Agitation of hydrating cement systems increases the rate of nucleation due to the disruption of previously formed crystals by impeller or by other particles to form additional small crystals.

Confirmation of this suggestion can be found by comparing the setting time of paste and concrete. George found that the paste setting time was longer than that of concrete (4). This can be attributed to the action of aggregate particles as heterogeneous nucleation sites and also to their effect of breaking down crystal nuclei during mixing.

The viscosity of the solution is also important with nucleation being supressed in a highly viscous solution due presumably to reduced ionic mobility.

After nucleation crystal growth occurs as ions moving near the crystal lattices approach closely enough to become orientated in their correct position. The decrease in surface energy which accompanies crystal growth acts as a driving force for spontaneous growth and results in the evolution of heat.

For the process described by equation {1} above, if ΔB is the heat evolution in J/mole and $\Delta B/s$ can be measured then the rate of reaction can be found.

The form of the reaction is shown in Figure 4.2. A difficulty with using the Avrami equation in this form for cement is that data arerequired for approximately 10 years before the fraction converted approaches unity. The problem is overcome by plotting the derivative form shown in Figure 4.3 whose equation is

$$\frac{dx}{dt} = n.K.t^{n-1}.e^{-K.t^n} \quad \ldots\ldots \quad \{3\}$$

where dx/dt is the rate of reaction at time t and can be equated to the rate of heat evolution if a suitable scaling factor for ΔB is calculated. The form of Figure 4.3 is seen to be similar to that of the main peak of heat evolution.

Figure 4.2. Avrami Equation

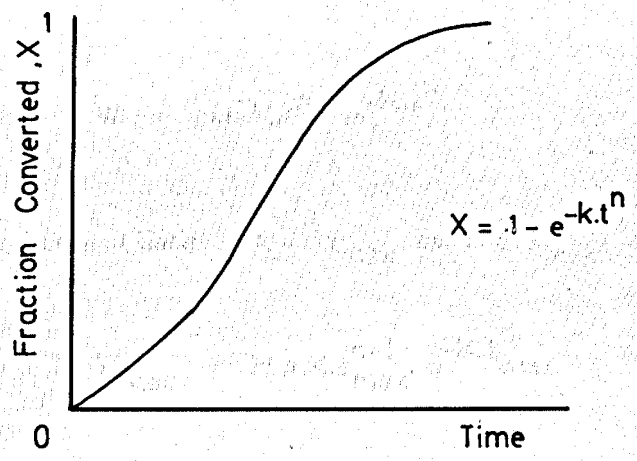

Figure 4.3. Derivative Avrami Equation

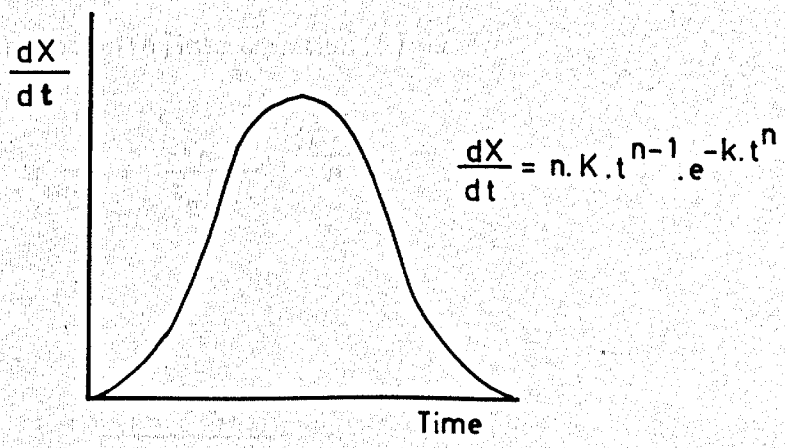

If dx/dt is related to W by a thermal conversion constant H, then

$$W = H.dx/dt$$

From equation {3}

$$W = H.n.K.t^{n-1}.e^{-K.t^n} \quad \ldots\ldots \quad \{4\}$$

From the experimental data $W = W_{max}$ at $t = t_{max}$, so

$$W_{max} = H.n.K.t_{max}^{n-1}.e^{-K.t_{max}^n} \quad \ldots\ldots \quad \{5\}$$

Also at $t = T_{max}$, $\frac{d}{dt}\left(\frac{dx}{dt}\right) = 0 = \frac{dW}{dt}$ and therefore $\frac{d^2X}{dt^2} = 0$

And thus $$-n.K.t^n + (n-1) = 0$$

Thus at the peak $t_{max}^n = \frac{n-1}{n.K}$ or, $K = \frac{n-1}{n.t_{max}^n}$ $\ldots\ldots$ $\{6\}$

Substituting equation {6} into equation {5} gives

$$W_{max} = \frac{H(n-1)}{t_{max}}.e^{\frac{(1-n)}{n}}$$

from which

$$H = \frac{W_{max}.t_{max}}{n-1}.e^{\frac{(n-1)}{n}} \quad \ldots\ldots \quad \{7\}$$

To obtain the best fit between experimental and calculated data the value of n is varied, typically between 2 and 3.5, whilst the origin for the Avrami equation must be shifted to take account of the dormant period in cement hydration as shown on Figure 1.8, Chapter 1.

The following interpretation of the physical significance of n is due to Dr. J.H. Sharp ((2)). He suggests that the significance is twofold and concerns the mechanisms of nucleation (n_1) and growth (n_2) of the new phase in the material. For a linear nucleus n_1 is around 1, for a platy, two dimensional nucleus n_1 is around 2 while for a cubical, three dimensional morphology n_1 is approximately 3. The value of n_2 is similarly affected by the form of crystal growth and the overall Avrami parameter n is obtained by adding n_1 and n_2. Thus the maximum value of n is 6, corresponding to 3-dimensional growth from cubic nuclei. The significance of the rate constant K cannot easily be defined since it is dependent on the value of n.

4.3 EXPERIMENTAL PROCEDURES

4.3.1 Oxford Conduction Calorimeter (Calox)

4.3.1.1 Calibration

The calibration procedure has already been described in section 4.2.1 above. Calibration runs were carried out for cement blocks containing 10g and 15 g of Ciment Fondu at w/c 0.25 and 0.50 with the input voltage varying from 3V to 5V.

4.3.1.2 Operation

The Calox unit is shown diagrammatically in Figure 4.4. Two such units were available and could be used simultaneously. The Calox calorimeter is capable of giving information on heat evolution from the instant when cement and water first come into contact. As the reaction

Figure 4.4. Calox Calorimeter

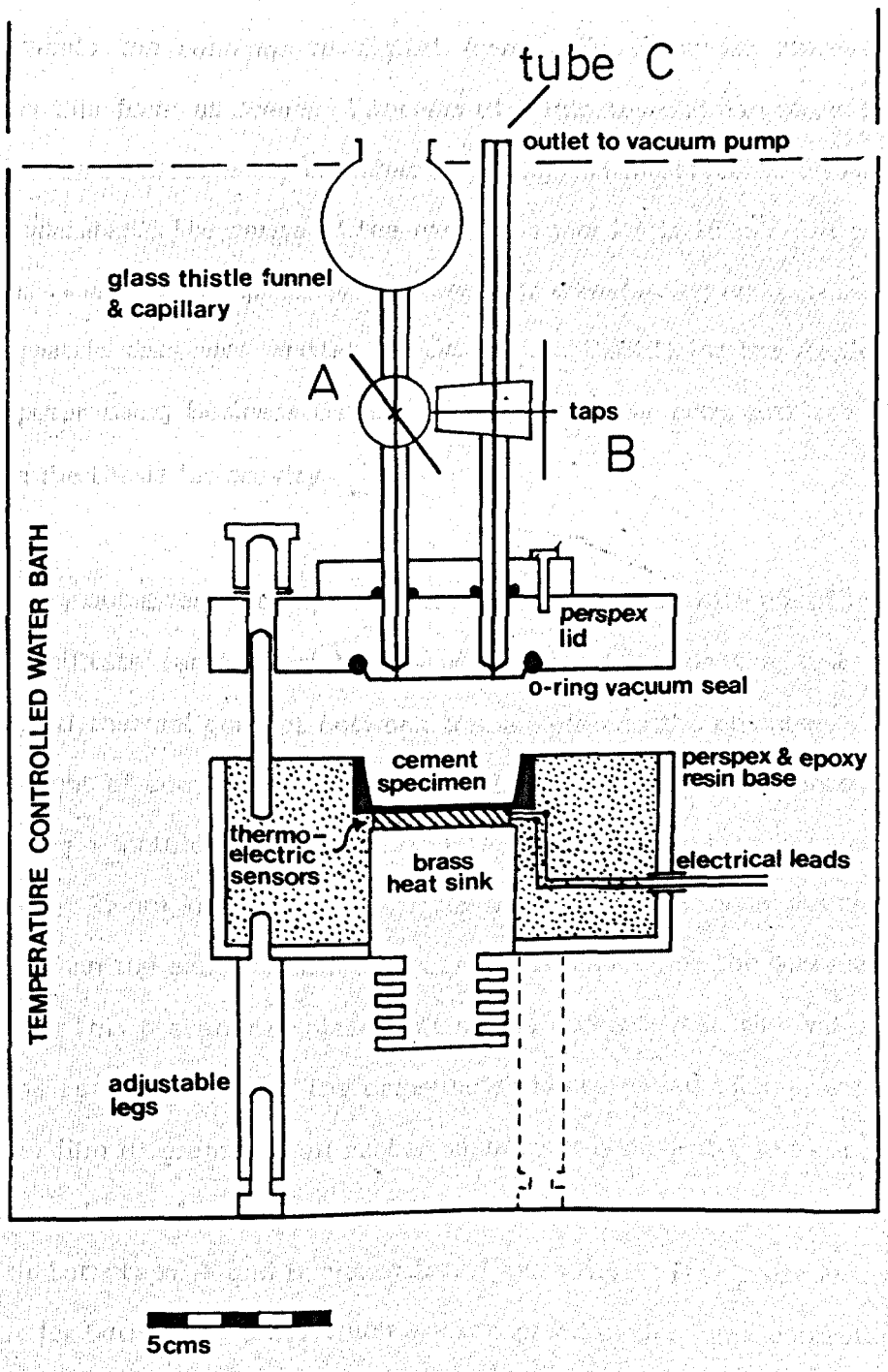

proceeds and heat is evolved the small temperature difference across thermocouples between the experimental chamber and a heat sink produces an electromotive force which is detected by a potentiometric chart recorder. The voltage output is also fed to a solid state memory recorder which converts the readings to digital form. The recorder stores the voltages in this form at preset intervals of 5 minutes and can store 1024 values which are subsequently transferred through an interface to an Apple III microcomputer. The range of the memory recorder is 10 mV full scale deflection. A suite of computer programmes for transferring and processing the calorimetric data was written by Dr. P.F.G. Banfill for the Apple III microcomputer using Business Basic. Details of these programs are not included in the thesis for brevity.

To carry out a test the experimental chamber is lined with clingfilm in order to facilitate removal of the hardened sample after the test yet maintain good thermal contact between the sample and the chamber. The required weight of cement, weighed to $\pm$ 0.01g, is carefully loaded into the chamber using a spatula and firmly compacted using a brass tamping rod of approximately 25mm diameter. A circle of filter paper with diameter slightly less than the experimental chamber is then placed on the surface of the cement. This prevents displacement of the cement when the water is run onto the cement surface. The calorimeter is assembled taking care to apply a thin film of grease to all rubber seals to prevent water ingress and the required volume of water, or admixture solution, is placed in the thistle funnel with both taps A and B closed (see Figure 4.4). This procedure is carried out for both Calox units which are immersed in the same controlled temperature ($\pm$ 0.1°C) water bath and left to reach the required temperature. The experimental chamber is evacuated by using a vacuum pump to apply suction via the glass tube C for 30 seconds. The tap B is then

closed and the vacuum pump hose removed before opening tap A allowing water to be drawn into the chamber. As the water is drawn in, the memory recorder is reset and the chart recorder started with chart speed and full scale deflection set at values appropriate to the sample under test. The test is said to be completed when the voltage output is seen to be virtually returned to zero; for most samples the run length was 2 days.

4.3.1.3 Testing on plain pastes

Tests were carried out on plain pastes at w/c 0.30 and 0.40 at the following test temperatures:

5, 10, 15, 20, 25, 27, 30, 35, 40, 45 °C

All pastes at w/c 0.30 were tested in Calox 1 and pastes at w/c 0.40 in Calox 2.

4.3.1.4 Pastes containing admixtures

Pastes listed in Table 4.1 at w/c 0.30 and 0.40 were tested at 5, 20, 30 and 40°C, maintaining the use of Calox 1 for w/c 0.30 as for plain pastes.

Table 4.1 Pastes Containing Admixtures Tested by Calorimetry

Paste No	Admixture Dosage %		
	Accelerator	Superplasticiser S1	S2
1	0.025	0	0
2	0.1	0	0
3	1.0	0	0
4	0	0.3	0
5	0	0.6	0
6	0	1.0	0
7	0	0	0.3
8	0	0	0.6
9	0	0	1.0
10	0.025	0.3	0
11	0.025	1.0	0.3
12	0.025	0	0.3
13	0.025	0	1.0

4.3.2 Vicat Testing

The Vicat test for initial set was used to determine the effect of the accelerating admixture on the setting time of the pastes listed in Table 4.2

Table 4.2 Pastes Tested for Initial Set

Temperature (°C)	w/c	Accelerator Dosage (%)
5	0.30	0
5	0.40	0, 0.01, 0.025, 0.05, 0.1, 0.5, 1.0, 2.0
20	0.30	0, 0.01, 0.025, 0.05, 0.1, 0.5, 1.0, 2.0
20	0.40	0, 0.01, 0.025, 0.05, 0.1, 0,5, 1.0, 2.0
30	0.30	0
30	0.40	0, 0.01, 0.025, 0.05, 0.1, 0.5, 1.0, 2.0
40	0.30	0
40	0.40	0, 0.01, 0.025, 0.05, 0.1, 0.5, 1.0, 2.0

The Vicat apparatus was partially immersed in a controlled temperature water bath ($\pm$ 0.1°C) with a polythene bag used to prevent water ingress into the paste specimen and a polystyrene insulating layer above the mould. The apparatus is shown diagrammatically on Figure 4.5. A copper-constantin thermocouple was embedded in the paste, with a reference thermocouple maintained at 0°C in ice, and connected to a potentiometric chart recorder. The thermocouple output voltage was calibrated against known temperatures allowing paste temperature to be continuously recorded.

An additional thermocouple was placed between the mould and its polythene covering to check that the apparatus was at the required temperature.

To prepare the pastes 400g of Ciment Fondu was mixed by hand for 1 minute then for an additional 2 minutes using a laboratory stirrer. After mixing the paste was poured into the Vicat mould and the thermocouple inserted.

To ensure that the paste was at the required test temperature after mixing the materials were stored overnight at the temperatures shown in Table 4.3

Table 4.3 Material Storage Temperatures for Vicat Testing

Test Temperature	Storage Temperature (°C)
5	3
20	16.5
30	31.5
40	43

Figure 4.5. Apparatus Used for Vicat Testing

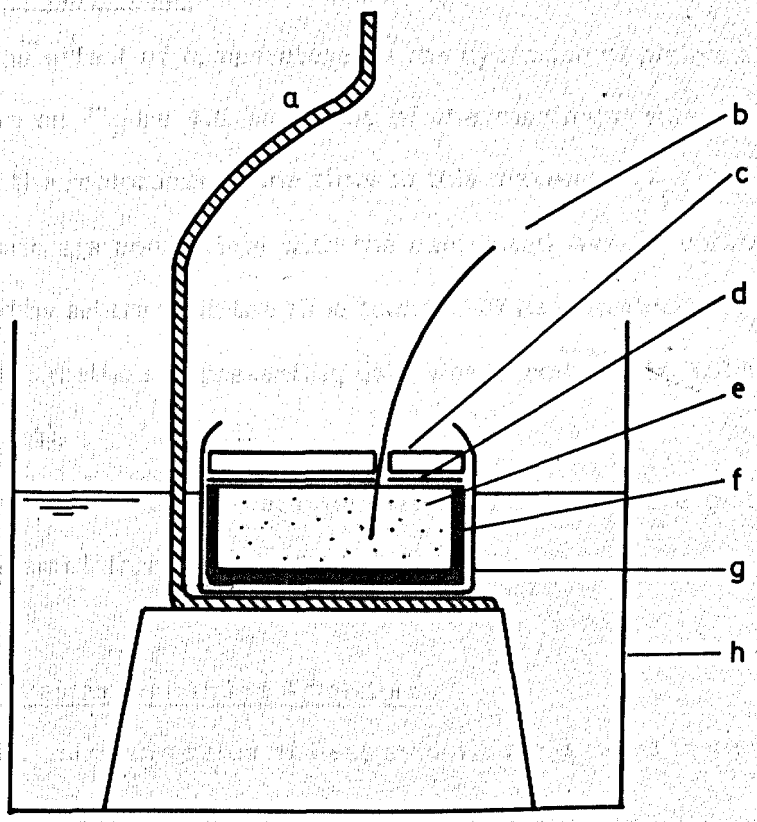

a Vicat stand
b Thermocouple
c Polystyrene disc
d Polythene disc
e Paste sample
f Vicat mould
g Polythene bag
h Controlled temperature water bath

4.4 RESULTS

4.4.1 Calox

4.4.1.1 Calibration

The results of calibration runs for Ciment Fondu are given in Table 4.4 with results for other types of cement included for comparison.

4.4.1.2 Plain Pastes

The effect of temperature on the hydration of plain pastes at w/c 0.30 is shown on Figure 4.6 as a plot of the maximum rate of heat evolution against the reciprocal of the time to this maximum (T_{peak}). To ensure that these data are compatible with the calculated Avrami parameters T_{peak} is adjusted by subtracting the time to onset of heat evolution (T_{off}).

This method of presenting data was introduced by Wilding, Walter and Double (84).

Tabulated kinetic data for w/c 0.30 and 0.40 are given in Table 4.5 with Avrami information in Table 4.6.

4.4.1.3 Pastes Containing Admixtures

The maximum rates of heat evolution and times to these maxima are presented in tabular form as follows:

Table 4.7	5 °C
Table 4.8	20 °C
Table 4.9	30 °C
Table 4.10	40 °C

The letters A-F are used to denote the possible forms of the graph of rate of heat evolution against time as shown on Figure 4.7.

Figure 4.6. Effect of Temperature on Heat Evolution, Paste, w/c 0·30

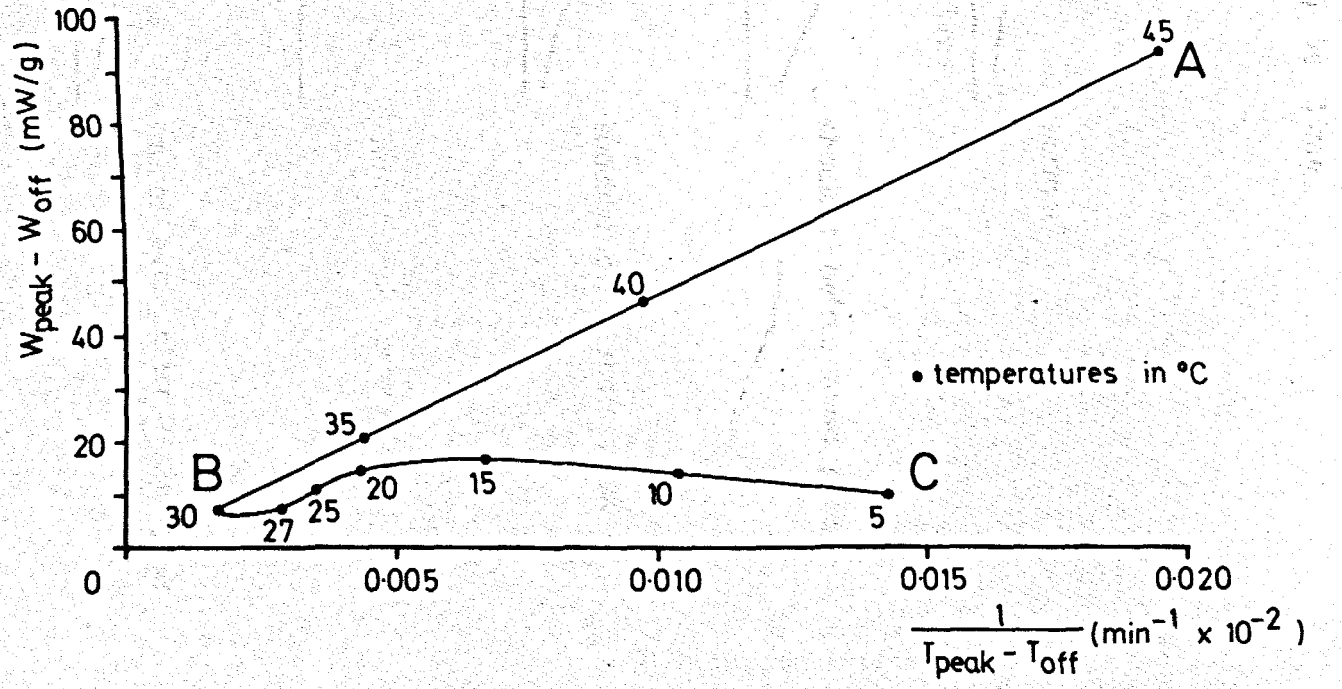

Figure 4.7. Possible forms of Graph of Rate of Heat Evolution (W) vs Time

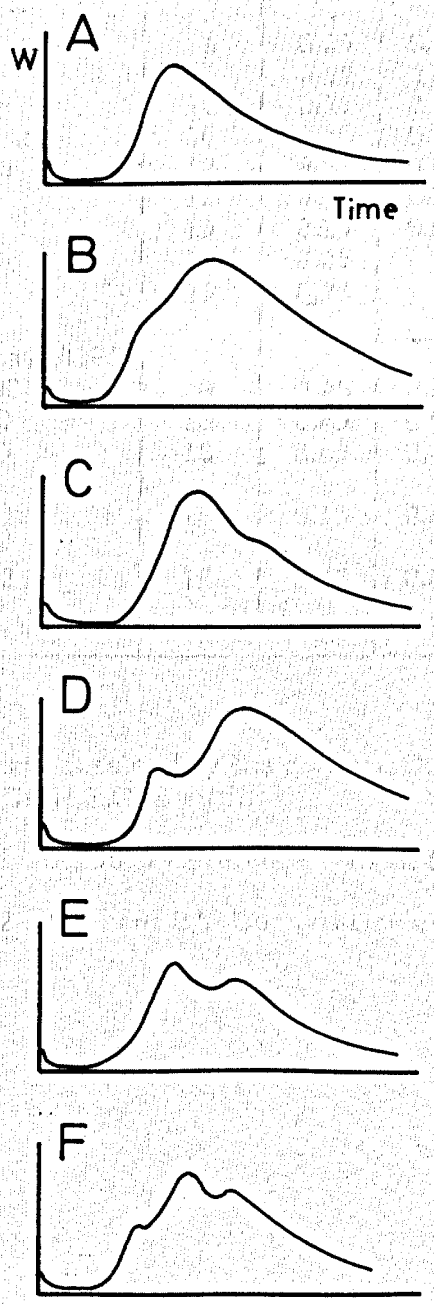

normal

shoulder before main peak

shoulder after main peak

minor peak before main peak

minor peak after main peak

multiple peaks

Table 4.4 Calox Calibration Results

Cement	Weight	w/c	Calox 1		Calox 2	
			k_1 (J/s.mV)	k_2 (J/mv)	k_1 (J/s.mV)	k_2 (J/mV)
	6	0.25	0.0178	9.94	0.0175	8.88
	10	0.25	0.0178	9.67	0.0164	7.93
	10	0.25	0.0182	8.60	-	- *
Ciment	10	0.50	0.0171	8.13	0.0174	9.77
Fondu	12	0.25	0.0183	9.75	0.0172	10.29
	12	0.50	0.0176	11.34	0.0171	9.78
	15	0.25	0.0176	11.27	0.0175	10.35
	15	0.25	-	-	0.0178	9.81 *
	15	0.25	-	-	0.0176	9.80 *
Cemsave/OPC						
0:100	18	0.45	0.0186	12.8	0.0173	11.9
40:60	18	0.45	0.0185	12.9	0.0184	12.3
70:30	18	0.45	0.0179	14.7	0.0180	12.8
OPC 1	18	0.55	0.0195	12.7	0.0182	10.4
OPC 2	18	0.35	0.0170	9.9	0.0167	10.7

* Result obtained by the author. Other results as private communication from Dr. P.F.G. Banfill.

OPC 1 BC 5075 Reference cement (Ribble)

OPC 2 "Cement B". Composition available on request (Blue Circle)

Table 4.5 Kinetic Data for Plain Pastes

Temp (°C)	Initial Peak (mW/g)	Main Peak Height (mW/g)	Main Peak Time (mins)
w/c 0.30			
5	7.7	11.3	250
10	9.0	14.2	290
15	7.3	17.0	340
20	7.2	15.1	495
25	7.7	10.7	725
27	7.4	7.0	895
30	7.6	8.1	1285
35	7.4	23.1	640
40	7.4	47.3	290
45	4.1	97.7	140
w/c 0.40			
5	7.4	9.9	255
10	9.6	14.3	280
15	8.2	18.6	315
20	6.7	19.0	435
25	7.6	16.6	655
27	6.7	10.9	890
30	8.0	9.4	1295
35	6.1	25.1	630
40	5.4	46.1	290
45	5.7	85.9	140

Note : Tian's analysis not valid at 45°C, doubtful at 35, 40°C. Peak heights included since these values were used to prepare Figure 4.6

Table 4.6 Data Relating to Avrami Equation, Plain Pastes

Temp (°C)	Avrami Parameters H (mJ/g)	n	K	False Origin Time (mins)	False Origin Heat (mW/g)	Fit Parameter, F **
w/c 0.30						
5	38700	3	8×10^{-13}	180	0.5	160
10	66000	4	5×10^{-14}	195	0.4	670
15	76000	3	1×10^{-15}	240	2.1	550
20	97000	4	5×10^{-16}	325	2.2	1150
25	140000	4	1×10^{-15}	440	0.6	190
27	107000	4	2×10^{-16}	550	0.4	20
30	120000	4	2×10^{-17}	895	1.2	585
35 *						
40 *						
45 *						
w/c 0.40						
5	38000	3	4×10^{-12}	185	0.6	560
10	58000	4	6×10^{-16}	180	0.7	625
15	88000	5	2×10^{-20}	170	0.8	535
20	131000	5	2×10^{-21}	220	0.6	115
25	160000	5	3×10^{-20}	385	0.5	425
27	180000	4	6×10^{-18}	495	0.6	280
30	212000	5	6×10^{-25}	560	0.4	140
35 *						
40 *						
45 *						

* Tian's analysis doubtful or not valid

** Fit parameter

	$F < 10$		excellent
$10 < F < 100$			very good
$100 < F < 1000$			good
$1000 < F < 5000$			acceptable

Table 4.7 Effect of Admixtures on Main Peak in Heat Evolution at 5°C

	Main Peak Height (mW/g)	Main Peak Time (mins)	Other Peak Height (mW/g)	Other Peak Time (mins)	Form of Graph (see Fig. 4.7)
w/c 0.30					
Control	11.3	250			
0.025% A	10.6	120	2.0	40	B
0.1% A	9.8	115	7.2	60	D
1.0% A	13.7	50			A
0.3% S1	9.2	265			A
0.6% S1	10.5	305			A
1.0% S1	9.6	580			A
0.3% S2	7.4	855			A
0.6% S2	4.9	1775	0.9	645	D
1.0% S2	3.0	3920			A
0.3% S1 + 0.025% A	10.0	85	3.1	30	D
1.0% S1 + 0.025% A	11.6	120	1.6	35	D
0.3% S2 + 0.025% A	10.3	120	1.8	30	D
1.0% S2 + 0.025% A	7.9	530	1.4	45	D
w/c 0.40					
Control	9.9	255			A
0.025% A	9.9	120	2.0	50	B
0.1% A	9.0	135	5.8	60	D
1.0% A	12.9	50			A
0.3% S1	10.9	250			A
0.6% S1	10.7	270			A
1.0% S1	10.1	440			A
0.3% S2	7.7	780	v. slight		B
0.6% S2	6.5	1430			A
1.0% S2	5.1	3050			A
0.3% S1 + 0.025% A	10.2	95	3.0	30	B
1.0% S1 + 0.025% A	11.9	115	2.4	30	B
0.3% S2 + 0.025% A	9.4	115	1.8	30	B
1.0% S2 + 0.025% A	8.5	455	1.7	25	D

Table 4.8 Effect of Admixtures on Main Peak in Heat Evolution at 20°C

	Main Peak Height (mW/g)	Main Peak Time (mins)	Other Peak Height (mW/g)	Other Peak Time (mins)	Form of Graph (see Fig. 4.7)
w/c 0.30					
Control	15.1	495			A
0.025% A	17.8	140	6.8	20	D
0.1% A	24.5	30	16.3	100	E
1.0% A	*1	17	*1	2	D
0.3% S1	14.1	420			A
0.6% S1	14.1	490			A
1.0% S1	14.5	660			A
0.3% S2	11.5	780			A
0.6% S2	10.6	1360			A
1.0% S2	7.5	2020			A
0.3% S1 + 0.025% A	18.9	90	11.4	5	D
1.0% S1 + 0.025% A	20.8	160			A
0.3% S2 + 0.025% A	21.2	120			A * 2
1.0% S2 + 0.025% A	15.5	240			A
w/c 0.40					
Control	19.0	435			A
0.025% A	18.6	150	5.2	20	D
0.1% A	22.8	30	16.6	100	E
1.0% A	51.0	22	21.8	2	D
0.3% S1	15.7	400			A
0.6% S1	16.1	430			A
1.0% S1	14.4	580			A
0.3% S2	13.1	650			A
0.6% S2	13.3	1185			A
1.0% S2	9.4	1550			A
0.3% S1 + 0.025% A	18.9	90	10.7	5	D
1.0% S1 + 0.025% A	22.8	105	3.6	20	D
0.3% S2 + 0.025% A	19.4	115	2.7	20	D
1.0% S2 + 0.025% A	16.5	235	2.9	20	D

*1 Tian's analysis not valid
*2 Several very small peaks before main peak

Table 4.9 Effect of Admixtures on Main Peak in Heat Evolution at 30°C

	Main Peak Height (mW/g)	Main Peak Time (mins)	Other Peak Height (mW/g)	Other Peak Time (mins)	Form of Graph (see Fig. 4.7)
w/c 0.30					
Control	8.1	1290			A
0.025% A	14.4	250	13.0	5	D
0.1% A	*1	16	*1	3	D
1.0% A	*1	10	*1	2	D
0.3% S1	9.1	680	3.1	960	E
0.6% S1	15.5	320	*2		C
1.0% S1	23.0	330			A
0.3% S2	10.6	860	7.0	1020	E
0.6% S2	11.6	630	4.0	900	C
1.0% S2	29.5	700			A
0.3% S1 + 0.025% A	24.8	85	23.7	5	F * 3
1.0% S1 + 0.025% A	47.0	40	13.9	15	D
0.3% S2 + 0.025% A	29.0	80	17.5	15	D
1.0% S2 + 0.025% A	53.4	60	2.4	30	D
w/c 0.40					
Control	9.4	1295			A
0.025% A	13.5	255	11.9	5	D
0.1% A	*1	19	*1	3	D
1.0% A	*1	13	*1	2	D
0.3% S1	7.5	650	6.0	1080	E
0.6% S1	10.8	395	3.0	900	E
1.0% S1	19.9	250	2.3	135	B
0.3% S2	11.1	860	8.8	1000	E
0.6% S2	10.1	595	5.7	940	E
1.0% S2	27.6	535	4.5	820	E
0.3% S1 + 0.025% A	23.8	90	22.6	5	F * 4
1.0% S1 + 0.025% A	43.7	35	22.0	20	B
0.3% S2 + 0.025% A	31.2	75	16.1	15	D
1.0% S2 + 0.025% A	48.5	60	2.3	30	D

*1 Tian's analysis not valid
*2 Very faint shoulder
*3 Additional peak 10.6 mW/g at 35 minutes
*4 Additional peak 12.9 mW/g at 30 minutes

Table 4.10 Effect of Admixtures on Main Peak in Heat Evolution at 40°C

	Main Peak Height (mW/g)	Main Peak Time (mins)	Other Peak Height (mW/g)	Other Peak Time (mins)	Form of Graph (see Fig. 4.7)
w/c 0.30					
Control	47.3	290			A
0.025% A	*1	9	*1	3,15	F
0.1% A	*1	10	*1	3	D
1.0% A	*1	6	*1	2	D
0.3% S1	27.3	150	22.4	230	E
0.6% S1	41.3	105	12.5	200	E
1.0% S1	54.2	105	16.0	160	E
0.3% S2	*1	250			A
0.6% S2	*1	220			A
1.0% S2	*1	265			A
0.3% S1 + 0.025% A	*1	4			A
1.0% S1 + 0.025% A	*1	15	*1	2	D
0.3% S2 + 0.025% A	*1	9			A
1.0% S2 + 0.025% A	*1	30			A
w/c 0.40					
Control	46.1	290			A
0.025% A	*1	3	*1	9,17	F
0.1% A	*1	10	*1	3	D
1.0% A	*1	8	*1	2	D
0.3% S1	24.2	245	23.9	150	D
0.6% S1	34.8	110	18.5	200	E
1.0% S1	53.8	85	23.0	135	E
0.3% S2	44.3	210			A
0.6% S2	46.5	195			A
1.0% S2	*1	220			A
0.3% S1 + 0.025% A	*1	4			A
1.0% S1 + 0.025% A	*1	10			B * 2
0.3% S2 + 0.025% A	*1	8	*1	4	D
1.0% S2 + 0.025% A	*1	30			A

*1 Tian's analysis not valid
*2 Slight shoulder before peak

The inapplicability of Tian's analysis where the temperature rise exceeds 1°C has already been mentioned. It will be shown in the next section that rapid reactions can cause a temperature rise exceeding 1°C and therefore Tian's analysis is not always valid. Data on T_{peak} from such tests is however included in Tables 4.7-4.10 since it gives a good qualitative indication of the degree of acceleration caused by the admixtures.

Figure 4.8 shows the effect of superplasticiser dosage on the Calox voltage output against time for S1 at 40°C.

The effect of temperature and admixture dosage on the initial peak in rate of heat evolution is given in Table 4.11.

4.4.2 Vicat

The effect of temperature, w/c ratio and accelerator dosage is shown graphically on Figure 4.9.

4.5 DISCUSSION

4.5.1 Calox

4.5.1.1 Plain Pastes

Calibration

To avoid any doubt concerning the validity of the constants k_1 and k_2 the calibration should be checked for each test. This process is however time consuming thus mean values of k_1 and k_2 were obtained as described below and used for all tests.

Statistical analysis of the results in Table 4.4 using the F test to compare variances showed that for Ciment Fondu the constants k_1 and k_2 are not significantly affected by the sample weight or w/c ratio. The effect

Figure 4.8. Effect of S1 on Heat Evolution During Hydration at 40 °C. Paste w/c 0·30

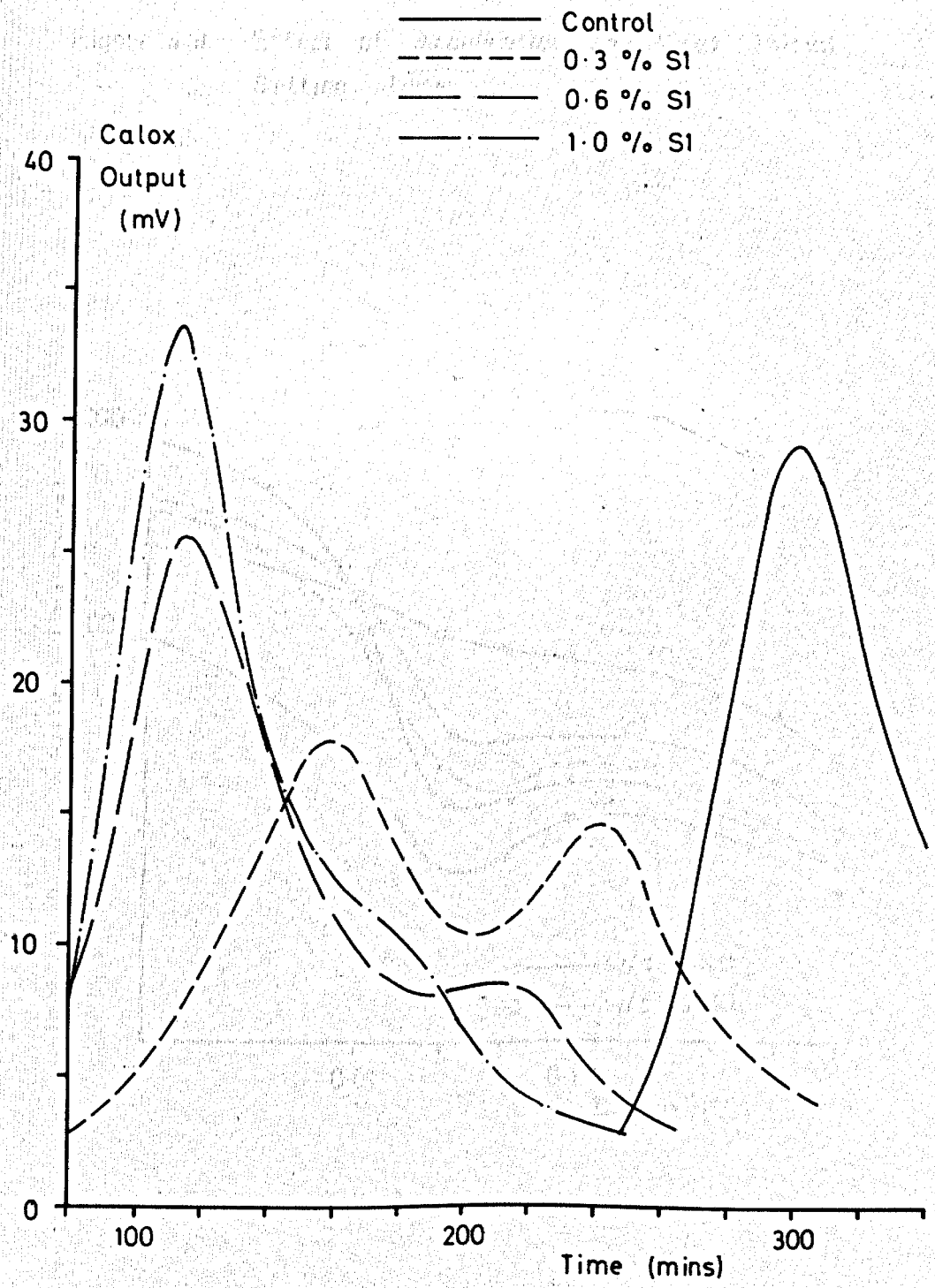

Figure 4.9. Effect of Accelerator on Vicat Initial Setting Time

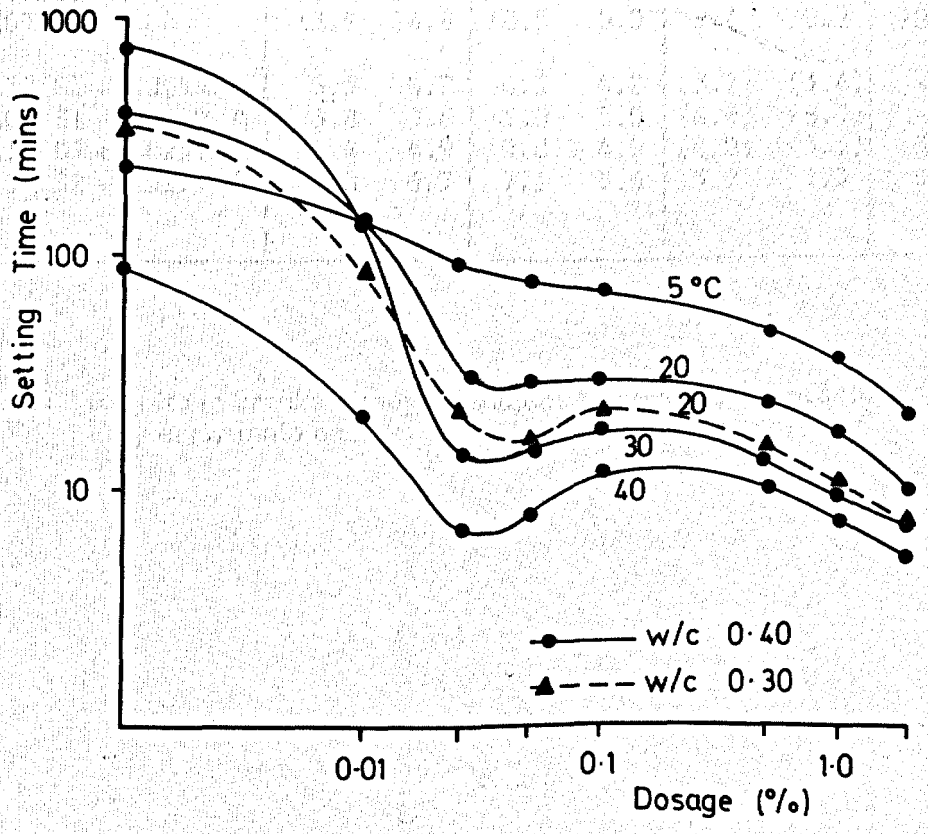

Table 4.11 Effect of Admixture on Initial Peak Height (mW/g)

	5°C		20°C		30°C		40°C	
w/c	0.30	0.40	0.30	0.40	0.30	0.40	0.30	0.40
0.025% A	8.0	8.7	4.4	4.9	(4.4)	(3.6)	3.4	3.4
0.1% A	4.1	3.9	5.0	4.6	(3.4)	(2.9)	-	-
1.0% A	8.3	7.7	2.7	-	-	-	-	-
0.3% S1	9.4	13.5	11.5	10.8	9.6	10.3	9.6	7.0
0.6% S1	7.5	12.9	9.9	8.5	10.3	9.0	11.4	9.3
1.0% S1	8.9	10.8	8.7	7.6	8.7	8.6	9.7	11.5
0.3% S2	12.4	12.8	8.7	9.9	8.9	8.6	8.4	5.7
0.6% S2	11.8	17.1	8.6	9.0	9.3	7.9	10.3	6.5
1.0% S2	13.9	16.8	10.5	8.0	8.6	8.2	10.8	8.6
0.3% S1 + 0.025% A	8.3	8.7	4.7	4.2	(3.7)	(3.6)	-	-
1.0% S1 + 0.025% A	3.8	3.6	5.0	5.0	(6.8)	(8.3)	-	-
0.3% S2 + 0.025% A	4.4	4.9	5.0	4.9	(4.0)	(5.5)	3.7	2.2
1.0% S2 + 0.025% A	5.0	6.3	7.1	5.6	5.9	5.3	8.1	7.2

Note: Results in brackets may be subject to error due to proximity of very early main peak

of cement type is significant at the 5% level in influencing k_1 although k_2 is not affected.

For the series of tests on Ciment Fondu described in this chapter values of k_1 and k_2 were taken to be the mean of 6 results (one result at each weight:w/c combination) and are as follows:

Calox 1	k_1	0.0177 J/s.mV	k_2	10.02 J/mV
Calox 2	k_1	0.0172 J/s.mV	k_2	9.50 J/mV

The weight of cement used for the main test programme was 12g, chosen after a number of trial runs at 15°C and 20°C to determine typical peak heights in the rate of heat evolution.

Validity of Tian's Analysis

It was stated in section 4.2.1 that Tian's analysis is valid provided that the temperature of the sample under test does not increase by more than about 1°C. The actual temperature rise for 2 pastes at w/c 0.30 was monitored using a thermocouple embedded in the sample; the results are shown in Table 4.12.

Table 4.12 Temperature Rise in Calox Specimens

Sample	Max' Rate of Heat Evolution (mW/g)	Temp' rise (°C)
Control hydrated at 20°C	15	1.0
1% A hydrated at 40°C	373	8.0

The increase in sample temperature is due to the inability of the heat sink to conduct all the heat away from the sample during hydration. For pastes with an increase in temperature exceeding 1°C the measured rates of heat evolution underestimate the actual rates and the Calox behaves as a semi-isothermal calorimeter. The error is compounded by the increased temperature causing a further increase in the rate of hydration in the sample.

Tian's analysis is clearly inappropriate for the paste at 40°C (which gave the maximum rate of heat evolution of all the pastes tested) and it would be misleading to quote quantitative kinetic data obtained from such experiments. However it is considered that for tests during which the sample temperature rises by no more than 2°C Tian's analysis may be used with the proviso that the results are interpreted with caution. If a simple linear relationship between temperature rise and maximum rate of heat evolution is assumed then the validity of Tian's analysis may be summarised as in Table 4.13.

Table 4.13 Validity of Tian's Analysis

Max' Rate of Heat Evolution (mW/g)	Tian's Analysis
< 15	valid
15 - 60	some doubt
> 60	not valid

The effect of this problem on the interpretation of data from plain pastes and pastes containing admixtures is considered later in this discussion.

Use of the Avrami Equation

Results will be considered only for plain pastes at 5-30°C since Tian's analysis is inappropriate at higher temperatures.

Values of the Avrami parameter n in Table 4.6 are in the range 3-5. The results are reported to the nearest whole number although the best fit curve is obtained by successive trial and error fit using values of n to the first decimal place. This rounding was carried out since for the same curve it is possible to obtain a reasonable fit with widely differing values of n by adjusting the position of the false origin as shown by the data for plain paste at 30°C in Table 4.14.

Table 4.14 Differences in Avrami n for Same Goodness of Fit

Avrami n	False Origin Time (mins)	False Origin Heat (mW/g)	Fit Parameter
3.8	895	1.2	585
5.7	645	0.6	640

It may be thought that the false origin should be placed at the onset of the increase in heat evolution. It is often found however that this results in a poor fit with the experimental data regardless of varying n and the heat co-ordinate of the false origin. This problem leads to difficulty in the interpretation of n since little significance can be attributed to the difference between values of 3 and 5.

It is considered that the difficulty in obtaining a good fit may be partly due to the simultaneous hydration of different anhydrous phases, each of which should be described by a different Avrami equation.

Effect of Temperature on Hydration - Main Peak in Heat Evolution

Figure 4.6 illustrates the very considerable influence of temperature on the hydration of Ciment Fondu. The increase in time to main peak (T_{peak}) with increasing temperature up to 30°C followed by a rapid decrease at higher temperature agrees well with previously published results (1, 4, 53, 91, 92).

Whilst it is inappropriate to refer to numerical kinetic data for pastes at temperatures above 30°C it is evident that the rate of reaction increases dramatically above this temperature. The underestimation of true rate of heat evolution by Tian's analysis in this region causes the section of curve AB on Figure 4.6 to appear as a straight line when it is probably a curve tending away from the x axis as the temperature increases.

The following is suggested as a plausible interpretation of Figure 4.6.

Section BC : The maximum rate of heat evolution in this section occurs between 15-20°C. Above 20°C the formation of CAH_{10} is not favoured and the predominant hydrate formed is C_2AH_8. No detailed explanation is offered here for the apparent retarding action of C_2AH_8 although it is relevant to note that the difference between T_{off} and T_{peak} changes with temperature in the same way as the individual values of T_{peak} and T_{off}. This shows the tendency for the peak in heat evolution to become progressively flatter and longer up to 30°C and provides evidence for the slow growth and crystallisation of C_2AH_8 up to this temperature as suggested by Bushnell-Watson and Sharp (93).

Section AB : There is a very rapid reduction in both T_{off} and T_{peak} above 30°C accompanied by a considerable increase in peak height. It is likely that above 30°C the formation of C_2AH_8 becomes progressively more favoured with C_3AH_6 also being formed. According to the published work

discussed in Chapter 1 it is unlikely that the direct formation of C_3AH_6 occurs below 45°C although at such temperatures the conversion of hexagonal to cubic hydrates can occur very quickly (18, 161).

It is relevant to note at this stage the difference between the nominal and actual w/c ratios. Several hardened Calox samples were weighed immediately after removal from the calorimeter and the results are given in Table 4.15.

Table 4.15 Differences Between Nominal and Actual w/c for Calox Samples

Nominal w/c	Measured w/c	Difference (%)
0.30	0.24	20
0.40	0.33	18
0.50	0.35	30
0.60	0.42	30

It is apparent that the series of tests described in this chapter were carried out at w/c ratios somewhat less than planned. This difference is probably due to incomplete absorption of the mixing water by the cement as it is run onto the cement under vacuum. There remains however a difference of 0.09 between the 2 w/c ratios which is close to the planned difference of 0.10. The nominal w/c ratios of 0.30 and 0.40 will be used throughout the remainder of this chapter to avoid confusion.

In order to carry out calorimetric tests at actual w/c exceeding approximately 0.35 it is clear that some method of mixing the paste within the calorimeter should be found rather than simply running the water onto the cement under vacuum.

Effect of Temperature on Height of Initial Peak

The coefficient of variation for results at different hydration temperatures (17%) was less than the coefficient of variation for 7 repeat tests on plain pastes at 5°C (23%). There is thus no evidence that change in hydration temperature affects the height of the initial peak.

Cement Variability

Calox tests on plain pastes at 5°C were carried out on cement samples taken from 5 bags of cement as these were used throughout the project over a period of approximately 18 months. The results in Table 4.16 are the mean of tests at 0.30 w/c and 0.40 w/c. Samples from the top and bottom of bags 1 and 2 were tested to check the effect of ageing in an opened bag.

Table 4.16 Cement Variability

Bag No.	Mean T_{peak}	Mean W_{peak}	No. of Results
1	259	10.8	4
2	245 *	12.7 *	4
3	261	11.1	2
4	234 *	9.9	2
5	253	12.0 *	2
Overall mean	251	11.3	
Overall s.d.	11	1.1	

* Result significantly different from bag 1, at 5% level using the t test.

The results show that there are significant differences between some bags in respect of both time to main peak and height of main peak. There is however no trend with increasing cement age and it is possible that the differences noted above are due to factors other than cement variability,

for example experimental error. No significant difference was found between results obtained at the top and bottom of a bag indicating that the storage arrangement was satisfactory. All bags were stored in airtight metal drums.

4.5.1.2 Pastes Containing Admixtures

Effect on Main Peak in Rate of Heat Evolution

The results show that the hydration of kinetics of Ciment Fondu are profoundly altered by the presence of admixtures. The hydration temperature is crucial and the same dosage of admixture can cause retardation at 5°C and yet acceleration at 40°C.

The presentation of a large amount of numerical data in Tables 4.7-4.10 is rather difficult to interpret. The alternative option of presenting each combination as a heat evolution graph would be preferable but is not feasible due to the number of runs involved.

At 5°C superplasticised mixes without accelerator all exhibit retardation. 1.0% S2 causes a 16 fold increase in T_{peak} over the control mix. This corresponds to a setting time of approximately 60 hours. Addition of 0.025% accelerator is sufficient to overcome the retardation for all except the 1.0% S2 mix. At 20°C the behaviour is similar though retardation is less marked and 0.3% S1 causes slight acceleration. At 30 and 40°C all mixes are accelerated with T_{peak} reduced to less than 5 minutes for some pastes.

Use of the accelerating admixture alone is very effective in accelerating the set at all test temperatures.

A noticeable feature is the presence of multiple peaks in heat evolution for many pastes, particularly at 30 and 40°C. This leads to great

difficulty in applying the Avrami equation to the data. In theory the peaks could be analysed separately but in practice it was found that most peaks were too close together and could not be separated by the original processing program. A further difficulty in applying the Avrami equation is that with increasingly rapid rates of reaction it becomes more difficult to achieve a satisfactory fit between predicted and calculated data. The processing program was therefore amended so that no attempt was made to fit the Avrami equation to data from pastes containing admixtures.

The effect of admixture dosage at 40°C is evident in Figure 4.8. At the lowest dosage used (0.3%) there are 2 peaks in voltage output of similar magnitude. Both peaks occur considerably before the much higher peak for the control paste. At higher dosages the main peak becomes larger and occurs earlier with the second peak much diminished. A feasible explanation for such behaviour could be that the admixture favours production of a certain hydrate or combination of hydrates which form more readily at 40°C, the lowest dosage of S1 being insufficient to alter the hydrate formation completely. It is interesting to note that the presence of S2 does not cause multiple peaks at 40°C yet both S1 and S2 do so at 30°C.

Experiments were carried out in an attempt to identify the hydration products corresponding to each peak in heat evolution. Details of the technique used and discussion of the results are given in Chapter 5.

Effect on Initial Peak

The presence of admixtures was found to have a significant effect, at the 5% level, on the height of the initial peak as follows (t tests carried out comparing the effect of each admixture in turn with the variability observed from repeat runs on plain paste) :

Initial peak height is increased by either S1 or S2 at 5 and 20°C and by S1 at 30 and 40°C.

Initial peak height is reduced by the accelerator at $\geqslant$ 20°C and by the use of accelerator/plasticiser combinations at 5 and 20°C. There are insufficient valid results for accelerator/plasticiser combinations at 30 and 40°C to allow comparison.

The explanation for such behaviour is likely to be based on i) changes to the dissolution characteristics of the anhydrous cement and ii) the possible formation of complexes of lime, alumina or ferrous hydrates with admixture molecules. Further discussion of likely mechanisms for admixture action is deferred until Chapter 6 when the results from all of the tests will be considered together.

4.5.2 Vicat Testing

The Vicat test results illustrate the dramatic effect of the accelerator on setting time. At dosages exceeding only 0.01% by weight of cement the 30°C delay is masked and setting times decrease consistently with increasing temperature. As dosage increases, a minimum setting time is observed at about 0.025%; this effect being more noticeable as temperature increases.

An attempt was made to correlate the Vicat initial setting time with parameters obtained from the calorimetry result; for example T_{off} or T_{cum}, the time at which a predetermined cumulative amount of heat has been evolved. The presence of multiple peaks caused difficulty in establishing any correlation and it was impossible to produce a quantitative relationship between setting time and any of the 3 parameters listed above. Comparison of the data in Tables 4.7-4.10 with that on Figure 4.9 shows that the time to initial set is normally slightly less than T_{peak}. This confirms the findings of Casson et al (87).

The use of a thermocouple embedded in the test sample was found to be helpful for the following reasons;

(i) It can be verified that the paste temperature during the test is as required.

(ii) A gradual rise in temperature is observed before the initial set. This reduces the number of needle penetration tests which must be carried out and is particularly useful for a paste with unknown setting time. The only sample for which no temperature rise was observed was for the plain paste at 30°C. In this case the rate of heat evolution is so slow that heat is dissipated to the surroundings at the same rate as it is generated.

4.6 CONCLUSIONS

4.6.1 Plain Pastes

1. Tian's analysis should not be used for conduction calorimeter tests when the rate of heat evolution exceeds 60mW/g and results obtained from tests with heat evolution rate between 15-60mW/g should be interpreted with caution.

2. The Avrami equation is of limited use in the interpretation of kinetic data from tests on Ciment Fondu. Difficulties are (i) the invalidity of Tian's equation, (ii) application of the equation to multiple peaks in heat evolution and (iii) the position of the false origin can have a considerable effect on the value of n.

3. To carry out Calox tests at $w/c > 0.35$ some method of in situ mixing should be used for the paste in the experimental chamber.

4. The calibration constants k_1 and k_2 are not affected by changes in the weight or w/c ratio of the Ciment Fondu paste under test.

5. The considerable retardation of the hydration of Ciment Fondu at around 30°C has been confirmed. As the temperature increases up to 30°C the main peak in heat evolution becomes progressively longer and flatter. This is indicative of the difficulty of nucleation and growth of C_2AH_8 up to 30°C.

6. The height of the initial peak in heat evolution which occurs as soon as water comes into contact with cement is independent of hydration temperature.

7. Checks on the heat evolution of pastes containg cement taken from different bags as used throughout the research showed no effect of age for the storage conditions used.

4.6.2 Pastes Containing Admixtures

1. Lithium citrate is extremely efficient in overcoming the retardation at 30°C.

2. Superplasticisers retard the hydration of Ciment Fondu at 5 and 20°C but accelerate slightly at 30 and 40°C. The retardation by superplasticisers may be overcome by simultaneous use of lithium citrate.

3. The hydration kinetics of Ciment Fondu pastes containing superplasticisers are extremely complex with some combinations, particularly at higher temperatures producing double or multiple peaks in the rate of heat evolution.

REFERENCES

Reference numbers contained in double brackets refer to publications mentioned only in this chapter. Reference numbers contained in single brackets refer to those included in the literature review in Chapter 1.

1. TIAN A ; "Util. de la Methode Cal. Dyn. Chem." Soc. Chim de France, Vol. 33, No. 4, 1923.

2. SHARP J.H ; Private communication Dec 1986.

CHAPTER 5 STRENGTH DEVELOPMENT AND HYDRATION PRODUCTS

5.1 INTRODUCTION

The objectives of the work described in this chapter are to determine (i) the effect of the superplasticising and accelerating admixtures on the strength development of Ciment Fondu mixes and (ii) the effect of these admixtures on the types and relative amounts of hydrates produced. The experiments were designed so that a statistical analysis of variance (ANOVA) could be carried out to determine the significance of the main factors and their interaction. The admixture dosages and hydration temperatures are as used for the conduction calorimetry tests described in Chapter 4 so that the two sets of results are directly comparable.

Compressive strength testing of mixes containing a large number of admixture combinations at several test temperatures and test ages would have required an unreasonably large number of specimens to be cast. A non-destructive test was preferred and accordingly the Pundit apparatus was used to monitor the ultrasonic pulse velocity (upv) of mortar cubes up to 18 months old. An additional advantage of non-destructive testing is that the same sample can be tested repeatedly. The correlation between upv and compressive strength was determined by crushing a number of cubes from which samples were removed for test by DTG with hydrate identification confirmed by XRD.

Throughout the chapter strength refers to compressive strength.

5.2 EXPERIMENTAL PROCEDURES

5.2.1 Upv/Strength Testing

Twelve mixes, detailed in Table 5.1, containing various combinations of admixtures were tested at 5, 20, 30 and 40°C. All mortars were 1:1.5

Table 5.1 Mix Details and Cube Ages at Test

Mix	Cube Ages at Test							
	5°C		20°C		30°C		40°C	
Control (1)	1d	12m	3d	6m	14d	3m	7d	2m
Control (2)	3d	12m	21d	2m	2d	18m	14d	3m
0.025% A (1)	1d	18m	2d	28d	7d	28d	21d	6m
0.025% A (2)	3d	6m	21d	6m	7d	28d	1d	28d
0.3% S1	3d	6m	3d	2m	1d	18m	14d	3m
0.3% S1 + 0.025% A	3d	28d	14d	18m	1d	3m	2d	12m
1.0% S1	7d	2m	2d	18m	21d	28d	21d	18m
1.0% S1 + 0.025% A	14d	12m	2d	12m	21d	3m	2d	2m
0.3% S2	7d	3m	1d	2m	14d	18m	2d	12m
0.3% S2 + 0.025% A	7d	6m	1d	3m	21d	28d	3d	12m
1.0% S2	7d	6m	14d	2m	7d	2m	21d	3m
1.0% S2 + 0.025% A	2d	18m	1d	28d	14d	12m	3d	6m

Note : d = day m = month

cement:sand at w/c 0.40 using sand 2 as described in Chapter 2 with each batch containing 1300g cement. Four 70.7mm cubes were cast from each mix, 2 of which were tested for strength at randomly chosen ages as shown on Table 5.1. The only restriction on these timings was that the first cube was crushed at one of the initial 6 test ages and the second cube at one of the remaining test ages. This ensured that both cubes were not tested either at a very early or late age. Great care was taken to ensure that materials were stored at the appropriate temperature prior to mixing. The mortar was mixed for 5 minutes using a Kenwood planetary mixer with 3 litre mixing bowl, the admixture solution was added gradually to the dry materials during the first minute. Three mixes at 40°C with extremely rapid setting times were mixed for only 3 minutes to enable cubes to be made before stiffening occurred.

Immediately after casting the moulds and their contents were placed inside polythene bags in water at the correct temperature. A slightly different technique was used for mixes cast at 20°C which were cured in air in the laboratory, covered with polythene sheeting to prevent evaporation. Cubes were demoulded as soon as possible, typically at 6 hours after casting though considerably longer for some mixes. The first upv readings were taken 24 hours after casting with readings also taken at 2, 3, 7, 14, 21, 28 days, 2, 3, 6, 12, 18 months.

The density of each cube was determined immediately prior to strength testing by weighing in both air and water. The strength was determined in general accordance with BS 915 Part 2:1972 (80).

Early results obtained from the main programme at 20°C suggested that the presence of admixtures influenced conversion. A secondary series

of mixes was therefore prepared at 20°C, using the same materials and mix proportions, to enable this behaviour to be studied in more detail. Four cubes were cast from each of the mixes listed below and upv measurements were made at intervals of 2 weeks up to an age of 4 months. One cube from each mix was crushed at 1, 2, 3 and 4 months with cube density measured prior to test and a sample removed for analysis by DTG as described for the main series.

Additional Mixes Tested at 20°C

Control
0.025% A
1.0% S1
1.0% S2
1.0% S1 + 0.025% A
1.0% S2 + 0.025% A

5.2.2 DTG Procedure

A sample of mortar was obtained from each cube after strength testing by drilling into the cube using a 5mm diameter masonry bit. Care was taken to use a sharp drill bit and to drill slowly thus preventing excessive heat production which may affect the composition of the hydrates formed. The sample was seived and acetone added to the fraction passing the 75μm seive which was then used for the DTG test. The evaporation of the acetone combined with any free water in the sample prevents any further hydration. This quenching procedure was adopted after consideration of published information and discussions with Dr. J.H. Sharp ((1)). After quenching the samples were stored in sealed plastic bags in a refrigerator at approximately 5°C until they were tested to prevent the possibility of conversion occurring during storage. Storage for up to 3 days before testing was found to have no effect on the results obtained although the DTG test was usually carried out on the same day as the cube was crushed.

A Stanton-Redcroft TG-750 thermobalance was used with 21mg samples heated in air at a uniform rate of 30°C/minute up to approximately 500°C. This heating rate is in accordance with the recommendations of the Thermal Methods group of the Analytical Division of the Chemical Society (105).

In addition to the DTG tests carried out on the samples as shown in Table 5.1, extra tests were done to ensure that results were available for all mixes at 12 months.

5.2.3 XRD Procedure

The powder samples, obtained as for DTG testing but ground slightly finer by use of a pestle and mortar, were mounted for analysis by packing into the central circular window of solid aluminium holders.

Samples from mixes at w/c 0.40 listed in Table 5.2 were tested using a Siemens D-500 X-ray diffractometer producing CuK_{α} radiation at 20kV, 6mA. A monochromator was attached to prevent background "noise" due to fluorescence and the scanning rate used was 1° 2θ/minute.

Table 5.2 XRD Samples

Sample Number	Description
1	Mortar, 5°C, Control, 6 months
2	Mortar, 20°C, Control, 6 months
3	Mortar, 40°C, Control, 6 months
4	Mortar, 20°C, 1.0% S2, 6 months
5	Paste, 5°C, Control, 1 day
6	Paste, 20°C, 0.3% S2, 1 day
7	Paste, 20°C, 0.3% S2, +0.025% A, 1 day
8	Paste, 30°C, Control, 1 day
9	Paste, 40°C, Control, 1 day
10	Anhydrous Ciment Fondu

5.3 RESULTS

The effect of age on upv is shown graphically on Figures 5.1-5.8 for mixes as detailed below with results from the control and accelerated mixes at the appropriate temperature shown on all graphs.

	Superplasticiser	Temperature (°C)
Figure 5.1	S1	5
Figure 5.2	S2	5
Figure 5.3	S1	20
Figure 5.4	S2	20
Figure 5.5	S1	30
Figure 5.6	S2	30
Figure 5.7	S1	40
Figure 5.8	S2	40

A program written in Business Basic for the Apple III micro-computer was used to carry out the ANOVA treatment of results ((2)). The main factors and treatment levels are given in Table 5.3.

Table 5.3 Main Factors and Treatment Levels for ANOVA

Factor	Treatment Levels
A	Superplasticiser S1, S2
B	Superplasticiser dosage 0, 0.3, 1.0%
C	Accelerator Dosage 0, 0.025%
D	Hydration temperature 5, 20, 30, 40°C

Values of upv for 2 cubes from each mix are required for the program which calculates variances due to the main effects A-D listed above and to interactions such as AxB, AxC. These calculated variances are compared with the error variance using the F ratio and tested for significance. The

Figure 5.1 Upv vs Age, 5 °C, S1

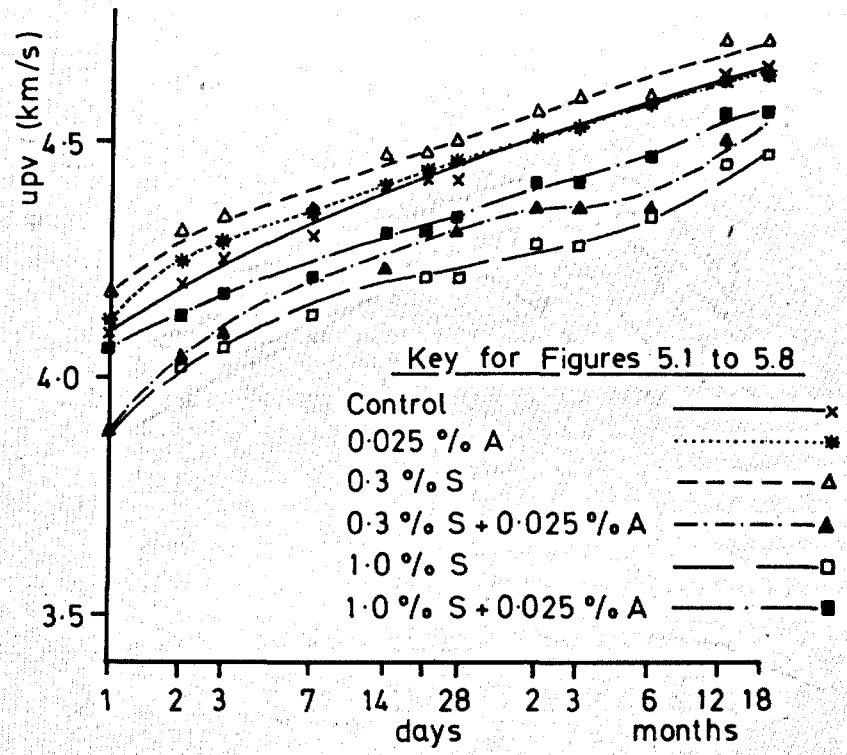

Figure 5.2 Upv vs Age, 5 °C, S2

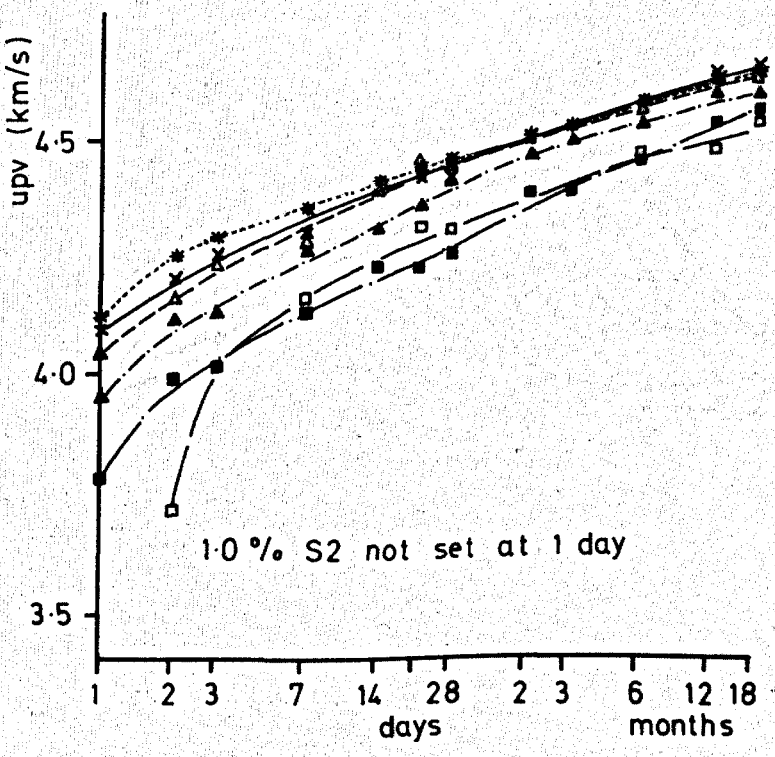

Figure 5.3 Upv vs Age, 20 °C, S1

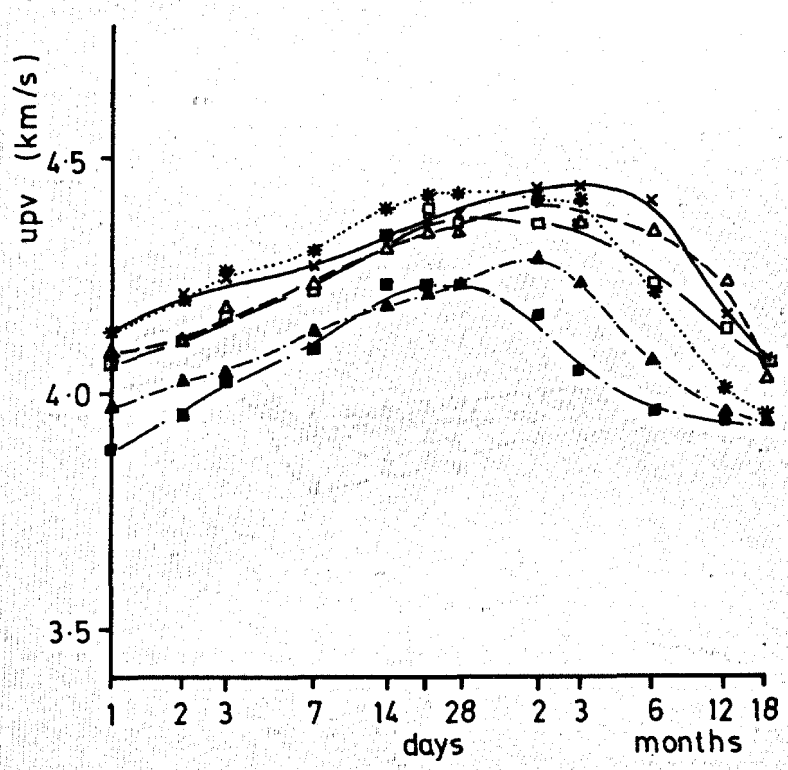

Figure 5.4 Upv vs Age, 20 °C, S2

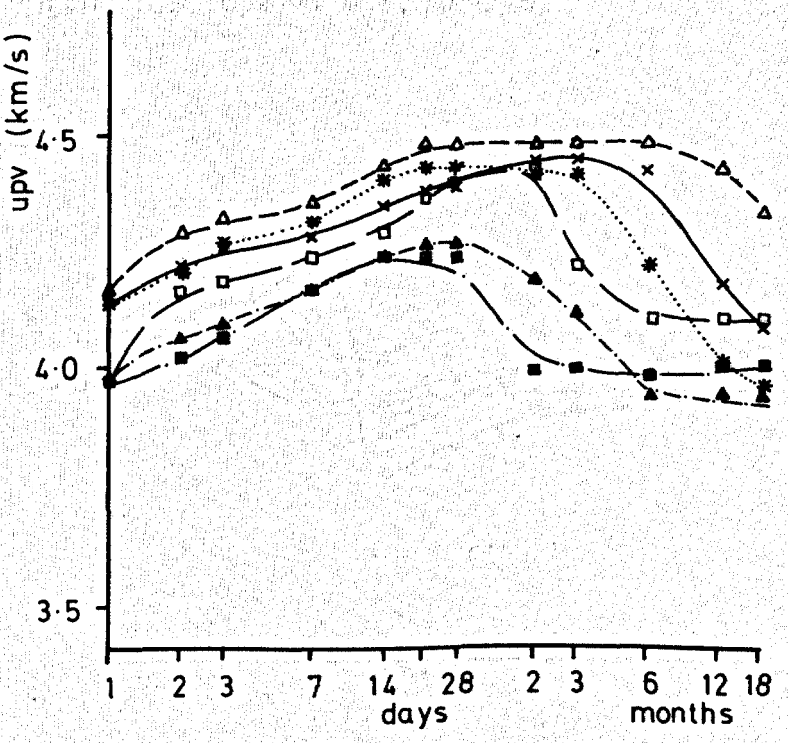

Figure 5.5 Upv vs Age, 30 °C, S1

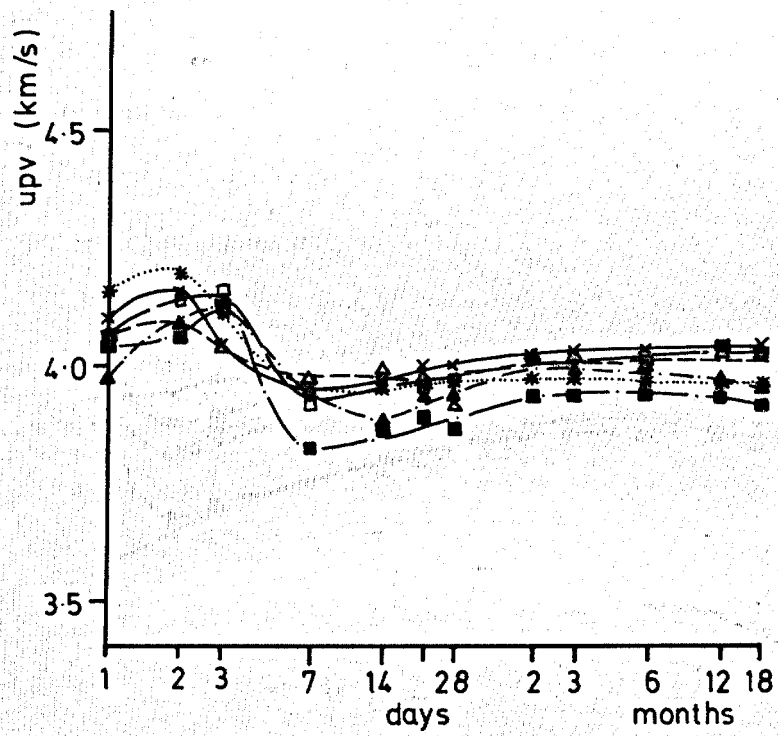

Figure 5.6 Upv vs Age, 30 °C, S2

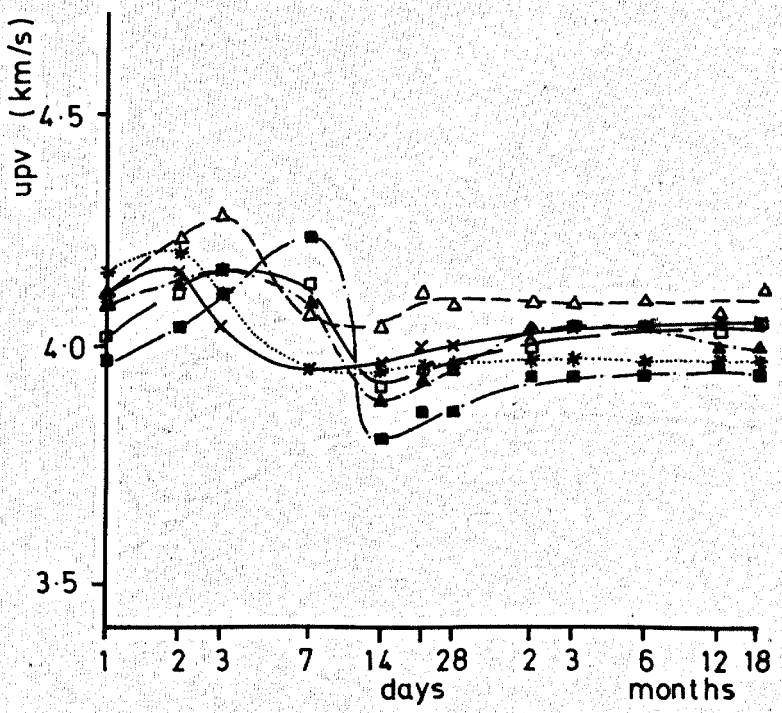

Figure 5.7 Upv vs Age, 40 °C, S1

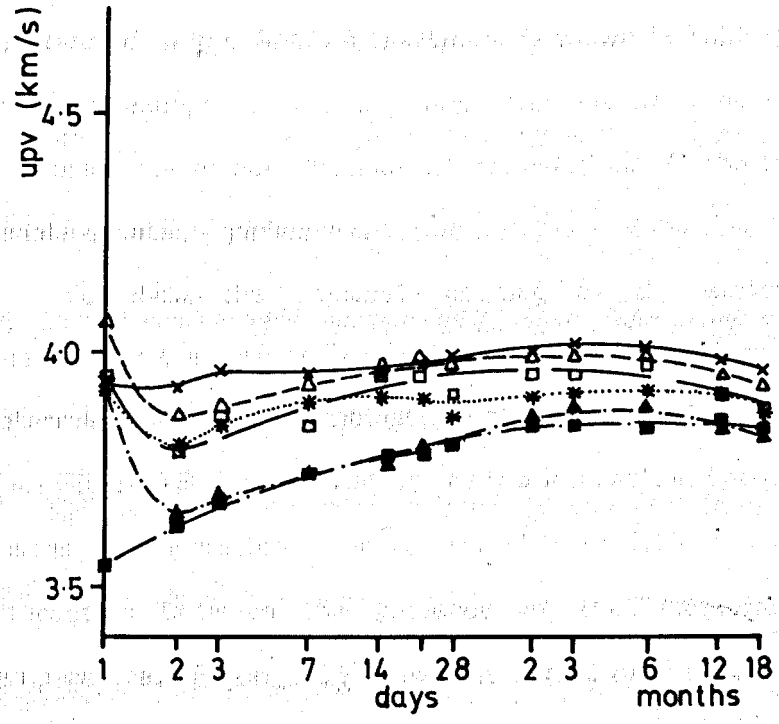

Figure 5.8 Upv vs Age, 40 °C, S2

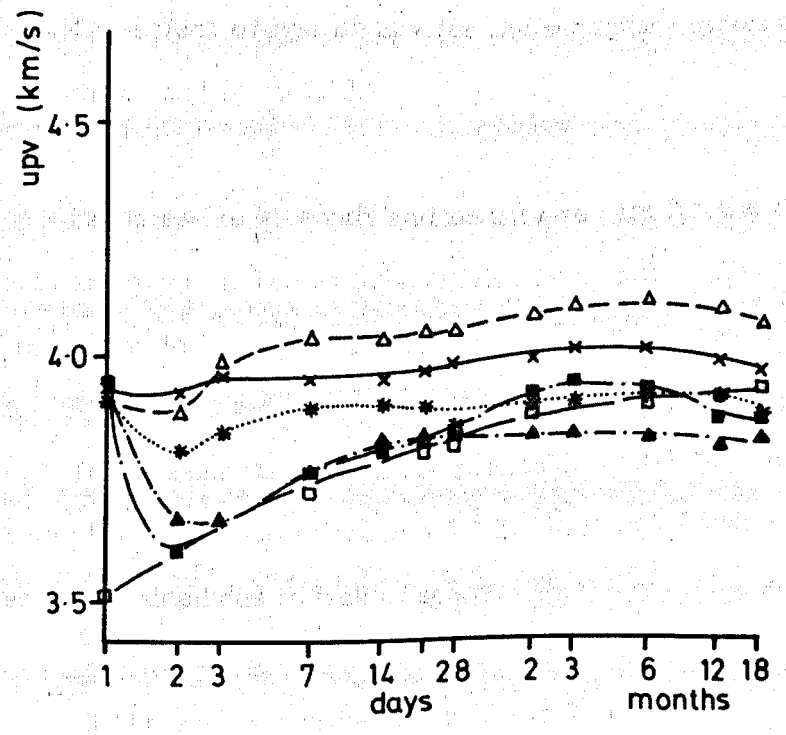

error variance is obtained by combining the 3 and 4 factor interactions (AxBxC etc and AxBxCxD) which are extremely unlikely to be significant.

The statistical significance of the main factors and of interactions determined by the ANOVA treatment is shown in Table 5.4 for all test ages with the exception of 1 day when the upv of some mixes could not be measured due to considerable set retardation. In the table, higher figures denote greater significance.

To show the physical meaning of the statistically significant interactions the data of Figures 5.1-5.8 are replotted to show mean upv values determined at all the combinations of the levels of the 2 factors concerned. Thus Figure 5.9 shows the effect of the interaction between superplasticiser dosage and hydration temperature. Figure 5.10 shows the effect of the interaction between the presence of the accelerator and hydration temperature. Figure 5.11 shows the effect of the interaction between the presence of the accelerator and superplasticiser dosage.

The effect of age on upv for the secondary series of mixes at 20°C is shown on Figure 5.12.

Compressive strength and density results for the main programme of tests are given in Tables 5.5-5.8 with results from the secondary series of mixes given in Tables 5.9 and 5.10.

The presentation of DTG results is restricted to those referred to during the discussion in section 5.4.2. It is not feasible to present all the results obtained due to lack of space.

XRD results are presented in Table 5.11.

Figure 5.9 Effect of Interaction Between Superplasticiser Dosage (factor B) and Temperature (factor D) on Upv

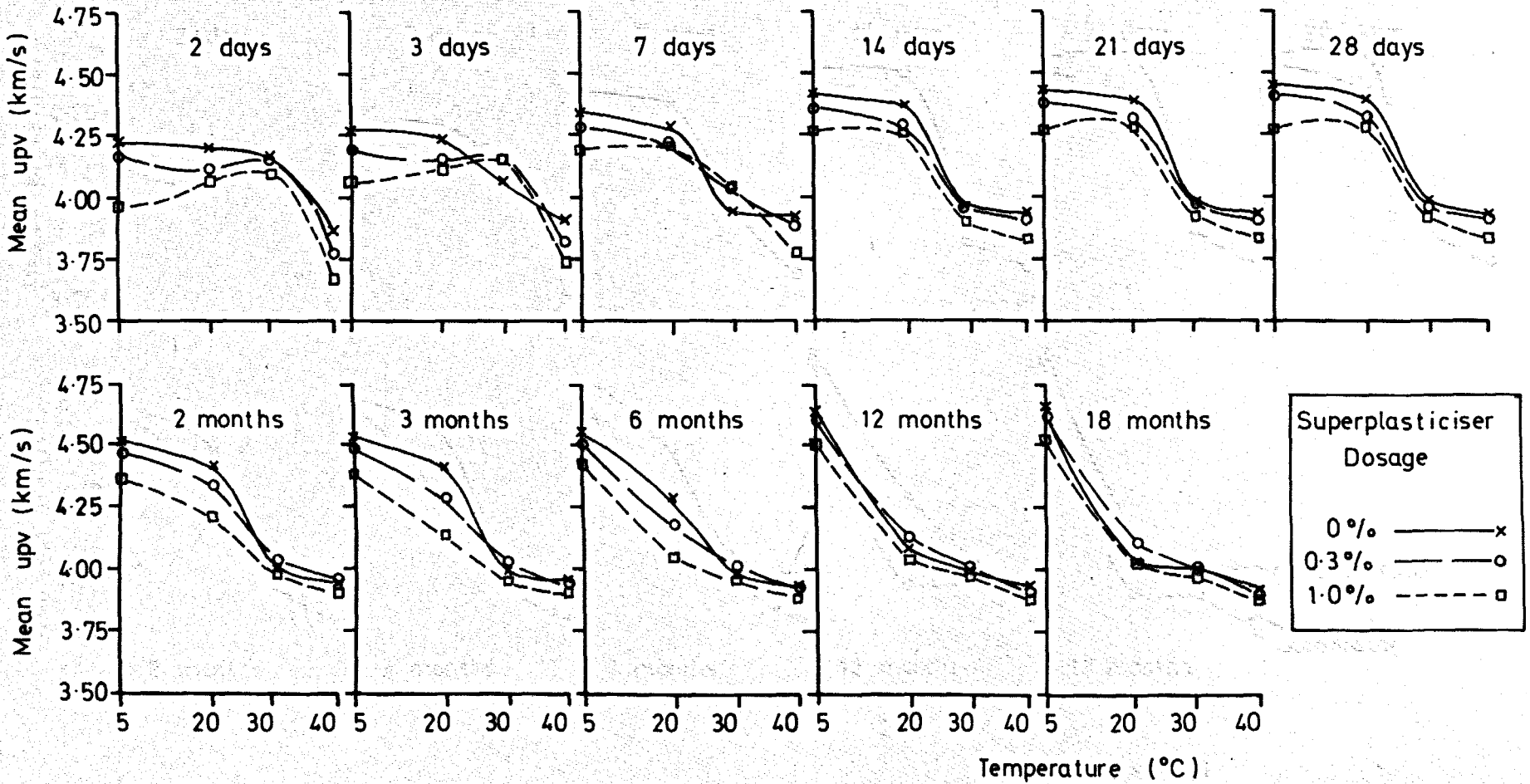

Figure 5.10 Effect of Interaction Between Accelerator Presence (factor C) and Temperature (factor D) on Upv

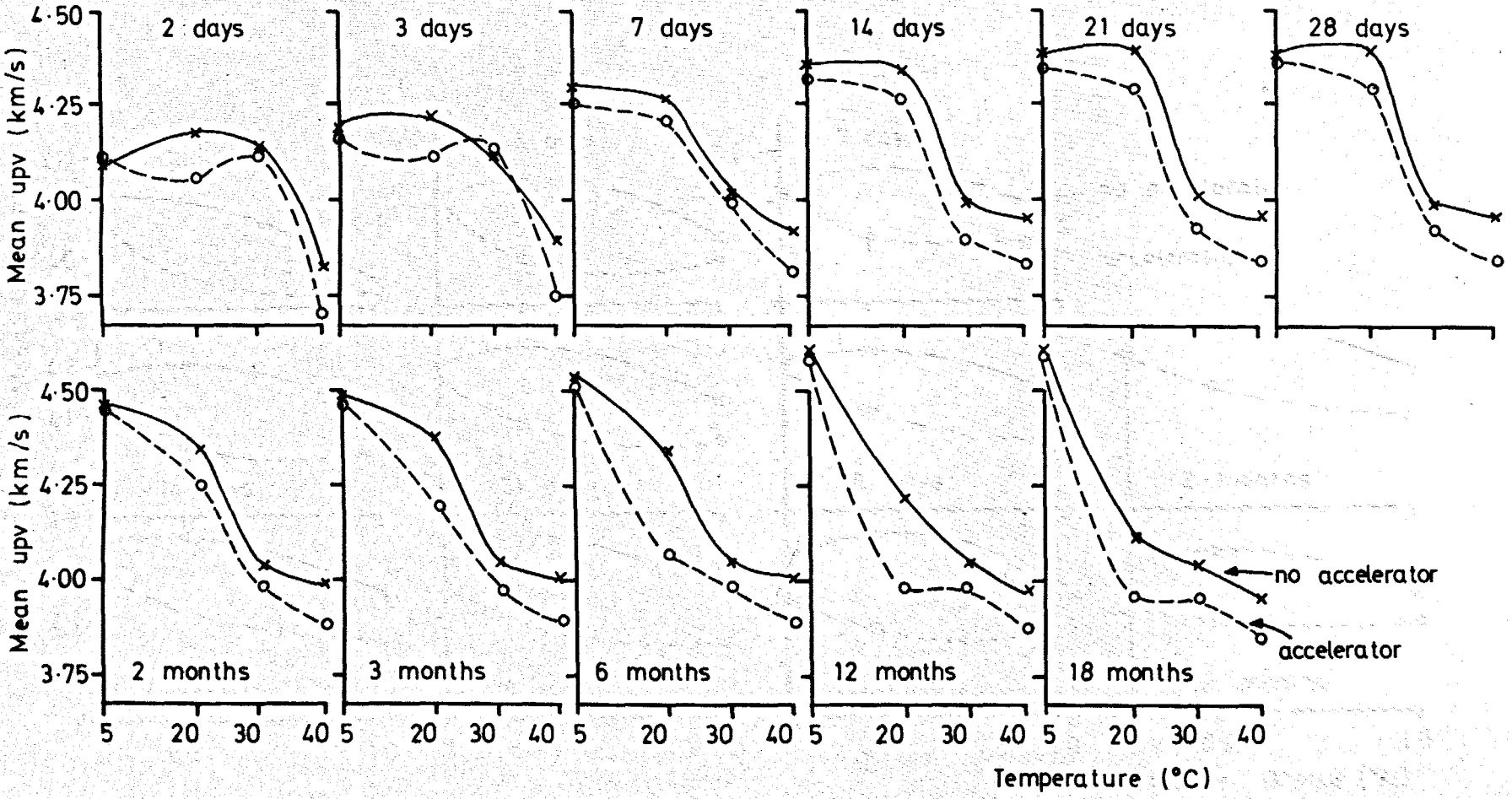

Figure 5.11 Effect of Interaction Between Superplasticiser Dosage (factor B) and Accelerator Presence (factor C) on Upv

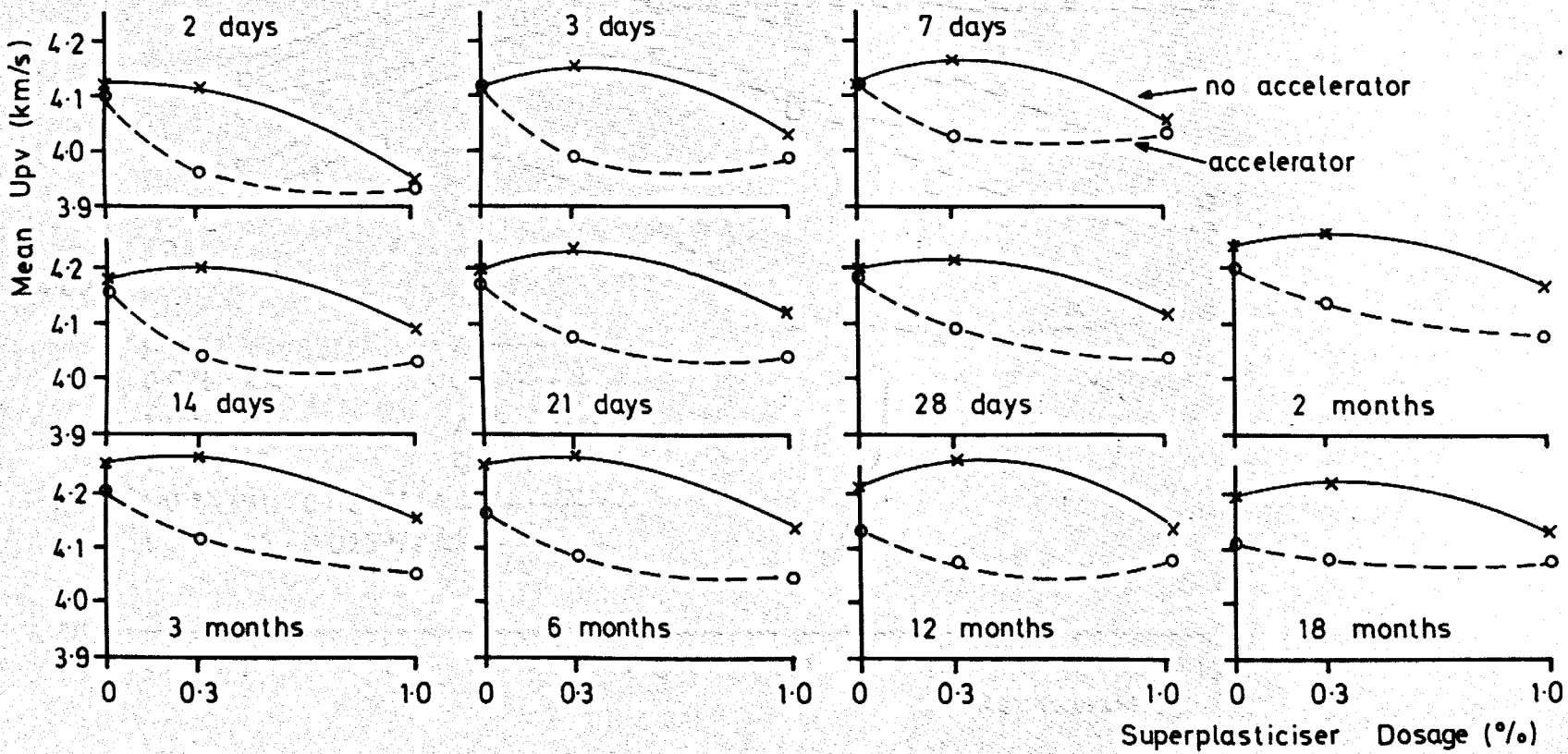

Figure 5.12 Effect of Age on Upv: Secondary Series of Mixes at 20 °C

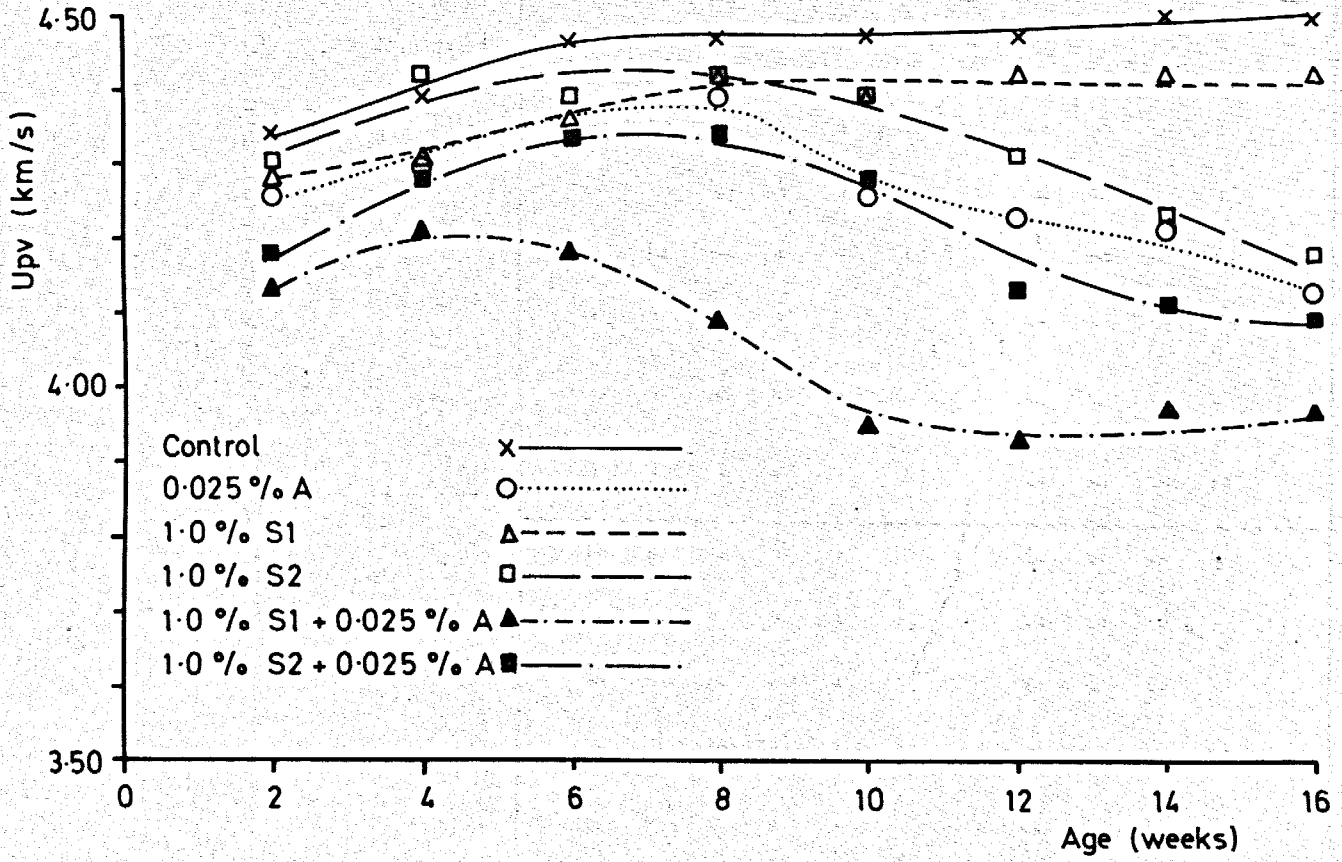

Table 5.4 Summary of Statistical Significance of Main Factors and Interactions on Upv Results from ANOVA

	Test Age										
	2	3	7	14	21	28	2	3	6	12	18
	days						months				
Main Effects											
A	-	-	2	-	1	2	-	-	-	1	2
B	3	3	2	3	3	3	3	3	3	3	2
C	2	3	2	3	3	3	3	3	3	3	3
D	3	3	3	3	3	3	3	3	3	3	3
Interactions											
A x B	-	-	-	-	-	-	-	-	-	-	-
A x C	-	-	-	-	-	-	-	-	-	-	-
A x D	-	-	-	-	-	-	-	-	-	-	-
B x C	2	3	2	3	2	1	2	2	2	3	3
B x D	2	3	2	-	-	-	2	3	3	-	1
C x D	1	2	-	-	-	-	2	2	3	3	2

Factors: A superplasticiser S1, S2

B superplasticiser dosage 0, 0.3, 1.0%

C accelerator dosage 0, 0.025%

D hydration temperature 5, 20, 30, 40°C

Significance levels : 1 = 10% : 2 = 5% : 3 = 1%

Table 5.5 Compressive Strength and Density Results, 5°C

Mix	Cube 1			Cube 2		
	Age	Strength (N/mm^2)	Density (kg/m^3)	Age	Strength (N/mm^2)	Density (kg/m^3)
Control (1)	1d	64.5	2285	12m	128.5	2360
Control (2)	3d	91.5	2335	12m	139.0	2345
0.025% A (1)	1d	69.0	2300	18m	124.0	2360
0.025% A (2)	3d	88.0	2340	6m	128.0	2360
0.3% S1	3d	89.5	2355	6m	111.0	2380
0.3% S1 + 0.025% A	3d	59.5	2320	28d	89.5	2340
1.0% S1	7d	64.0	2310	2m	88.5	2270
1.0% S1 + 0.025% A	14d	81.0	2275	12m	107.0	2320
0.3% S2	7d	64.0	2340	3m	93.0	2350
0.3% S2 + 0.025% A	7d	58.5	2340	6m	97.0	2350
1.0% S2 + 0.025% A	7d	51.0	2320	6m	80.5	2335
1.0% S2 + 0.025% A	2d	45.0	2315	18m	96.0	2340

Note d = day m = month

Table 5.6 Compressive Strength and Density Results, 20°C

Mix	Cube 1			Cube 2		
	Age	Strength (N/mm^2)	Density (kg/m^3)	Age	Strength (N/mm^2)	Density (kg/m^3)
Control (1)	3d	88.0	2320	6m	83.0	2365
Control (2)	21d	110.0	2330	2m	98.0	2320
0.025% A (1)	2d	79.0	2325	28d	105.0	2335
0.025% A (2)	21d	104.0	2345	6m	65.5	2370
0.3% S1	3d	76.0	2305	2m	96.0	2310
0.3% S1 + 0.025% A	14d	83.0	2315	18m	40.0	2360
1.0% S1	2d	66.0	2265	18m	51.5	2340
1.0% S1 + 0.025% A	2d	55.5	2250	12m	44.0	2335
0.3% S2	1d	79.0	2325	2m	109.0	2355
0.3% S2 + 0.025% A	1d	54.0	2310	3m	51.5	2340
1.0% S2	14d	68.0	2320	2m	70.0	2345
1.0% S2 + 0.025% A	1d	42.0	2315	28d	65.0	2350

Note d = day m = month

Table 5.7 Compressive Strength and Density Results, 30° C

Mix	Cube 1			Cube 2		
	Age	Strength (N/mm^2)	Density (kg/m^3)	Age	Strength (N/mm^2)	Density (kg/m^3)
Control (1)	14d	40.5	2365	3m	38.5	2350
Control (2)	2d	65.5	2260	18m	42.0	2375
0.025% A (1)	7d	39.0	2335	28d	38.0	2365
0.025% A (2)	7d	41.0	2360	28d	37.0	2340
0.3% S1	1d	55.0	2325	18m	37.0	2365
0.3% S1 + 0.025% A	1d	49.0	2265	3m	36.0	2300
1.0% S1	21d	39.0	2340	28d	41.5	2290
1.0% S1 + 0.025% A	21d	40.0	2330	3m	39.0	2280
0.3% S2	14d	46.0	2360	18m	45.0	2385
0.3% S2 + 0.025% A	21d	31.0	2340	28d	29.5	2350
1.0% S2	7d	53.0	2320	2m	36.0	2335
1.0% S2 + 0.025% A	14d	35.5	2305	12m	40.5	2380

Note d = day m = month

Table 5.8 Compressive Strength and Density Results, 40°C

Mix	Cube 1			Cube 2		
	Age	Strength (N/mm^2)	Density (kg/m^3)	Age	Strength (N/mm^2)	Density (kg/m^3)
Control (1)	7d	42.5	2350	2m	44.5	2335
Control (2)	14d	42.0	2350	3m	40.0	2360
0.025% A (1)	21d	33.0	2300	6m	30.5	2360
0.025% A (2)	1d	47.0	2330	28d	37.0	2345
0.3% S1	14d	38.0	2355	3m	38.0	2340
0.3% S1 + 0.025% A	2d	23.0	2325	12m	26.5	2355
1.0% S1	21d	40.5	2345	18m	37.0	2355
1.0% S1 + 0.025% A	2d	25.0	2290	2m	29.5	2290
0.3% S2	2d	34.5	2355	12m	44.0	2400
0.3% S2 + 0.025% A	3d	25.5	2335	12m	26.0	2350
1.0% S2	21d	36.0	2355	3m	39.0	2355
1.0% S2 + 0.025% A	3d	25.0	2345	6m	36.0	2370

Note d = day m = month

Table 5.9 Compressive Strength Results from Secondary Series of Mixes at 20°C

Mix	Age (weeks)			
	4	8	12	16
Control	109.5	113.0	111.0	107.5
0.025% A	104.0	93.5	86.0	73.5
1.0% S1	92.5	97.5	98.0	93.0
1.0% S2	85.0	81.0	69.0	57.0
1.0% S1 + 0.025% A	65.0	53.5	42.5	44.0
1.0% S2 + 0.025% A	74.0	78.5	62.5	60.0

Table 5.10 Density Results from Secondary Series of Mixes at 20°C

Mix	Age (weeks)			
	4	8	12	16
Control	2325	2345	2350	2355
0.025% A	2330	2350	2360	2355
1.0% S1	2295	2315	2320	2325
1.0% S2	2345	2370	2365	2365
1.0% S1 + 0.025% A	2265	2285	2295	2305
1.0% S2 + 0.025% A	2335	2350	2355	2355

Table 5.11 Phases Identified by XRD (peak heights given in mm)

Mix Pastes Tested at 1 day	CAH_{10}	C_2AH_8	C_3AH_6	AH_3	CA
5°C Control	√ (26)				√ (44)
20°C 0.3% S2	√ (14)	√ (7)			√ (34)
20°C 0.3% S2 + 0.025% A	√ (8)	√ (20)			√ (33)
30°C Control	√ (10)	√ (45)			√ (29)
40°C Control		√ (45)	√ (17)		√ (27)
Mortars tested at 6 months					
5°C Control	√ (16)				√ (10)
20°C Control			√ (36)	√ (12)	
20°C 1.0% S2			√ (50)	√ (8)	
40°C Control			√ (56)	√ (16)	

Notes : i) The peak heights of paste and mortar samples cannot be directly compared due to the presence of sand. The ratio of peak heights is therefore of more use.

ii) The height of the CA peak for anhydrous Ciment Fondu was 120 mm.

iii) Peak height measurements were made at the angles listed below :

Phase	CAH_{10}	C_2AH_8	C_3AH_6	AH_3	CA
Angle (°2θ)	12.32	8.4	17.24	18.3	30.1

5.4 DISCUSSION

5.4.1 Upv and Strength

5.4.1.1 Interpretation of Upv Measurements

The propagation of longitudinal ultrasonic waves through a solid medium depends on the elastic modulus and density of the material in accordance with equation {1}.

$$c = \sqrt{\frac{E}{\rho}} \qquad \ldots\ldots \quad \{1\}$$

where c = wave velocity

E = bulk modulus of elasticity

ρ = density

Ciment Fondu mortars may be considered as comprising a mixture of air voids, voids filled with solutions of lime and alumina, gels of either alumina or calcium aluminates, crystalline hydrates, unhydrated cement and sand. The propagation of ultrasonic waves through such a material would be expected to vary considerably with changes in the relative amounts of these materials present.

Use of the same mix proportions, materials and compaction procedure should ensure that the amount of sand and air voids is the same for all cubes although it is recognised that there will be unavoidable slight differences in compaction and sand content.

The upv of air is 0.33 km/s whereas the upv of water is approximately 1.5 km/s. The presence of air voids would thus have a considerable effect on the measured upv of a mortar cube. Storage of the cubes in water and wet testing should however ensure that voids were filled with water rather than air.

If imaginary cubes were made entirely from one of the components listed above then the upv would be expected to increase in the sequence: saturated solutions, gels and crystalline hydrates due to the predominating effect of the increasing bulk modulus.

The following factors are considered likely to affect the upv of cubes containing different crystalline hydrates.

(i) differences in the shape, strength and specific gravity as reported in Chapter 1.

(ii) differences in the amount of water required for hydrate production as shown below.

$$6CA \longrightarrow 6CAH_{10} \qquad w/CA\ 1.14$$

$$6CA \longrightarrow 3C_2AH_8 + 3AH_3 \qquad w/CA\ 0.63$$

$$6CA \longrightarrow 2C_3AH_6 + 4AH_3 \qquad w/CA\ 0.46$$

The disagreement concerning the intrinsic strength of the crystalline hydrates was discussed in section 1.6 of the literature review. Whilst the true order of strength remains uncertain it seems likely that the considerable differences in the amount of water required for hydration have a more powerful influence. Complete hydration of CA to C_3AH_6 requires only 40% of the amount of water required to form CAH_{10}. All mixes for upv testing were prepared at w/c 0.40 thus it would be expected that mortars containing mainly C_3AH_6 rather than CAH_{10} would show lower upv values if hydrated to the same extent. Conversion is an additional complication and it is considered that the lower predicted level of upv for formation of C_3AH_6 could be confirmed only by hydration above 55°C to ensure that conversion does not occur.

Guidance is given in Table 2 BS 1881:1986 Part 203 to ensure that the sample size exceeds the wavelength for a transducer of given frequency ((5)). It is recognised that the samples tested in this programme were near the lower limit for the 54 kHz transducer used.

5.4.1.2 Effect of Age and Hydration Temperature

The differences in upv vs age relationships for mixes hydrated at different temperatures are readily seen on Figures 5.1-5.8. Leaving aside for the moment the effect of the admixtures it is worthwhile to note the following general trends.

At 5°C there is a slow but continuous increase in upv up to 18 months. At test ages exceeding 28 days the highest upv measurements are always obtained for mixes at 5°C.

At 20°C upv increases up to 1-6 months after which a steady decrease occurs.

At 30°C there are early increases in upv with values approximately the same as for mixes at 5 or 20°C. However after 3-7 days there is a sharp decrease in upv and although there is some later recovery the final upv values are much reduced compared to mixes at 5°C.

At 40°C it appears that there is a similar abrupt decrease in upv as for 30°C but that this occurs at or before 1 day. Subsequently there is a slight increase in upv up to 18 months.

The most likely explanation of the observed decreased in upv is the conversion of CAH_{10} and C_2AH_8 to C_3AH_6 as described in section 1.6, Chapter 1. DTG evidence in support of this explanation will be presented in section 5.4.2 of this chapter. It is considered that the reduction in upv can be attributed to the increased porosity of the converted paste although no

direct evidence is available to support this proposal. Such a change in porosity would not necessarily be reflected in a reduction in density since the density of C_3AH_6 exceeds that of either CAH_{10} or C_2AH_8.

Although great care was taken to maintain the correct storage temperature at all times a small number of tests to monitor cube temperature during setting showed that considerable increases did occur as result of the heat evolved on hydration. The test results given in Table 5.12 show that cubes stored nominally at 20°C were in fact subjected to curing at >30°C for about 3 hours. It will be shown in section 5.4.2 that this has a considerable influence on the early hydration products. The temperature of the mortar hydrated at nominally 40°C, selected because it had the maximum rate of heat evolution, exceeded 55°C for only 10 minutes which is probably not long enough to cause direct formation of C_3AH_6.

Table 5.12 Temperature Increase in Mortar Cubes During Hydration

Mix	Hydration Temperature (°C)	Maximum Temperature in Mortar Cube (°C)
Control	20	34 (>30°C for 3 hours)
0.3% S2 + 0.025% A	20	37 (>30°C for 3 hours)
0.1% A	40	58 (>55°C for 10 minutes)

5.4.1.3 Effect of Admixtures

Figures 5.1-5.8 show that the presence of either of the superplasticisers usually causes a reduction in upv at all of the hydration temperatures studied for all test ages. The only exceptions to this observation are 0.3% S1 at 5°C and 0.3% S2 at 20, 30 and 40°C. The

reduction in upv increases with increasing dosage and is compounded by the additional presence of the accelerator. Mixes containing only the accelerator do not show marked differences compared to the control except at 20°C when the conversion reaction appears to begin at an earlier age. The general form of the relationship between upv and age at each hydration temperature remains unaltered from the descriptions given in section 5.4.1.2. The effect of both superplasticisers is very similar at all temperatures. The only notable exception occurs at 30°C when the presence of S2 extends the initial period during which upv is increasing. The subsequent minimum value of upv at 30°C is the same for all mixes, about 3.8 km/s, thus the early reduction in upv is greater for S2 mixes as shown in Table 5.13.

Table 5.13 Early Reduction in Upv at 30°C

	Reduction in Upv Occurring at 3-14 Days (km/s)	
	S1	S2
0.3%	0.12	0.24
0.3% + 0.025% A	0.25	0.28
1.0%	0.25	0.25
1.0% + 0.025% A	0.31	0.43

It might be expected that mortar mixes containing admixtures would show early differences in upv in accordance with the acceleration/retardation of hydration as noted in Chapter 4. Figures 5.1-5.8 show however that this is not always so, although the severe retardation of the 1.0% S2 mix at 5°C is reflected in the very low early upv.

The statistical significance of the main factors and of interactions can be clearly identified from the ANOVA treatment of results which is summarised in Table 5.4. The 3 factor interaction was not found to be significant at any age when checked against the 4 factor interaction. The 3 and 4 factor interactions were therefore combined to give a mean square with 23 degrees of freedom against which the F ratios for main factors and interactions could be tested to give the following results:

MAIN FACTORS

Superplasticiser (factor A). While the presence of either superplasticiser caused a reduction in upv at all ages, this decrease was slightly less for mixes containing S2 rather than S1 at 7, 21, 28 days, 12 and 18 months. At other ages there was no significant difference between mixes containing S1 or S2.

Superplasticiser Dosage (factor B). The reduction in upv caused by increasing superplasticer dosage is significant at all ages.

Accelerator (factor C). The presence of the accelerator causes a significant reduction in upv at all ages.

Hydration Temperature (factor D). As expected the hydration temperature has a significant effect on upv with increased temperature causing reduced values.

INTERACTIONS

Table 5.4 shows that the only interactions which are statistically significant are as follows: B x C, B x D and C x D. The interpretation of these interactions in physical terms is simplified by referring to Figures 5.9-5.11.

Figures 5.9 (B x D) shows that at 7-28 days there is a clear contrast between the upv of mixes at 5 or 20°C and those at 30 or 40°C, the higher upv values at 5 and 20°C being for unconverted mortars. After 28 days the upv of mixes at 20°C decreases, due presumably to conversion. It is interesting to note that mixes containing superplasticisers show an earlier and larger drop in upv, this effect being more marked as the dosage increases from 0.3 to 1.0%. It was these observations which led to the preparation of an additional series of mixes at 20°C to enable the changes to be studied more closely. Figure 5.12 shows that the behaviour was confirmed and clarified that the presence of the accelerator exacerbates the drop in upv and causes it to occur earlier than for mixes containing only a superplasticiser.

The effect of the accelerator in reducing upv at all ages is seen on Figures 5.10 (C x D) and 5.11 (B x C). Figure 5.10 shows that there is very little reduction in upv at 5°C but at higher temperatures the reduction is about 0.1 km/s. Figure 5.11 shows that the effect of the accelerator in reducing upv in unplasticised mixes becomes progressively greater with increasing age. At all ages the upv reduction is greater for mixes containing only 0.3% superplasticiser compared to 1.0% superplasticiser.

The results for the secondary series of mixes given in Table 5.10 show a statistically significant increase in density with age (at 5% level using 2 way ANOVA with age and admixture combination as the 2 factors) whilst upv is reduced. Mixes at 5°C also showed an increase in density with increasing age but this was accompanied by increasing upv. The density measurements cannot therefore be used to make any predictions on upv.

The reductions in upv are accompanied by considerable strength reductions as recorded in Table 5.9. The correlation between upv and strength will be discussed in section 5.4.1.4 whilst the changes in hydrates

associated with the reduction in upv and strength will be discussed in section 5.4.2.

5.4.1.4 Correlation Between Upv and Strength

All results obtained from the main programme are plotted on Figure 5.13. There is seen to be reasonable correlation between upv and strength. Presentation of the data in this form clearly shows that greater strengths were obtained for mortars stored at 5 or 20°C compared to higher temperatures.

The relationship between upv (v) and strength (f) for mortar or concrete is generally taken to conform to either equation {2} or {3} where A,B,C and D are constants.

$$f = A.v^{B} \quad \ldots\ldots\ldots \quad \{2\} \qquad ((3))$$

$$f = C.e^{D.v} \quad \ldots\ldots\ldots \quad \{3\} \qquad ((4))$$

Guidance on the effect of sample temperature on measured upv is given in Table 1 BS 1881:1986 Part 203 ((5)). It is suggested that measurements at 40°C should be increased by 1.7% whilst measurements at 5°C should be reduced by 0.75%. Tests on cubes normally at 40°C allowed to cool to 20°C did not however show any alteration in measured upv; thus it appears that no corrections should be made to the experimental data.

It was thought that alterations in hydrate composition may lead to slightly differing values of the constants in equations {2} and {3} thus the correlation between upv and strength at each hydration temperature was investigated. Using equation {2} it was found that the best fit curves for 20, 30 and 40°C were within the 95% confidence limits calculated for 5°C. The confidence intervals for 5°C were selected since the best correlation (r = 0.92) was obtained for this temperature.

Figure 5.13 Correlation Between Upv and Strength, All Results

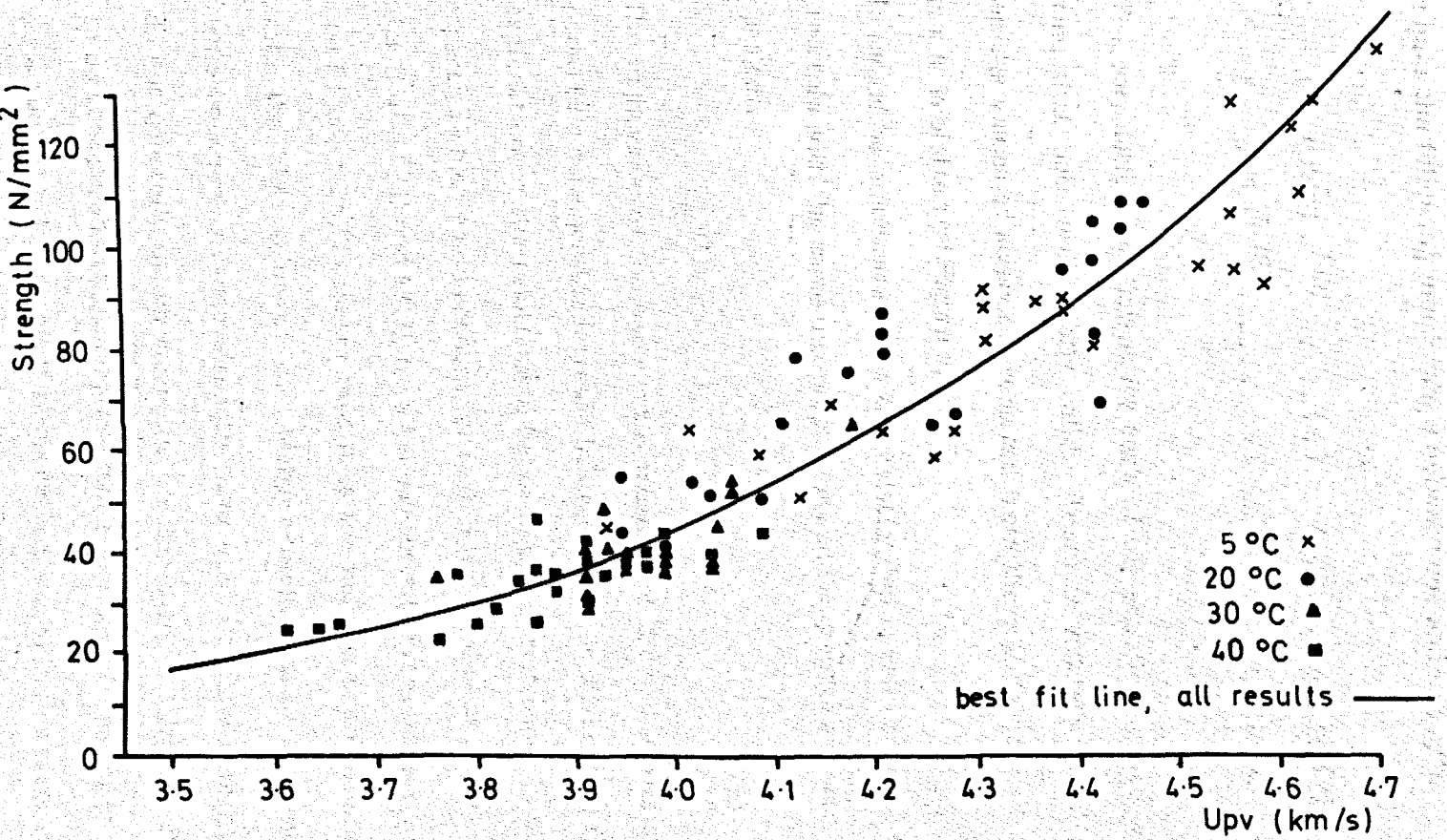

There is therefore no evidence that differences in hydrate composition caused either by initial hydration temperature or by conversion have any effect on the correlation between upv and strength. Consideration of all results gave the following relationships between upv and strength.

$$f = 0.0025.v^{7.08} \quad \ldots\ldots \{4\} \qquad \text{(applying equation \{2\})}$$

$$f = 0.05.e^{1.70.v} \quad \ldots\ldots \{5\} \qquad \text{(applying equation \{3\})}$$

The correlation coefficient for each of the equations above was 0.94 indicating that both are equally valid. There is virtually no difference between the values of strength predicted from these 2 equations thus only equation 4 is plotted on Figure 5.13.

It should be emphasised that this relationship is valid only for Ciment Fondu mortars with the same mix proportions and aggregate as those studied in this project.

The high value of the exponent B means that a small increase in upv corresponds to a considerable increase in strength. It is difficult to find any clear explanation of the relationship between upv and strength in terms of bulk properties which could account for such a large value of B. Previously, values for B of 4 ((6)) and 6 ((7)) have been reported. From inspection of the results on Figure 5.13 it appears that it is the high strength results which necessitate the high value of B. Many experiments to determine the relationship between upv and strength have used Portland cement mixes which do not generally attain strengths greater than 70 N/mm^2. Another factor to be considered is that very few experiments on Ciment Fondu have been carried out at below ambient temperature, shown in this programme to produce the highest strength results.

Calculation of the 95% confidence intervals for equation {4} show that

the predicted strength at a given upv is as shown in Table 5.14

Table 5.14 Predicted Strength from Upv Measurement

Upv (km/s)	95% Confidence Intervals for Predicted Strength (N/mm^2)
3.7	18 - 37
4.0	32 - 64
4.3	53 - 107

5.4.2 Hydrate Composition

5.4.2.1 Identification of DTG Peaks

The association of DTG peaks with particular hydrates was made after consideration of:

(i) Published information on peak temperature

(ii) Comparison of DTG and XRD results from the same specimens

(iii) Anticipated hydrate compositions for plain pastes at various temperatures.

Several problems were encountered in interpretation of DTG results which will now be discussed.

Effect of Amount of Hydrate Present

Assuming that dehydration of a given hydrate does not begin until a certain, critical temperature it is reasonable to suppose that the DTG peak temperature will increase as the amount of hydrate increases. Dr. H.G. Midgley suggests that a graph of ln (peak height) against peak temperature gives a series of straight lines corresponding to different hydrates ((10)). A

graph was therefore produced using data from DTG traces produced during the main test programme and is included as Figure 5.14. The points are seen to lie on a series of almost parallel straight lines each of which corresponds to dehydration of a particular hydrate. The graph is extremely useful in differentiating between peaks occurring at similar temperatures, particularly in the range 40-100°C. In this temperature range the predominance of CAH_{10} peaks at 5 and 20°C can clearly be seen whilst the gel peaks occur for mixes hydrated at higher temperature. XRD results from mixes hydrated at 30 and 40°C showed that no CAH_{10} was present, as expected at these temperatures. It is recognised however that CAH_{10} is often present in a poorly crystalline state and therefore the confirmation of CAH_{10} by XRD may be difficult, particularly at early ages. The production of gels of either alumina or calcium aluminates has been suggested by several researchers ((8-10)). The composition of the phase corresponding to the low temperature peak was therefore assumed to be a gel of some description in which the water molecules are loosely bound. The possibility of the presence of residual water from the paste can be discounted since the acetone quench procedure and subsequent storage of the specimens ensures that they are completely dry. Comparison of the temperature range observed for the gel compared to that for other phases led to the tentative suggestion that there are 2 different gel forms. This is supported by the observation of 2 distinct "gel" peaks on some traces.

Initially it was considered that the wide range of temperatures thought to correspond to AH_3 may be due to the presence of more than one form of AH_3. However no DTG graph showed 2 distinct AH_3 peaks in addition to a C_3AH_6 peak and it seems that only 1 line for AH_3 should have been drawn on Figure 5.14. The relatively wide range of temperature then associated with the AH_3 peak is possibly due to AH_3 of differing maturity. Pure

Figure 5.14 Effect of DTG Peak Height on Peak Temperature

5 °C × 20 °C ○ 30 °C △ 40 °C □

● A pure C_3AH_6

● B pure AH_3 (gibbsite)

● C CAH_{10} } confirmed by XRD

● D C_2AH_8 }

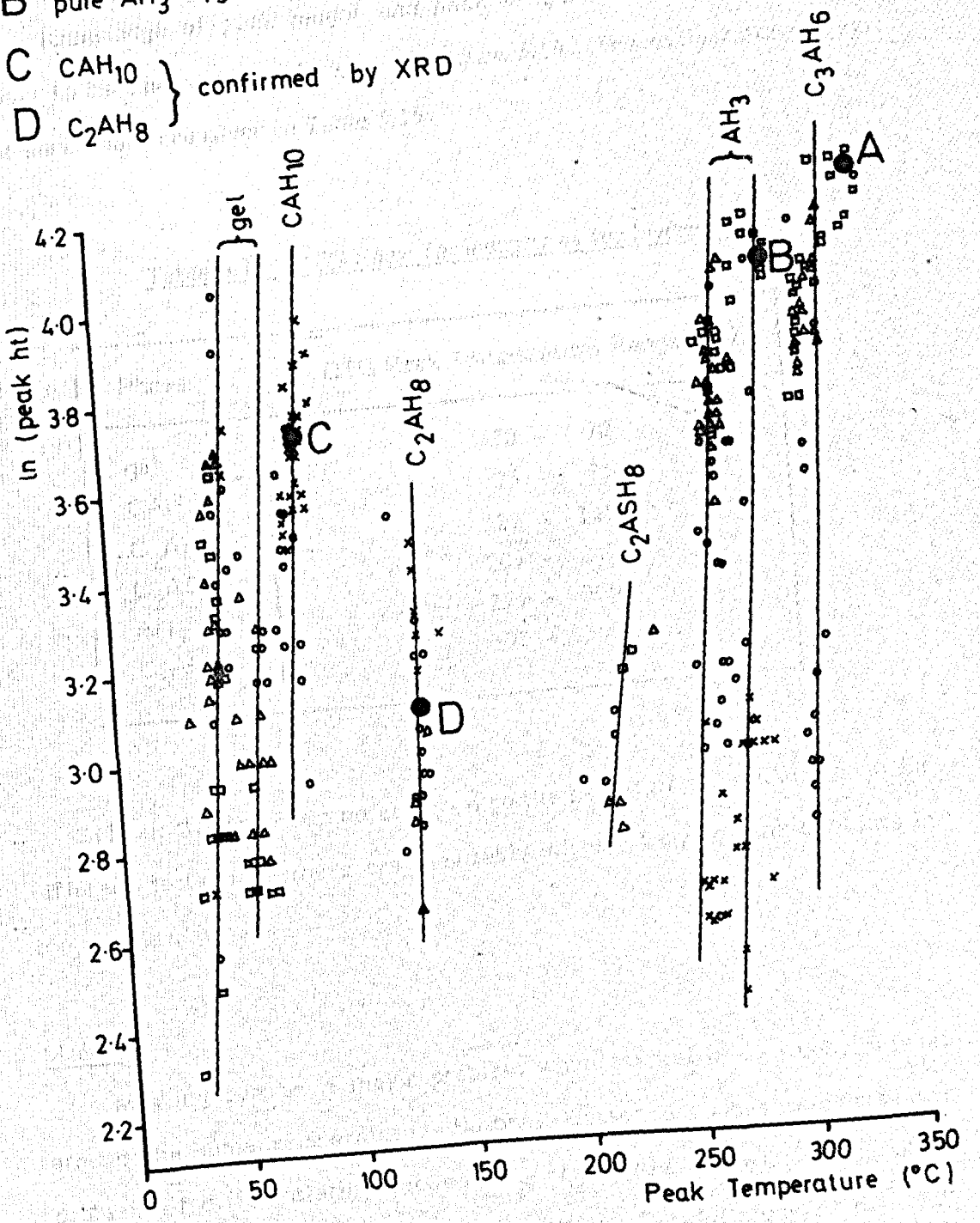

samples of C_3AH_6 and Gibbsite were kindly supplied by Dr. H.G. Midgley and the DTG peak positions are shown on Figure 5.14 as points A and B respectively. These results suggest that the lower temperature AH_3 peaks are perhaps due to less crystalline AH_3.

Knowledge of peak height and peak temperature thus enables DTG peaks to be assigned by reference to Figure 5.14. The temperature ranges for each phase are given in Table 5.15.

Table 5.15 DTG Peak Temperatures for Hydrates

Phase	DTG Peak Temperature Range (°C)
gel	30 - 70
CAH_{10}	75 - 95
C_2AH_8	125 - 145
C_2ASH_8	205 - 240
AH_3	255 - 300
C_3AH_6	305 - 340

No significance can be attached to the height of a particular peak for different tests since there are inevitably slightly varying sand contents in the samples.

Masking

Masking can be a major problem when several phases dehydrate at around the same temperature. Bushnell-Watson describes the particular problem of differentiating between C_2AH_8, C_4AH_{13} and $C_4A\bar{C}H_{11}$ which all show peaks at a similar temperature ((8)). Careful study of the XRD

results for 6 month samples did not however show either of the 2 latter hydrates thus the peak at 125-145°C is most likely to be C_2AH_8. It is recognised that XRD analysis should ideally be carried out for all samples in addition to DTG testing and that "C_2AH_8" peaks may have been incorrectly ascribed for some mixes.

Masking causes a problem in determining the presence of C_2AH_8 when there is also a large amount of CAH_{10}. The C_2AH_8 peak is then present as a shoulder and the relative peak heights are difficult to distinguish. It is likely that the greater amount of combined water in CAH_{10} will lead to a greater weight loss compared to either C_2AH_8 or C_3AH_6 for a given weight of hydrate.

Estimation of Degree of Conversion

The accepted formula depends on measurements of the amounts of CAH_{10} and AH_3. Some of the drawbacks associated with the use of the formula have already been discussed in section 1.6.2, Chapter 1. Additional problems became apparent during the experimental work. Firstly the difficulty in distinguishing between the gel and CAH_{10} peaks, or the masking of a gel peak by a large amount of CAH_{10} may cause errors. Secondly no account is taken of conversion of C_2AH_8 to C_3AH_6 which will be the dominant reaction when the hydrate originally formed is C_2AH_8. Thirdly, although the conversion of CAH_{10} produces approximately equal quantities of C_3AH_6 and AH_3, the conversion of C_2AH_8 produces considerably more C_3AH_6. It therefore seems sensible to discuss the degree of conversion qualitatively rather than quantitatively.

5.4.2.2 Results for Plain Pastes

The problem of considerable temperature increases within cubes during early hydration was described in section 5.4.1.2. The need for great

care to be taken in interpretation of DTG results can clearly be seen on Figures 5.15 and 5.16 which compare DTG results for pastes and mortars of the same composition hydrated at 5°C (Figure 5.15) and 20°C (Figure 5.16). Pastes were prepared at w/c ratio 0.40 using only 10g of Ciment Fondu to ensure that there was no significant temperature rise in the sample during hydration. The effect of temperature increases in the larger, mortar specimens is immediately apparent for both mixes. At 5°C the temperature rise in the mortar cube, although not monitored, was clearly sufficient to allow formation of C_2AH_8 and AH_3 in addition to the CAH_{10} found in the paste.

At 20°C the same effect is observed although it is more pronounced than at 5°C.

The size of cube samples used is comparable to the thickness of grout likely to be used in industrial applications thus the effects observed during this test programme provide a practical indication of long term behaviour.

At 5°C Figure 5.17 shows that there is little change in hydrate composition from 1 day to 1 year, although it appears that conversion has occurred to a very slight extent. Figures 5.1 and 5.2 showed no decrease in upv up to 18 months which implies that the low rate and/or degree of conversion observed is insufficient to cause a reduction in either upv or strength. It has been shown that the initial presence of any C_2AH_8 and AH_3 was due to the temperature rise in the cubes during hydration.

At 20°C the main initial hydration products are CAH_{10}, C_2AH_8 and AH_3. If the temperature during hydration had been maintained at exactly 20°C the proportion of CAH_{10} would have been higher. Figure 5.18 clearly shows the conversion of CAH_{10} and C_2AH_8 to C_3AH_6 with increasing age. The conversion reaction proceeded most rapidly between 3 and 6 months

Figure 5.15 DTG Results at 5°C, Control Mixes, 1 Day

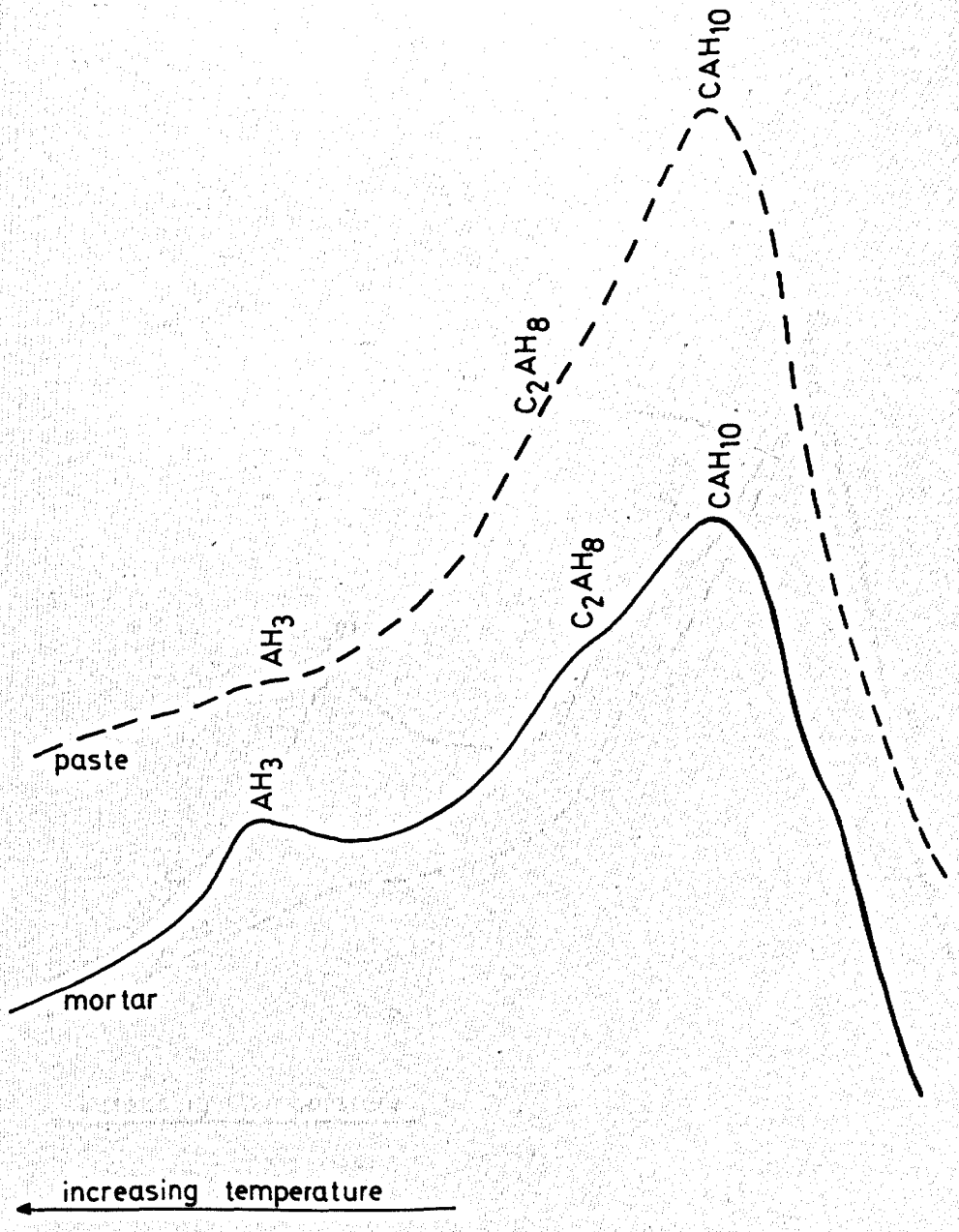

Figure 5.16 DTG Results, 20 °C, 0·3 % S2 + 0·025 % A, 1 day

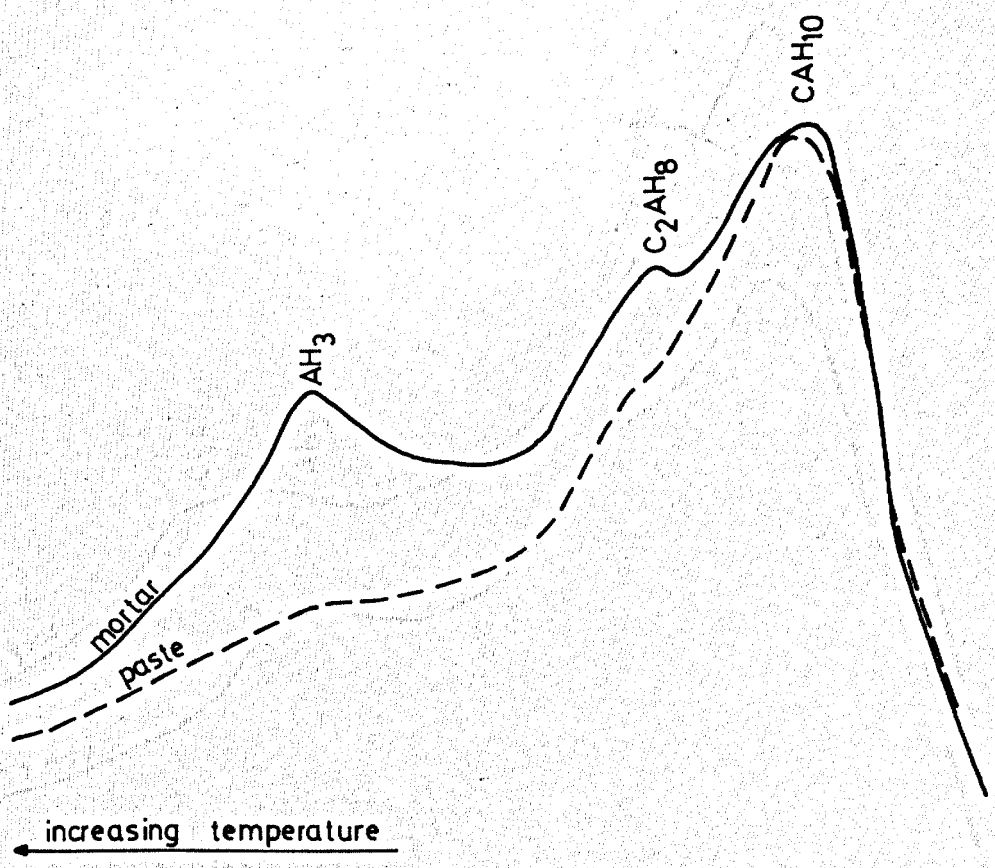

Figure 5.17 DTG Results, Control Mortar Mix at 5°C

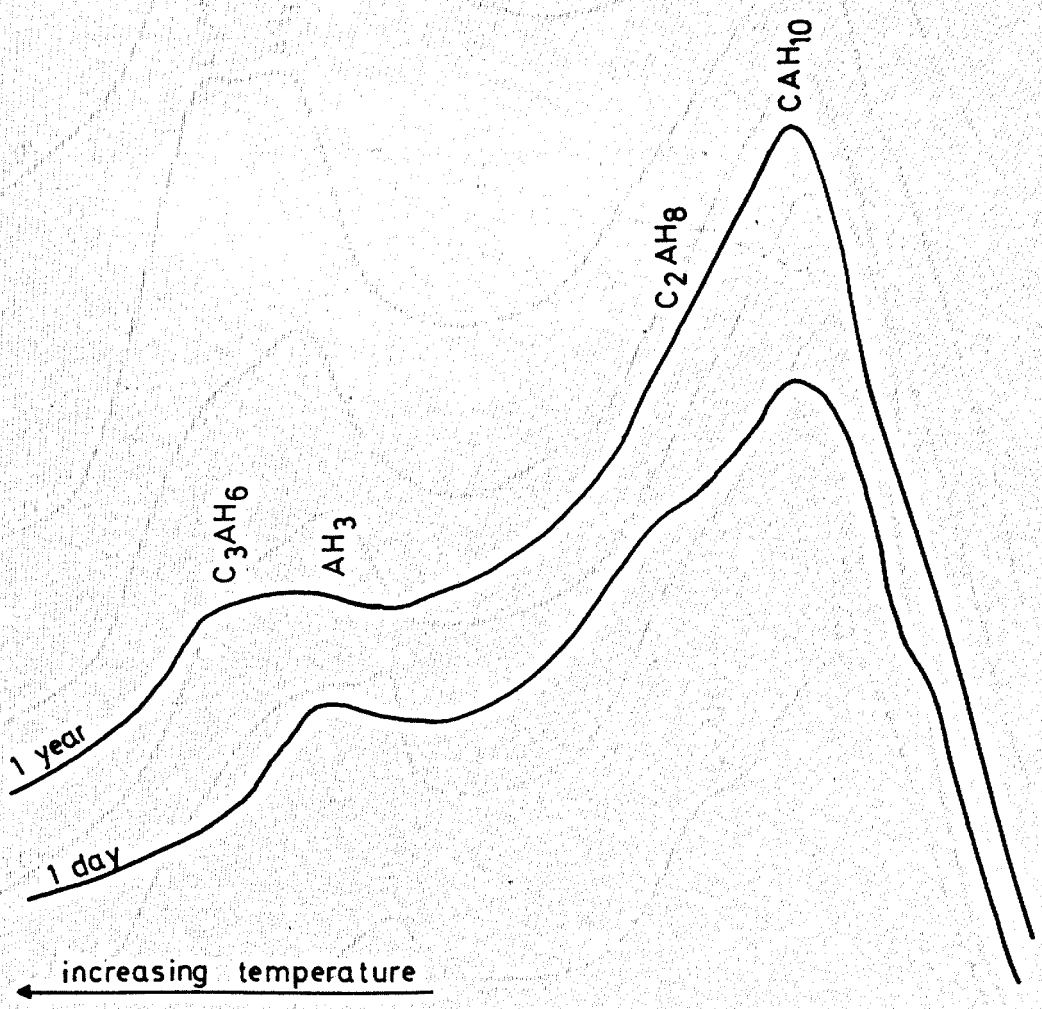

Figure 5.18 DTG Results Showing Effect of Age on Control Mortar Cubes Stored at 20°C

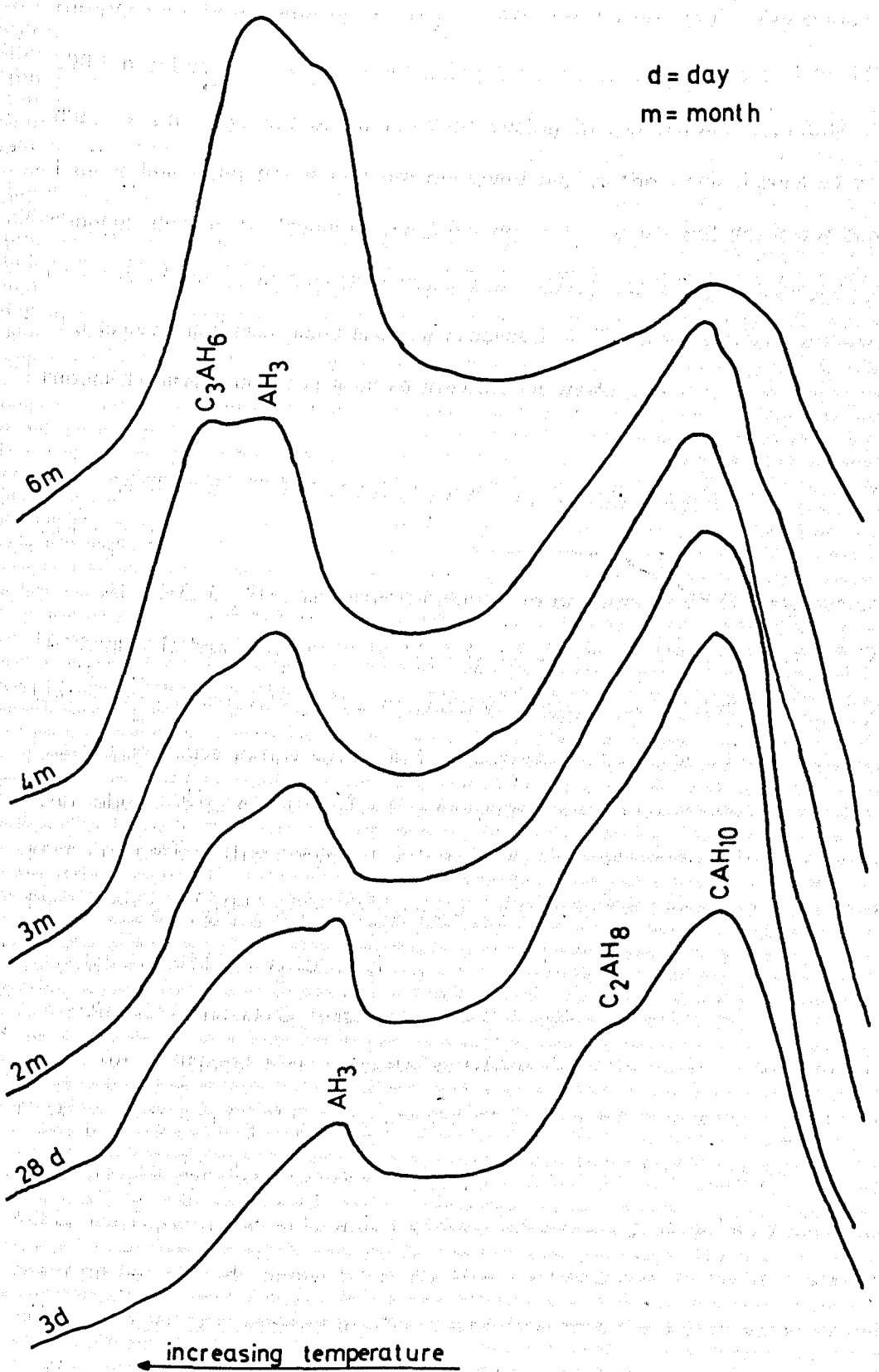

which corresponds well with the decreasing upv recorded on Figures 5.3 and 5.4. The level of conversion observed after only 6 months is higher than that reported by Teychenne for curing at 18°C for 1 year (127). Teychenne used 100mm cubes of concrete containing 1 : 3 cement:aggegate and found that the maximum temperature reached during hydration was typically 25°C. This is less than the maximum observed during the work described in this chapter, due to the lower nominal curing temperature and the lower cement content which must together more than offset the effect of larger cubes. The lower maximum temperature recorded by Teychenne thus explains the reduced conversion compared to the current work.

At 30 and 40°C the main hydration products are amorphous gel, AH_3 and C_3AH_6.

At 30°C C_2AH_8 is formed initially in preference to C_3AH_6 but after 14 days this has converted to C_3AH_6 as shown by the sequence of DTG traces on Figure 5.19. The conversion reaction correlates well with the marked decrease in upv which in turn corresponds to a decrease in strength from about 65 to 40 N/mm². The gel peaks remain quite distinct even at 1 year indicating that crystallisation is a slow process. The continued formation of C_3AH_6 after 14 days can be seen in the increased ratio of the peak heights of C_3AH_6 to AH_3.

At 40°C no DTG tests were carried out on mortar samples until 7 days. An additional test on paste at w/c 0.40 cured at 40°C showed that C_2AH_8, AH_3 and C_3AH_6 were present at 1 day. At 7 days the C_2AH_8 had converted to C_3AH_6. If it is assumed that the initial hydration products at 40°C are C_2AH_8 and AH_3 which convert very rapidly, it is likely that this reaction has already begun by 1 day thus no reduction in upv is observed. This argument is supported by the observation that the initial value of upv at 1 day is virtually the same as for mortar at 20 and 30°C after conversion.

Figure 5.19 DTG Results Showing Effect of Age on Control Mortar Cubes Stored at 30 °C

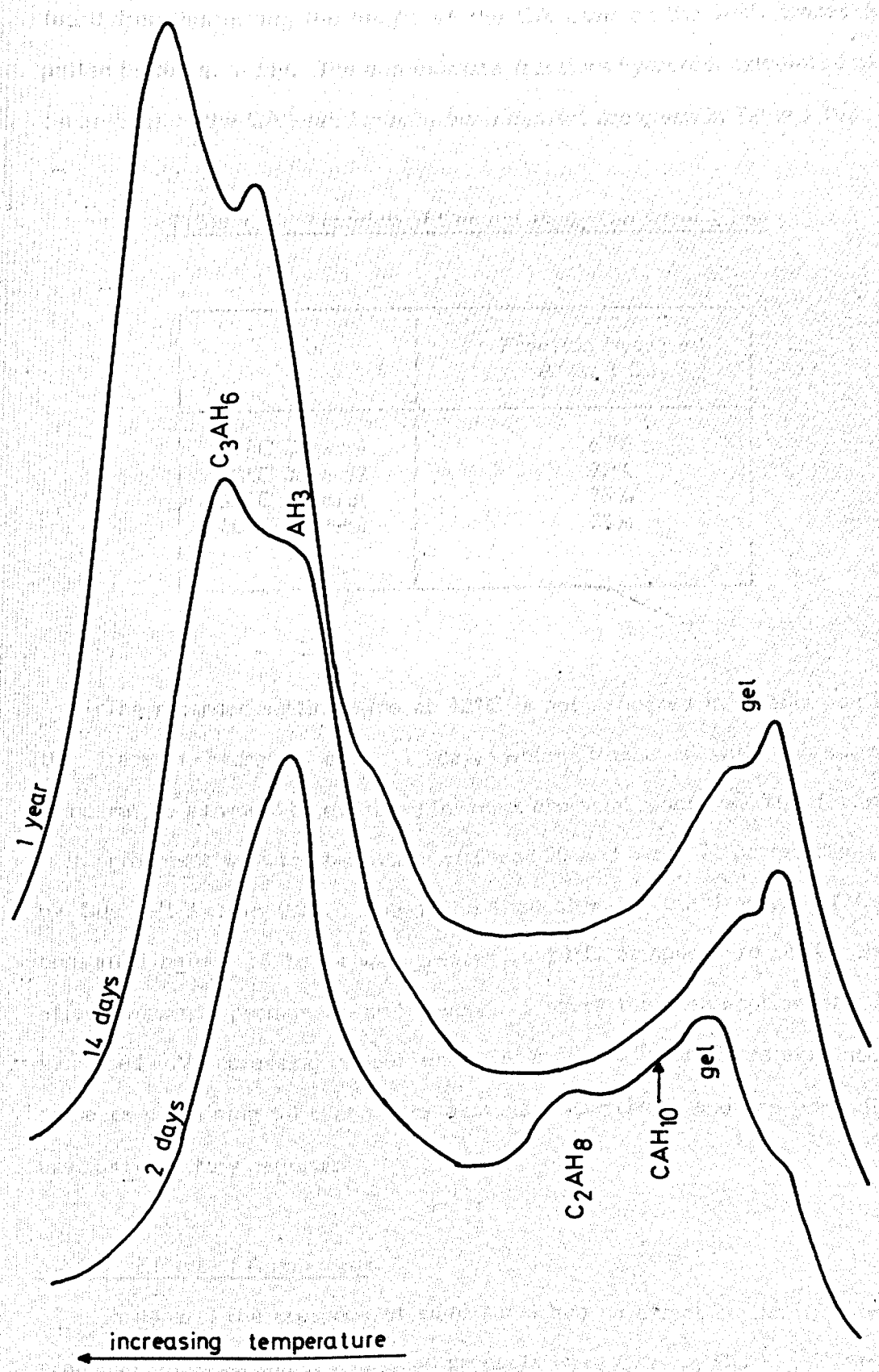

An indication of the fraction of cement hydrated after 1 day can be found from inspecting the height of the CA peak on the XRD traces for pastes tested at 1 day. The approximate fractions hydrated, calculated as a percentage of the CA peak for anhydrous cement are given in Table 5.16,.

Table 5.16 Fraction of Cement Hydrated After 1 day

Mix	Fraction Hydrated After 1 Day
5°C Control	63%
20°C 0.3% S2	72%
30°C Control	76%
40°C Control	78%

The retarded setting time at 30°C is not reflected in a reduction in the fraction hydrated after 1 day, which increases with increasing temperature as would be expected for most chemical reactions. This finding is in agreement with the behaviour of Secar 50 and Secar 71 pastes studied by Bushnell-Watson ((8)). She found that although the fraction of CA consumed before 16 hours was greater at 20°C compared to 30°C, the effect was not permanent and beyond 16 hours the consumption of CA increased with increasing temperature. Secar 50 and Secar 71 are aluminous cements containing 50% and 71% alumina respectively and are normally used as refractory cements.

5.4.2.3 Effect of Admixtures

In general the presence of admixtures had no effect on the hydrates produced since the major hydration products were CAH_{10}, C_2AH_8, C_3AH_6 and AH_3 as for plain mixes.

Rodger and Double suggested that the presence of lithium ions favours production of C_2AH_8 at the expense of CAH_{10} (14). The DTG results from this test programme suggest however that it is not the presence of lithium per se but simply the increase in temperature caused by the accelerating effect of lithium. For example Figure 5.20 shows that there is no difference between plain paste and paste containing 0.025% accelerator after 1 day at 5°C; indeed there is slightly more C_2AH_8 and AH_3 in the plain paste. Also shown on Figure 5.20 are results from pastes hydrated at 20°C which show that neither S2 or S2 with the lithium salt have a significant effect on the hydrates produced compared to the control mix.

The size of sample used by Rodger and Double to investigate hydrate composition was not stated although during adiabatic calorimetry temperatures of up to 100°C were recorded for hydration at 22 $\pm$ 2°C. Such extreme temperatures during hydration provide an explanation for the appearance of C_2AH_8 rather than CAH_{10} and clearly illustrate the need to record the temperature during hydration of any sample which is subsequently to be analysed for hydrate composition.

At 5°C there is clear evidence of a gel peak for a few mixes although its occurrence seems to be random. Since this gel occurs more often at higher hydration temperatures it is thought that its presence in a cube stored at 5°C is indicative of an increased temperature during hydration. An increase in temperature to only about 15°C would be sufficient to account for formation of C_2AH_8, AH_3 and perhaps the amorphous gel. Such an increase could be caused by poor circulation of cold water around the cube moulds.

At 20°C the admixtures did have a considerable effect on the conversion reaction as mentioned in section 5.4.1.3 when it was shown that

Figure 5.20 DTG Results Showing Effect of Admixtures on Mortars at 5°C, Pastes at 20°C, 1 Day

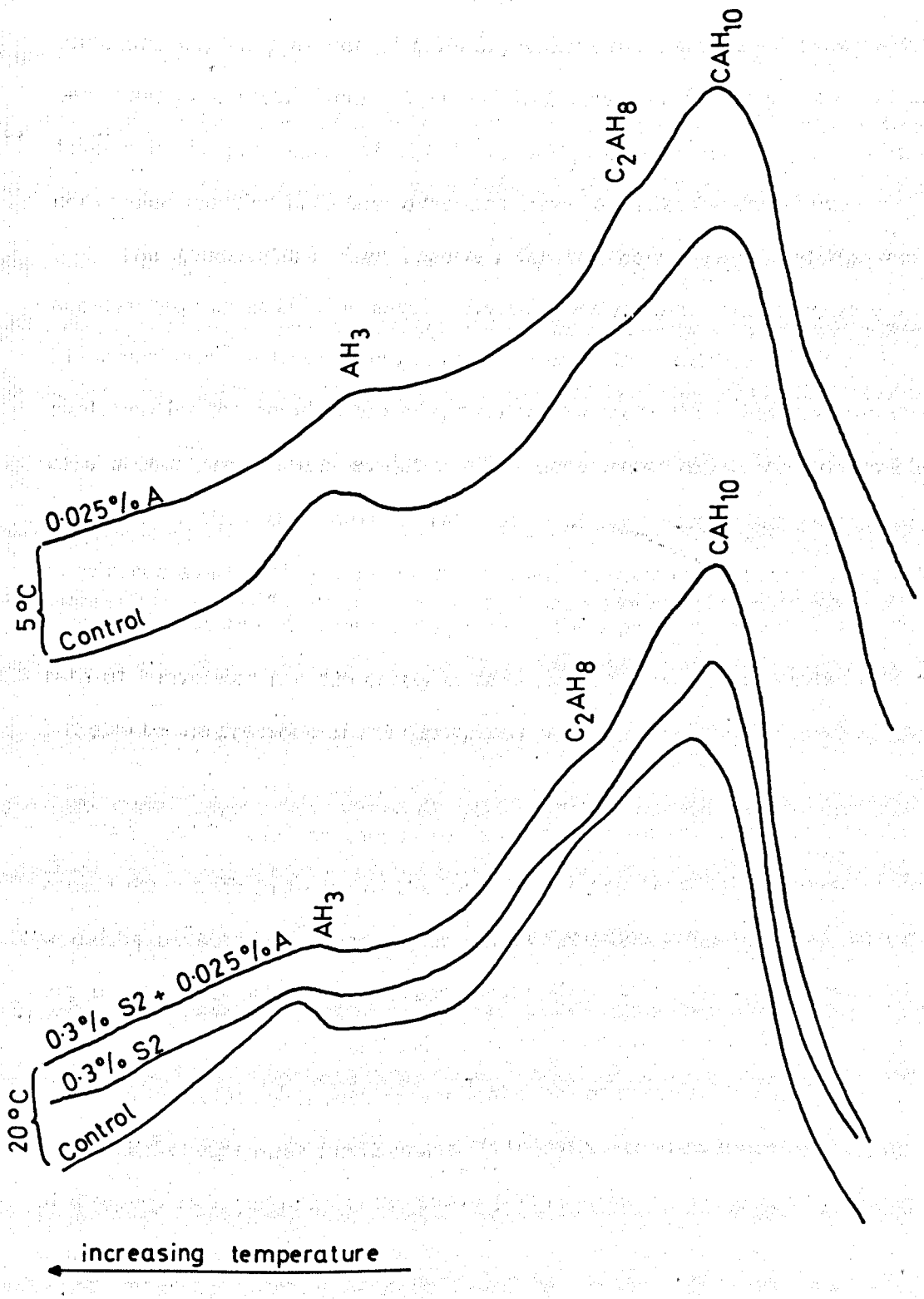

the upv of cubes containing admixtures reduces earlier and more rapidly than for the control. It was initially thought that this was again due to the increased temperature of the accelerated mixes. Although this would have some impact, the presence of 1.0% S2, which causes severe set retardation, does have an effect. Figures 5.21 and 5.22 show that (i) the presence of S2 favours initial production of C_2AH_8 and AH_3 rather than CAH_{10} and (ii) the conversion reaction is further advanced after 16 weeks for the S2 mix.

The temperature rises reported for the control mix and the most accelerated mix at 20°C in section 5.4.1.2 were similar. This observation is in accordance with the very small increase in maximum rate of heat evolution for the accelerated mix, a complicating factor being the presence of a double peak in heat evolution. For accelerated mixes showing double peaks it is thus the maxium rate of heat evolution which should be considered as affecting the hydrates formed. It seems reasonable to suggest therefore that the observed changes in hydrate production and subsequent rate of conversion are due partly to temperature rises in accelerated mixes but also to the presence of the superplasticisers.

At 30°C the presence of any admixture caused considerable acceleration both in terms of the peak height and time to the peak. This would be expected to cause higher actual hydration temperatures than for the control mix which would accelerate the early conversion reaction. Reference to Figures 5.5 and 5.6 shows however that the reduction in upv (shown to correlate well with conversion) does not occur earlier for S1 mixes and indeed occurs later for S2 mixes. It therefore appears that the presence of a superplasticiser inhibits the conversion reaction as suggested by Young who proposed that organic compounds are absorbed into the hydrates (47).

At 40°C the behaviour is very similar to that at 30°C.

Figure 5.21 DTG Results Control Mortar 20°C

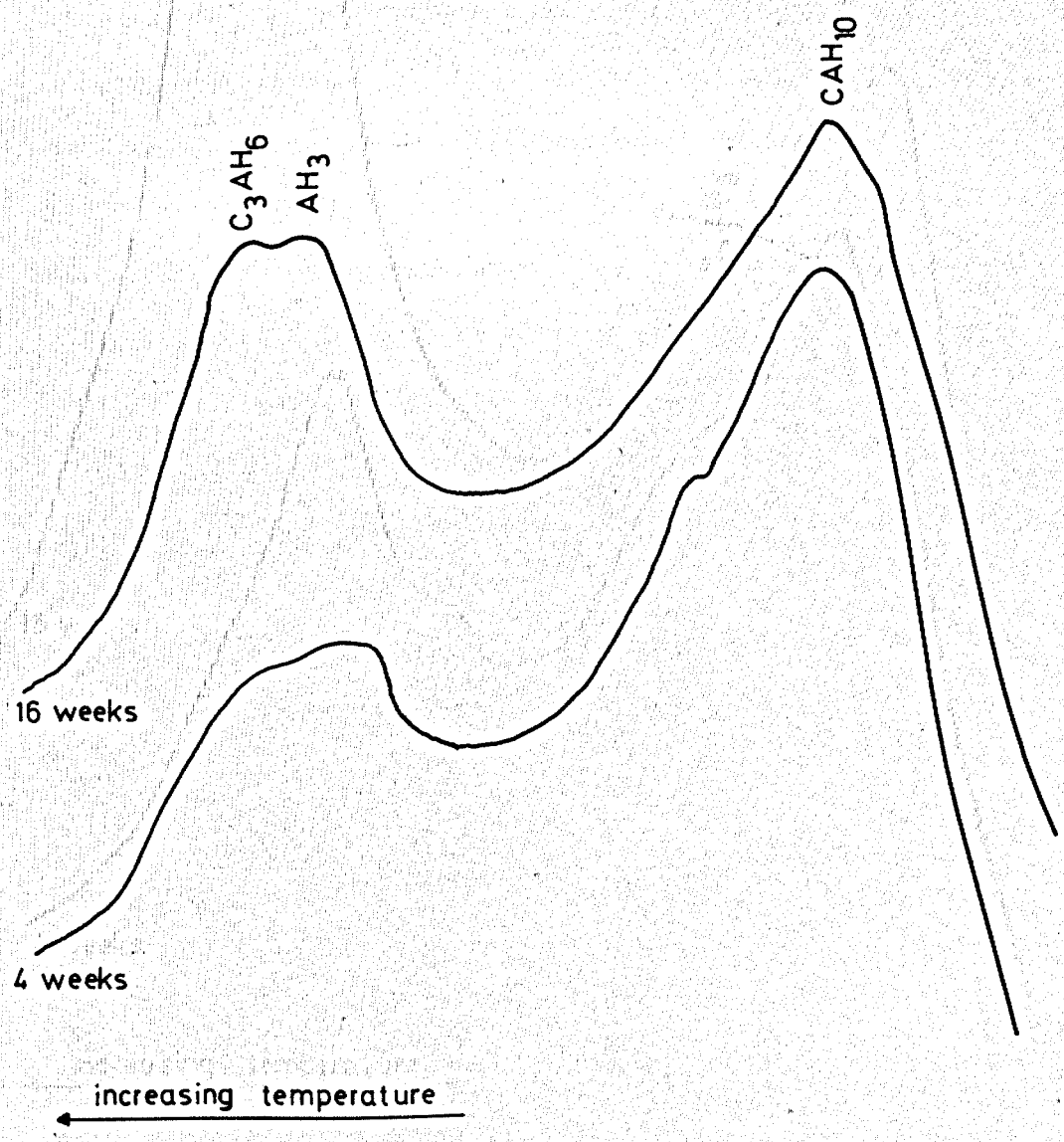

Figure 5.22 DTG Results 10% S2 Mortar 20°C

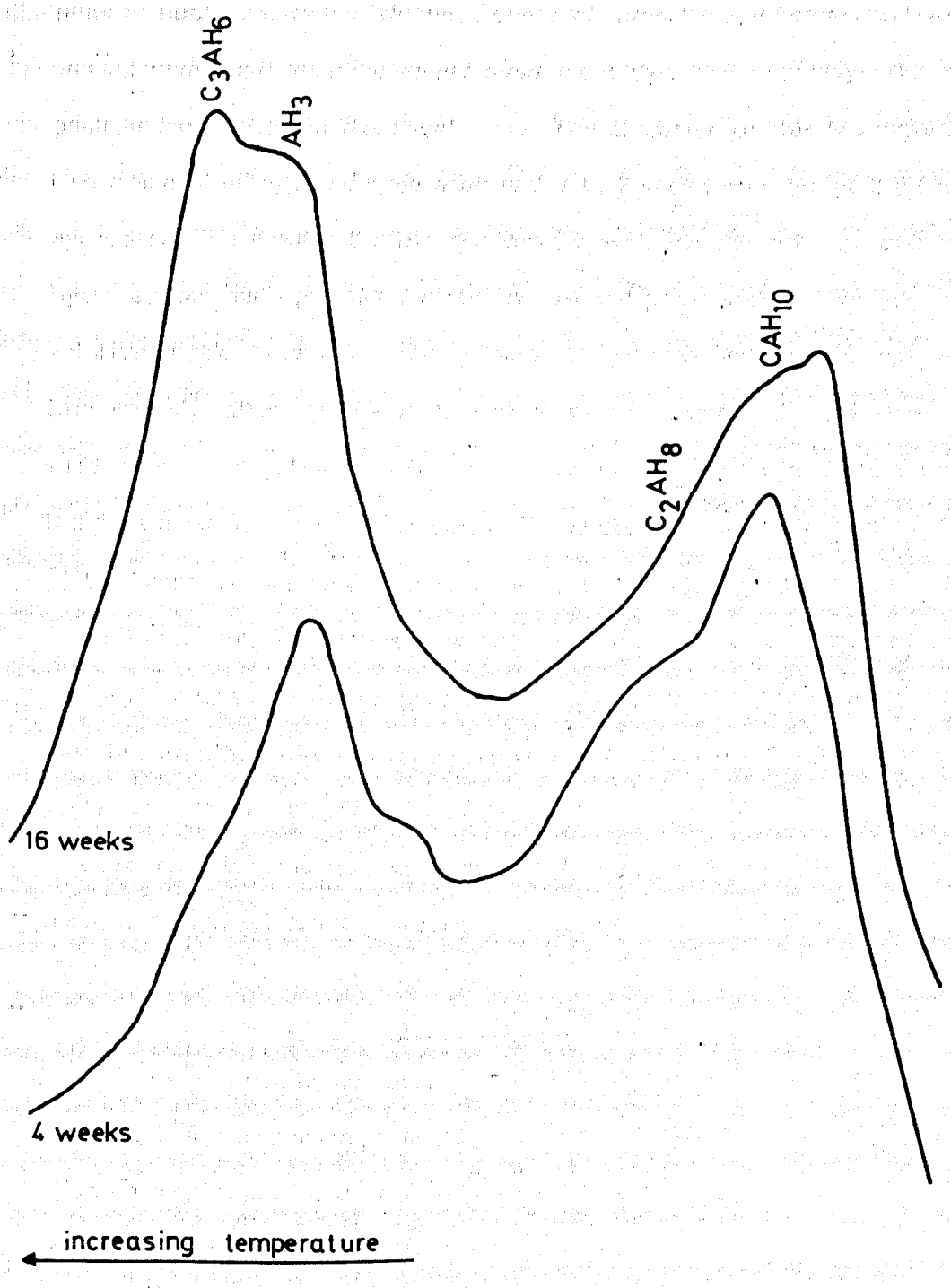

5.4.2.4 Investigation of Double Peak in Heat Evolution

The double peak in heat evolution for some mixes containing admixtures at 30 and 40°C was reported in Chapter 4. A sample of paste at w/c 0.40 containing 0.3% S1 hydrated at 40°C was known to show a double peak in heat evolution with the 2 peaks of almost equal height. DTG tests were carried out on samples removed from this paste slightly after each peak and quenched in the usual way. The objective of this testing was to determine whether the double peak is due to 2 step formation of 2 different hydrates. The results for the quenched specimens showed only that more hydrates had been produced after the second peak with no change in the relative peak heights. DTG tests on unquenched specimens tested immediately after grinding showed a much larger gel peak than the specimens. The gel peak was particularly large for the sample taken after the first maximum in heat evolution. These observations may simply reflect (i) the increased amount of free water in both unquenched samples and (ii) the greater amount of free, unhydrated water in the sample removed earlier. It was considered possible that the quenching procedure removes loosely associated water from amorphous gels although testing on 2 day old pastes showed no such effect.

There was thus no evidence that the 2 peaks were caused by the precipitation of different hydrates.

5.5 CONCLUSIONS

1. There was good correlation ($r = 0.94$) between upv and strength for the mortar cubes tested during this project. The correlation was not sigificantly affected by the presence of different hydrates and the overall relationship between upv (v) and strength (f) was as follows :

$$f = 0.0025\, v^{7.08}$$

2. The occurrence of conversion, confirmed by DTG, was accompanied by a significant reduction in upv and therefore in strength. The minimum value of upv for converted mortar was approximately 3.9km/s regardless of initial hydration temperature. This corresponds to a strength of about 40 N/mm^2. The upv of unconverted mortars at ages exceeding 7 days was typically 4.3-4.5km/s, corresponding to a strength of about 75-105 N/mm^2. The strength loss associated with conversion was thus approximately 50%.

3. The heat generated during hydration can cause a considerable increase in mortar temperature sufficient to affect the type of hydrates produced. This is particularly a problem when curing specimens at about 20°C since it is in the range 20-30°C that the hydration of Ciment Fondu is most sensitive to changes in temperature. If very close control of hydration temperature is required then the sample size should be minimised and an efficient water circulation system should be used to maintain the correct temperature.

4. DTG results suggest the presence of one or possibly 2 forms of amorphous gel particularly at hydration temperatures > 30°C. These gels may contain aluminium, calcium and iron in variable proportions and could be formed (i) as intermediate hydration products before crystallisation or (ii) as intermediate products during conversion.

5. The wide range of DTG peak temperatures associated with AH_3 is thought to be due to differences in its maturity.

6. The presence of any admixture generally causes a reduction in upv and therefore in strength at all test ages and at all temperatures.

7. The behaviour of S1 and S2 is broadly similar with increasing dosage causing larger upv reductions.

8. The presence of the accelerator either alone or in combination with a superplasticiser reduces upv. Contrary to published work it was shown that the presence of lithium does not promote preferential formation of C_2AH_8 rather than CAH_{10} (14).

9. There was no DTG or XRD evidence that the presence of admixtures caused the formation of hydrates other than those normally found in Ciment Fondu systems.

10. Apart from the overall strength reduction, typically 10-20%, the only notable effect of the superplasticisers was to encourage the conversion reaction to occur earlier for mortars stored at 20°C. After 18 months however the strengths of control and superplasticised mixes were virtually identical.

REFERENCES

Reference numbers in double brackets refer to references used only in this chapter. Reference numbers in single brackets refer to references in the literature review in Chapter 1.

1. SHARP J.H; Private communication 1985

2. BANFILL P.F.G; Private communication 1984

3. BS 4408, 1974, Part 5. Measurement of the velocity of ultrasonic pulses in concrete. Superceded by BS 1881 Part 203, 1986.

4. ELVERY R.H; "Estimating strength of concrete in structures". Current Practice Sheet 10. Concrete, 7, No. 11, Nov 1973 pp 49-51.

5. BS 1881:1986 Part 203; Recommendations for measurement of velocity of ultrasonic pulses in concrete.

6. L'HERMITE R; "The strength of concrete and its measurement", Annales, L'Institute Technique de Batiment et des Travaux Publics (Paris) No 12, Jan 1950.

7. CHEFDEVILLE J; "Application of the method toward estimating the quality of concrete", RILEM bulletin No. 15, Aug 1953.

8. BUSHNELL-WATSON S.M.; Ph.D thesis 1987, Department of Ceramics, Sheffield University.

9. FENTIMAN C; Private communication 1987

10. MIDGLEY H.G; Private communication 1987

CHAPTER 6 ADMIXTURE MECHANISMS

6.1 INTRODUCTION

The results presented in Chapters 3, 4 and 5 showed that the rheology, hydration kinetics and long term strength of Ciment Fondu mixes are considerably altered by the presence of admixtures.

Before any improvements can be made to admixture formulations it is necessary to understand the interaction between the admixtures and hydrating cement.

Experiments were therefore carried out to investigate the effect of the admixtures on the dissolution of lime and alumina and to monitor changes in superplasticiser concentration during early hydration.

Consideration of these results together with those from earlier chapters enables a tentative explanation of admixture mechanisms to be proposed.

6.2 SOLUTION CHEMISTRY

6.2.1 Experimental Procedures

Note : All tests were carried out at laboratory temperature 18-22°C.

6.2.1.1 Determination of Calcium Concentration in Solution

Ion Selective Electrode

An Orion 93-20 calcium electrode was used in conjunction with an Orion 90-02 reference electrode. These were connected to a Linear chart recorder to monitor the calcium ion concentration in the cement pastes. Monitoring was undertaken for periods of either 15 or 30 minutes from the time of addition of cement to the solution. Cement was added gradually over 45 seconds to the mixing solution which was continually stirred at constant speed by a propeller shaped impeller. The weight of cement used

for each test was 100g and the w/c ratio was 0.60. Tests were carried out on pastes containing the combinations of admixtures listed below using both S1 and S2. Before each test the electrode was calibrated using solutions of known calcium concentration.

Control
0.025% A
0.3% S
0.3% S + 0.025% A
1.0% S
1.0% S + 0.025% A

These dosages are as used for the tests described in Chapters 4 and 5 so that the results are directly comparable.

The calcium electrode consists of an electrode body and a sensing module which, according to the manufacturer, must be replaced after about 6 months of use ((1)). The sensing module contains a liquid internal filling solution in contact with a gelled organophilic membrane containing a calcium-selective ion exchanger. When the membrane is in contact with a calcium solution, an electrode potential develops across the membrane. This potential, which depends on the level of free calcium ions in solution, is measured against a constant reference potential with a digital pH/mV meter. The measured potential corresponding to the level of calcium ion in solution is described by the Nernst equation;

$$E = E_o + S. \log (X)$$

where E = measured electrode potential

E_o = reference potential (a constant)

X = calcium ion level in solution

S = electrode slope (about 27 mV per decade)

The level of calcium ion, X, is the activity of free calcium ions in solution and can be considered to be the effective concentration since the electrode does not respond to bound or complexed ions. At high, constant ionic strength the calcium ion activity is directly proportional to the free calcium ion concentration. It is therefore standard practice to add a solution of high ionic strength, such as 4M potassium chloride, to the test solution. The recommended addition of KCl produces an ionic strength (I) of about 0.1. (Ionic strength is calculated using the equation below where C_i is concentration and Z_i is ionic charge).

$$I = 0.5 \sum C_i Z_i^2$$

The ionic strength of the solution in contact with hydrating Ciment Fondu, calculated on the basis of published data for lime and alumina, is approximately 0.2 thus no adjustment of ionic strength was required for the pastes under test (9).

EDTA Titration

The samples tested were obtained by filtering the cement paste under vacuum using the apparatus shown in Figure 6.1. Paste at w/c 0.60 containing 100g Ciment Fondu was mixed for 5 minutes using a laboratory mixer with propeller shaped impeller. A vacuum was applied at intervals to remove the 5ml of filtrate required for the titration and the calcium content was determined using the method described in BS 4551 : 1980 ((2)).

This technique was used to determine the calcium content after 15 to 30 minutes for the following mixes

Control
1.0% S1
1.0% S2

Figure 6.1 Apparatus Used to Extract Filtrate From Cement Paste

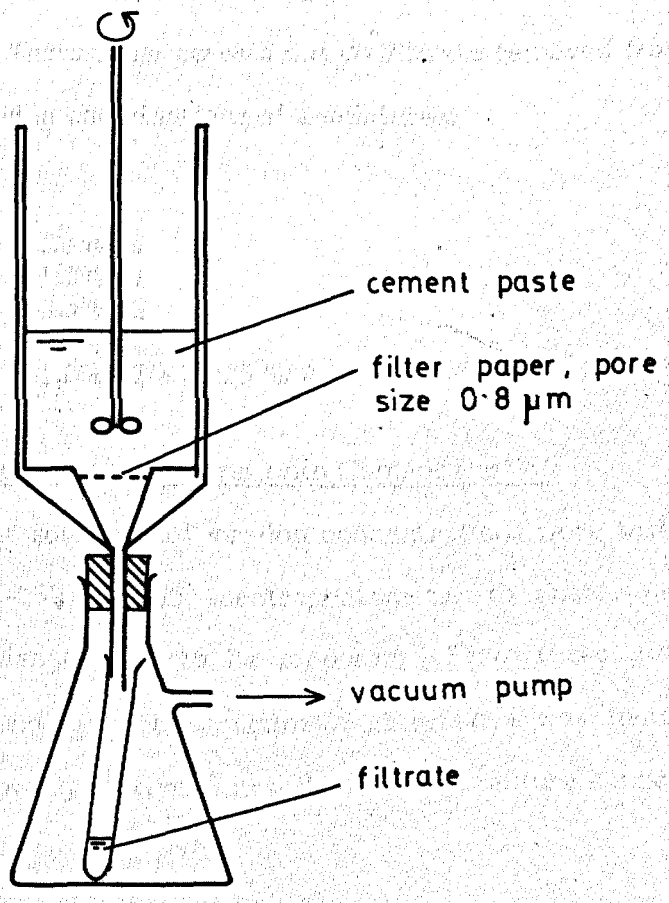

6.2.1.2 Determination of Aluminium Concentration in Solution

Pastes were prepared as described in section 6.2.1.1 except that (i) 200g cement was used for each mix and (ii) the paste was stirred continuously and filtrate samples withdrawn at 10 minute intervals. These samples were diluted with deionised water at 1 : 100 before immediate test using atomic absorption spectroscopy. The instrument used was supplied by Instrumentation Laboratory and the aluminium content determined from the absorption at 309.2nm after calibrating against standard solutions. Tests were carried out on filtrate removed from pastes containing the following combinations of admixtures:

Control
1.0% S1
0.3% S2
1.0% S2
1.0% S2 + 0.025 % A

6.2.1.3 Adsorption of Superplasticiser onto Cement Particles

Superplasticiser solutions of varying concentrations were tested using a Pye Unicam SP6-550 UV/VIS spectrophotometer to enable graphs of absorbance vs wavelength (λ) to be prepared. From these graphs the wavelength corresponding to the maximum absorbance was found and a calibration curve showing maximum absorbance vs admixture concentration was drawn.

The relationship between absorbance (A_b) and admixture concentration (c) is given by Beers law ((3)):

$$\epsilon = \frac{A_b}{c.l}$$

where ϵ = extinction coefficient

l = path length; i.e. width of spectrophotometric test cell

Calculation of the extinction coefficients for S1 and S2 enables superplasticiser concentration to be determined from measurement of absorbance.

Pastes containing 100g cement at w/c 0.60 were prepared containing 0.1, 0.5 and 1.0% S1 or S2. Two batches of each mix were made using the mixing procedures detailed below:

A 1 minute by hand followed by 2 minutes mechanical stirring at constant speed.

B 1 minute by hand followed by 9 minutes mechanical stirring at constant speed.

Filtrate samples were withdrawn at 20 minutes and were tested for superplasticiser concentration after appropriate dilution. The reduction in measured superplasticiser concentration indicates the amount adsorbed onto the cement.

6.2.2 Results

The effect of admixtures on the calcium ion concentration of pastes measured using the ion electrode is shown on Figure 6.2 (S1) and Figure 6.3 (S2). The results obtained by EDTA titration are recorded in Table 6.1.

The effect of admixtures on the aluminium concentration is shown on Figure 6.4.

Results from spectrophotometric testing of S1 and S2 are given in Table 6.2.

The adsorption isotherms for S2, showing the effect of mixing procedures A and B on the amount of S2 adsorbed vs equilibrium concentration, are plotted on Figure 6.5. The results for S1 are not reported due to problems described in section 6.2.3.3

Figure 6.2 Effect of S1 on [C], 20 °C

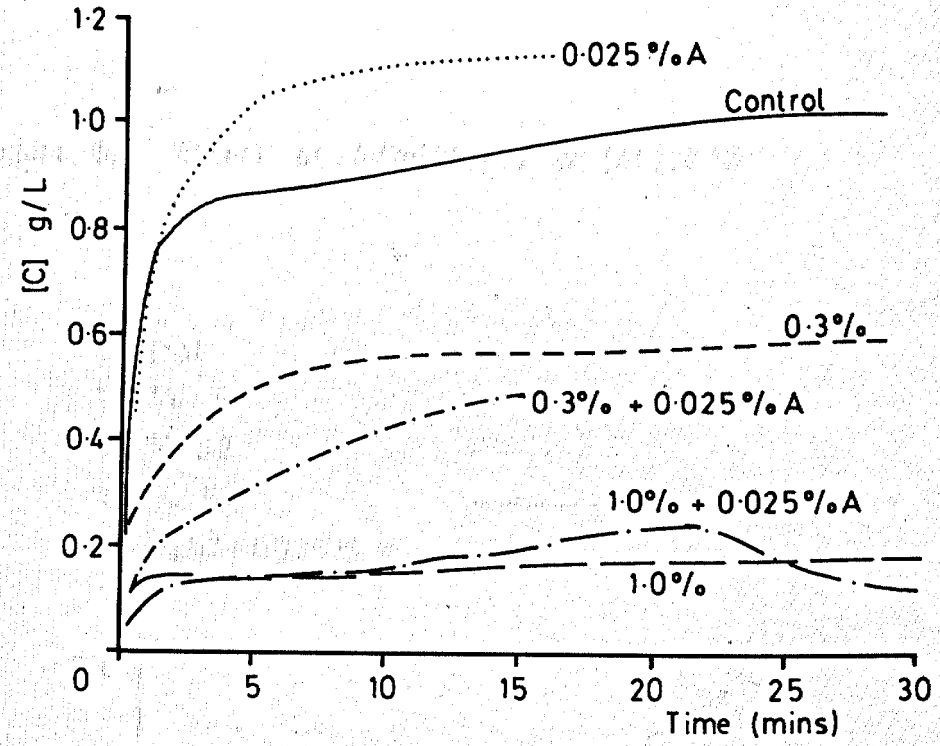

Figure 6.3 Effect of S2 on [C], 20 °C

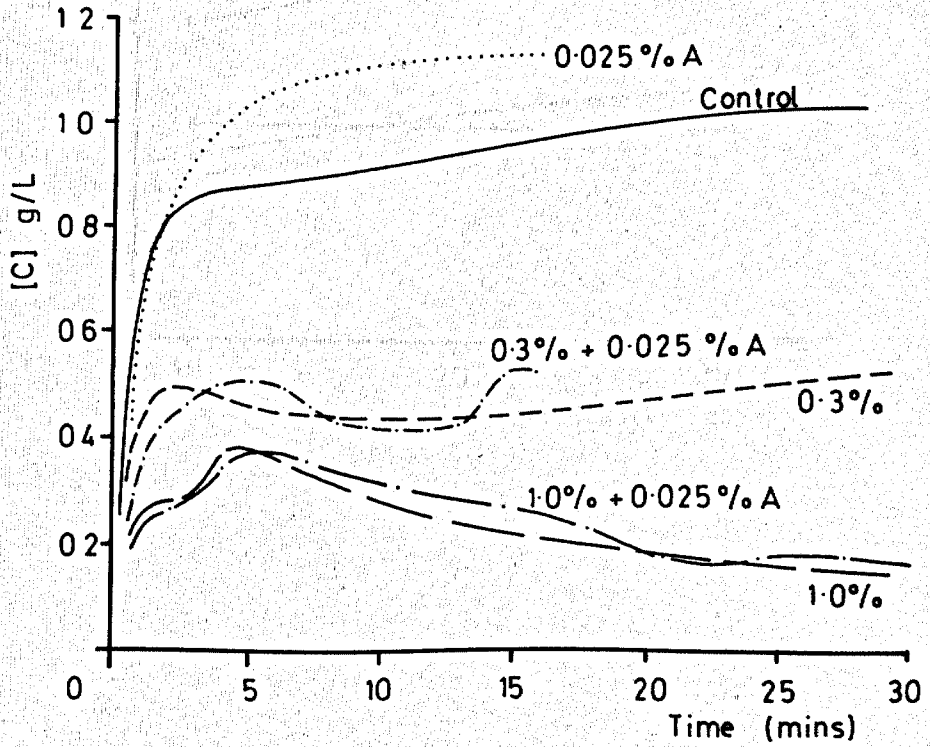

Figure 6.4 Effect of Admixtures on [A], 20 °C

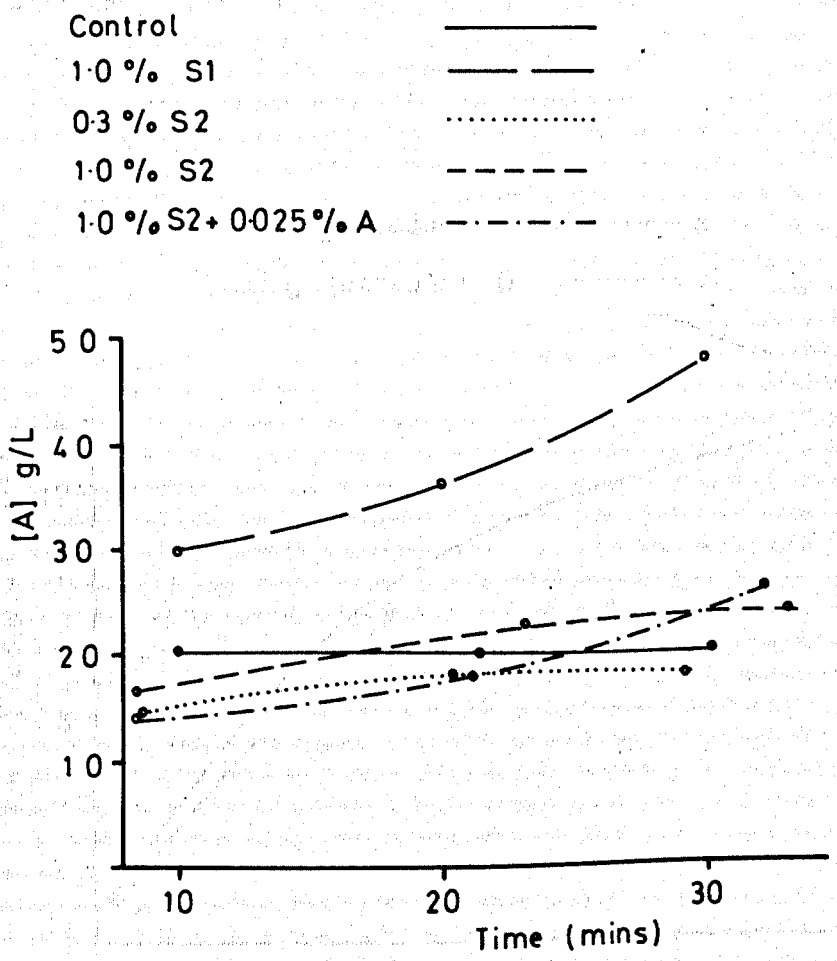

Figure 6.5 Adsorption Isotherms for S2

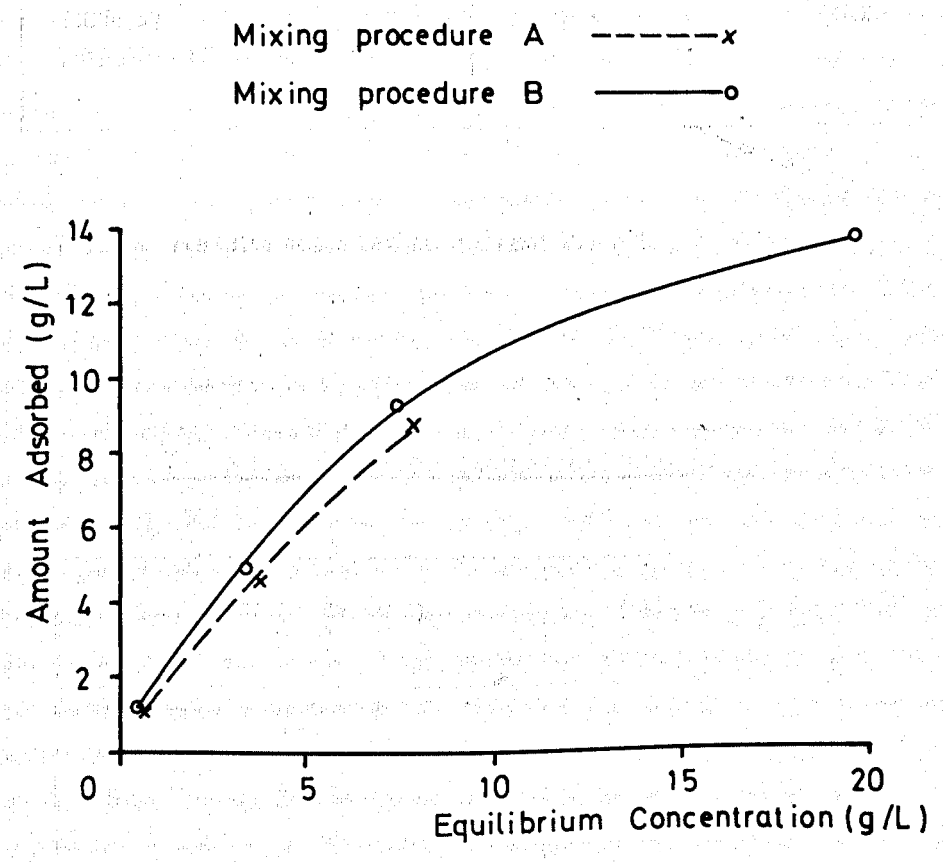

Table 6.1 Effect of Admixtures and Measurement Technique on [C] for Pastes at w/c 0.60, 20°C

Paste	[C] (g/L)	
	EDTA Titration	Electrode
Control (mean of 2 tests, at 10 & 20 minutes)	1.0	1.0
1.0% S1 (sampled at 25 minutes)	0.2	0.2
1.0% S2 (sampled at 15 minutes)	0.6	0.2

Note : Results reported to nearest 0.1 g/L

Table 6.2 Spectrophotometric Data for S1 and S2

	Peak Wavelength (nm)	Extinction Coefficient (L/g.m)
S1	295	1695
S2	280	570

6.2.3 Discussion

6.2.3.1 Concentration of CaO and Al_2O_3 in Solution

Other researchers have used very high paste water contents, typically w/c = 10, which are known to result in the formation of different hydration products to those formed at lower w/c (9,35). For this work it was considered desirable to use the same w/c ratio, 0.30-0.40, as for the experiments described in Chapters 3-5. However it was found that a w/c ratio of 0.60 was necessary to maintain a continuous flow of paste across the electrode surface. As the paste stiffens this flow cannot be maintained and so pastes which stiffened rapidly could be monitored for only 15 minutes.

For plain paste at 20°C the concentration of CaO in solution, [C], increased very rapidly during the initial minute after addition of cement to water. Subsequently [C] continued to increase slowly up to 30 minutes. The value of 1.0 g/L attained after 30 minutes agrees well with the results for pure aluminates and Ciment Fondu obtained by other researchers (9, 13, 19, 21) and was confirmed by titration with EDTA.

The presence of admixtures has a considerable influence on the results obtained and Figures 6.2 and 6.3 show that the effect of S1 and S2 is broadly similar. Addition of superplasticiser appears to cause a reduction in [C] which increases with increasing dosage. The results in Table 6.1 indicate however that these graphs must be interpreted with caution. There is very good agreement between [C] values obtained using the electrode and EDTA titration for both the control and 1.0% S1 mix. In contrast the considerable discrepancy between the 2 values for the 1.0% S2 mix indicates a fundamental difference between the action of S1 and S2.

To reconcile this behaviour it is necessary to consider how each test responds to the presence of "free" and complexed calcium ions. The

electrode responds only to "free" calcium ions whereas EDTA can remove calcium ions bound in complexes. However if very strong complexes are formed between calcium and superplasticiser then EDTA is unlikely to remove the calcium ions.

The reduction in [C] caused by both superplasticisers is attributed to the formation of a calcium-superplasticiser complex. The difference between the [C] results for S1 and S2 may be resolved if the S2 complex is weaker than the S1 complex and so some calcium complexed with S2 can be chelated by the EDTA whereas no calcium is removed from the S1 complex. Calcium bound in complexes with either S1 or S2 is not detected by the electrode.

Despite the difficulty in interpretation of results there remains sufficient evidence to confirm that there is a real reduction in [C] for mixes containing either S1 or S2.

The presence of the accelerator alone is seen to cause an increase in [C] compared to control. The calcium concentration of mixes containing both superplasticiser and accelerator appears to be mainly influenced by the superplasticiser. This is perhaps not surprising considering the much higher dosage of superplasticiser compared to accelerator.

The aluminium content of the control mix expressed as the concentration of Al_2O_3, [A], remained constant at 2.0g/L between 10 and 30 minutes. This value agrees well with the results reported by other researchers for pure aluminates and Ciment Fondu (9, 13, 19, 21).

The presence of S2 alone or with accelerator appears to have little effect on [A] although in the mix containing accelerator aluminium content continually rises in contrast to the other mixes for which [A] appears to

stablise after 20 minutes. The aluminium content is however considerably affected by S1 with increases of 50% and 150% compared to the control after 10 and 30 minutes respectively. This is further evidence of a different mechanism of action for S1 and S2.

6.2.3.2 Spectrophotometric Testing of Superplasticisers

The position and magnitude of the peak of absorbance as a function of wavelength gives useful information on the structure of the superplasticiser molecules. Compared with S2, S1 has a much higher extinction coefficient and a slightly higher peak wavelength at a certain concentration. These phenomona are both consistent with the larger delocalised electron system of the double benzene ring in naphthalene compared to the single benzene ring of phenol.

6.2.3.3 The Adsorption of Superplasticiser onto Cement

The adsorption isotherms for S2 shown on Figure 6.5 are consistent with normal Langmuir adsorption of molecules onto a surface when it becomes progressively more difficult for the same proportion of solute molecules to find a vacant site as the equilibrium concentration increases ((4)). Similar adsorption isotherms were found by Al-Kurwi for the adsorption of superplasticisers onto Portland Cement ((5)). The differences in amount adsorbed due to the different mixing procedures seem reasonable. The adsorption of a higher proportion of S2 after a longer mixing time is consistent with deflocculation and the presence of freshly exposed particle surfaces.

The adsorption isotherms for S1 are not reported due to the following problems encountered during testing which invalidated the results.

Whilst studying the adsorption of superplasticiser onto the cement it was observed that the peak in absorbance shifted to a lower wavelength as shown in Table 6.3.

Table 6.3 Shift in Spectrophotometric Peak for S1 and S2

	Peak Position (nm)	
	Deionised Water	Cement Filtrate
S1	295	275
S2	280	255

A similar shift in peak wavelength was noted by Al-Kurwi for sulphonated naphthalene and melamine formaldehyde condensates in Portland Cement ((5)) and was also noted by Gregory ((6)) although no explanations were presented.

For S2 the shift could be accurately reproduced by preparing solutions of S2 in sodium hydroxide at pH 11; approximately the same pH as in the hydrating Ciment Fondu system. However for S1 the shift could not be reproduced by preparing solutions in sodium hydroxide. Although no explanation can be found for this behaviour it provides a further indication of the difference between the action of S1 and S2. To permit quantitative determination of S1 content in cement filtrate it was thought necessary to prepare solutions of S1 in cement filtrate at known concentration. A further problem then became apparent when it was noted that the addition of S1 to cement filtrate caused the formation of a white colloidal precipitate. When diluted ten-fold with deionised water this precipitate was no longer visible but presumably was still present and would lead to an

artificially high absorbance. It seems possible that the precipitate, which could be removed by filtering, is an insoluble complex containing superplasticiser and other ions such as calcium and aluminium. If so then determination of S1 content is not possible since

i) if the sample is filtered, an unknown amount of superplasticiser is lost.

ii) if the sample is not filtered, absorbance will be considerably increased due to the presence of the opaque precipitate.

After encountering this problem for S1 it was subsequently found that addition of S2 to cement filtrate also resulted in the formation of a white, colloidal precipitate. This then casts considerable doubt on the results obtained for the adsorption of S2 onto cement although the qualitative interpretation of normal adsorption is still thought to be valid.

During the collection of filtrate samples for [C] or [A] tests it was noted that the filtrate colour changed from brown to colourless with increasing time. The brown colour, almost certainly due to the presence of superplasticiser, was noticeable up to 5-10 minutes. The gradual change to a colourless filtrate which occurred over 10-40 minutes is probably due to the adsorption of superplasticiser onto cement and/or the formation of complexes in solution.

This is qualitatively confirmed by spectrophotometric measurements which show a continuing decrease in superplasticiser concentration with age. Quantitative details will not be reported here due to the uncertainty in their validity.

6.3 CALCIUM SUPERPLASTICISERS

6.3.1 Preparation

It was considered that the relatively poor workability of mixes containing superplasticiser may be associated with the reduction in [C] and that a method of artificially raising [C] while incorporating superplasticiser could overcome the problem.

To test this hypothesis calcium forms of S1 and S2 were prepared by ion exchange using a column filled with Amberlite IR-120 resin. A concentrated solution of sodium superplasticiser was passed through the acidified ion exchange resin leading to the replacement of sodium by hydrogen ions. Neutralisation of this solution with calcium carbonate produced the calcium form of the superplasticiser whose concentration was checked by spectrophotometry. No shift in the peak of absorbance vs wavelength was observed for the calcium forms which indicates that the calcium complex is not formed in deionised water. The neutralisation process causes precipitation of insoluble calcium sulphate which is removed by filtration. The calcium superplasticisers are therefore sulphate free, unlike the sodium forms of S1 and S2 which contain 5% and 15% sulphate respectively. It may be recalled that Banfill showed this level of sulphate to have no significant effect on hydration (156).

Several experiments, detailed in section 6.3.2, were carried out to investigate the effect of calcium superplasticisers on Ciment Fondu.

6.3.2 Experimental Procedures

Rheology

The time dependent behaviour under continuous shear of pastes at w/c 0.40 containing the following combination of admixtures was monitored at 5 and 20°C. The procedure used was as described in Chapter 3, section 3.4.1.2. The results are shown on Figures 6.6 and 6.7.

Figure 6.6 Torque vs Time Behaviour, Calcium Superplasticisers at 5 °C

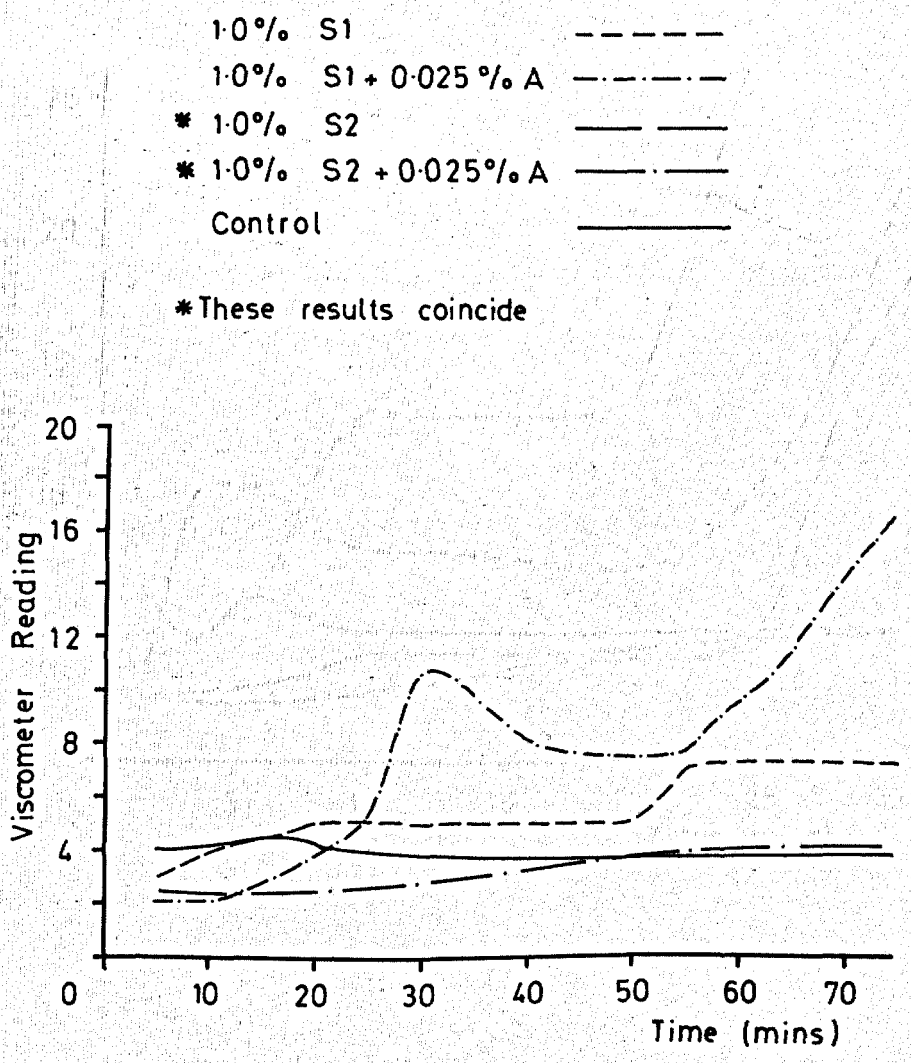

Figure 6.7 Torque vs Time Behaviour, Calcium Superplasticisers at 20 °C

key as on Figure 6.6

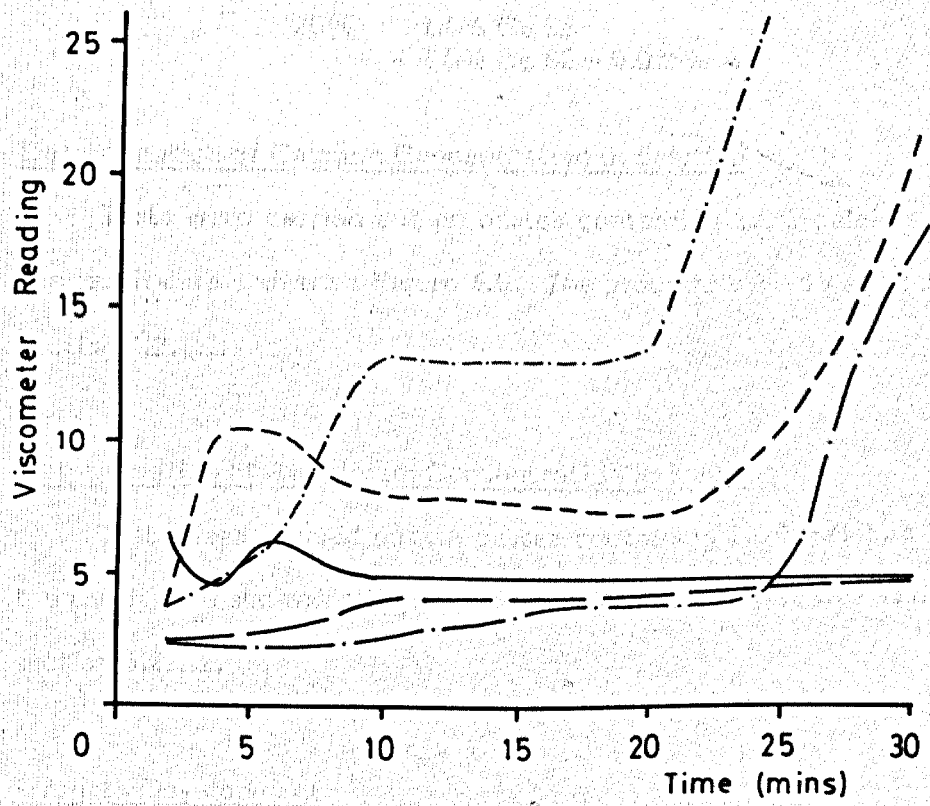

1.0% Ca S1
1.0% Ca S2
1.0% Ca S1 + 0.025% A
1.0% Ca S2 + 0.025% A

Hydration Kinetics

Conduction calorimetry tests were carried out on the following pastes at 0.40 w/c and the results are given in Table 6.4. The procedure used was as described in Chapter 4, section 4.3.1.

5°C	1.0% Ca S1
	1.0% Ca S2
	1.0% Ca S1 + 0.025% A
	1.0% Ca S2 + 0.025% A
20°C	1.0% Ca S2
	1.0% Ca S2 + 0.025% A

Determination of Calcium Concentration in Solution

Tests were carried out on pastes containing 1.0% calcium S1 and S2, the results are shown on Figure 6.8. The procedure used was as described in section 6.2.1.1.

Determination of Aluminium Concentration in Solution

Tests were carried out on pastes containing 1.0% calcium S1 and S2, the results are shown on Figure 6.9. The procedure used was as described in section 6.2.1.2.

Strength Development

The upv at 20°C of 3 mortar cubes from each of the mixes listed below was monitored up to 6 months. The results are shown on Figure 6.10. The procedure used was generally as given in Chapter 5, section 5.2.1.

1.0% Ca S2
1.0% Ca S2 + 0.025% A

Figure 6.8 Effect of Calcium Superplasticisers on [C] , 20 °C

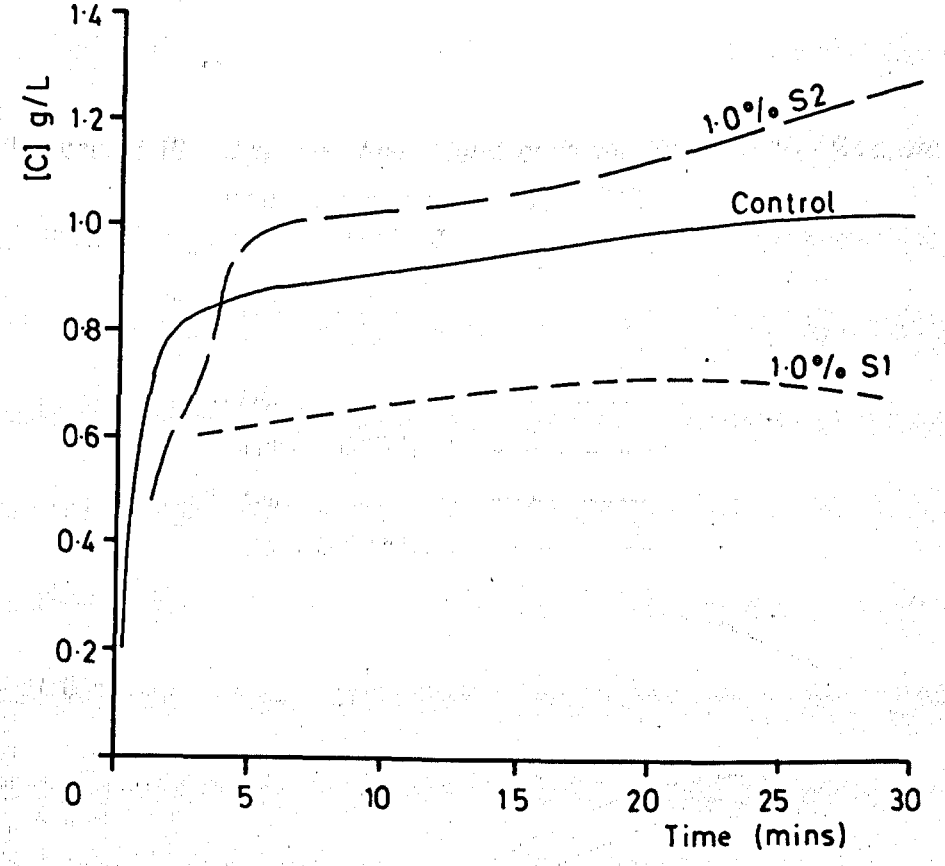

Figure 6.9 Effect of Calcium Superplasticisers on [A], 20 °C

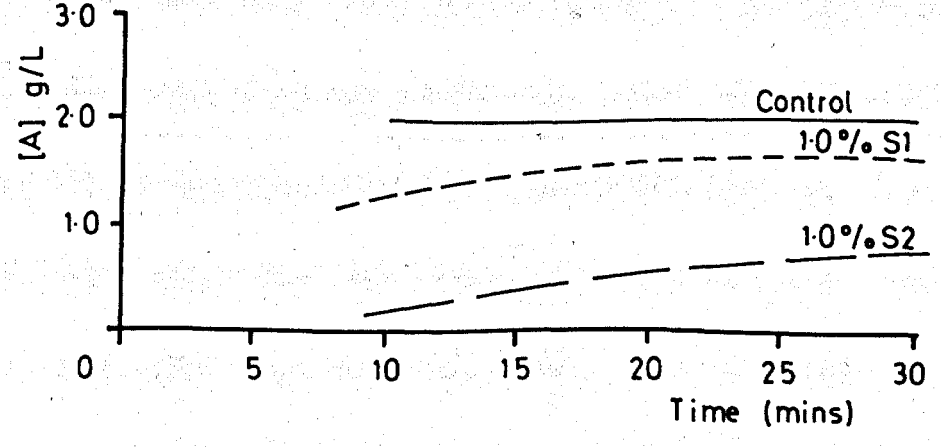

Figure 6.10 Upv vs Age Relationships for 1·0% Sodium and Calcium S2 at 20°C

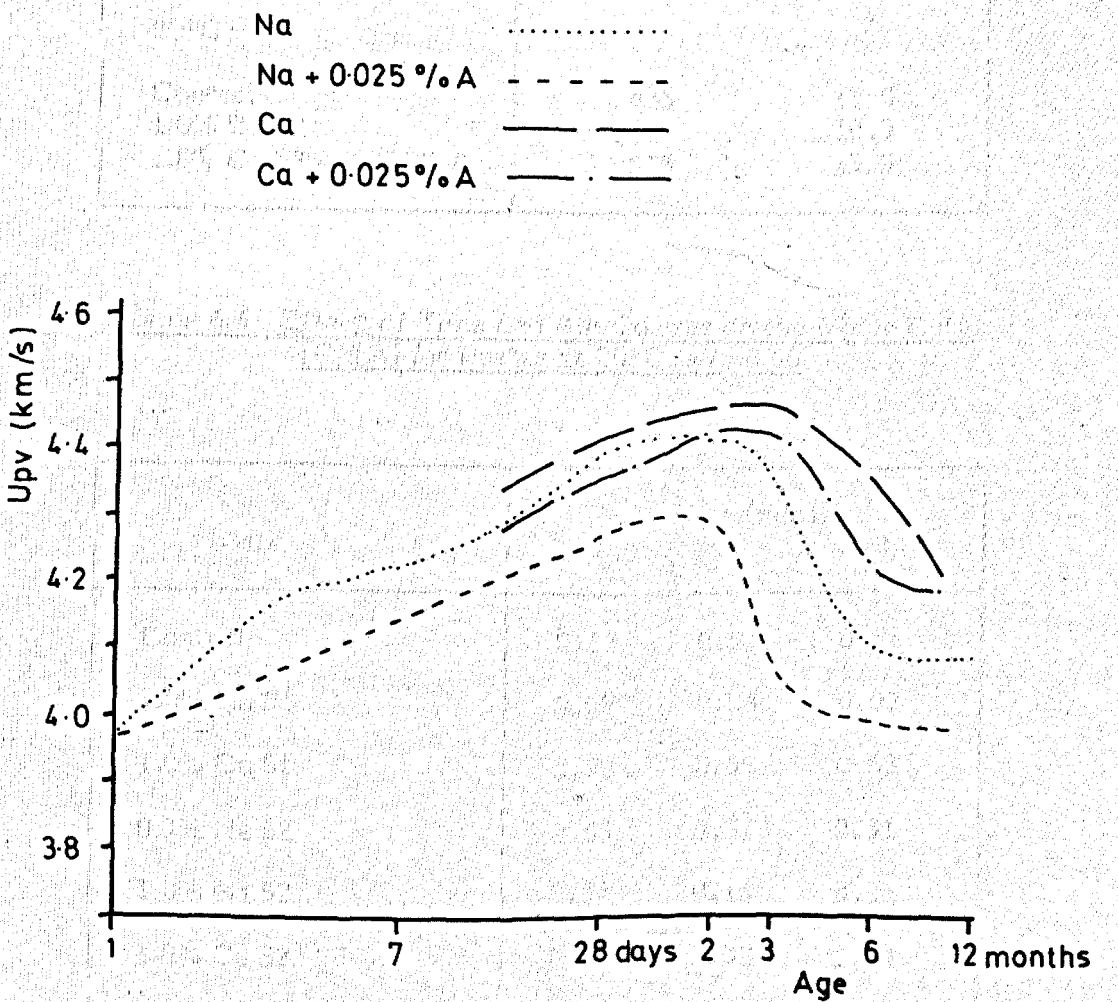

Table 6.4 Conduction Calorimetry, Results for Calcium Superplasticisers, w/c 0.40

Mix	Main Peak Time (mins)	Main Peak Height (mW/g)
5°C		
Control	255	9.9
1.0% Ca S1	280	8.3
1.0% Ca S2	1230	5.2
1.0% Ca S1 + 0.025% A	120	9.0
1.0% Ca S2 + 0.025% A	350	6.5
20°C		
Control	435	19.0
1.0% Ca S2	1180	10.3
1.0% Ca S2 + 0.025% A	215	15.0

Table 6.6 Effect of Time and Admixtures on the Molar Ratio [C]/[A] for Pastes at 20°C, w/c 0.60

Mix	Time (mins) 10	20	30
Control	0.82	0.91	0.91
1.0% Na S1	0.09	0.08	0.07
1.0% Ca S1	0.98	0.80	0.68
0.3% Na S2	0.65	0.51	0.51
1.0% Na S2	0.34	0.15	0.11
1.0% Ca S2	8.90	3.32	2.97
1.0% Na S2 + 0.025% A	0.39	0.18	0.11
1.0% Ca S2 + 0.025% A	*	9.70	3.27

* No alumina detected at 10 minutes

Hydration Products

DTG tests were carried out on the pastes listed below hydrated at 20°C in accordance with the procedure described in Chapter 5, section 5.2.2. Tests were also carried out on sodium superplasticiser pastes to enable a comparison to be made. The times at test, i.e. the times at which the hydration reaction was quenched, were selected in an effort to ensure that each paste had undergone the same degree of hydration. The test times were 16 hours for Ca and Na S1, 26 hours for Ca S2 and 32 hours for Na S2. Paste samples contained only 10g cement to prevent any significant temperature increase due to hydration. The DTG traces are shown on Figure 6.11.

6.3.3 Discussion

Rheology

At 20°C the effect of calcium S2 is very similar to that of sodium S2. At 1.0% workability is improved up to at least 30 minutes compared to the control. For 1.0% with accelerator workability is improved up to 24 minutes when sudden stiffening occurs.

The calcium form of S1 causes stiffening to occur earlier than for the sodium form and increases the degree of stiffening. There is an initial improvement in workability compared to the control but this is lost by 2-3 minutes.

There are fewer results available at 5°C although it seems that the same pattern of behaviour is followed as at 20°C. Thus the best performance is shown by 1.0% calcium S2 which provides improved workability for 45 minutes compared to the control.

Figure 6.11 Effect of 1·0 % Sodium and Calcium Superplasticisers on Initial Hydration Products at 20 °C (DTG Results)

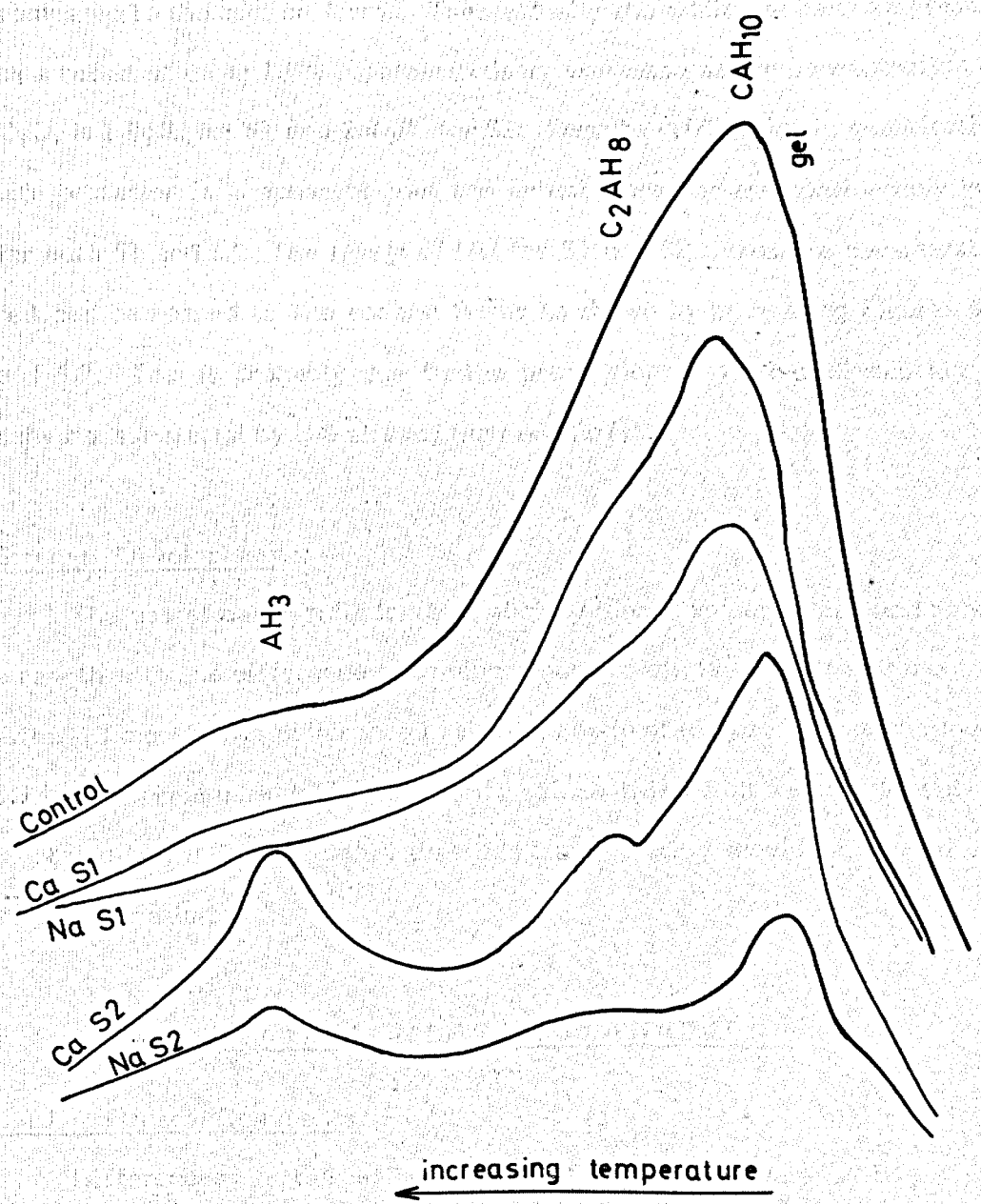

Hydration Kinetics

At 5 and 20°C the calcium forms cause less retardation than the sodium superplasticisers although there is still considerable retardation compared to the control.

Solution Chemistry

As expected the use of calcium S1 and S2 causes an increase in [C] compared to the sodium forms. Theoretically the additonal calcium present as a result of using 1.0% superplasticiser, expressed as the concentration of CaO, is 1.8g/L for S1 and 2.4g/L for S2. Despite difficulties in quantitative interpretation it is apparent that the actual increases are considerably less for both S1 and S2. The levels of [A] for S1 and S2 mixes are considerably reduced compared to the sodium forms as shown by comparing Figures 6.4 and 6.9. This is probably due to the prevention of further dissolution of anhydrous material by the already high level of [C].

Strength Development

The use of calcium S2 leads to slightly higher values of upv and hence strength with the difference becoming progressively larger up to 10 months. After 10 months the difference in strength estimated by reference to Figure 5.13, is approximately 10-15 N/mm^2. Since this result relates to only 6 mortar cubes it is considered that additional testing should be carried out for confirmation.

6.4 ACTION OF SUPERPLASTICISERS

6.4.1 General Comments

Differences in the effectiveness of superplasticisers with cement paste must be due in some way to the differences in their chemical structures, shown on Figure 6.12. It can be seen that all three

Figure 6.12 Molecular Structure of Sodium Superplasticisers
(other isomers will also be present)

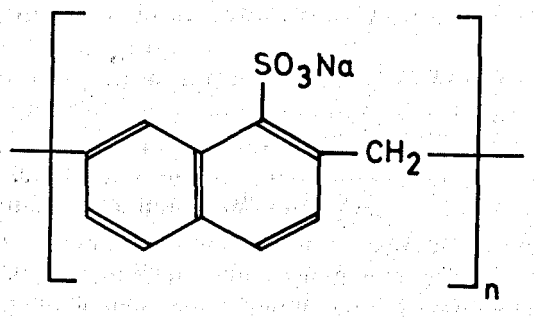

S1

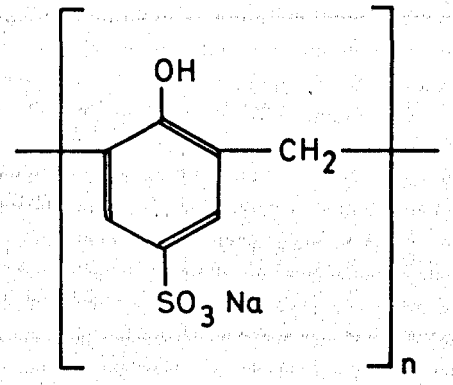

S2

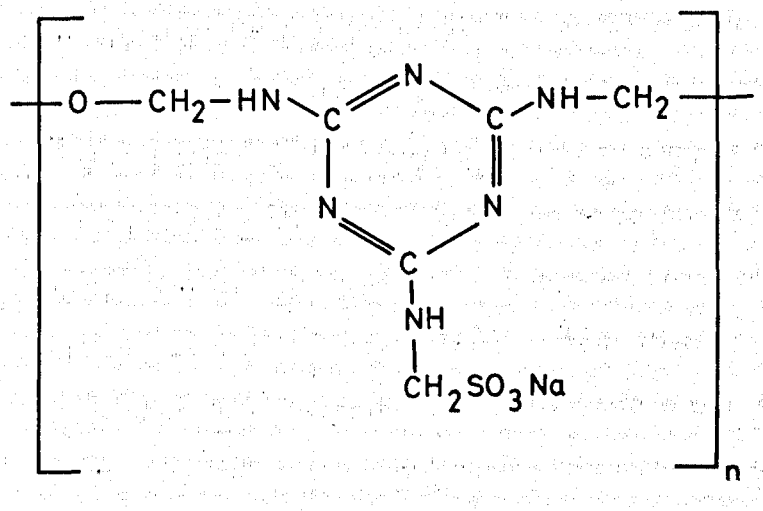

S3

superplasticisers are polymers with repeat unit which comprises an aromatic ring structure with a sulphonate group which is capable of adsorption onto a positively charged surface. The information given in Table 6.5 shows that a typical molecule of S3 is considerably larger than that of S1. This may be expected to lead to a difference in behaviour of mixes containing the 2 superplasticisers. Unfortunately no information is available concerning the likely degree of polymerisation of S2.

Table 6.5 Superplasticiser Structure

	S1	S2	S3
Molecular Weight of Repeat Unit (g) (not including sodium atoms)	219	186	261
Typical Number of Repeat Units	7-9	unknown	100-150

In research on Portland cement the amount of superplasticiser required to ensure coverage of all cement particles is frequently quoted. The approximate dosages of S1, S2 and S3 required to achieve monolayer coverage of the Ciment Fondu are 0.04, 0.06 and 0.05% respectively by weight of cement. This may be thought to suggest that at the dosages used in this project each cement particle must be covered by an adsorbed layer of superplasticiser. It must be remembered however that the hydration of Portland cement is very different from that of aluminous cement. In Portland cements hydration occurs by surface growth and little dissolution occurs. Superplasticiser molecules can therefore remain adsorbed onto the particle surfaces. In aluminous cements the rapid dissolution of the

anhydrous particles reduces the amount of superplasticiser molecules which remain adsorbed on the particles. This fundamental difference in the hydration mechanism is probably responsible for the relatively poor performance of superplasticisers with Ciment Fondu. This proposal is in accordance with observations that at very low dosages (0.01-0.05%) both superplasticisers S1 and S2 had a marked plasticising effect up to 25-50 seconds depending on dosage. After this period there was a rapid loss of workability and stiffening compared to the control. This rapid stiffening can be attributed to the dissolution of anhydrous material together with adsorbed superplasticiser from particle surfaces. At these low dosages there is then insufficient superplasticiser remaining on the particles to have an effective plasticising action.

6.4.2 Superplasticiser Mechanisms

Any proposals must take account of the observed effects on rheology, hydration kinetics, strength development, hydration products and solution chemistry previously described.

The system is so complex that a major research programme would be necessary to obtain sufficient evidence to permit a quantitative analysis thus the following discussion is presented as a qualitative outline. Suggestions for further work are given in Chapter 7.

Adsorption onto Cement and Effect on Dissolution

At the first moment of contact between anhydrous cement and the admixture solution the system may be considered as 2 discrete phases. The solid phase consists of heterogeneous particles of widely varying size with surface active sites. The liquid phase is an aqueous solution containing fully dissociated superplasticiser molecules. Immediately after the contact of these phases the following reactions occur:

i) Dissolution of the solid material.

ii) Adsorption of superplasticiser ions onto the solid particle surfaces.

The evidence presented in section 6.2 suggested that complex formation occurred between superplasticiser and calcium ions. In this case the superplasticiser ions may exist in 3 different states within the system as listed below:

i) Freely in solution.

ii) Adsorbed onto cement particles.

iii) Bound in complex form with calcium ions in solution.

The proportions of these 3 forms are likely to depend on the solution pH and temperature and on the relative bond strengths of the adsorbed and complexed forms.

The data for [C] obtained by EDTA titration suggest that the proportion of complexed superplasticiser at 20°C is greater for S1 than S2 and imply that more S2 remains adsorbed on cement surfaces than S1. This would be expected to cause (i) improved plasticisation and (ii) prolonged set retardation due to a reduction in the rate of cement dissolution for mixes containing S2 compared to S1. The experimental evidence presented in Figures 3.10, 3.11 and Table 4.5 shows that this is indeed the case. Figures 6.2 and 6.3 confirm that the presence of adsorbed superplasticiser reduces the rate of dissolution of calcium from the surface.

During the first few minutes of hydration changes in solution composition may be responsible for the preferential formation of the complexed form of S1 with molecules desorbing from the surface. This could account for the progressive stiffening of S1 mixes up to about 10

minutes after mixing as the increasing level of calcium in solution leads to an increase in the amount of S1 complex formed. The same occurs for S2 but at a lower rate. The later very sudden increase in stiffness observed for mixes containing S1 may be due to the precipitation of solid phases to restore the solution equilibrium.

Effect on Solution Equilibrium

The latter suggestion will now be considered in more detail. A minimum instability curve was proposed to account for the existence of a dormant period during the hydration of CA (20). It seems reasonable that a similar curve of minimum instability would apply to Ciment Fondu even though there is no true dormant period. Thus if the usual balance between lime and alumina in solution was disturbed, precipitation of a solid phase would occur to restore equilibrium. The effect of time and admixtures on the molar ratio of [C]/[A] which is relevant to the following discussion is shown in Table 6.6.

For a mix containing S1 it is suggested that the reduction in [C] caused by the formation of the strongly bound calcium-superplasticiser complex is countered by increasing dissolution of anhydrous material. Further formation of the complex prevents an increase in [C] but the increased dissolution leads to the considerably increased level of [A] as shown on Figure 6.4. When [A] reaches a certain, critical level precipitation of an alumina rich phase would (i) restore solution equilibrium and (ii) cause sudden stiffening.

It was expected that similar arguments should apply to the action of S2 although the experimental evidence does not support this proposal. At present no satisfactory explanation can be found for this anomaly. However the observation for S2 mixes that [A] is approximately the same as for the control whilst workability remains improved supports the suggestion that the

precipitation of an alumina rich phase is responsible for the sudden stiffening of pastes containing S1.

For calcium superplasticisers the discrepancy between the expected and actual increase in [C] compared to the sodium forms was mentioned in section 6.3.3. A possible explanation for this is incomplete neutralisation of the acidic superplasticiser or, more likely, formation of a higher proportion of the calcium/superplasticiser complex.

At a dosage of 1.0% calcium S1, [C] is restored to almost that of the control mix. The ratio of [C]/[A] is however much larger than for the control and precipitation of lime rich phases could be expected. This may account for the considerable early stiffening.

The argument presented above for S1 could apply to S2 although no stiffening was observed during the rheological testing. It is possible that such stiffening occurs rather later than for S1 mixes.

The additional calcium introduced by the use of calcium S2 is much more than that required to maintain the [C]/[A] ratio at the level of the control mix. A superplasticiser containing both sodium and calcium ions may provide the correct amount of additional calcium to the system. This suggestion could be evaluated by preparing and testing a series of S2 solutions at various Na/Ca ratios.

Effect on Hydration Products

An alumina rich gel is thought to be the first hydration product of normal Ciment Fondu mixes ((7, 8)). It is therefore possible that the early precipitation of this gel which apparently occurs for mixes containing sodium S1 does not lead to any significant alteration in the hydration products. This is confirmed by the DTG results on Figure 6.11. The same figure shows that the calcium S1 also has no apparent effect on hydrate

production. This evidence appears to conflict with the suggested action of calcium S1 presented above in which the precipitation of a lime rich phase was postulated. The disagreement cannot easily be reconciled although it may indicate that (i) the results of [C] and [A] are doubtful, (ii) the system is far too complex to be resolved by the limited amount of work carried out or (iii) the difficulties in DTG interpretation first noted in Chapter 5 section 5.4.2.1 mean that the presence of gels of differing composition cannot be confirmed.

In contrast pastes containing either the sodium or calcium form of S2 show a marked difference in initial hydration products compared to the control. The production of C_2AH_8 and AH_3 is favoured rather than CAH_{10}. It is very difficult to confirm the presence of any CAH_{10} and the early DTG peak may correspond to gel 2. For the calcium S2 it could be argued that the lime rich solution ultimately precipitates a lime rich gel, possibly gel 2 from which hydrates with high lime content are formed. The argument does not however hold for the sodium S2 since the ratio of [C]/[A] is not significantly altered compared to the control. There is clearly a need for far more information on the chemistry of the hydrating system before adequate theories can be put forward. The change in hydration products due to the presence of S2 is however real and also occured for the mortar mixes described in Chapter 5 as shown by Figures 5.21 and 5.22.

During her research on pure CA Bertrandie confirmed that alteration in the [C]/[A] ratio caused by addition of lime led to a change in the nature of the initial hydration products (23). At [C]/[A] less than 1.16 the initial hydration product was CAH_{10} whereas at greater than 1.16 the initial products were C_2AH_8 with some CAH_{10}.

The results presented in this thesis do not however appear to be in agreement with these observations since the dominant factor determining hydrate production is superplasticiser type rather than the [C]/[A] ratio. This evidence leads to the conclusions that (i) results of testing on pure CA cannot be assumed to apply to Ciment Fondu and (ii) the formation of hydrates is dependent on unknown factors in addition to lime and alumina concentrations.

Effect on Setting and Strength

It should be noted that reduction in [C] caused by the presence of either S1 or S2 does not necessarily lead to an extended setting time; paste containing 0.3% S1 showed acceleration despite reduced [C]. Mixes containing accelerator in addition to superplasticiser also had reduced [C] but an accelerated set. It should also be noted that the early precipitation of gel does not necessarily result in accelerated setting. A possible explanation is that the formation of crystalline calcium aluminate hydrates cause setting and hardening whereas gels cause stiffening.

It would be expected that changes in hydrate production due to the presence of superplasticisers would affect the strength of Ciment Fondu mixes. It has been shown in Chapter 5 that the presence of either S1 or S2 causes a reduction in strength compared to the control which is approximately the same for both superplasticisers. The results presented in this chapter show however that the effect of S1 and S2 on the hydrating Ciment Fondu system is quite different. A tentative proposal to account for the strength reduction is that it is due to the formation of excessive amounts of gel, rich in alumina for S1 and lime for S2. This is in accordance with the observation that after about 12 months there is virtually no difference in upv between the control and mixes containing superplasticiser.

Thus increasing age could promote the crystallisation of hydrates from gel phases.

Effect of Temperature

The effect of temperature on the action of the superplasticisers was shown to be considerable (see Tables 4.4-4.7). Generally both S1 and S2 caused retardation at $\leqslant 20°C$ and acceleration at $\geqslant 30°C$. Whilst little supporting evidence is available, the following factors may be responsible for the retardation at low temperatures:

i) Reduced rate of dissolution of cement due to adsorption of superplasticiser.

ii) Possible adsorption of superplasticiser onto hydration products which would prevent crystal growth.

iii) Tendency for formation of C_2AH_8 which is not favoured at low temperature.

iv) The formation of complexes which interfere with crystallisation.

At high temperatures there is virtually no available evidence although if factor (iii) above is true then hydration would be accelerated since formation of C_2AH_8 is favoured above 30°C.

Behaviour of S3

Although no studies were made of the action of S3 apart from the rheologicial investigation it is useful to consider why its performance was so poor. With Portland cement superplasticisers based on melamine resins have proved very effective although as with other such admixtures the plasticising action is shortlived. Little research has been carried out to provide an explanation for this behaviour.

A major difference between S1 and S3 is the degree of polymerisation which results in S3 molecules being very much larger than S1. For Portland cement each S3 molecule could partly cover one particle and contribute to the plasticising effect until the particle surface is disrupted by crystal growth. In contrast if an S3 molecule is adsorbed initially onto one particle of Ciment Fondu it is likely that dissolution would still occur causing the melamine chain to become partially detached from the cement particle. Entangling of the long chained molecules would almost certainly cause considerable stiffening.

6.5 ACTION OF ACCELERATOR

Most of the work described in this thesis has focussed on the superplasticisers thus there are fewer data available concerning the accelerator.

It was noted that accelerated pastes showed an early improvement in workability compared to the control and did not show the early peak in stiffness seen for the control (see Figures 3.9-3.13). It is suggested that the accelerator alters the interparticle forces so that deflocculation is encouraged. Deflocculation would promote easier access of water to the cement surface and so increase the rate of dissolution. The observed increase in [C] compared to the control supports this argument.

The calorimetry results presented in Chapter 4 showed that lithium citrate is an extremely effective accelerator for Ciment Fondu. Reference to Figure 4.9 shows that addition of >0.025% accelerator is sufficient to overcome the delayed setting observed for plain pastes at about 30°C. If, as suggested by Bushnel-Watson (161), the phenomenon for plain paste is caused by difficulty in nucleation then the accelerator must promote nucleation. This proposal was also made by Rodger and Double (14) and Crepaz and Raccanelli (157).

It seems likely that the mechanism of acceleration is that suggested by Midgley and described in Chapter 1, section 1.8.3.

6.6 CONCLUSIONS

1. An ion selective electrode can be used in Ciment Fondu pastes at w/c 0.60 to monitor the calcium concentration. The results obtained from pastes containing admixtures should be interpreted with care and additional tests using EDTA titration should be carried out.

2. The spectrophotometric determination of superplasticiser concentration in cement filtrate is complicated by
   i) formation of a gel, thought to contain superplasticiser and other ions
   ii) a reduction in the wavelength associated with maximum absorbance compared to solutions in deionised water.

3. For S2 the shift in peak wavelength appears to be due to the high pH of cement filtrate. For S1 high pH did not reproduce the shift noted for cement filtrate and no other explanation could be found. This is evidence for the different mechanisms of S1 and S2.

4. The differences between calcium concentrations measured using the ion electrode and EDTA titrations for the same mixes provide additional evidence of different action mechanisms for S1 and S2.

5. The presence of either S1 or S2 causes a considerable reduction in the calcium concentration. The formation of complexes containing superplasticiser and calcium ions is proposed as an explanation for about 50% of the reduction caused by S2 and may also account for the action of S1.

6. The presence of S2 has little effect on the aluminium content. In contrast the presence of S1 leads to a considerably higher aluminium content.

7. The addition of S1 does not lead to noticeable alterations in hydration products at 20°C compared to plain paste. The addition of S2 favours the initial production of C_2AH_8 and AH_3 rather than CAH_{10}. These findings agree with the results for mortar presented in Chapter 5.

8. The use of calcium rather than sodium superplasticisers does not lead to any further improvement in the workability of Ciment Fondu mixes. There is some evidence which suggests that mortar strength is improved.

REFERENCES

Reference numbers in double brackets refer to references used only in this chapter. Numbers in single brackets refer to references included in the review of literature in Chapter 1.

1. Orion Research; Instruction manual for calcium ion electrode.
2. BS 4551:1980; Methods of testing mortars, screeds and plasters.
3. DYER, J.R; Applications of Absorption Spectroscopy of Organic Compounds, Prentice-Hall, 1965.
4. GILES C.H, MacEWAN T.H, NAKHWA S.N, SMITH D; J. of Chem Soc. 1960 pp 3973-3993.
5. AL-KURWI A; The effect of superplasticisers on the rheological properties of cement. M.Phil Thesis, Dept of Ceramics, University of Leeds, 1982.

6. GREGORY T; Private Communication 1986.

7. FENTIMAN C; Private Communication 1986.

8. MONTGOMERY R; Private Communication 1985.

CHAPTER 7 CONCLUSIONS

7.1 None of the three superplasticisers investigated in this project produced the considerable improvement in workability normally observed when superplasticisers are used with Portland cement. The generally poor performance is attributed to the different hydration mechanism of Ciment Fondu. The continual dissolution of calcium and aluminium from the surface probably prevents the adsorption of a sufficiently high superplasticiser concentration to cause effective plasticisation.

7.2 Each of the three superplasticisers tested did cause initial plasticisation although the improvement in workability was shortlived. The subsequent loss of workability can occur very rapidly and is particularly severe for S3. The most effective superplasticiser was S2 followed by S1 and then S3.

7.3 The admixture formulation which proved most successful in meeting the objectives of the study was 0.3% S2 with 0.025% accelerator. At 5°C pastes containing this formulation showed improved workability compared to the control up to 25 minutes after mixing (see Figure 3.8). At 20°C paste workability is improved for 10 minutes for the same admixture formulation (see Figure 3.10). This admixture combination does not retard setting. The improvement in workability can be maintained for a longer period by increasing the dosage of superplasticiser although some set retardation may result.

7.4 The results demonstrate the considerable effect of hydration temperature on the setting time, hydration products and the long term behaviour of plain Ciment Fondu mixes.

The retardation of setting at about 30°C previously reported for both pure CA and Ciment Fondu was confirmed (1, 4, 53, 91, 92).

At 5°C the major hydration product is CAH_{10} whilst at 20°C the initial hydration products are CAH_{10}, C_2AH_8 and AH_3. At 30 and 40°C C_2AH_8 and AH_3 with a small amount of CAH_{10} are formed initially although there is rapid conversion to C_3AH_6. The rate of conversion is much greater at 40°C than at 30°C.

The strength of mortar cube cast at 20, 30 or 40°C was approximately the same after 18 months whereas cubes cast at 5°C were considerably stronger. The strength loss is caused by the conversion of CAH_{10} and C_2AH_8 to C_3AH_6 and AH_3. Typically the strength reduction caused by this conversion was 50-60%. For applications where strength is important it would be necessary to allow for this reduction.

7.5 The influence of the admixtures was also highly dependent on temperature. The previously reported retardation caused by the use of a superplasticiser alone was confirmed for both S1 and S2 at 20°C or below (153, 154). However at 30°C or above either superplasticiser causes acceleration. The behaviour of superplasticised Ciment Fondu mixes is thus highly susceptible to temperature variations within the range 20-30°C. It is unfortunate that this coincides with the likely range of working temperatures encountered in practice. This problem may necessitate the production of two formulations suitable for either low or high temperature applications.

This effect also means that any laboratory investigations of Ciment Fondu should be carried out at carefully controlled temperature which should be clearly stated with the experimental results.

7.6 The inclusion of almost all admixture combinations caused a reduction in the strength of mortar cubes, particularly at early ages. However by 18 months the reduction in strength caused by the admixtures was very slight.

Strength up to 18 months was slightly increased for mixes containing (i) 0.3% at S2 at 20°C or above (ii) 0.025% accelerator at 5 and 20°C (iii) 0.3% S1 at 5°C.

7.7 For the mixes tested there was good correlation between ultrasonic pulse velocity (upv) and strength which demonstrates that upv testing is an effective method for monitoring the long term behaviour of Ciment Fondu mixes.

RECOMMENDATIONS FOR FURTHER WORK

Further work is necessary to clarify why some results could not be explained by the available evidence.

In particular it is suggested that knowledge of the surface charge and dissolution of Ciment Fondu particles would assist in understanding the action of admixtures.

The surface charge of cement particles is dependent on solution pH. It would therefore be sensible to monitor solution pH in further investigations of the effect of admixtures.

In addition the nature and stability of the superplasticiser complex should be studied. This would be particularly useful in analysing the results of spectrophotometric testing and could also provide confirmation of the tentative suggestions of admixture action proposed in this thesis.

Further investigation of superplasticisers containing both sodium and calcium ions may prove fruitful. There is also scope for a wide ranging investigation of anionic and cationic surfactants not necessarily already in use with hydraulic cements.

It must be remembered that the results presented in this thesis relate only to one batch of Ciment Fondu. Since it is known that both chemical composition and particle size distribution vary from batch to batch it would be useful to check the behaviour of additional samples of Ciment Fondu.

REFERENCES

1. ROBSON T.D; High alumina cements and concretes. Contractors Record 1962
2. SORRENTINO F.P, GLASSER F.P; Trans.J.Brit.Ceram.Soc pp 253-256 Vol 74 1975, pp 95-103, 1976, Vol 75
3. CALLEJA J; 7th Int Cong on Chemistry of Cements. Paris 1980. Vol III, V-102
4. GEORGE C.M; Structure and Performance of Cements. Edited P Barnes Chap 9. 1983
5. ABDEL RAZIG B.E.I, PARKER K.M, SHARP J.H; Proc 7th Int Conf on Thermal Analysis. Vol 1, Chichester 1982, pp 571-577
6. BRISI C, LUCCO BORLERA M, MONTANARO L, NEGRO A; Cem & Concr Res 1986 pp 156-160 Vol 16
7. ROBSON T.D; 5th Int Symp on Chemistry of Cement, Tokyo 1969, Part 1, Section 4.
8. BENSTED J; 7th Int Cong on Chemistry of Cements. Paris 1980. Vol III, II-1
9. LEA F.M; The Chemistry of Cement and Concrete. 3rd edition, 1970 Arnold
10. HARCHAND K.S, VISHWAMITTER C.K; Cem & Conc Res 1984, pp 19-24 Vol 14
11. MIDGLEY H.G; Cem & Conc Res 1979, pp 623-630 Vol 9
12. GALTIER P; Thesis, Ecole Nationale Superieure des Mines de St Etienne 1981
13. COSTA U, MASSAZZA F, TESTOLIN M; Ind Chim Belg Vol 39, 1974, pp 579-586
14. RODGER S.A, DOUBLE D.D; Cem and Concr Res 1984, pp 73-82 Vol 14
15. TREFFNER W.S, WILLIAMS R.M; J.Amer Ceram Soc 1963, pp 399-406 Vol 46

16. AFSHAR W, McCARTER W.J; J. Mat Sci Letters 1985, pp 851-854 Vol 4

17. McCARTER W.J, AFSHAR W; J.Mat Sci Letters 1984, pp 1083-1086 Vol 3

18. RETTEL A, GESSNER W, MULLER D, SCHELER G; Transactions and Journal of British Ceram Soc 1985 pp 25-28 Vol 84

19. BARRET P, MENETRIER D, BERTRANDIE, D; Cem and Concr Res 1974 pp 545-556, pp 723-733 Vol 4

20. BARRET P, BERTRANDIE D; 7th Int Cong on Chemistry of Cements, Paris 1980. Vol. III, V-134

21. FUJII K, KONDO W, UENO H; J. Amer Ceram Soc 1986 pp 361-364 Vol 69

22. PARKER K.M, SHARP J.H; Transactions and Journal of the British Ceramic Society 1982, pp 35-42 Vol 81

23. BERTRANDIE D; Thesis, University of Dijon 1977

24. BARRET P, BETRANDIE D, BEAU D; Cem & Concr Res 1983 pp 789-800 Vol 13

25. SOUSTELLE M et al; Cem & Concr Res 1985 pp 421-430 Vol 15

26. SOUSTELLE M et al; Cem & Concr Res 1985 pp 655-661 Vol 15

27. BARRET P, BERTRANDIE D, BEAU D; Cem & Concr Res 1986 pp 785-788 Vol 16

28. BACHIORRINI et al; 8th Int Conf on Chem of Cem Brazil 1986 Vol IV pp 376-382

29. MISHIMA K; Proc. 5th Int Symp on Chemistry of Cement, Tokyo 1968, Vol 3, pp 167-174

30. TSEUNG A.C.C, CARRUTHERS K.G; Trans Brit Ceram Soc 1986, p305 Vol 85

31. COTTIN B; Cem and Concr Res 1971, pp 177-186 Vol 1

32. MURAT M, GALTIER P, GUILHOT B, NEGRO A; C.R.Acad Sci Paris Series C,291, pp 113-115, 1980

33. NIKUSHCHENKO V.M, KHOTIMCHENKO V.S, RUMYANTSEV P.F, KALININ A.I;Cem and Concr Res 1973, pp 625-63 Vol 3

34. SCHWIETE et al; Beton Steinzeitung Vol 32, 1966, p141 cited by Lea (9)

35. WELLS, CARLSON; J.Nat Bur Stand 1956, Vol. 57, pp 335-353 cited by George (4)

36. HALSEY Y, PRATT P.L; 8th Int Conf on Chem of Cem Brazil 1986 Vol IV pp 317-321

37. MISHIMA K, IWASE N, KOIDE S; Proc 13th Jap Congr on Mater Res, Tokyo 1969 pp 216-218

38. COTTIN B; Cem and Concr Res 1971, pp 273-284 Vol 1

39. CHATTERJI S, JEFFERY J.W; Trans Brit Ceram Soc May 1968, pp 171-183 Vol 67

40. MIDGLEY H.G, PETTIFER; Trans J.Brit Ceram Soc 1972, pp 55-59 Vol 71

41. KITTL, P, CASTRO J.H.C, POMPEU L.C; 7th Int Cong on Chemistry of Cements. Paris 1980. Vol III, V-10

42. PLATRET G; Thesis, University of Dijon, 1983

43. MEHTA P.K, LESNIKOFF; J.Amer Ceram Soc 1971, pp 210-212 Vol 54

44. BENSTED J; World Cement Technology 1982, pp 117-119 Vol 13

45. PARKER K.M, SHARP J.H; Unpublished Results

46. MIDGLEY H.G; J.Thermal Analysis 1978, pp 515-524 Vol 13

47. YOUNG J.F; Cem and Concr Res 1971, pp 113-122 Vol 1

48. GALTIER P, GUILHOT B; Cem and Concr Res 1984, pp 679-685 Vol 14

49. TEOREANU, I, ANGELESCU N, TUCLEA D; Rev Roum Chim Vol. 29, 1984, pp 113-120

50 MENETRIER-SORRENTINO D, GEORGE C.M, SORRENTINO F.P; 8th Int Conf on Chem of Cem Brazil 1986 Vol. IV pp 334-338

51. FOURNIER et al; Cem and Concr Res 1985, pp 151-158 Vol 15

52. CARLSON E.T; J.Res Natn Bur Stand 1964, p 453 cited by Lea (9)

53. GEORGE C.M; Trans J. Brit Ceram Soc 1980, pp 82-90 Vol 79

54. VAN AARDT J.H, VISSER S; C.S.I.R Res Report Vol. 594, 1983, pp 1-13

55. MIDGLEY H.G, BHASKARA RAO P; Cem and Concr Res 1978, pp 169-172 Vol 8

56. AVRAMI M; J.Chemical Physics Vol. 7 Dec 1939, Vol. 8, Feb 1940 Vol. 9 Feb 1941

57. LE SUEUR P.J, DOUBLE D.D; Unpublished results

58. URZHENKO, A. USHEROV-MARSHAK A; Izv Akad Navk SSR, Neorg Mater 1974 pp 888-892

59. SAKOVITCH; cited by Le Sueur and Double (42)

60. DOMONE P.L, THURAIRATNAM H; London Centre Report No. MC35 May 1984, Dept of Civ. Eng., University College London

61. TATTERSALL G.H, BANFILL P.F.G; The rheology of fresh concrete. Pitman, London 1983

62. TATTERSALL G.H; Nature 1955, p 166

63. TATTERSALL G.H; Brit J.Appl Physics 1955, pp 163-167

64. BHATTY J, BANFILL P.F.G; Cem and Concr Res 1984, pp 64-72 Vol 14

65. BANFILL P.F.G, SAUNDERS D; Cem and Concr Res 1981, pp 363-370 Vol 11

66. BANFILL P.F.G; Mag of Concr Res 1981, pp 37-47 Vol 33

67. ROY D.M, ASAGA K; Cem and Concr Res 1979, pp 731-739 Vol 9

68. JONES T.E.R, TAYLOR S; Silicates Industriels 1978, pp 142-151

69. JONES T.E.R, TAYLOR S; Mag of Concr Res 1977, pp 207-212 Vol 29

70. ORBAN J.A, PARCEVAUX P.A, GUILHOT D.J; Soc of Petroleum Engineers Special Paper 15578 1986

71. VOM BERG W; Mag of Concr Res 1979 Vol 31

72. DIMOND C.R; Ph.D Thesis, Sheffield University 1975

73. TATTERSALL G.H, DIMOND C.R; Proc of Conference held at Sheffield University Publ No 15.121, Slough Cement and Concrete Association 1976, pp 118-133

74. LOBANOV V.P; Kolloinduii Zhurnal 12(5) 1950, pp 352-358 (Library communication No. 579, BRS Garston 1951)

75. ASAGA K, ROY D.M; Cem and Concr Res 1980, pp 287-295 Vol 10

76. ROY D.M, ASAGA K; Cem and Concr Res 1980, pp 337-344 Vol 10

77. MANNHEIMER R.J; Oil & Gas Journal 1986 pp 94-100

78. BHATTY J, BANFILL P.F.G; Cem and Concr Res 1982, pp 69-78 Vol 12

79. Feb Ltd. Private communication 1984.

80. BRITISH STANDARDS INSTITUTIONS; BS 915:Part 2:1972 High Alumina Cement. London pp 16

81. MAGNAN R; Amer Ceram Soc Bul 1970, pp 314-316 Vol 49

82. CURRELL B.R, GRZESKOWIAK R, MIDGLEY H.G, PARSONAGE J.R; Cem and Concr Res 1987 pp 420-432 Vol 17

83. MURAT M, NEGRO A, BACHIORRINI A; C.R. Acad Sci Paris Series C, 1980, pp 287-290

84. WILDING C.R, WALTER A, DOUBLE D.D; Cem and Concr Res 1984, pp 185-194 Vol 14

85. MUNIR Z.A, TAYLOR M.A; J.Mater Sci 1979, pp 640-646 Vol 14

86. DOMONE P.L, CASSON R.B; Int Conf on concrete at early ages, Paris, April 1982

87. CASSON R.B, DOMONE P.L, SCRIVENER, JENNINGS, GILHAM, PRATT ; Proc Symp "Concrete Rheology" Nov 1-4 1982, Boston. Materials Research Society.

88. WILDING C.R, DOUBLE D.D; British Ceramic Proc No 35, Sept 1984, pp 349-357.

89. MUNIR Z.A, TAYLOR S; J.Mater Sci, Mar 1979, pp 647-652

90. PERIANI Ann Lavori Oct 1925 cited by Robson (1)

91. FRENCH P.J, MONTGOMERY R, ROBSON T.D; Mtg of Brit Ceram Soc Belfast 1970

92. GEORGE C.M, COTTIN B; Int Sem on calcium aluminates, Turin 1982

93. BUSHNELL-WATSON S & SHARP J.H; Cem & Concr Res in press 1986

94. RAMACHANDRAN V.S, FELDMAN R.F; Cem & Concr Res 1973, pp 729-750 Vol 3

95. KULA T.M, MEISER M.D, TRESSLER R.E; Cem and Concr Res 1980, pp 491-497 Vol 10

96. GEORGE C.M.; The Structural Use of High Alumina Cement Concrete. Publ of Lafarge Aluminous Cement Co Ltd. Not dated.

97. BEAUDOIN J.J.; Cem and Concr Res 1982, pp 289-299 Vol 12

98. COTTIN B, REIF P; Rev Mat Constr No 661, 1970, pp 293-305

99. MIDGLEY H.G, RYDER J.F; Cem and Concr Res 1977, pp 669-672 Vol 7

100. NEVILLE A; 11 Cemento 1978, pp 291-302

101. ALEGRE, R; Rev Mat Constr No 630, 1968 pp 101-108

102. NEVILLE A; High alumina cement and concrete. Construction press 1975

103. Report on the collapse of the roof of the assembly hall of the Camden School for Girls, BRE report for the Secretary of State for Education and Science, HMSO 1973 16 pp

104. BATE S.C.C; Report on the failure of roof beams at Sir John Cass's Foundation and Red Coat Church of England School in Stepney, BRE Current paper CP 58/74 18 pp

105. WILBURN F.W, KEATTCH C.J, MIDGLEY H.G, CHARSLEY E.L; Thermal methods group. Analytical division of Chemical Society London 1975

106. EL-JAZAIRI B; Report of Civ Eng Dept, Kings College, London, 1976

107. B.R.E. Information Paper 22/81

108. FRENKEL M, GLASNER A, SARIG S; J. Phys Chem 1980 507-510

109. OGER A; Internal Report Lafarge Ltd, 1975

110. BARNES P.A, BAXTER J.H; Thermochim Acta 1985, pp 427-431

111. BUSHNELL-WATSON S, SHARP J.H; Thermochim Acta 1985, pp 613-616

112. RUIZ DE GAUNA A, TRIVINO F, VAZQUEZ T; Mater Constr Espagnol Vol 157 1975 pp 43-64

113. MIDGLEY H.G; Private communication 1985

114. Concrete Society Technical Report Number 11

115. QUON D.H.H, MALHOTRA V.M; J.Amer Concr Inst 1982, pp 180-183

116. BUNGEY J.H; Paper given at Symp on HAC, Thames Polytechnic, 10 Dec 1974

117. BUNGEY J.H; Concrete, Sept 1974, pp 39-41 Vol 8

118. MAYFIELD B, BETTISON M; Concrete, Sept 1974, pp 36-38 Vol 8

119. REYNOLDS W.N; Brit Journal of NDT, Jan 1984, pp 11-14

120. BRADBURY C, CALLAWAY P.M, DOUBLE D.D; Mat Sci and Eng 1976, pp 43-53

121. LAFUMA H; Rev Mat Constr Trav Publ No 305 1935, pp 29-30

122. NEVILLE A; Proc Inst Civ Eng Vol 25, 1963, pp 287-324

123. MIDGLEY H.G, MIDGLEY A, Mag of Concr Res 1975, pp 59-77

124. NEVILLE A; Proc Inst Civ Eng Vol 10, 1958, pp 185-192

125. MIDGLEY H.G; Trans Brit ceram Soc 1976, pp 161-187

126. BROCARD; C.R. Acad Sci 1961, pp 413-415

127. TEYCHENNE D.C; Mag of Concr Res 1975, pp 78-102 Vol 27

128. MIDGLEY H.G; 7th Int Cong on Chemistry of Cements, Paris 1980, Vol III, V-68

129. CHATTERJI A.K, MAJUMDAR A.J; Indian Concrete Journal 1966, 40(51)

130. LEHMAN H, LEERS K.J; Tonindustrie Zeitung Vol 87, 1963, pp 29-41 cited by Ramachandran & Feldman (94)

131. GEORGE C.M; Seminar on cement and concrete science. Thames Polytechnic April 1979

132. MIDGLEY H.G; Int Sem on calcium aluminates, Turin 1982

133. BRE CP 34/75 1975

134. PEREZ M, VAZQUEZ T, TRIVINO F; Cem and Concr Res 1983, pp759-770 Vol 13

135. PEREZ M, VAZQUEX T, TRIVINO F; Cem and Concr Res 1984, pp161-169 Vol 14

136. FENTIMAN C.H; Cem & Concr Res 1985 pp 622-630 Vol 15

137. TRIVINO F; 8th Int Conf on Chem of Cem Brazil 1986 Vol IV pp417-422

138. MEHTA P.K; Proc 5th Int Symp on Chemistry of Cement 1968, Vol 2, pp148-152

139. BHASKARA RAO P, VISWANATHAN V.N; 7th Int Cong on Chemistry of Cements, Paris 1980, Vol III, V-51

140. BENSTED J; World Cem Tech Vol 12, 1981, pp 178-179, 182-184

141. Feb. Ltd; Private communication, 1984

142. MIDGLEY H.G; 7th Int Cong on Chemistry of Cements, Paris 1980, Vol III, V-85

143. LAFUMA H; Rev Mat Constr Trav Publ 243, p441, 1929 and Publ 244, p4, 130 cited by Lea (8)

144. BACHIORRINI A, CUSSINO L; 8th Int Conf on Chem of Cem Brazil 1986 Vol IV pp 383-388

145. GEORGE C.M; Performance of concrete in Marine Environment, New Brunswick, Aug 1980, ACI SP 68.

146. RAASK E; Seminar on carbonation of concrete, Slough UK, April 1976, Rilem Proc.

147. BLENKINSOP R.D, CURRELL B.R, MIDGLEY H.G, PARSONAGE J.R; Cem and Concr Res, 1985 pp 276-284, 385-390 Vol 15

148. CUSSINO L, NEGRO A; 7th Int Cong on Chemistry of Cements, Paris 1980. Vol III, V-62

149. SOUKATCHOFF P; Mater et Constr Vol 18 1985 pp 115-122

150. MASSAZZA F, COSTA U, BARRILA A; J.Amer Ceram Soc 1982, pp 203-207 Vol 65

151. MICHAUX, M, DEFOSSE C; Cem & Concr Res 1986 pp 23-30 Vol 16

152. SAKAI et al; Cem & Concr Res 1980 pp 311-319 Vol 10

153. QUON D.H.H, MALHOTRA D.H; Conference on Developments in the use of superplasticisers. Ottawa June 1981. ACI sp 68-10 pp173-187

154. LANKARD D.R, HACKMAN L.E; Amer Ceram Soc Bul Sept 1983, pp 1019-1025

155. DRAGOMAN I; Metalurgia (Bucharest) Vol 35, 1983, pp 194-197

156. BANFILL P.F.G; Cem & Concr Res 1986 pp 602-604 Vol 16

157. CREPAZ E, RACCANELLI A; Ind Ital Cem 1965 pp 333-338

158. VAN STRATEN H.A, SCHOONEN M.A.A, De BRUYEN P.L; J. Coll & Interfacial Sci Vol 103 No 2 1985 pp 493-507.

159. CREPAZ E, RACCANELLI A; Ind Ital Cem Vol 35, 1965, pp 761-766

160. PARKER T.W; Proc of 3rd Int Conf on Chem of Cem London 1952 Sect 14

161. BUSHNELL-WATSON S, SHARP J.H; Unpublished results

162. BASILE F, BIAGINI S, FERRARI G, COLLEPARDI M; 8th Int Conf on Chem of Cem, Brazil 1986 Vol VI pp 260-263

163. RIXOM M.R; Chemical Admixtures for Concrete. Spon, London 1978

APPENDIX 1. PROPERTIES OF THE CIMENT FONDU

Setting Time (BS 915: 1972) — Initial 280 minutes, Final 293 minutes

90 μm Residue: 3.8%

Surface Area (Blaine): 276 m^2/kg

Chemical Composition (%):

SiO_2	4.14	CaO	38.5
Al_2O_3	38.67	Na_2O	0.06
Fe_2O_3	10.43	K_2O	0.04
FeO	5.63	SO_3	0.19
TiO_2	1.98	CO_2	0.42

APPENDIX 2. GRADING OF SAND 1

Sieve	% Passing
5.00 mm	100
2.36 mm	89
1.18 mm	63
600 μm	32
300 μm	8
150 μm	1

APPENDIX 3. CALIBRATION OF HELICAL IMPELLER

THEORETICAL BACKGROUND

Dimensional analysis of mixing shows that for a Newtonian fluid

$$Np = B.Re^{x} \quad \ldots\ldots\ldots \qquad \{1\}$$

where Np = power number Re = Reynolds number

$$Np = \frac{P}{N^3.D^5.\rho} \qquad Re = \frac{D^2.N.\rho}{\eta}$$

P = power consumption during mixing
B = constant
η = viscosity
ρ = density

Equation {1} can also be written

$$\ln Np = \ln B + x.\ln Re$$

If T is the torque then $P = 2.\pi\, T.N$ and the power number may be written

$$Np = \frac{T}{N^2.D^5.\rho}$$

The omission of 2π here simply modifies the value of B by a factor of $1/2\pi$.

By plotting ln Np against ln Re it is found that the slope of the graph (x) is equal to -1 for laminar flow with resistance to flow caused only by viscous forces.

Newtonian Materials

For a Newtonian material $\tau = \eta.\gamma$ and it is found experimentally that

with a helical impeller system, $T = G.\eta.N$. Substitution of T into equation {1} gives $x = -1$ if $G = B.D^3$. Conversely, if the results of an experiment on a Newtonian material are plotted as ln Np against ln Re, the points would be expected to fit on a straight line of slope -1 and, if they do, the system is operating under laminar flow conditions.

Bingham Materials

For a Bingham material equation {1} can be assumed to apply if the apparent viscosity is used:

$$\eta app = \frac{\tau_o}{\dot{\gamma}} + \mu$$

and if it is assumed that the effective shear rate in the mixer is simply proportional to the rotational speed of the impeller:

$$\dot{\gamma} = K.N$$

$$\text{Then} \quad Re = \frac{D^2.N.\rho}{\left(\tau_o/K.N\right) + \mu} \quad \ldots\ldots\ldots \quad \{2\}$$

Substitution in equation {1} with $x = -1$ gives:

$$\frac{T}{\rho N^2 D^5} = B\left(\frac{\tau_o}{K D^2 N^2 \rho} + \frac{\mu}{D^2 N \rho}\right)$$

which may be written as:

$$T = \frac{B.D^3}{K}.\tau_o + B.D^3.N.\mu \quad \ldots\ldots \quad \{3\}$$

For a Bingham material such as cement paste it is found experimentally that $T = g + h.N$ for the helical system where g,h are as below by comparison with equation {3} and represent the intercept and slope respectively of the graph of T vs N.

$$g = \frac{B.D^3}{K}.\tau_o \qquad h = B.D^3.\mu$$

Expressions for yield value and plastic viscosity may then be written as below (recalling that $G = B.D^3$)

$$\tau_o = \frac{K}{G}.g \qquad \mu = \frac{1}{G}.h$$

Pseudoplastic Materials

For a pseudoplastic fluid of a type that obeys the power law

$$\tau = r.\dot{\gamma}^s \quad ..... \qquad \{4\}$$

$$Re = \frac{D^2.N.\rho}{r(KN)^{s-1}}$$

and since $T = g.\eta.N$

$$T = B.D.^3.r.K^{s-1}.N^s$$

Initially it is assumed that the power in this equation may not be the same as in equation {4} and so it is written as

$$T = p.N^q \quad ..... \qquad \{5\}$$

Thus since $\eta_{app} = T/G.N$

$$\eta_{app} = p.N^{q-1}/G ..... \qquad \{6\}$$

Equating the values of η_{app} obtained from equations {4} and {6} gives

$$\dot{\gamma} = \left(\frac{p}{r.G}\right)^{\frac{1}{s-1}} . N^{\frac{q-1}{s-1}}$$

If the powers s and q are equal as expected then

$$\dot{\gamma} = \left(\frac{p}{r.G}\right)^{\frac{1}{s-1}} .N$$

Thus

$$K = \left(\frac{p}{r.G}\right)^{\frac{1}{s-1}} \quad \ldots\ldots \quad \{7\}$$

It must be emphasised that this analysis is valid only for laminar flow.

CALIBRATION PROCEDURE

The procedure is illustrated by results from the IHB/CC system. Numerical details are not given for the other systems for brevity.

To Determine G

The relationship between viscosity and temperature for a Newtonian material (heavy oil) was determined using ICD/CD coaxial cylinders.

The relationships between T and N were found for the helical impeller in the heavy oil over a range of temperatures. The constant G may then be found as the gradiant of a graph of T/N vs μ which for the IHB/CC systems was $0.787 \times 10^{-3} m^3$.

To Determine K

Aqueous solutions of carboxymethyl cellulose (CMC) which are pseudoplastics of the power law type were prepared at several concentrations.

Tests using the ICD/CD system gave graphs of scale reading vs rotational speed which, after conversion to τ and Ω, enabled plots of ln τ vs ln Ω to be prepared.

The gradient n of each line was determined and used to calculate the shear rate factor α:

$$\alpha = \frac{2}{n.R_b^{2/n}\left[\left(\frac{1}{R_b}\right)^{2/n} - \left(\frac{1}{R_c}\right)^{2/n}\right]}$$

Values of Ω are then converted to shear rate, $\dot{\gamma}$, using $\dot{\gamma} = \alpha.\Omega$ so that the graphs of ln τ vs ln $\dot{\gamma}$ can be plotted. Values of slope, s, and intercept ln r were as follows:

	CMC Solution				
	1	2	3	4	5
s	0.471	0.511	0.498	0.507	0.523
r	8.109	8.723	10.044	14.055	23.500
Correlation Coefficient	0.999	0.999	0.999	0.999	0.999

Plots of ln T vs ln N for the same range of CMC concentrations were then obtained for the helical system from which the constants p and q were as follows:

	CMC Solution 1	2	3	4	5
p	0.00224	0.00222	0.00281	0.00314	0.00653
q	0.474	0.556	0.508	0.626	0.546

A value of K for each CMC solution, calculated using equation {7}, is shown below together with values of q-1/s-1

	CMC Solution 1	2	3	4	5
K	7.24	10.06	7.85	12.86	8.87
q-1/s-1	0.994	0.908	0.980	0.759	0.952

For all except strength 4 values of q-1/s-1 are close to 1 as predicted from the theory. The mean value of K (excluding the result from strength 4) is 8.5.

APPENDIX 4

Published Papers

The Effect of Superplasticisers on the Hydration of Aluminous Cement

Gill S.M., Banfill P.F.G., El-Jazairi B.

Proceedings 8th International Congress
on the Chemistry of Cement, Brazil 1986
Vol. IV pp 322-327

S.M. GILL, P.F.G. BANFILL, B. EL-JAZAIRI
School of Architecture and Building Engineering, University of Liverpool, P.O. Box 147, Liverpool L69 3BX,
FEB (Great Britain) Ltd., Swinton Hall Road, Swinton, Manchester M27 1DT, U.K.

THE EFFECT OF SUPERPLASTICISERS ON THE HYDRATION OF ALUMINOUS CEMENT
L'EFFET DES ADJUVANTS SUPERPLASIFIANTS SUR L'HYDRATATION DU CIMENT ALUMINEUX

SUMMARY

The use of superplasticisers to produce aluminous cement mixes at low water content is an attractive proposition which is hindered by their retarding effects. In order to examine the possibility of overcoming the retardation the influence of two superplasticisers and an accelerator, both singly and in combination, on Ciment Fondu has been systematically studied.

The setting time of cement pastes was determined by the Vicat needle penetrometer and the kinetics of hydration studied in a conduction calorimeter.

The strength of mortar cubes was monitored by ultrasonic pulse velocity which was correlated with compressive strength in a subsidiary series of tests.

Both superplasticisers have a severe retarding effect at 5°C and 20°C, extending the time to the main heat evolution peak by up to 60 hours depending on the concentration used. At 30°C both admixtures overcome the well known retardation which occurs at this temperature in plain Ciment Fondu pastes and at 40°C slight acceleration occurs. The severe retardation at low temperatures may be overcome by simultaneous use of a lithium salt accelerator.

INTRODUCTION

The use of superplasticisers with Portland cement is now well established enabling the production of extremely workable mixes or of mixes with significantly reduced water content. Superplasticised aluminous cement mixes with similar characteristics are an attractive proposition. Highly workable mixes could be used where high early strength or improved chemical resistance is required whilst reduction of water content to less than 0.40 water/cement ratio (w/c) significantly reduces the rate of conversion. (1). Previous studies on such systems have however shown the tendency for unacceptable set retardation (2).

The hydration of Ciment Fondu will not be described in detail in this paper since much work has already been reported (3-7). A major feature however is the effect of temperature, since, unlike Portland Cement, the products of hydration are not the same at all temperatures. Hydration of Ciment Fondu may be described in terms of the hydration of CA, its major constituent (typically 50%) but there is disagreement over the temperature ranges for the formation of each hydrate (8,11) and over the hydration reactions. At low temperatures (<20°C) CAH_{10} is formed, above approximately 30°C the products of hydration are C_3AH_6 and alumina gel. The equations given below are not established but represent a possible reaction scheme (4):

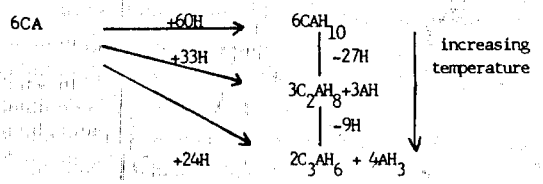

It is important not to neglect the influence of other phase components such as $C_{12}A_7$, CA_2, C_2AS, C_4AF and other minor constituents. Variation in Ciment Fondu composition further complicates understanding of the processes involved. The main manifestation of all this complexity is that the hydration rate slows above about 20°C until 30°C at which temperature the rate starts to increase rapidly. This behaviour causes delayed setting of pastes and concretes (6,7).

This paper describes a systematic study of the influence of 2 superplasticisers and an accelerator, both singly and in combination, on the setting, hydration and strength development of Ciment Fondu at temperatures between 5 and 40°C.

While the mortar test programme described here will eventually provide strength data over a much longer period, at the time of preparing this paper results were available up to 28 days.

EXPERIMENTAL PROCEDURES

MATERIALS

Cement: Ciment Fondu from one production batch was used for all tests on pastes and mortars. The chemical composition and physical properties are given in Appendix 1.

Superplasticisers: S1 sulphonated naphthalene resin, S2 development product. (Admixture dosages in % by weight of cement.) Accelerator: Lithium salt
Water: Deionised water used in all experiments.

CONDUCTION CALORIMETRY

Tests were carried out using Oxford Conduction Calorimeter (Calox) units. This type of calorimeter is capable of giving information on the heat evolution from the instant when cement and water first come into contact. As the reaction proceeds, and heat is evolved the small temperature difference across thermocouples between the experimental chamber and a heat sink produces an emf which is detected by a potentiometric chart recorder. The voltage output is also fed to a solid state memory recorder which converts the readings to digital form. The recorder stores the voltages in this form at preset intervals of 5 minutes and can store 1024 values which are subsequently transferred through an interface to an Apple III microcomputer. For pastes which show considerable acceleration, data can be taken from the chart output at shorter intervals and added to the stored data. This ensures that the peak in rate of heat evolution is well defined. A suite of computer programs was written for the Apple III microcomputer to process and analyse the results.

For plain pastes runs were made over the range of 5 to 45°C at 5°C intervals. An additional test at 27°C was made to provide a comparison with results obtained by French workers (11). Runs were also made on pastes containing various admixture combinations. A total of 14 combinations, listed in Table 1, were all tested at 5, 30 and 40°C. All tests were carried out using 12g of cement at both 0.30 and 0.40 w/c.

It should be noted that only a limited amount of the data produced can be reported in a paper of this length.

SETTING TIMES

The Vicat needle penetrometer was used to measure the initial setting time of pastes with the following accelerator dosages at 5, 20, 30 and 40°C w/c and at 20°C only at 0.30 w/c:

0, 0.01, 0.075, 0.05, 0.01, 0.5, 1.0, 2.0%.

STRENGTH DEVELOPMENT

PUNDIT equipment was used to monitor the ultrasonic pulse velocity (UPV) of 70.7 mm cubes of 1:1½ cement:sand mortar stored in water at 5, 20, 30 and 40°C. A total of 12 mixes, detailed in Table 1, were tested at each of the four temperatures. Four cubes were cast from each mix, 2 of which are tested for compressive strength at randomly chosen ages to enable the correlation between UPV and strength to be investigated. Great care was taken to ensure that materials were stored at the appropriate temperature prior to mixing. Immediately after casting the moulds and their contents were placed inside plastic bags in water at the correct temperature. The exception to this was that cubes cast at 20°C were cured in air in the laboratory, covered with plastic sheeting to prevent drying. Cubes were demoulded as soon as possible, typically 6 hours after casting though considerably longer for some mixes. The first UPV readings were taken 24 hours after casting. Other test ages are 2, 3, 7, 14, 21, 28 days, 2, 3, 6, 12, 18 months.

UPV testing is advantageous since the same specimen is repeatedly checked thus eliminating the effects of variability between samples tested to destruction.

TABLE 1. MIX DETAILS FOR PASTES AND MORTARS.

Paste	Mortar	Admixture Dosage (%) Superplasticiser. S1	S2	Accelerator
P1	M1	0	0	0
P2	M3	0.3	0	0
P3	-	0.6	0	0
P4	M4	1.0	0	0
P5	M5	0	0.3	0
P6	-	0	0.6	0
P7	M6	0	1.0	0
P8	M2	0	0	0.025
P9	-	0	0	0.1
P10	-	0	0	1.0
P11	M7	0.3	0	0.025
P12	M8	1.0	0	0.025
P13	M9	0	0.3	0.025
P14	M10	0	1.0	0.025

RESULTS

HYDRATION OF PLAIN PASTE

A typical graph obtained from calorimetry testing is shown as Figure 1. The effect of temperature on the hydration of plain paste at 0.30 w/c is shown on Figure 2. The method of presentation used is that of Wilding, Walter and Double (13). The pattern of results at 0.40 w/c is very similar.

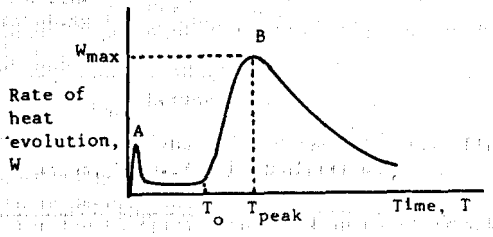

FIGURE 1. Variation of rate of heat evolution with time in conduction calorimeter.

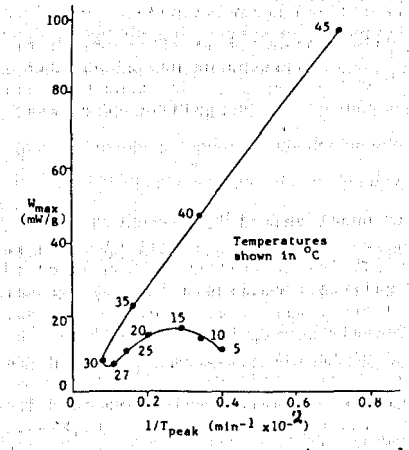

FIGURE 2. Effect of temperature on heat evolution.

HYDRATION AND SETTING OF PASTE CONTAINING ACCELERATOR ALONE

Figure 3 shows the results of Vicat testing. Results obtained from calorimetry testing showed that a second distinct peak in rate of heat evolution was produced by some mixes, as shown in Figure 4, though the highest peak is not always the second to occur. This leads to difficulties in interpretation of results. Throughout this report, W_{max} and T_{peak} refer to the highest peak present.

Values of Vicat initial set and T_{peak} are given in Table 2.

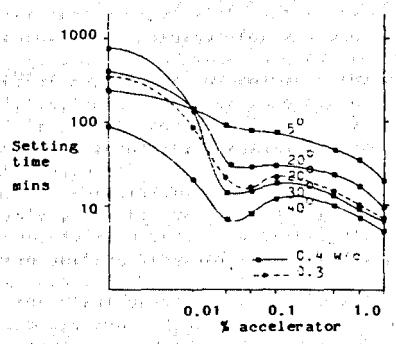

FIGURE 3. Effect of accelerator on Vicat initial setting time.

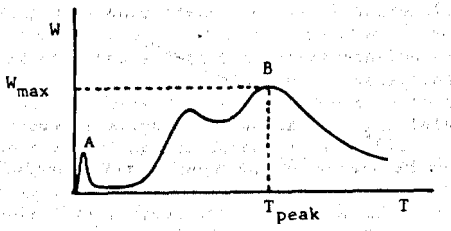

FIGURE 4. Double peaks observed in conduction calorimeter with certain mixes (see Table 3).

TABLE 2. CORRELATION OF VICAT INITIAL SET WITH CALORIMETER T_{peak}

Temperature	%Accelerator	Vicat Initial Set (Minutes)	T_{peak}	Number of peaks
5°C	0	240	250	1
w/c 0.40	0.025	90	120	1
	0.1	75	115	2
	1.0	35	50	1
20°C	0	350	495	1
w/c 0.30	0.025	22	140	2
	0.1	23	30	2
	1.0	10	17	2
20°C	0	395	435	1
w/c 0.40	0.025	32	150	2
	0.1	30	30	2
	1.0	17	22	2
30°C	0	745	1290	1
w/c 0.40	0.025	14	250	2
	0.1	19	16	2
	1.0	9	10	2
40°C	0	85	290	1
w/c 0.40	0.025	7	9	1
	0.1	12	10	2
	1.0	7	6	2

EFFECT OF SUPERPLASTICISERS ALONE AND WITH ACCELERATOR

Calorimetry

Several mixes produced more than one peak in the rate of heat evolution as shown in Figure 4. Table 3 summarises the peak pattern.

TABLE 3. EFFECT OF SUPERPLASTICISERS AND ACCELERATOR ON CALORIMETER OUTPUT.

MIX	5°C	20°C	30°C	40°C
P2	P	P	Pp	PP
P3	P	P	Pp	Pp
P4	P	P	P	Pp
P5	P	P	pp	P
P6	Pp	P	Pp	P
P7	P	P	P	P
P11	Ppp	PP	PP	P
P12	Ppp	P	Pp	Pp
P13	Ppp	Ppp	PP	P
P14	Pp	P	Ppp	pP

P denotes one major peak. PP denotes 2 major peaks; Pp denotes one major and one considerably smaller peak, etc.,.

Figure 5 summarizes the acclerating/retarding action of the admixtures. The vertical axis of this figure shows the ratio of the time to W_{max} for the particular combination of admixture and temperature to the time to W_{max} for the plain paste at the same temperature i.e.:

$$X = \frac{T_{peak\ (admixture)}}{T_{peak\ (control)}}$$

Deviation of the curve above X = 1 signifies retardation, below X = 1 acceleration.

Strength Development

For the 48 results obtained up to 28 days the relationship between UPV (v) and compressive strength (f) is:

$$f = 0.0019\ v^{7.3} \quad \text{(correlation coefficient = 0.93)}$$

This is shown on Figure 6 together with the upper and lower 95% prediction intervals.

Figures 7-10 show the changes in UPV occurring up to 28 days after casting.

DISCUSSION

PLAIN PASTE

During the hydration of Ciment Fondu heat is evolved as shown in Figure 1. The initial peak A is thought to be due to wetting of solids, chemical dissolution and partial hydration occurring when water first comes into contact with cement (14). This is followed by a dormant period whose length is determined by temperature, water content and chemical composition. After this dormant period, the rate of heat evolution increases rapidly at T_o until a clearly defined peak, B, is seen.

The well known delay affect around 30°C is confirmed in Figure 2. Above 30°C the relationship between W_{max} and $1/T_{peak}$ is linear and corresponds to the acceleration of a single hydration reaction (the formation of C_3AH_6) by increasing temperature (13). Between 5 and 30°C the behaviour is more complex, due possibly to interactions in the simultaneous production of several hydrates. The maximum delay in hydration occurred at 30°C as compared to the 27°C reported by Murat et al for pure CA (11).

ACCELERATED PASTES

Figure 3 illustrates the dramatic effect of the lithium salt accelerator on setting time. At dosages exceeding only 0.01% by weight of cement the 30°C delay is masked and setting times decrease consistently with increasing temperature. As dosage increases, a minimum setting time is observed at about 0.025%; this effect being more noticeable as temperature increases. Setting times were longer at higher paste water content. This behaviour may be explained by the longer time required to achieve the saturated solution from which initial hydrate precipitation occurs.

An attempt was made to correlate the Vicat initial setting time with parameters obtained from the calorimetry results; for example, T_o, T_{peak}, or T_{cum}, the time at which a predetermined cumulative amount of heat has been evolved. The onset of bulk precipitation of hydrates (and hence production of heat) is said to correspond with the time at which measureable mechanical resistance begins to develop in the paste (6). However, a difficulty in establishing the correlation is caused by the presence of multiple peaks for many mixes. It thus proved to be impossible to produce a quantitative relationship between setting time and any of the 3 parameters listed above. DTA results have led to the suggestion that the first peak is due to the formation of a calcium aluminate hydrate gel and the second to a more stable monocalcium aluminate decahydrate (15). Further work on the chemical differentiation between these peaks is planned as a later stage of this research. Additional problems arise in correlating setting time with calorimetry results because of the different patterns of heat evolution when forming different hydrates and in the interpretation of Vicat results in fundamental terms. Inspection of the data in Table 2 shows that the time to initial set is normally slightly less than T_{peak}. This confirms the findings of Casson et al (16).

Relatively little work has been carried out on the mechanism of lithium salt accelerators. Rodger and Double (17) propose that formation of lithium aluminate promotes nucleation of calcium aluminate hydrates. This was confirmed by Crepaz and Raccanelli (18) by solution analysis studies.

EFFECT OF SUPERPLASTICISERS

The presence of multiple peaks in heat evolution again causes difficulty in interpretation. Times to the maximum rate of heat evolution were used to prepare Figure 5 which clearly shows the dramatic effect of temperature on superplasticised mixes.

At 5°C mixes without accelerator all exhibit retardation. 1.0% S2 causes a 16 fold increase in T_{peak} over the control mix. This corresponds to a setting time of approximately 60 hours. Addition of 0.025% accelerator is sufficient to overcome the retardation for all except the 1.0% S2 mix. At 20°C the behaviour is similar though retardation is less marked and 0.3% S1 causes slight acceleration. At 30 and 40°C all mixes are accelerated.

Sulphates retard the hydration of Ciment Fondu at room temperature (19), and the behaviour of S1 and S2 which contain 5% and 15% w/w free sodium sulphate, respectively, may perhaps be attributed to this. Further work is planned to increase the understanding of this aspect.

It may be expected that mortar mixes containing admixtures would show early differences in UPV in accordance with the acceleration/retardation of hydration. Figures 7-10 show however that this is

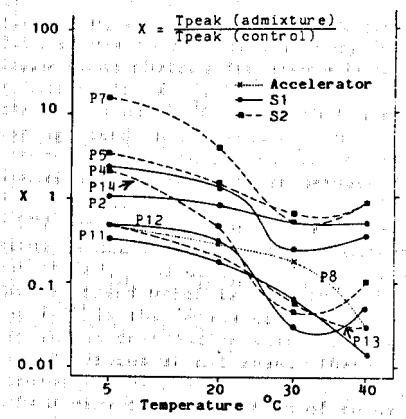

FIGURE 5 - Effect of temperature on T_{peak} of pastes.

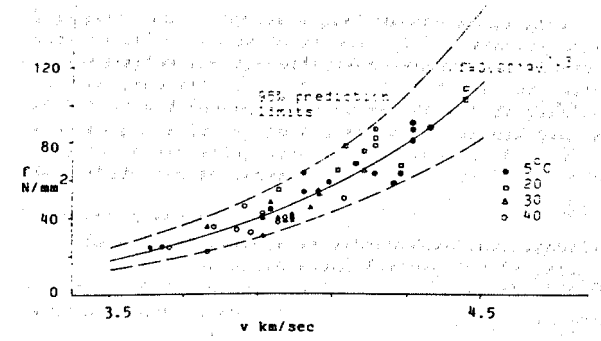

FIGURE 6 - Relationship between UPV and strength for 70.7 mm mortar cubes.

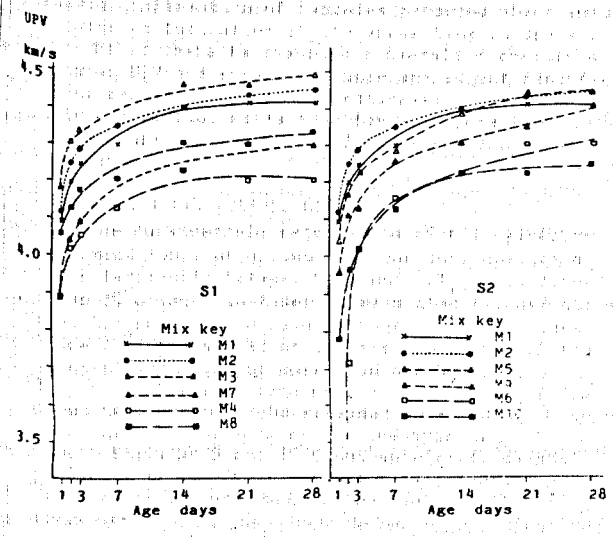

FIGURE 7 - UPV/Age relationship for mortars at 5°C.

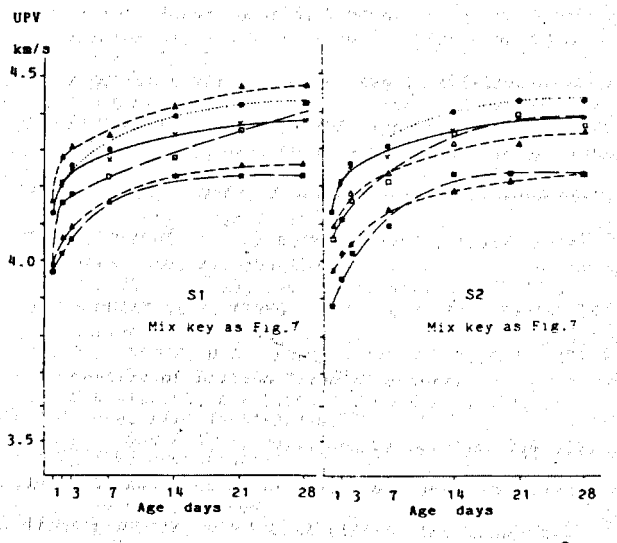

FIGURE 8 - UPV/Age relationship for mortars at 20°C.

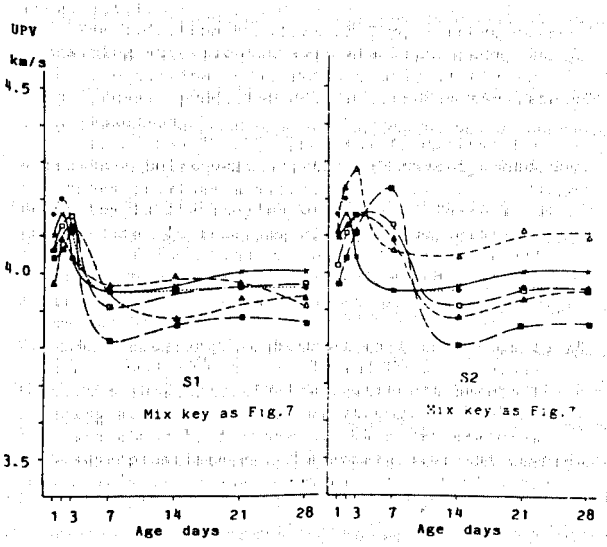

FIGURE 9 - UPV/Age relationship for mortars at 30°C.

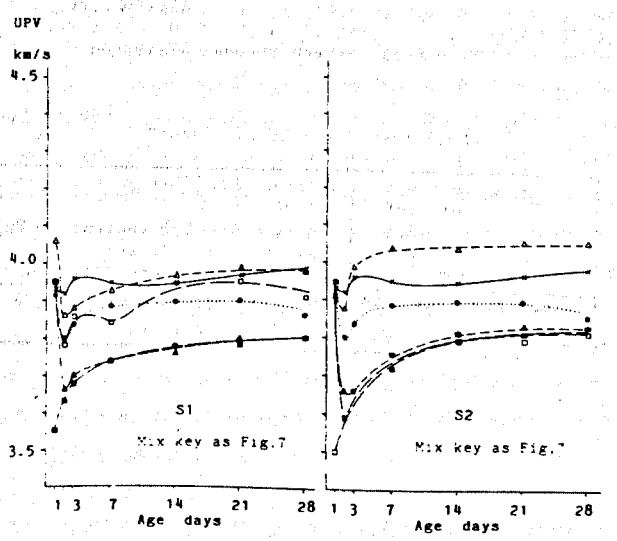

FIGURE 10 - UPV/Age relationship for mortars at 40°C.

not always so, although the extreme retardation of the 1.0% S2 mix is reflected in very low early UPV.

There is an obvious difference between the UPV/age relationships at 5, 20°C and those at 30, 40°C. The mixes at 5 and 20°C all exhibit a steadily increasing trend in UPV with age up to 28 days. At 30°C there is the same initial rapid increase in UPV but a maximum is reached after between 2 and 7 days. At 40°C the maximum is reached before 1 day, thereafter UPV decreases before increasing again. This behaviour is characteristic of the conversion reactions of CAH_{10} and C_2AH_8 to C_3AH_6 and AH_3 (6).

Another trend which is clearly visible from figures 7-10 is that mixes containing a superplasticiser in combination with accelerator show reduced UPV values at all ages. These low values are accompanied by low compressive strengths. Thus there is a very complex pattern of behaviour since setting and early hydration is accelerated whilst strength is reduced. Further testing is planned to enable confirmation of hydrates produced which should provide an indication of the mechanisms in operation.

Whilst there is reasonable overall correlation between UPV and strength, there are as yet insufficient results at each temperature to confirm that this correlation holds true for all hydration temperatures and hence for different hydrate compositions.

CONCLUSIONS AND FURTHER WORK.

1. The considerable retardation of the hydration of Ciment Fondu at around 30°C has been confirmed. The relationship between W_{max} and $1/T_{peak}$ is linear above 30°C which is taken to mean that the hydration reaction remains the same above this temperature. Below 30°C the situation is very complex with the parallel formation of more than one hydrate.
2. A lithium salt accelerator is extremely efficient in overcoming the retardation at 30°C.
3. Superplasticisers retard the hydration of Ciment Fondu at 5 and 20°C but accelerate slightly at 30 and 40°C. The retardation is tentatively ascribed to the presence of free sulphate in the admixtures.
4. The retardation by superplasticisers may be overcome by simultaneous use of the lithium salt accelerator.
5. The hydration kinetics of Ciment Fondu pastes containing superplasticisers are highly complex with some combinations, particularly at higher temperatures, producing double peaks in the rate of heat evolution.
6. Use of the PUNDIT apparatus to monitor the ultrasonic pulse velocity through Ciment Fondu mortar cubes provides a valuable indication of changes occurring in the samples with time. There is a good general correlation with the compressive strength of the cubes which enables the variation in strength with time to be determined with economy in terms of the effort involved in specimen preparation and storage.
7. Mortar strength continues to increase up to 28 days at 5 and 20°C but at 30 and 40°C it passes through a substantially lower strength before increasing slowly. The 28 day strengths at 30 and 40°C are about half those at lower temperatures. Both superplasticisers, the accelerator and combinations affect the variation in strength with time in different ways.

This paper has reported a preliminary stage in a substantial research programme. Other aspects under investigation are the effects of superplasticisers on flow properties, on changes in hydrate composition with time and consequently on mechanical properties. When complete it is hoped that more progress can be made in interpreting some of the complex effects described in this paper.

ACKNOWLEDGEMENTS

The authors gratefully acknowledge the financial assistance of the Science and Engineering Research Council and the provision of materials by the Lafarge Aluminous Cement Co Ltd.

REFERENCES

1. H G MIDGLEY, A MIDGLEY (1975), Mag Con Res 27, 59.
2. D H QUON, V M MALHOTRA (1981), in "Developments in the use of superplasicisers", ACI SP 68-10,173.
3. F M LEA (1970), "The chemistry of cement and concrete", Edward Arnold, London.
4. K M PARKER, J H SHARP (1982), Trans J Brit Ceram Soc 81, 35-42.
5. B COTTIN (1971), Cem Conc Res 1, 177-186.
6. C M GEORGE (1983), in "Structure and performance of cements", ed P. BARNES, Applied Science, Lond.
7. T D ROBSON (1962), "High alumina cements and concretes", Contractors Record Ltd, London.
8. K MISHIMA (1968), Proc. 5th Int. Symp. Chemistry of Cement, Tokyo 3, 167-174.
9. A C TSEUNG, K G CARRUTHERS (1963), Trans. Brit. Ceram. Soc. 62, 305-309.
10. B COTTIN (1971), Cem. Conc. Res. 1, 273-284.
11. M MURAT et al (1980), C.R. Acad. Sci. Paris, 291, Series C, 113-115.
12. P J FRENCH, N G J MONTGOMERY, T D ROBSON, (1970), Meeting of British Ceramic Society.
13. C R WILDING, A WALTER, D D DOUBLE (1984), Cem. Concr. Res. 14, 185-194.
14. R MAGNAN (1970), Bull. Am. Ceram. Soc. 314-315.
15. H G MIDGLEY (1985), Private communication.
16. R B CASSON et al (1982), Proc. Symp. "Concrete rheology", Boston.
17. S A RODGER, D D DOUBLE (1984), Cem. Conc. Res. 14, 73-82.
18. E CREPAZ, A RACCANELLI (1975), Ind. Ital. Cem. 35, 761-768.
19. V S RAMACHANDRAN, R FELDMAN, J J BEAUDOIN (1981), "Concrete science", Heyden, London.

APPENDIX

Properties of the Ciment Fondu

Setting time (BS 915): Initial	280 min
Final	293 min
90 μm residue (%)	3.8
Surface Area (Blaine) (m^2/kg)	276
Chemical Composition (%):	

SiO_2	Al_2O_3	Fe_2O_3	FeO	TiO_2	CaO	Na_2O	K_2O	SO_3	CO_2
4.14	28.67	10.43	5.63	1.98	38.5	0.06	0.04	0.19	0.42

The Rheology of Aluminous Cement Pastes

Banfill P.F.G, Gill S.M

Proceedings: 8th International Congress
on the Chemistry of Cement, Brazil 1986.
Vol. VI pp 223-227

P.F.G. BANFILL, S.M. GILL
School of Architecture and Building Engineering, The University of Liverpool,
P.O. Box 147, Liverpool L69 3BX, U.K.

THE RHEOLOGY OF ALUMINOUS CEMENT PASTES
LA RHEOLOGIE DES PATES DU CIMENT ALUMINEUX

SUMMARY

While the rheology of cement pastes has been studied over many years almost no information seems to be available on aluminous cement pastes. In view of the industrial importance of Ciment Fondu grouts, which are very durable in offshore applications, it is useful to compare the rheology of Ciment Fondu pastes with that of ordinary Portland cement. Ciment Fondu pastes were tested in a coaxial cylinders viscometer and the effect of test regime on the shape of the flow curve determined. Using a short flow cycle time, the effects of mixing method, age and water/cement ratio on the measured rheological parameters was studied systematically. Experiments at constant steady shear rate were carried out to study the breakdown of structure.

The rheology of Ciment Fondu pastes is as complex as that of Portland cement pastes. While they are thinner at a given water/cement ratio, they still undergo structural breakdown, manifested by a reduction in apparent viscosity on shearing. This shearing may be as a result of mixing prior to testing, or in the viscometer during the course of the test. The shape of the flow curve depends in a complex way on the cycle time but the pattern of curves is very similar to those obtained for Portland cement pastes. All these phenomena may be explained by flocculation and deflocculation processes.

INTRODUCTION

The rheology of cement pastes has been studied over several decades, but work has concentrated almost entirely on Portland cement (1), and no information seems to be available on aluminous cement pastes. In view of the industrial importance of Ciment Fondu grouts, particularly in marine applications where their superior durability and rapid strength gain are advantageous, it is useful to compare the rheology of Ciment Fondu pastes with that of ordinary Portland cement. This paper reports work carried out with a typical Ciment Fondu to provide this information.

RHEOLOGY OF CEMENT PASTES

The principal features of the rheology of cement pastes have been described in detail elsewhere (1), but may be briefly summarised as follows:

1. The flow curve of cement paste has been described in terms of various models:

Bingham $\tau = \tau_o + \mu\dot{\gamma}$

Hershel-Bulkely $\tau = \tau_o + A\dot{\gamma}^B$

Robertson-Stiff $\tau = A(\dot{\gamma}+C)^B$

Ostwald-De Waele $\dot{\gamma} = B\sinh(\tau-\tau_o)/A$

with associated observations in each case of shear thinning behaviour at high shear rates (τ shear stress, $\dot{\gamma}$ shear rate).

2. The existence of a yield value indicates that structure exists in the paste, due to the interactions between cement particles in the suspension. This structure breaks down on shearing because the energy input to the links between particles is sufficient to break the bonds. This structural breakdown manifests itself in two ways. Firstly, the yield value and plastic viscosity of the paste decrease with prolonged mixing, so that the method of preparing the paste affects the measured rheological parameters. Secondly, the torque, T, exerted by the paste on a continuously rotating cylinder or cone in a rotational viscometer decreases with time, t, according to an exponential relationship of the form

$$T - T_e = ke^{-bt}$$

where Te is the torque reached at equilibrium and k and b constants. The latter effect was treated theoretically by Tattersall (2) in terms of the number of links between particles in the paste.

3. The structural breakdown can also account for the variation in the reported flow curve shapes. Banfill and Saunders (3) found that when the time taken to complete an up and down cycle in a coaxial cylinders viscometer was short the flow curve showed a hysteresis loop with the downcurve falling to lower shear stresses than the upcurve (structural breakdown), whereas when the cycle time was long the loop was reversed. At intermediate cycle times flow curves with more than one loop were obtained. Furthermore the cycle times producing these types of curve varied from cement to cement. Only at cycle times of two minutes or less were the loop shapes consistent. They explained this in terms of the competition between shear-induced structural breakdown and the buildup of structure due to continuing hydration reactions. In addition, prolonged mixing results in reversible flow curves (up- and downcurves superimposable).

4. Variations in yield value over a 20-fold range and in plastic viscosity over a 50-fold range have been reported by different workers and can be explained by differences in experimental technique (4). In addition to the effect of mixing on the structural breakdown, cement pastes slip at the walls of the viscometer. This is assumed to be overcome by profiling or serrating the surfaces but no-one has shown conclusively that this is so. Nevertheless, Mannheimer showed that slippage could result in a sixfold reduction in the measured yield value of a cement paste (5).

5. Because of the variation of shear stress across the gap of a coaxial cylinders viscometer fluids with a yield value exhibit plug flow at low shear rates where the stress does not exceed the yield value at all points in the fluid, as shown by the Reiner-Rivlin equation:

$$\Omega = \frac{T}{4\pi\mu h}\left(\frac{1}{R_b^2} - \frac{1}{R_c^2}\right) - \frac{\tau_o}{\mu}\ln\frac{R_b}{R_c}$$

only when $T/2\pi R_b^2 h \geq \tau_o$ does all the fluid flow. This may be taken account of in the evaluation of data, but Tattersall and Dimond found that plug flow also occurred at much higher shear rates and stresses in conditions of steady continuous shear (6). They observed discontinuities in the exponential decay of torque with time which on visual examination of the paste were found to coincide with the times at which a solid plug of material broke up. When the observed width of the sheared zone was used in calculations instead of the instrument gap width, previously irreconcilable data on the effect of shear rate on the structural breakdown kinetics could be understood.

This complex behaviour of Portland cement pastes forms the background against which the rheology of Ciment Fondu pastes must be compared.

EXPERIMENTAL DETAILS

All experiments were carried out using a typical Ciment Fondu with the composition and other properties given in Table 1. The viscometer used in this work was a Haake Rotovisco RV2 with PG142 external speed programmer. Two coaxial cylinders geometries were used: (i) the Haake system MVIIP with inner cylinder radius 18.4mm, outer cylinder radius 21mm, height 60mm, both cylinders profiled with vertical ribs of 0.1mm square section, spaced 2mm apart round the circumference; (ii) the system S13/15 used by Tattersall and Dimond with inner cylinder radius 13mm, outer cylinder radius 15mm, height 50mm, both cylinders profiled with vertical serrations of 0.5mm square section, spaced 0.5mm apart round the circumference.

Pastes were prepared in batches of not more than 250g measured by weight and blended either by hand mixing with a spatula in a beaker for one minute or in a propellor type laboratory mixer at a speed of 1000 rpm for a predetermined time. Time and temperature were carefully controlled; all mixes were prepared and tested at 20 C.

The experimental programme studied the following: the effect of cycle time on flow curve shape; the effects of mixing time, concentration in water and age after mixing; and the behaviour under continuous shear.

Table 1 Properties of the Ciment Fondu

Setting time (BS 915): Initial							280 min			
Final							293 min			
90 μm residue (%)							3.8			
Surface Area (Blaine) (m^2/kg)							276			
Chemical Composition (%):										
SiO_2	Al_2O_3	Fe_2O_3	FeO	TiO_2	CaO	Na_2O	K_2O	SO_3	CO_2	
4.14	28.67	10.43	5.63	1.98	38.5	0.06	0.04	0.19	0.42	

RESULTS

EFFECT OF CYCLE TIME ON FLOW CURVE SHAPE

Pastes of 0.325 w/c were hand mixed and tested in the MVIIP geometry with shear starting 2.5 minutes after the first contact of cement and water. The total cycle time was varied from one minute to one hour and the maximum speed of rotation was 500 rpm. Figure 1 shows the three types of flow curve obtained, classified according to Banfill and Saunders, and Table 2 gives the cycle times at which these occurred. The relationship between speed and torque shown by the section XX in Figure 1, whether downcurve or upcurve, was independent of cycle time and conformed to the Reiner-Rivlin equation for a Bingham fluid. In view of these results the cycle time in all subsequent experiments was kept short to produce Type 1 flow curves, from the downcurve of which the yield value and plastic viscosity were calculated using that equation.

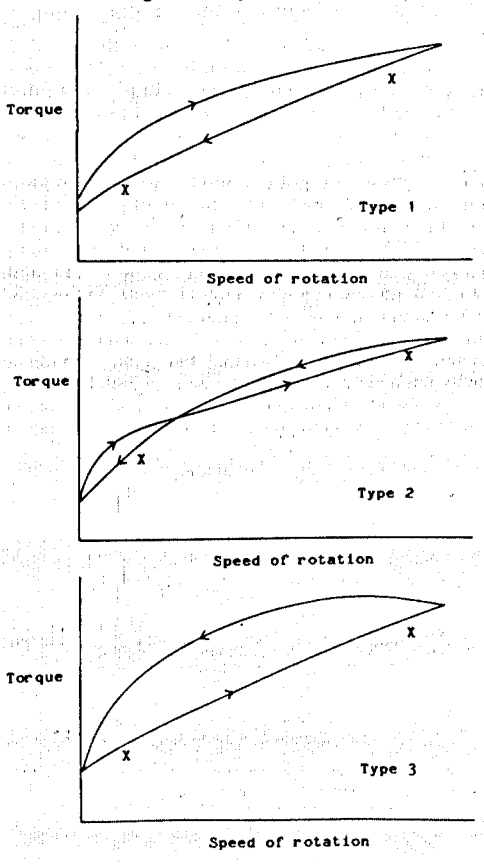

FIGURE 1 - Classification of flow curve types.

Table 2 Variation in flow curve with cycle time

Cycle time (min)	1	2	5	9.8	12	24	36	48	60
Flow curve type	1	1	1	1	2	3	3	3	3

EFFECT OF MIXING TIME

Pastes of 0.3 and 0.4 w/c were mechanically stirred for up to 10 minutes and tested in the MVIIP geometry with shear starting one minute after the end of stirring (i.e. up to 11 minutes from first contact of cement and water). The maximum speed was 500 rpm and the cycle time one minute. Figure 2 shows the effect of mixing time on the yield value and plastic viscosity.

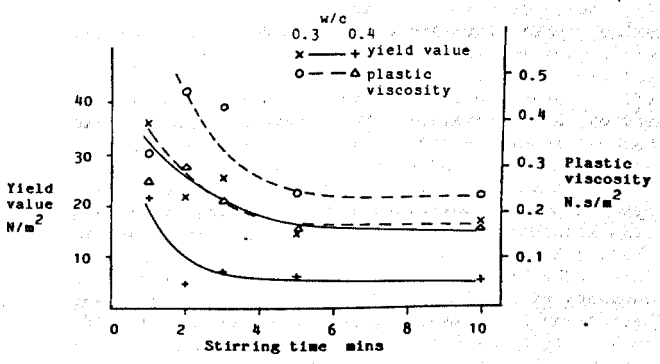

FIGURE 2 - Effect of mixing time on the rheology of Ciment Fondu pastes.

EFFECT OF CONCENTRATION OF PASTE

Pastes of different w/c ratios were mechanicaliy mixed for 5 minutes then tested in the MVIIP geometry to a maximum speed of 999 rpm and in the S13/15 geometry to 500 rpm, in both cases with a one minute cycle time. This mixing time was chosen in the light of the results in Figure 2. Separate paste samples were prepared for each test in both geometries. Figure 3 shows the variation in yield value and plastic viscosity with w/c ratio with comparative information on Portland cements drawn from Tattersall and Banfill's survey of the literature (1).

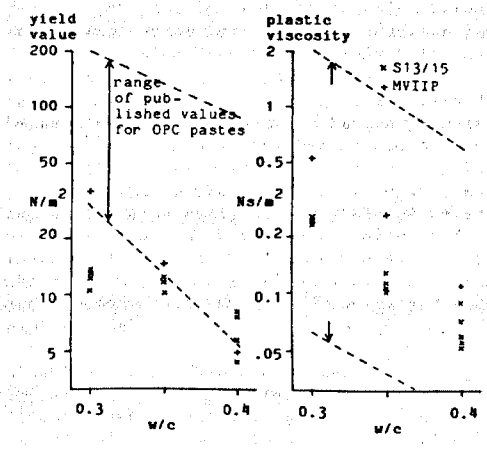

FIGURE 3 - Effect of w/c ratio on the rheology of Ciment Fondu and Portland cement pastes.

EFFECT OF AGE

Separate samples of paste at 0.3 w/c ratio were mechanically mixed for 5 minutes then left to stand for up to 90 minutes before testing in the S13/15 geometry to a maximum speed of 999 rpm or in the MVIIP geometry to 500 rpm with a one minute cycle time. Figure 4 shows the variation with age in yield value and plastic viscosity calculated as before.

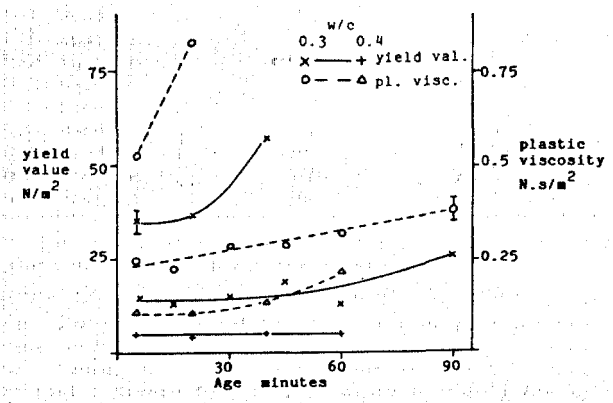

FIGURE 4 - Variation of yield value and plastic viscosity of Ciment Fondu pastes with standing time.

STRUCTURAL BREAKDOWN IN STEADY SHEAR

Hand mixed and mechanically mixed pastes of 0.3 and 0.4 w/c ratio were sheared in both geometries at several speeds of rotation. Typical torque-time behaviour observed in both geometries, as recorded on a continuous chart trace, is shown in Figure 5. However, plug flow taking the form of a stationary zone of paste up to 1mm thick adjacent to the stationary outer cylinder was observed in the MVIIP geometry but never in the S13/15 geometry. It occurred only in the pastes of 0.3 w/c, which suggests that it may be related to the stiffness of the paste. Because of the quantitative uncertainties introduced by this plug flow, only those results obtained in the S13/15 system will be reported here, but it must be borne in mind that the results from the two systems show close qualitative agreement. Table 3 summarises the results.

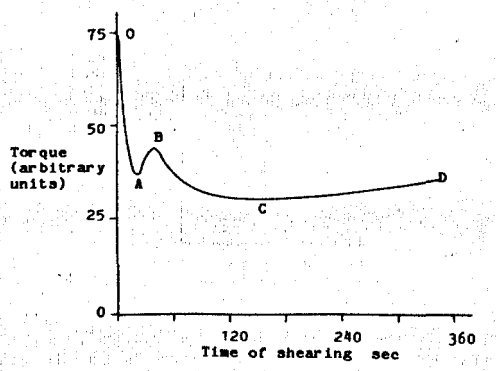

FIGURE 5 - Variation in torque with time during continuous steady shearing of Ciment Fondu paste.

DISCUSSION

Most of the features of the rheology of Portland cement pastes described earlier have been observed in these experiments on Ciment Fondu pastes, but some novel features are also present.

FLOW CURVES

Ciment Fondu pastes may be described by the Bingham model provided it is also realised that structural breakdown occurs on shearing which may distort the flow curve and give apparent shear thinning behaviour. Structural breakdown results in the greater effect on the yield value than on the plastic viscosity (Figure 2), exactly as is observed in Portland cements (7).

The changing flow curve/hysteresis loop pattern shown in Figure 1 follows the same sequence as for Portland cements. Loops indicative of structural breakdown are obtained at short cycle times, while the sense of the loop is reversed at long cycle times. At intermediate times of 10-20 minutes curves with more than one loop are observed. While Banfill and Saunders (3) attribute this to the competition in Portland cement between shear induced breakdown and hydration causing buildup, this cannot apply to Ciment Fondu because of the different chemistry involved. The hydration of Ciment Fondu proceeds via a "through solution" mechanism with dissolution of calcium aluminates. Structure development is delayed until their subsequent precipitation when the saturation level is exceeded (8). In contrast, in Portland cement the growth and interlocking of hydration products takes place from the first contact of cement and water (9). Therefore the observed changes in flow curve/hysteresis loop shape in both types of cement are probably due to physical effects arising from flocculation and deflocculation processes. Hattori and Izumi have explained the hysteresis loops by a theoretical model based on these considerations (10).

EFFECT OF CONCENTRATION AND AGE

Figure 3 shows that the yield value and plastic viscosity of Ciment Fondu pastes are related to w/c ratio in a similar way to Portland cement pastes but that the values determined are somewhat lower. Consequently a Ciment Fondu grout will be easier to pump but may show a slightly greater tendency to bleed. It also accounts for the well known harshness of Ciment Fondu concretes (11).

Because of the low rate of reaction between Ciment Fondu and water during the induction period, the relatively slow increase in yield value and plastic viscosity of undisturbed paste with time (Figure 4) is not surprising. There is a marked difference between results obtained in the two geometries which may be explained by the occurrence of plug flow in the MVIIP system as noted above. This would increase the effective shear rate in the paste and cause the apparently higher yield value and plastic viscosity which have been calculated from the instrument dimensions for Figure 4. In view of the observation of plug flow during continuous shear experiments this must be considered a plausible explanation.

STRUCTURAL BREAKDOWN AND BUILDUP

In general the structural breakdown behaviour of Ciment Fondu pastes is similar to that of Portland cement pastes, but this is the first time that observations of a double minimum in the torque-time behaviour have been reported.

3.3

Table 3 Structural breakdown under steady shear (S13/15 geometry)

Experimental Conditions					Torque (Nmm) at				Time (sec) from 0 to			Slope of semi-log plot (sec^{-1})	
W/C	Mixing method	Time (min)	Shearing speed (rpm)		0	A	B	C	A	B	C	OA	BC
0.3	Hand	1	200	)mean	35.7	16.9	19.3	12.9	22	41	175	10.3	1.84
	(4 replicates)			)s.d.	1.9	0.8	0.5	1.5	2.3	2	33	1.7	0.23
0.3	Hand	1	400		>46	19.7	21.2	18.6	45	72	160	3.7	0.73
0.3	Hand	1	500		>46	20.6	21.6	20.3	40	55	120	5.7	0.70
0.3	Machine	5	500		35.4	-	-	17.7	-	-	135	-	1.37
0.3	Machine	10	500		34.5	-	-	16.7	-	-	160	-	1.18
0.4	Hand	1	200		16.9	4.6	6.0	5.5	40	72	140	4.3	*
0.4	Hand	1	400		25.6	6.4	-	-	40	-	-	4.8	-
0.4	Hand	1	500		23.0	6.1	7.4	6.7	20	45	100	3.9	*
0.4	Machine	5	500		28.1	7.1	-	-	65	-	-	7.6	-
0.4	Machine	10	500		26.2	6.9	-	-	60	-	-	4.6	-

* The differences between the torques at points B and C are too small to allow accurate calculation of the slope of the semi-logarithmic graph.

The general form of the torque-time relationship under conditions of steady continuous shear is shown in Figure 5. The main features are the rapid initial decrease to a minimum at point A followed by a small peak B and another minimum C, after which torque steadily rises (D). When the torque reading, T, taken from the chart record is plotted in the form log(T-TeA) or log(T-TeC) against time, where TeA and TeC are the torques at the two minima A and C respectively, both portions fit a straight line relationship (Figure 6). The peak after the initial rapid fall in torque is generally well defined and two minima are clearly evident. However, in some experiments, particularly in mechanically mixed and less concentrated pastes the double minimum tends to merge into a single shallow one (Table 3). In the S13/15 geometry the second minimum is always below the first, but in the MVIIP geometry it is normally at the same torque or slightly above. This could be due to differences in the relative rates of breakdown and buildup at the higher shear rates prevailing in the MVIIP geometry when plug flow is taking place.

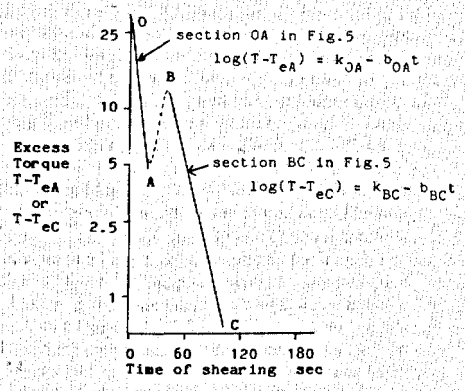

FIGURE 6 - Exponential form of the relationship between torque and time in continuous steady shear.

The linear relationship between log(T-TeA) and time is exactly as first reported by Tattersall for Portland cement pastes (2). However the slopes of the semilogarithmic plots shown in Figure 6 are different for the two portions of the torque-time curve. For the initial breakdown OA (Figure 5) the slope is 5-10 times that of the portion BC. There are insufficient data to confirm Tattersall's observations that the slope of the semilogarithmic plot is steeper at higher shear rates. The slope of the portion OA is not significantly affected by w/c ratio. No conclusion can be drawn about section BC because at 0.4 w/c the second minimum is either not present or so shallow that it is not possible to produce a semilogarithmic plot of the data.

Increasing the w/c ratio moves the whole curve to lower torques but has no significant effect on the times to any of points A, B or C. Mechanical mixing has the same effect but results in a single minimum, the position of which depends on w/c ratio (Table 3). At 0.3 w/c ratio the overall shape of the single minimum is shallow with the lowest torque occurring at times corresponding to point C of the curves with double minima, whereas at 0.4 w/c the minimum is sharply defined with the lowest torque corresponding in time to point A.

These observations tend to support the hysteresis loop behaviour. If the buildup of structure were of chemical origin the time after initial contact of water and cement would be critical whereas mechanical mixing for 10 minutes leaves the shape of the torque-time relationship unchanged. Thus the critical time is that from the start of shearing in the viscometer and the explanation of structural buildup must be sought in physical, flocculation changes.

STRUCTURAL MODEL

Tattersall's model for the structural breakdown of Portland cement pastse was proposed on the basis of the work done in a rotational viscometer (i) in overcoming normal viscous forces, (ii) in breaking linkages and (iii) in keeping them broken (2). Since he observed no rebuilding of structure, item (iii) was not considered. His model correctly predicts the exponential form of the experimental relationship between the excess torque (T-Te) and

time and gives the breakdown constant as

$$b = \frac{2\pi K}{n_0 \psi} w(w - w_1)$$

where w is the shear rate, n_0 and ψ are structural parameters - the initial number of linkages present and their strength repectively, and K, w_1 constants. Hattori and Izumi's structural model (10) explicitly allowed structural rebuilding or reflocculation and, as already noted, this accounted for the observed flow curve/hysteresis loop shapes.

If it is considered that the new structure which forms has different structural parameters then it too will undergo structural breakdown but at the same shear rate the value of the breakdown constant, b, will be different. For example, stronger linkages or more of them, perhaps arising from a different geometrical arrangement in the new structure, will result in a smaller constant b.

The existence of different types of flocculation structure in clay suspensions is well known and documented (12). The flat particles may associate through edge-edge, face-face or edge-face linkages and these types of linkage have different strengths arising from the different arrangements of atoms in the surface layers in these parts of the particles. These structural variations produce different rheological properties. Bombled (13) and Legrand (14) consider that the charge distribution on a grain of cement is not uniform. Ridges and other points where there are abrupt changes in direction of the surface are thought to be charged differently from flat faces. Consequently there is the possibility of face-ridge association relying on electrostatic charges. Because of the heterogeneity of cement particles the strength of this association may well depend on the relative orientation of the particle contacts.

The following model is therefore a plausible suggestion to account for the observed rheological behaviour of Ciment Fondu pastes. Particles are in contact when they are first mixed with water and remain together in the form of flocs, where the interparticle attraction is the resultant of attractive Van der Waals forces and the mutual repulsion of the electrical double layers around each charged particle in water. The particles in a floc are arranged randomly with some strong and some weak linkages. Shear breaks these flocs down, reduces the apparent viscosity of the suspension and individual particles can flow past one another and reorientate themselves. Particles collide but because of their freedom of movement are able to take up relative positions such that only the strongest linkages are formed. This results in a net increase in the strength of the structure, which is then followed by further breakdown, but at a lower rate because of the stronger linkages.

The model is somewhat speculative at this stage but further experimental evidence in support is provided by the effect of superplasticisers, to be described in a later publication. These admixtures remove the second minimum in the torque-time relationship, as would be expected for materials which adsorb all over the particle surfaces thereby obliterating any differences in the charge distributions. Consequently a single type of structure only is involved.

CONCLUSIONS

The rheology of Ciment Fondu pastes is broadly similar to that of Portland cement pastes. They show Bingham type behaviour with slightly lower yield value and plastic viscosity. They exhibit structural breakdown in the form of a dependence on the time of mixing. The flow curves show similar hysteresis loop behaviour to that shown by Portland cement pastes and which can be explained by the competition between structural breakdown and buildup due to flocculation.

In continuous steady shear experiments the behaviour shows novel features in the form of a double minimum in the torque-time curve. This behaviour can also be explained by a change in the flocculation structure upon shearing.

ACKNOWLEDGEMENTS

We gratefully ackowledge the financial support of the Science and Engineering Research Council and FEB (Great Britain) Ltd; provision of materials by Lafarge Aluminous Cement Co Ltd; and the experimental assistance of Miss P. Hooper.

REFERENCES

1. G.H. TATTERSALL, P.F.G. BANFILL (1983), The Rheology of Fresh Concrete, London, Pitman.
2. G.H. TATTERSALL (1955), Brit. J. Appl. Phys. 6 (5), 165-7.
3. P.F.G. BANFILL, D.C. SAUNDERS (1981), Cem. Concr. Res. 11, 363-70.
4. P.F.G. BANFILL (1985), 4th Nat. Conf. on Mechanics and Technology of Composite Materials, Varna, Bulgaria, 423-6.
5. R.J. MANNHEIMER (1983), Oil and Gas J. Dec 5, 144-7.
6. G.H. TATTERSALL, C.R. DIMOND (1976), Hydraulic Cement Pastes, Publicn. 15.121, Slogh, Cement and Concrete Association, 118-33.
7. P.F.G. BANFILL (1981), Mag. Concr. Res. 33 (114), 37-47.
8. F.M. LEA (1970), Chemistry of Cement and Concrete, London, Arnold.
9. D.D. DOUBLE, S.J. PERRY, A. HELLAWELL (1978), Proc. Roy. Soc. Lond. A 359,435-51.
10. K. HATTORI, K.IZUMI (1982), J. Dispersion Sci. Tech. 3 (2), 129-45; 147-67; 169-93.
11. T.D. ROBSON (1962), High Alumina Cements and Concretes, London, Contractors Record Ltd.
12. H. VAN OLPHEN (1977), An Introduction to Clay Colloid Chemistry, New York, Wiley.
13. J.P. BOMBLED (1974), Revue des Materiaux de Construction (688), 137-55.
14. C. LEGRAND (1981), Cahiers de la Groupe Francaise de Rheologie, (Special Number) October, 129-36.